

**INTRODUCTION
TO
ASTROPHYSICAL
RADIATIVE TRANSFER**

Robert J. Rutten

Copyright ©1988 R.J. Rutten, Sterrekundig Instituut Utrecht, The Netherlands
Reproduction in any form of any part of this work is not permitted without prior consent of the author.

First edition: Autumn 1988, based on previous lectures of the third year course OTS by C. Zwaan and R.J. Rutten. Set in LaTeX by M. van der Klomp.

Second edition: Autumn 1989, revised (with restoration from disk by H.M.G. Burn) and expanded (Chapter 8, with LaTeX assistance from F. van der Wolf).

Third edition: Autumn 1990, revised (with contributions by A. Schadee) and expanded (Appendices A–C).

Fourth edition: Autumn 1991, revised and expanded (Chapter 8).

English translation of the fourth edition: Spring 1992, by Ruth C. Peterson, corrected by L. Strous, with assistance from C. Zwaan and the author.

March 1995: fresh compilation of the fourth edition by Dan Kiselman, including revised version of Chapters 2 and 3 by Rob Rutten, and new figures Chapter 4.

Autumn 2015: fresh compilation of the fourth edition by Luc Rouppe van der Voort, including corrections.

Contents

1	Introduction	1
1.1	Why this book?	1
1.1.1	EM radiation as a diagnostic	1
1.1.2	EM radiation as a driver of structure formation	2
1.2	These lecture notes	2
1.3	Other books	3
1.4	Main themes	3
1.4.1	Wavelength, frequency and energy	3
1.4.2	Spectral lines and continua	4
1.4.2.1	Spectral lines	4
1.4.2.2	Continua	7
1.4.3	Collisional transitions and radiative transitions	9
1.4.4	Photon creation, photon destruction, photon scattering and photon conversion	11
1.4.5	Optically thin and optically thick	12
1.4.6	Thermal and nonthermal	13
1.5	Crucial questions	13
2	Radiation quantities	15
2.1	Introduction: from luminosity to intensity	15
2.2	Intensity and related quantities	19
2.2.1	Intensity	19
2.2.2	Mean intensity	21
2.2.3	Flux	22
2.2.4	Radiation density and radiation pressure	23
2.2.5	Stokes parameters	24
3	Transport equation	27
3.1	Introduction: emission and extinction	27
3.2	Emission coefficient	27
3.3	Extinction coefficient	28
3.4	Transport equation	30
3.5	Optical path length, optical thickness, optical depth	31
3.6	Source function	32
3.7	Formal solution of the transport equation	34
3.7.1	Integral form of the transport equation	34
3.7.2	Radiation from a homogeneous medium	35
3.7.3	Radiation from a thick medium	37
4	Radiation and matter in equilibrium	41

4.1	Introduction: thermodynamical equilibrium	41
4.2	Radiation in thermodynamical equilibrium	41
4.2.1	Kirchhoff laws	41
4.2.2	Planck law	43
4.2.3	Related radiation laws	43
4.2.3.1	Wien approximation	43
4.2.3.2	Rayleigh-Jeans approximation	43
4.2.3.3	Wien displacement law	45
4.2.3.4	Stefan-Boltzmann law	45
4.2.4	Radiation temperatures	46
4.2.4.1	Brightness temperature	46
4.2.4.2	Antenna temperature	46
4.2.4.3	Color temperature	47
4.2.4.4	Effective temperature	47
4.3	Matter in thermodynamical equilibrium	47
4.3.1	Maxwell distribution	47
4.3.2	Boltzmann distribution	48
4.3.3	Saha distribution	49
4.3.4	Saha-Boltzmann partitioning	50
5	Discrete processes	53
5.1	Introduction: bound-bound transitions	53
5.2	Five transition processes	54
5.2.1	Spontaneous deexcitation	54
5.2.2	Radiative excitation	55
5.2.3	Induced deexcitation	56
5.2.4	Collisional excitation and collisional deexcitation	56
5.3	Einstein relations	57
5.4	Emission coefficient and extinction coefficient	58
5.5	Source function	60
6	Continuous processes	63
6.1	Introduction: four types of interaction	63
6.2	Radiation from an accelerating charge	63
6.3	Electrons and electric fields	65
6.3.1	Free-free transitions	65
6.3.2	Bound-free transitions	67
6.3.3	H ⁻ transitions	69
6.4	Electrons and photons	70
6.4.1	Elastic scattering	70
6.4.1.1	Rayleigh scattering	72
6.4.1.2	Resonant scattering	73
6.4.1.3	Thomson scattering	74
6.4.2	Inelastic scattering	74
6.4.2.1	Compton scattering	74
6.4.2.2	Inverse Compton scattering	75
6.5	Electrons and magnetic fields	77
6.5.1	Cyclotron radiation	77
6.5.2	Synchrotron radiation	78
6.6	Collective processes	79

6.6.1	Dust and droplets	79
6.6.2	Cherenkov radiation	79
6.6.3	Plasma cutoff	80
6.6.4	Faraday rotation	80
6.6.5	Razin cutoff	80
6.7	Nuclear reactions	81
6.7.1	Fusion and fission reactions	81
6.7.2	Pair annihilation and pair creation	81
7	Radiative transfer	83
7.1	Introduction: different types of equilibrium	83
7.1.1	Thermodynamical Equilibrium (TE)	83
7.1.2	Local Thermodynamical Equilibrium (LTE)	83
7.1.3	Statistical Equilibrium (SE)	84
7.1.4	Non-Local Thermodynamical Equilibrium (NLTE)	85
7.2	Radiative transfer in LTE	86
7.2.1	Radiation from a thin LTE slab	87
7.2.2	Radiation within a thick LTE medium: the Rosseland approx- imation	87
7.2.3	Radiation from a thick LTE medium	88
7.3	Radiative transfer with photon scattering	91
7.3.1	Pure scattering	92
7.3.2	Absorption and scattering in a two-level atom	93
7.3.3	Effective optical thickness	96
7.3.4	Radiation from a thin scattering slab	97
7.3.5	Radiation within a thick scattering inhomogeneous medium: the Eddington approximation	97
7.3.6	Radiation from a thick scattering medium	98
7.4	Radiative transfer with photon conversion	101
8	Applications	103
8.1	Introduction: between thick and thin	103
8.2	Spectra from stellar photospheres	103
8.2.1	Continua from the Sun	103
8.2.1.1	Extinction coefficient	103
8.2.1.2	Height of formation	104
8.2.1.3	Variation of emergent intensity and temperature stratification	106
8.2.1.4	Center-limb variation	108
8.2.2	Spectral lines from the Sun	109
8.2.2.1	Extinction coefficient	109
8.2.2.2	Height of formation	109
8.2.2.3	The Na I D lines	110
8.2.2.4	The Ca II K line	111
8.2.2.5	Emergent intensity and temperature stratification	113
8.2.2.6	Center-limb variation	114
8.2.2.7	Outside the limb	115
8.2.3	Spectra of stellar photospheres	115
8.3	Stellar envelopes	116
8.3.1	Stellar coronae	116

8.3.1.1	The solar corona in X-rays	120
8.3.1.2	The solar corona in the visible	121
8.3.1.3	The solar corona in radio waves	124
8.3.2	Stellar winds	126
8.3.3	Planetary nebulae	129
8.3.3.1	Zanstra mechanism	130
8.3.3.2	Fluorescence	132
8.3.3.3	Forbidden lines	132
8.3.3.4	Radio emission	133
A Tables and term diagrams		135
B Formulae		149
References		85

Chapter 1

Introduction

1.1 Why this book?

By “radiation” we are referring here exclusively to electromagnetic (EM) radiation. This radiation is of interest from both a diagnostic and an energetic standpoint.

1.1.1 EM radiation as a diagnostic

Practically all astrophysical data which reach us are encoded in the EM spectrum; it is “the astronomer’s treasure” (Pannekoek), a rich source of (diagnostic) information in that:

- all objects emit EM waves, i.e. photons, and so are observable provided that they are not obscured by another object. EM radiation travels with the speed of light, and photons do not decay;
- differences can be discerned in the direction (the image), time, wavelength and energy (spectrum), and direction of oscillation (polarization);
- encoded in the spectral lines is a rich probe of local conditions (composition, thermodynamical quantities of state, motions, magnetic fields).

The interpretation of the astrophysical EM diagnostics demands a knowledge of the generation and the transport of radiation. This is true throughout all subjects of astrophysics.

Question 1.1 Compare the wealth of diagnostic information provided by EM radiation with the output of the following additional carriers of astrophysical information:

- neutrinos;
- baryons;
- gravitational radiation;
- meteorites and comet impacts;
- radar;
- sounding rockets, orbiters, landers, flybys;
- astronauts and cosmonauts.

Question 1.2 Name some types of observations and domains of astronomical investigation in which a knowledge of the generation and transport of radiation is *not* important.

1.1.2 EM radiation as a driver of structure formation

Frequently radiation and radiation transport within an astrophysical object are energetically of importance, for example:

- energy transport in stars;
- stellar winds driven by radiation pressure;
- heating of gaseous nebulae by stars;
- Comptonization in accretion disks;
- the radiation-dominated epoch in the theory of the Big Bang.

1.2 These lecture notes

These lecture notes cover the generation and transport of radiation. Both subjects are difficult and extensive, and for both, only the basics are set forth here. They will appear again in more advanced courses.

These lecture notes are divided as follows:

- this chapter is an introduction to the central themes and problems of this subject, and provides definitions of various concepts;
- Chapters 2 and 3 contain macroscopic definitions of various measures of radiation, and of the equation of radiative transport;
- Chapter 4 treats radiation and matter in thermodynamic equilibrium;
- Chapter 5 details the discrete microscopic radiative processes;
- Chapter 6 details the continuous microscopic radiative processes;
- Chapter 7 treats radiation transport;
- Lastly, Chapter 8 provides a few astrophysical applications.

The astrophysical applications bring up the rear in these lecture notes in order not to disturb the more formal presentation of the basic material in Chapters 2–7. It pays, however, to refer to them during the treatment of the relevant formulae, as an example and a proving ground.

These lecture notes include many questions. They are intended to set the reader thinking, the reason being that much of the material offered here seems more transparent than it is. The equations are simple and demand not much more than college physics, except for Chapter 6. Nevertheless the optical thickness of this matter is considerable. The questions help to make that clear. Answers in Appendix ??.

These lecture notes use cgs units. The choice is however not important; most formulae are the same in the mksA system.

These lecture notes are concerned exclusively with radiation in and by *gases*, including ionized ones (“plasmas”). We therefore have only to deal with free atoms, ions, molecules and electrons, perhaps in a magnetic field. These simple forms of matter provide rather difficult material — until you can develop a physical intuition for gases that you can’t see through. The Sun is made of gas but is not transparent!

Question 1.3 For the investigation of which astrophysical objects is a knowledge of solid-matter physics required?

1.3 Other books

No book covers exactly the same material, but these lecture notes follow parts of:

- Mihalas: *Stellar Atmospheres*. A standard graduate text. Chapters 1 – 6 cover the topics of these lecture notes at a more advanced level and from a more mathematical and computational standpoint. Additional topics are covered in later chapters.
- Rybicki and Lightman: *Radiative Processes in Astrophysics*. Very good; more difficult than these lecture notes and therefore also good for more advanced courses in plasma- and high-energy astrophysics. Purchase strongly recommended. Chapters 2–5 and 7 of these lecture notes give an expanded treatment of the material which is summarized in the first chapter by Rybicki and Lightman, with the same notation; conversely, Chapter 6 of these lecture notes is a simplified summary of Chapters 3–8 by Rybicki and Lightman. Moreover this book contains additional subjects which are not treated in these notes.

Also useful are the following:

- Harwit: *Astrophysical Concepts*. Broad and good.
- Gray: *Observation and Analysis of Stellar Photospheres*. Simpler than these lecture notes; interesting on account of the emphasis on instrumentation and observational methods in optical stellar spectrometry.
- Novotny: *Introduction to Stellar Atmospheres and Interiors*. Somewhat simplistic and out of date.
- Bowers and Deeming: *Astrophysics I & II*. Here Volume I. Concise but very broad, sometimes sloppy.

Occasionally reference is made to the more specialized literature, especially in the applications in Chapter 8. The references are found in Appendix 5.5.

1.4 Main themes

We now give a short characterization of the main themes to which attention will be paid in these lecture notes, along with an introduction of the various terms and an overview of the most critical points. The intention is to outline the problems and provide a first grasp of the topics to be discussed in depth in the following chapters.

1.4.1 Wavelength, frequency and energy

EM radiation has a *wave character*. From the four Maxwell equations there follow the wave equations for the electric field \vec{E} and the magnetic field \vec{B} which are satisfied by transverse waves, with $\vec{E} \perp \vec{B}$, $\vec{B} \perp \vec{k}$ and $\vec{E} \perp \vec{k}$, in which the wave vector \vec{k} specifies the direction of propagation.

The third statement of perpendicularity holds in a vacuum and in isotropic media, in which the electric susceptibility χ is a scalar. In media such as birefringent crystals, χ is a tensor and the angle between \vec{E} and \vec{k} differs from 90° .

The frequency and wavelength are related according to:

$$\nu = c/\lambda \quad (1.1)$$

ν = frequency, units $\text{s}^{-1} = \text{Hz} = \text{cy/s}$ (cycles per second) = cps;
 c = speed of light; in vacuum $c = 3 \times 10^{10}$ cm/s;
 λ = wavelength, units cm or Ångstrom ($1 \text{ \AA} = 10^{-8}$ cm) or nm ($1 \text{ nm} = 10 \text{ \AA}$);
 σ = wave number, defined as $\sigma = 1/\lambda_{\text{vac}}$ or $\nu = c_{\text{vac}}\sigma$. Units cm^{-1} ;
 ω = angular or circular frequency, defined as $\omega = 2\pi\nu$.

In a medium both c and λ become smaller with increasing index of refraction n , while ν and σ do not change. In these lecture notes the index of refraction is neglected by setting $n = 1$. The following convention holds for the wavelengths of spectral lines: for $\lambda < 2000 \text{ \AA}$: $\lambda = \lambda_{\text{vac}}$; for $\lambda > 2000 \text{ \AA}$: $\lambda = \lambda_{\text{air}}$ (15° C , 760 mm Hg). A conversion table appears in Allen, *Astrophysical Quantities*, §32.

EM radiation also has a *particle character*. The Maxwell equations are not satisfied on the microscopic scale in which quantization becomes significant. The interaction between EM radiation and matter proceeds by means of *photons* with energy:

$$E = h\nu \quad (1.2)$$

with h = the Planck constant = 6.626×10^{-27} erg sec ($1 \text{ erg} = 10^{-7} \text{ J}$).

The EM spectrum used in astrophysics spans something like fifteen decades (Figure 1.1). Each wavelength region is characterized by its own radiative processes. The nature of the observed objects is related to this. Frequently the radiation at the extremes of the spectrum (radio and X-ray radiation) is entirely of nonthermal origin, while the radiation in the intermediate wavelengths is generally of thermal origin.

Each wavelength region also has its own characteristic observational techniques (Table 1.1). The access to the EM spectrum has widened considerably since the Second World War, thanks to radio astronomy, space travel, and advances in detector technology.

1.4.2 Spectral lines and continua

Astronomical spectra exhibit *continua* on which are superimposed *spectral lines*, in *absorption* or in *emission* with respect to the local continuum. See Figure 1.2 and Figure 1.3 for examples.

Spectral lines are called “lines” because spectrographs usually have linear entrance slits. The monochromatic image of the spectrum exhibits brighter or darker stripes perpendicular to the direction of the dispersion.

Question 1.4 What kind of spectral lines would the Sun show if no entrance slit was used? During eclipses people frequently photograph the spectrum of the outermost solar limb without a slit. What do these spectra look like? Why is this done?

1.4.2.1 Spectral lines

Spectral lines are the result of transitions between *discrete* energy levels, such as the jumps between bound levels of a valence electron in an atom: *bound-bound* transitions. *Excitation* to higher levels can occur via absorption of kinetic energy

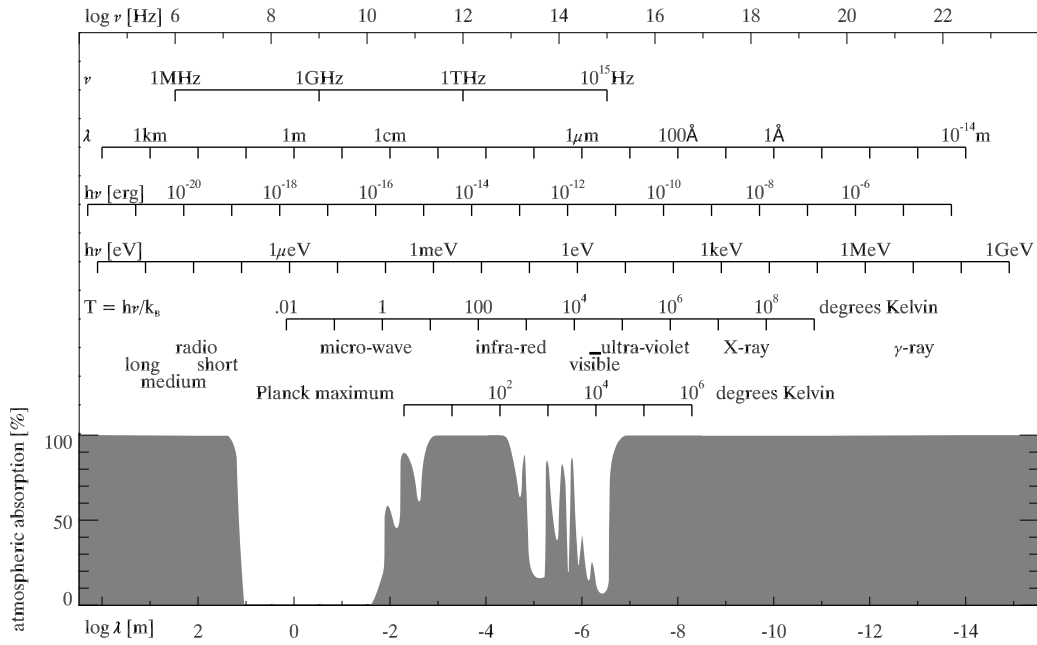


Figure 1.1: *The EM spectrum and the Earth atmosphere absorption. After A. Code, 1960 Astron. J. 65, 279*

(*collisional excitation*) or by photon absorption (*radiative excitation*). Likewise, *deexcitation* to lower levels can occur via collision (*collisional deexcitation*) or by photon emission (*radiative deexcitation*). This energy exchange proceeds by means of quanta with a frequency given by $h\nu = \Delta E_{mn}$, where $\Delta E_{mn} = E_m - E_n$ is the energy difference between the levels m and n ($m > n$) of the bb transition; the photons involved have the corresponding wavelength $\lambda = hc/\Delta E_{mn}$.

Note the abbreviation: bb = *bound-bound*.

Notation: Fe I is the spectrum of neutral iron, Fe II is the spectrum of singly ionized iron (Fe^+), etc.

Spectral lines are *broadened* with a statistical distribution determined by:

- *radiative damping*, a phenomenon arising from the finite lifetime of levels higher than the ground state, which are then no longer sharp (they possess a *natural line width* – as a result of the uncertainty principle);
- *collisional damping*, by disturbances due to neighboring particles;
- *Doppler broadening*, the average over the range of Doppler shifts for the radiating atoms (of the appropriate kind).

This statistical distribution of wavelengths is called the *line profile*.

Spectral lines are *split* by:

- (*hyper-*)*fine structure* as a result of isotopic splitting and interaction of the atomic nucleus with the electrons (spin and magnetic moment);
- magnetic fields (*Zeeman splitting*);
- large-scale motions in the line of sight direction (*Doppler splitting*).

	Radio	Micro-wave	Infra-Red	Visual	Ultra-Violet	X-ray	γ -ray
Jargon ν/λ Jargon E	MHz mJansky	GHz mJansky	μm T_B	\AA , nm erg, I/I_0	\AA , nm erg	keV	MeV/GeV
Facilities: first, notable	radar VLA, WSRT, LOFAR, SKA	COBE WMAP, Planck	IRAS ISO, Spitzer, Herschel, SOFIA	Galilei ESO Chile, Keck Hawaii, La Palma	IUE Hubble, GALEX	Uhuru Chandra, XMM Newton	balloons/ SAS-2/COS-B Compton Swift
Imaging Dispersion Detection	Aperture synthesis filters amplitude +phase	mirror filters energy	mirror filters energy	mirror, lens filters, grating photons collective	mirror filters, grating some photons	mask, mirror filters, grating individual photons	mask, mirror filters, grating individual photons
Continua Lines	Bremsstrahlung spin-spin	free-free molecules	free-free molecules	bound-free atoms	Thomson ions	Compton nuclei	Compton nuclei
Characteri stic object	galaxy, quasar	CMB	IM, protostar	cool star	hot star	accretion disk	GRB

Table 1.1: *Various facts concerning spectral regions*

When the instrumental *resolution* is not sufficient, (whether in λ , in x , y , z , t , or in the polarization direction), such splitting results in line broadening.

Spectral lines are always associated with discrete bb processes, but this does not mean that emission lines in an observed spectrum are always the direct consequence of photon emission by radiative deexcitation, or that absorption lines are always the direct consequence of photon absorption by radiative excitation. That depends on the radiation transport through the medium. In general spectral lines are the result of the *extra* bb processes which can occur at the specific line wavelength in the medium, in addition to the processes which give rise to the continuous spectrum at that and adjacent wavelengths.

Question 1.5 What is H I? And H II and H III?
Do these spectra have spectral lines? What is the 21 cm line associated with?
Does Fe XII have spectral lines? If so, in which wavelength region?

Question 1.6 Compare the observed wavelengths of the Na I D lines in Figure 1.2 and the $\text{Ly}\alpha$ line in Figure 1.3 with those of the associated bb transitions in the relevant term diagrams (Appendix ??). What is your conclusion?
Figure 1.3 shows a large number of spectral lines with $\lambda < 3530 \text{\AA}$: the *Ly α forest*. Do these arise from hyperfine structure, Zeeman splitting, or Doppler splitting?

Question 1.7 In Figure 1.2 the line identifications are given. Near the Na I D lines there are solar lines of Fe I and Ni I; the H_2O lines, however, originate in the Earth's

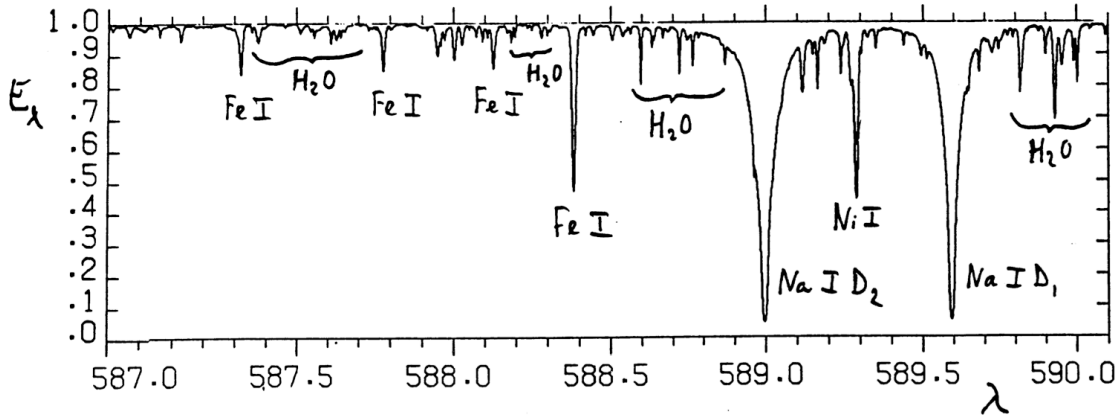


Figure 1.2: The Na I D lines in the solar spectrum. These are the resonance lines (the strongest lines arising from the ground level) of Na I; the name “D” is due to Fraunhofer who named in alphabetical order the most striking of the darker features in the solar spectrum. They correspond to the two transitions possible between the ground level and the first two excited levels of the neutral sodium atom (see the Na I term diagram in Appendix ??). They are the same spectral lines which appear in the yellow sodium lamps shining along the highways. These are the same lines which gave Fraunhofer the idea that darker lines in the solar spectrum and brighter lines in flame spectra have something to do with one another. Here they are in absorption: the brightness of the Sun is lower in the wavelengths of the lines than in the adjacent continuum. This piece of spectrum is taken from the flux atlas of Kurucz et al. (1984). On the y axis is plotted the intensity averaged over the visible disk of the Sun (irradiance), normalized to the continuum between the lines. Wavelength in nm is plotted along the x axis. The line identifications are taken from the standard tabulation of Moore, Minnaert and Houtgast (1966).

atmosphere. How can the origin of the lines be conclusively established?

1.4.2.2 Continua

Continua are the result of nondiscrete processes in which photons are absorbed or emitted:

- bound–free transitions of atoms and molecules.

The liberation of a valence electron from a bound state n , by absorption of a photon with energy larger or equal to the ionization energy $\Delta E_{\infty n} = E_{\infty} - E_n$ from that level (*radiative ionization*). Alternatively, the capture of a free electron (*recombination*) into a bound state, accompanied by the emission of a photon with energy larger or equal to $\Delta E_{\infty n}$ (*radiative recombination*). The free states above the *ionization limit* are not discrete because the free electron may have an arbitrary kinetic energy ($\frac{1}{2}m_e v^2$: $h\nu = \Delta E_{\infty n} + \frac{1}{2}m_e v^2$). Ionization and recombination can equally well occur by the absorption or release of kinetic energy (*collisional ionization and collisional recombination*), without a photon.

Note the abbreviation: bf = bound–free.

Notation: FeI bf is the continuous spectrum associated with the ionization of neutral iron (*series limit continuum* of Fe). FeII bf is the bound-free spectrum of Fe^+ , etc.

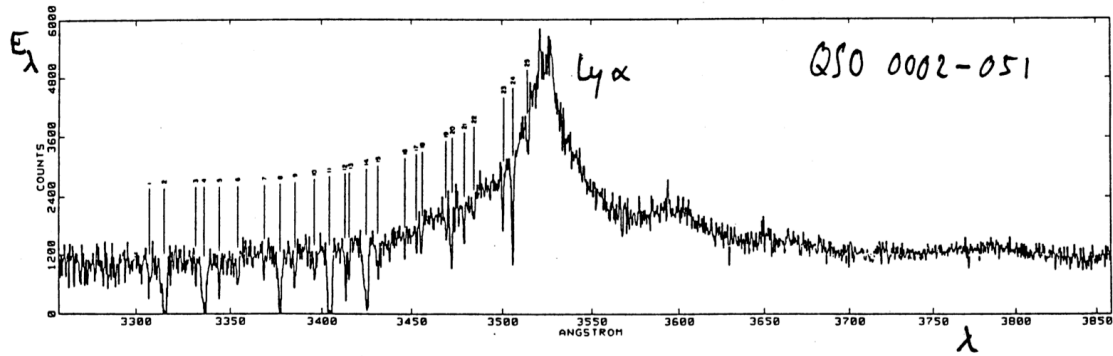


Figure 1.3: The H I Ly α line in the spectrum of the quasar Q0002+051. This resonance line arises from the transition between the ground level of hydrogen and the adjacent level (see Figure 1.4): it is the first line (of longest wavelength) of the Lyman series. It is evident here as a broad emission peak near 3530 Å. At shorter wavelengths, the Ly α “forest” appears: a forest of Ly α lines at smaller redshifts. They are all seen in absorption. The most obvious ones are numbered from 1 to 25, but there are probably many more that are buried in the noise. Observation with the 2.54 m reflector at Las Campanas (Chile), by Young et al. (1982).

- dissociation and association of molecules;
- nuclear fission and nuclear fusion;
- free-free transitions = Bremsstrahlung.

This is the emission or absorption of photons as a result of the acceleration or deceleration of an energetic particle in an electric field, for example in the collision of an ion and an electron.

Note the abbreviation: ff = free-free.

Notation: Fe I ff is the spectrum resulting from the interaction between a free electron and an Fe⁺ ion. Fe II ff is the free-free spectrum of Fe⁺⁺, etc.

- cyclotron radiation, synchrotron radiation.

As a result of acceleration of a charge in a magnetic field;

- pair annihilation, pair production;

- Cherenkov radiation.

The bow shock of a particle whose speed exceeds the local speed of light in a medium.

A special, astrophysically important, case concerns the bf and ff processes of neutral hydrogen with an extra electron, the H⁻ ion. H⁻ bf ionization is the removal of the second bound electron in H⁻; H⁻ bf recombination is capture of a free electron by a neutral hydrogen atom into the bound H⁻ state (in this case there is only one such state); H⁻ ff is emission or absorption resulting from the acceleration or deceleration of a free electron in the electrical field of a neutral hydrogen atom.

Question 1.8 What are the H I bf processes? What is the notation for the Bremsstrahlung spectrum resulting from collisions between free protons and electrons?

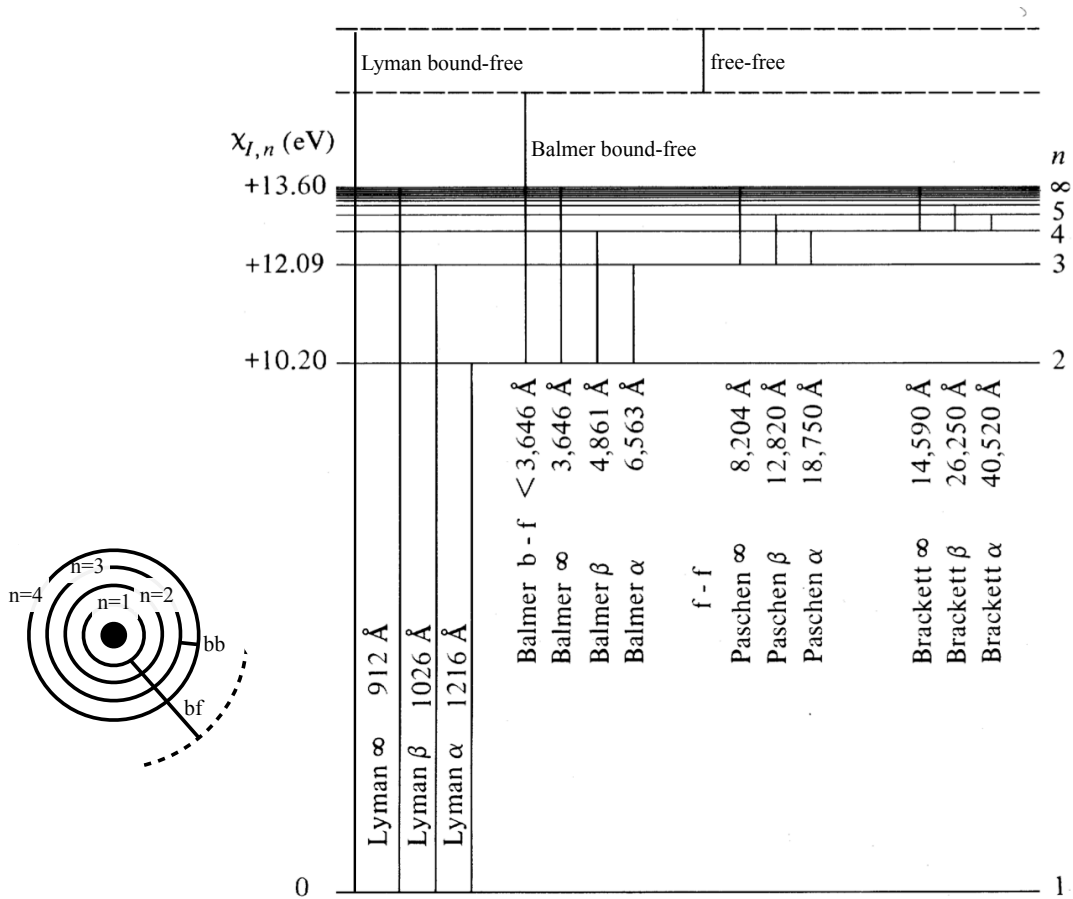


Figure 1.4: The Bohr atom and the energy level diagram for hydrogen. For the first four line series in the spectrum of hydrogen, the transitions corresponding to the first two lines (bb) and the series limit (∞) are given with their wavelengths. The free-free (ff) and bound-free (bf) transitions are also indicated. The wavelengths are in Å (10^{-10} m). It is customary to refer to the Balmer lines as $H\alpha$, $H\beta$ etc., and the bf Balmer continuum as Bacont; the bb Lyman transitions as $Ly\alpha$, $Ly\beta$ etc., and the bf Lyman continuum as $Lycont$.

1.4.3 Collisional transitions and radiative transitions

Bound-bound excitation and deexcitation, bound-free ionization and recombination, molecular dissociation and association etc. may occur, both by absorption or release of radiation energy in the form of photons and by absorption or release of kinetic energy by means of a collision with a particle. Figure 1.5 shows all of the five types of transitions possible between two discrete energy levels (bb) and between a bound and a free state (bf). In the second and fifth processes in each column, no photons are involved. The fourth process, respectively *induced deexcitation* and *induced recombination*, can be viewed as a resonant process: a photon of just the right energy triggers radiative deexcitation — that is, the target atom resonates with the incoming wave. The escaping photon has the same attributes (frequency, direction, phase) as the incident photon.

With more levels, even more circuitous routes are possible; see Figure 1.7.

Question 1.9 Check that a photon conversion sequence as shown in Figure 1.7 can consist

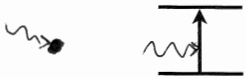



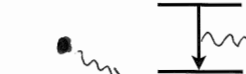



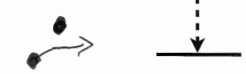

bound-bound (bb) processes		bound-free (bf) processes	
radiative excitation		radiative ionization	
collisional excitation		collisional ionization	
spontaneous de-excitation		radiative recombination	
induced de-excitation		induced recombination	
collisional de-excitation		collisional recombination	

Figure 1.5: The bb and bf processes.

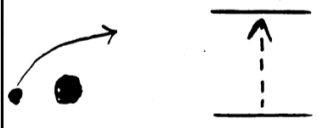



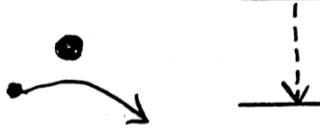

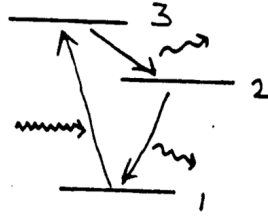
photon creation	photon destruction	photon scattering
		
		

Figure 1.6: Three pairs of bb interactions: creation, destruction and scattering of photons.

of $\text{Ly}\beta$ absorption, followed by $\text{H}\alpha$ and $\text{Ly}\alpha$ emission. Can such a triad also consist of bf transitions, for example the Lycont?

Question 1.10 Is kinetic energy involved in induced deexcitation? And in induced recom-

Figure 1.7: *Photon conversion.*

bination?

Question 1.11 Check that collisional recombination requires a three-body collision. Under what circumstances will collisional recombination be a rare process?

Question 1.12 Draw a diagram such as that in Figure 1.5 for ff transitions. Does this also comprise five processes? How many particles are involved in each process?

1.4.4 Photon creation, photon destruction, photon scattering and photon conversion

In Figure 1.6 the bb processes of Figure 1.5 are grouped into three *pairs*:

- collisional excitation followed by radiative deexcitation (spontaneous or induced) = *photon creation* = conversion of kinetic energy into radiation;
- radiative excitation followed by collisional deexcitation = *photon destruction* = conversion of radiation into kinetic energy;
- radiative excitation followed by radiative deexcitation = *scattering photon* = redistribution of radiation.

Scattering changes at least the direction between the incident and the scattered photon, possibly with an anisotropic redistribution (*directional redistribution*) depending on the process. The frequency can remain constant in bb processes between the same two levels, for example in *resonance scattering* out of the ground state; in that case the scattering is *coherent* or *monochromatic* if the frequency remains exactly the same. It can also happen that the frequency is slightly changed by redistribution over the line width: *frequency redistribution*.

The pairs of processes in Figure 1.6 hold for two levels; with more levels, *photon conversion* such as in Figure 1.7 can appear on the scene. In this case an energetic photon is converted into two other photons of longer wavelength.

In the first two pairs, local kinetic energy and radiation energy are transformed into one another. These pairs of processes couple the radiation field to conditions in the local medium. If collisions occur frequently enough, strong coupling is expected between the local radiation field and the local particle velocities: *equipartition* of energy.

However, if collisional excitations and collisional deexcitations are rare, the radiation field (at the wavelength of the spectral line corresponding to this bb transition) can be independent of the local particle energies. This will be the case if the particle density is so low that there are very few interactions, but also if primarily coherent scattering takes place at the particular wavelength in question. The radiation we see may not tell us anything about conditions at the place where we see the radiation

coming from, i.e., where the detected photons were emitted: the photon supplied by a scattering atom came from somewhere else, and the original creation of that quantum of radiation energy by a collisional excitation–radiative deexcitation pair happened perhaps many scattering processes earlier and in another place entirely. Throughout such a sequence of bb scattering processes a particular quantum keeps its own identity, with information that refers to its creation, namely the characteristic kinetic energy of the particles at the place where it was generated. With each scattering the photon briefly serves as potential energy of a target atom and then is sent out once again in another direction. This *nonlocally determined nature* of radiation owing to scattering forms the central issue of radiative transport.

This description concerns bb scattering, i.e., line photons; similarly, in elastic scattering of continuum photons *nonlocal* representation of the radiation field can also occur. For example, consider fog around a lantern. What you actually see is the fog, not the lantern; however the color temperature of the radiation is that of the lantern and not that of the fog.

Question 1.13 Figure 1.6 does not show all possible combinations of the five bb processes in Figure 1.5. How do the other pairs go?

Question 1.14 For bf processes, are there similar pairs for creation, destruction and scattering? What about for ff processes?

Question 1.15 Check that also in photon conversion the problem can crop up that observed photons are not created where you see them coming from. Are there triple processes between three levels in which there is coupling with the local kinetic energy of the particles?

Question 1.16 Is the color temperature of the daytime sky that of the Sun? What about the color temperature of the full moon?

1.4.5 Optically thin and optically thick

An object is *optically thin* at a given wavelength if it is transparent to radiation at that wavelength, and *optically thick* if such radiation does not shine through. The observer “sees” all the way through an optically thin object, but not through an optically thick object.

An optically thick object has an (outer) “surface” (*photosphere*) which your gaze cannot penetrate — where the photons which you detected had their last interaction. For a solid object this is a sharply defined layer, but also for an optically thick ball of gas we can speak of a surface to indicate the layer from which the photons escape. In the Sun, for example, the layer from which the visible light escapes is but a few hundred km thick, while the solar diameter amounts to 1400 Mm. The escaping radiation contains information about this layer. If the photons were created in that last process, this is then *local* information, but in the case of scattering that is not necessarily the case — such as for optically thick fog around a lantern.

An optically thin object, on the contrary, doesn’t change the majority of the photons passing through. Only a few will undergo an interaction (destruction, scattering, or conversion) and only a few new photons will be added (by creation, scattering, or conversion). There is no surface; only the fraction contributed to the radiation field contains *nonlocalized* information about the whole object.

Question 1.17 Is the Sun optically thick to all radiation? Does the “surface” where the sunlight comes from lie equally deep at all wavelengths? What will that depend upon?

Question 1.18 The Sun is “optically” thin to neutrinos. Does it make sense to try to detect neutrinos coming from the Sun? How can you distinguish these from neutrinos from other stars?

1.4.6 Thermal and nonthermal

In the pair of processes that provide photon creation, thermal kinetic energy is transformed into photons via collisions. The photons created in this way are *thermal*. If the frequency of collisions is sufficiently large, coupling is achieved between the radiation field and particle velocities: so many quanta of radiation are created and destroyed in collisions that there is equipartition between radiation energy and kinetic energy. Such radiation is then *thermal* at the bb wavelength: in accord (in “equilibrium”) with the kinetic temperature at that point.

In bb scattering the new photon is provided by a similar photon that originated elsewhere; with much scattering or photon conversion the coupling between radiation and local kinetic temperature can be lost. Depending on the origin of the photons, the entire radiation field can be nonthermal.

A radiation field that is in equilibrium with the Maxwellian distribution of particle velocities at the place where it is generated follows the Planck function corresponding to the temperature at that spot (Chapter 4).

Question 1.19 With a lower collisional frequency, the chances for bb scattering are increased. Why?

Question 1.20 If cyclotron and synchrotron radiation, pair annihilation, or collisions with nonthermal particles contribute, then the radiation field is not thermal as a rule. Why?

Question 1.21 Is the atmosphere of the Earth in thermal equilibrium with the solar radiation? And with the light of the daytime sky?

1.5 Crucial questions

The paragraphs above define the astrophysical questions which should be asked for each object observed, for the continuum as well as for each spectral line under study:

- is the object seen in emission or absorption?
- is the object optically thick or thin?
- from what layer does the observed radiation arise?
- what is the excitation, deexcitation, ionization, association, velocities, magnetic fields etc. at that point?
- which processes supply the observed photons?
- were the observed photons created in their last interaction, or is scattering or photon conversion important?

– is the radiation thermal or nonthermal?

The answers to these questions determine the diagnostics that the EM spectrum provides for doing astrophysics. In the following chapters these tools are sharpened.

Question 1.22 In a well-known scientific laboratory experiment a spectroscope is used to look at a flame into which salt (NaCl) is scattered. The NaID lines appear as emission lines. Such a flame is optically thin in the NaID lines; make use of this in answering the above questions.

Question 1.23 Following this, the same experiment is extended by viewing the flame with salt in projection against a brighter continuum source. The two NaI resonance lines then appear as absorption lines against the brighter background continuum. What has changed?

Question 1.24 The solar spectrum in Figure 1.2 also shows the NaID lines in absorption. In many textbooks this is explained by analogy with the second experiment, but by the end of these lecture notes we will be able to establish the extent to which this analogy is correct (only partially so). Why are the sodium lines of the Sun so much more difficult to understand than those of the flame?

Question 1.25 In the quasar spectrum in Figure 1.3 the Ly α line appears not in absorption but in emission. Does that mean that the origin of this line is easier to understand?

Chapter 2

Radiation quantities

2.1 Introduction: from luminosity to intensity

How to describe the radiation from an astrophysical object? The goal is to define a quantity with maximum information content; a heuristic introduction brings us to the concept of intensity. The formal definitions follow in Section 2.2.

Let us begin by defining the

total luminosity L [erg s⁻¹],

as the total energy radiated by an object per unit time. This is a number without much diagnostic value, except for its size (energy budget) and time dependence (variability, evolution).

A first refinement is to disperse the spectrum:

monochromatic luminosity L_ν [erg s⁻¹ Hz⁻¹]

is the energy emitted by the object per unit time and per unit spectral bandwidth at the frequency ν , with $L \equiv \int_0^\infty L_\nu d\nu$.

However, one cannot measure energy all around a faraway object. At Earth, one only detects:

irradiance \mathcal{R}_ν [erg cm⁻² s⁻¹ Hz⁻¹],

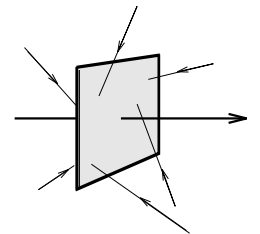
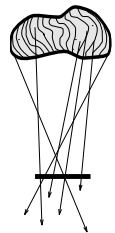
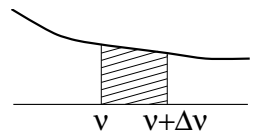
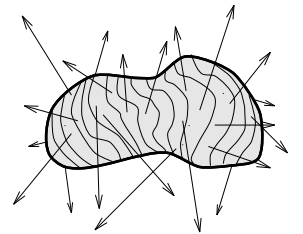
defined as the total energy of the photons from the object which pass per unit time and per unit spectral bandwidth at the frequency ν through a unit area at Earth, oriented perpendicular to the line of sight to the object.

Inward extrapolation to the surface of the object or to its interior provides a generalization:

flux \mathcal{F}_ν [erg cm⁻² s⁻¹ Hz⁻¹],

the total energy of the photons from or in the object that pass per unit time and per unit spectral bandwidth at the frequency ν through a unit area placed at a specified place and oriented at right angles to a specified direction. The point of measurement and the direction may be chosen freely. Also, photons may come from all sides; the energy of the photons coming from behind (against the specified direction) are counted as negative. The flux \mathcal{F}_ν therefore measures the *net* flow of energy through the unit area in the given direction. \mathcal{F}_ν is the *monochromatic flux*; the *total flux* \mathcal{F} is given by: $\mathcal{F} \equiv \int_0^\infty \mathcal{F}_\nu d\nu$.

In going from luminosity to flux, we have defined measurement of photons that arrive at or pass through a given location. It is more informative to specify the



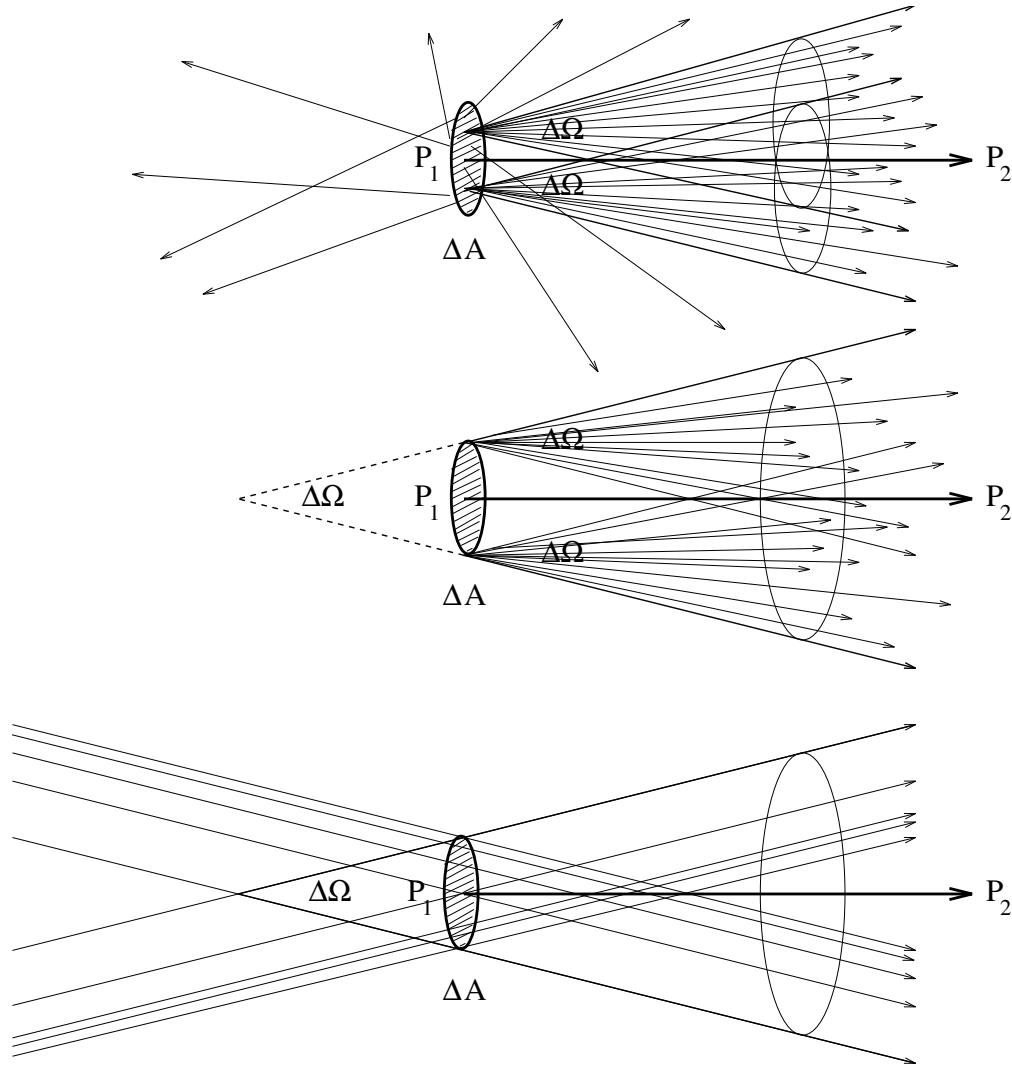


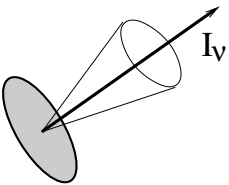
Figure 2.1: Cones (“pencils”) of radiation. Photons are emitted by a circular surface with area ΔA around P_1 in all directions. The photons that leave a particular point of ΔA with directions within solid angle $\Delta\Omega$ around direction P_1P_2 constitute a cone of radiation emerging from that point (top). The cones from all such points on ΔA merge into a larger, truncated cone with opening angle $\Delta\Omega$ (middle). Likewise for beams of parallel rays from elsewhere that pass through ΔA with the same opening angle $\Delta\Omega$ (bottom). The angle is the same in the propagation direction towards the right and in the line-of-sight direction towards the left. The amount of energy in the cone is proportional to ΔA and $\Delta\Omega$ as well as to the duration Δt and the frequency bandwidth $\Delta\nu$ of the measurement, if ΔA , $\Delta\Omega$, Δt and $\Delta\nu$ are all small enough that the radiation field is homogeneous across these intervals. After Novotny (1973).

propagation direction of the photons also. The best is to specify where photons come from and where they go to. That is achieved with:

intensity I_ν [$\text{erg cm}^{-2} \text{ s}^{-1} \text{ Hz}^{-1} \text{ ster}^{-1}$],

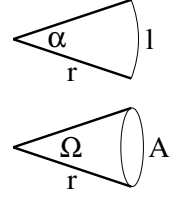
which is the flow of energy at a specific location in a specific direction, per unit time, per unit bandwidth, per unit solid angle around that direction, and per unit area oriented perpendicular to that direction at that location.

The unit “ster” stands for steradian. It is the unit of solid angle, the three-



dimensional equivalent of angular measure in a plane. Just as the angle $\alpha = l/r$ rad subtends a segment l of circular arc, a spherical surface segment A is subtended by the solid angle $\Omega = A/r^2$ ster.

Intensity specifies the flow of energy along a beam of radiation both at departure and at arrival. It describes the radiation along a “ray”, connecting the departure and arrival points. A single, infinitely thin ray doesn’t contain energy, so one speaks of a *bundle* or *beam* of rays, a “*pencil of radiation*”, with angular spreading over a cone $\Delta\Omega$. The rays travel towards us in the direction of propagation; their spreading is also measured when looking backwards along the line of sight. See Figure 2.1.



A cone of rays spreads, but intensity is measured per steradian, per unit of spreading. The spreading of a beam therefore does not affect its intensity, at least in vacuum where there is no matter present to absorb or emit photons. This property makes intensity the macroscopic quantity of choice to formulate radiative transfer with, i.e., to describe processes by which matter and photons interact. Using intensity ensures that *only* such interactions affect the measure of radiation, not the distance over which it has traveled.

The conservation of intensity along a beam is illustrated in Figure 2.2. There are two arbitrary surfaces at separation r , with area ΔA_1 at point P_1 and area ΔA_2 at P_2 . Photons of all frequencies travel through each surface in all directions. We seek to describe only those that pass through *both* surfaces, first through ΔA_1 and then through ΔA_2 . These photons represent on the one hand the flow of energy which “escapes” from ΔA_1 towards ΔA_2 , and on the other hand the flow of energy which “arrives” at ΔA_2 from ΔA_1 .

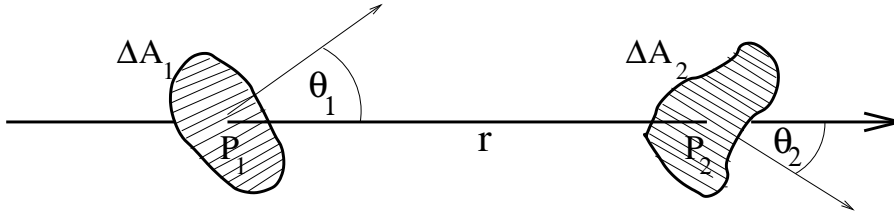


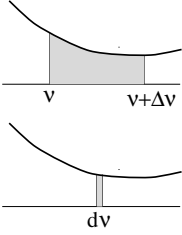
Figure 2.2: *Conservation of intensity along a beam. The intensity of a beam that passes along both P_1 and P_2 is the same at both points because intensity is measured per steradian. The projected detection area at one point represents the solid angle for the other, so that there is full symmetry between P_1 and P_2 .*

How large is this energy flow? Consider it first at the departure point P_1 , taking ΔA_1 as the measurement surface. Empirical experience and physical insight teach that the measured amount of energy is proportional to the measurement duration Δt and to the measurement bandwidth $\Delta\nu$; the larger each, the more photons are taken into account. The measured energy is also proportional to the cross-section posed by the measurement surface ΔA_1 . Since of all possible directions through ΔA_1 only those count that pass ΔA_2 as well, the energy flow is proportional to the projected surface $\Delta A_1 \cos \theta_1$, with θ_1 the angle between the normal to ΔA_1 and the direction $P_1 P_2$. The energy flow is also proportional to the solid angle $\Delta\Omega_1$ that is subtended by area ΔA_2 as seen from P_1 , since it defines the cone of directions from P_1 that pass through ΔA_2 . It is given by $\Delta\Omega_1 = \Delta A_2 \cos \theta_2 / r^2$ ster. There are no other proportionalities or dependencies (assuming vacuum). The energy flow ΔE_ν which departs from ΔA_1 towards ΔA_2 thus has:

$$\Delta E_\nu \propto \Delta t \Delta\nu \Delta A_1 \cos \theta_1 \Delta\Omega_1.$$

The spreading $\Delta\Omega_1$ must be sufficiently small that proportionality indeed applies, i.e., that the bundle is homogeneous across the solid angle $\Delta\Omega_1$. The same holds for the

other proportionalities; ΔA_1 , Δt and $\Delta\nu$ should be small enough that the radiation field can be considered homogeneous across each sampling interval. To ensure such homogeneity, we take the limit $\Delta \rightarrow 0$. We now *define* intensity by:



$$dE_\nu(P_1) \equiv I_1 dt d\nu dA_1 \cos \theta_1 d\Omega_1 = I_1 dt d\nu dA_1 \cos \theta_1 \frac{dA_2 \cos \theta_2}{r^2},$$

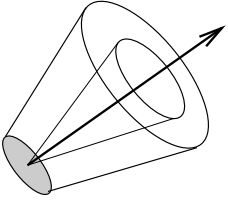
with the intensity I_1 the proportionality constant that holds at P_1 .

Now describe the same flow as it arrives at P_2 . It is again proportional to the cross-section of the sampling surface, now given by $\Delta A_2 \cos \theta_2$, and also to the solid angle subtended by A_1 at the distance r from P_2 . In the limit $\Delta \rightarrow 0$ the energy measured at P_2 is:

$$dE_\nu(P_2) \equiv I_2 dt d\nu dA_2 \cos \theta_2 d\Omega_2 = I_2 dt d\nu dA_2 \cos \theta_2 \frac{dA_1 \cos \theta_1}{r^2},$$

with I_2 defined as the proportionality constant that is valid at P_2 . These two expressions for locations P_1 and P_2 measure the same energy flow dE_ν , namely all photons that pass through ΔA_2 after passing through ΔA_1 . Equating the two expressions yields the result that $I_1 = I_2$. Thus, the proportionality constant does not change from P_1 to P_2 ; *intensity is constant along a ray*. It therefore suffices to define intensity at just one location, as

$$I_\nu \equiv \frac{dE_\nu}{dt d\nu dA d\Omega}$$



at that location, with I_ν the intensity of the beam which transports a quantity of energy dE_ν in a specific direction through a surface dA placed perpendicular to that direction, with the spreading of the beam confined to a solid angle $d\Omega$ around that direction, during a time dt at a specific moment, and limited to a frequency band $d\nu$ at a specific frequency ν .

Question 2.1 What are the units of dE_ν ?

Question 2.2 Does the intensity in a divergent beam diminish with the square of the distance? Or does it depend on the opening angle $\Delta\Omega$ of the beam?

Question 2.3 Monochromatic quantities such as L_ν , \mathcal{F}_ν and I_ν are expressed per unit bandwidth. The energy flow that is measured across a frequency band between ν and $\nu + \Delta\nu$ is given by $L_\nu \Delta\nu$, $\mathcal{F}_\nu \Delta\nu$ and $I_\nu \Delta\nu$, respectively. One may also use L_λ , for example with \AA as the unit of bandwidth in wavelength, or L_σ and L_ω for bandwidths expressed in wavenumber and angular frequency. The following questions address the conversions:

- show that $I_\nu d\nu = I_\lambda d\lambda$ if $|d\nu| = (c/\lambda^2) |d\lambda|$;
- show that $d\nu/\nu = -d\lambda/\lambda$;
- are I_ν and I_λ equal for a given beam?
- does the minus sign in $d\nu/\nu = -d\lambda/\lambda$ imply that I_ν or I_λ is negative?
- why is it useful to plot λI_λ or νI_ν in graphs instead of I_λ or I_ν ?
- show that $\int_0^\infty I_\nu d\nu = \int_0^\infty I_\lambda d\lambda$;
- what is the conversion factor between I_ν and I_σ ? And between I_ν and I_ω ?

Question 2.4 One might use the following units in place of $[\text{erg cm}^{-2} \text{s}^{-1} \text{Hz}^{-1} \text{ster}^{-1}]$ for intensity:

- $[\text{erg cm}^{-3} \text{s}^{-1} \text{ster}^{-1}]$;
- $[\text{erg cm}^{-2} \text{ster}^{-1}]$;
- $[\text{erg cm}^{-1} \text{s}^{-1} \text{ster}^{-1}]$,

by replacing Hz^{-1} with other bandwidth units. What are the latter for these three cases?

Question 2.5 Show that:

- an isotropic radiator produces at a distance D : $\mathcal{R}_\nu = L_\nu/(4\pi D^2)$;
- a spherical radiator has: $\int_A \mathcal{F}_\nu dA = L_\nu$;
- an isotropic radiation field has: $\mathcal{F}_\nu = 0$.

Question 2.6 Show that:

- $d\Omega = \sin\theta d\theta d\varphi$ in polar coordinates;
- a quarter hemisphere measures $\pi/2$ ster;
- a whole sphere measures 4π ster.

Question 2.7 The exposure meter in a camera is an intensity device which operates better if it accepts a smaller solid angle, as in a single-lens reflex camera where it meters through the lens, and optimally as a “spot meter” measuring only a small part of the image.

Does the exposure time given by such a spot meter vary between wide-angle close-up pictures and pictures of the same object taken from afar with a telephoto lens?

2.2 Intensity and related quantities

The heuristic description above demonstrates that intensity is the quantity best suited to describe radiation. The following are definitions of quantities related to intensity.

2.2.1 Intensity

The *intensity* I_ν is defined as the proportionality coefficient I_ν in:

$$\begin{aligned} dE_\nu &\equiv I_\nu(\vec{r}, \vec{l}, t) (\vec{l} \cdot \vec{n}) dA dt d\nu d\Omega \\ &= I_\nu(x, y, z, \theta, \varphi, t) \cos\theta dA dt d\nu d\Omega, \end{aligned} \quad (2.1)$$

where dE_ν is the amount of energy transported through the surface dA , at the location \vec{r} and with \vec{n} the normal to dA , between times t and $t + dt$, in the frequency band between ν and $\nu + d\nu$, and in the solid angle $d\Omega$ about the direction \vec{l} . The polar coordinate angles θ and φ are defined in Figure 2.3.

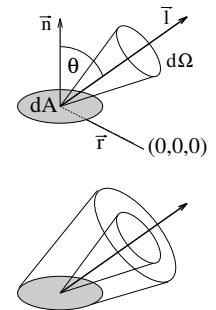
Dimension I_ν : [$\text{erg s}^{-1} \text{cm}^{-2} \text{Hz}^{-1} \text{ster}^{-1}$] or [$\text{W m}^{-2} \text{Hz}^{-1} \text{ster}^{-1}$].

This is the *monochromatic* intensity; the *total* intensity is $I \equiv \int_0^\infty I_\nu d\nu$.

The intensity depends on place, direction, time and frequency, and describes the radiation field completely unless it is polarized (§ 2.2.5). This definition holds both for the intensity emitted by a surface and for the intensity along a bundle of rays.

I_ν is often called *specific intensity* to emphasize that it is measured per steradian. Other names are *brightness* and *surface brightness*. In everyday language, “intensity” often implies flux or irradiance—even in astronomy the distinction is not always clear. With the above definition, intensity does not vary along rays in vacuum. It changes only if there is extinction (loss of photons out of the beam through absorption, scattering, or photon conversion) or emission (addition of photons to the beam from photon creation, scattering, or photon conversion) along the way, or when the index of refraction varies. The intensity differs within a sheet of glass from the incident value, but resumes the latter upon exit. The intensity in the image plane of an absorption-free telescope is as large as it is near the object.

Question 2.8 Show that the intensity along a beam from an object does not change when the object is imaged by a lens.



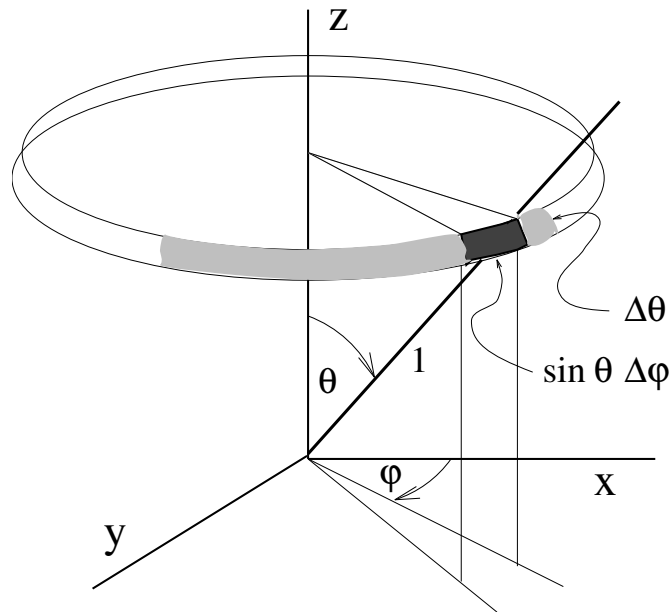


Figure 2.3: *Solid angle in polar coordinates. The annulus is part of the sphere with radius unity around the given location. The dark area defines solid angle $\Delta\Omega = \sin\theta \Delta\theta \Delta\varphi$ from the given location.*

- Question 2.9* A lamp radiates intensity I_0 isotropically. If it is placed in the focus of a lens, what is the intensity of the resulting collimated (parallel) beam?
- Question 2.10* Does an absorption-free prism change the intensity of the light which it disperses?
- Question 2.11* Use Snell's law $n_1 \sin\theta_1 = n_2 \sin\theta_2$ to demonstrate that the quantity I_ν/n^2 is conserved when a beam with intensity I_ν passes across the border between media 1 and 2 with indices of refraction n_1 and n_2 .
Why is it that astronomers tend to set $n = 1$ for their objects?
- Question 2.12* The intensity of the solar radiation has the same value near Earth as near Saturn, although Saturn is ten times further away. Does Saturn receive the same amount of energy as the Earth?
- Question 2.13* What exposure time do you need to take a picture of the full moon? How does it compare to the exposure time which an astronaut requires on the moon itself? And for a kosmonaut on Mercury?
- Question 2.14* Design an intensity meter for an amateur astronomer. Which constraints must be satisfied to measure the intensity of:
- the surface of the moon;
 - a sunspot;
 - Jupiter's red spot;
 - the Milky Way?
- Describe the appropriate measurement procedures.
- Question 2.15* Can the amateur astronomer in Problem 2.14 measure the intensity of Sirius A? Can a radio astronomer measure the intensity of a quasar?
- Question 2.16* The spatial resolution of the Hubble Space Telescope was expected to be much better than that of ground-based telescopes of similar size, because there is no atmospheric turbulence in space to spoil images (the so-called

seeing). Such an improvement in image sharpness results in considerable gain in sensitivity for stars, but not for extended objects such as gaseous nebulae. Why? Is a (good) space telescope a good choice to image galaxies? And quasars?

2.2.2 Mean intensity

The *mean intensity* J_ν is defined by:

$$J_\nu(\vec{r}, t) \equiv \frac{1}{4\pi} \int I_\nu d\Omega = \frac{1}{4\pi} \int_0^{2\pi} \int_0^\pi I_\nu \sin \theta d\theta d\varphi. \quad (2.2)$$

Dimension J_ν : [erg cm⁻² s⁻¹ Hz⁻¹ ster⁻¹], just as for I_ν .

The *total* mean intensity is given by:

$$J \equiv \frac{1}{4\pi} \int I d\Omega = \frac{1}{4\pi} \iint I_\nu d\nu d\Omega = \int_0^\infty J_\nu d\nu,$$

in which the “mean” means averaging $I_\nu(\theta, \varphi)$ over all directions, with $\Delta\Omega = \sin \theta d\theta d\varphi$ in polar coordinates (Figure 2.3) and $\int d\Omega = 4\pi$. An isotropic radiation field has $J_\nu = I_\nu$ and $J = I$; otherwise, J_ν and J indicate how much intensity is locally available for processes which are not sensitive to direction, such as radiative excitation and radiative ionization.

I will often discuss radiation from optically thick objects taking the convention that the z -axis is vertical, perpendicular to a horizontal surface (x, y), on the premise that thick objects are gravitationally bound. Then, z is equivalent to geometrical height h ; I will often use h to specify the direction away from the object rather than z . The zero point of the z and h scales is arbitrary; it is usually placed at “the surface”—which for gaseous objects needs to be defined.

Axial symmetry is often assumed for thick objects by permitting spatial variations to occur only along vertically, not in horizontal directions. The (x, y) planes are then homogeneous “slabs” or “plane-parallel layers”; they often represent a local approximation to the curved shells of spherical objects such as stars. The radiation field, whatever its origin, is then symmetrical around the z -axis ($\theta \equiv 0$): $I_\nu = I_\nu(z, \theta)$. Then

$$d\Omega = 2\pi \sin \theta d\theta = -2\pi d\mu,$$

where

$$\mu \equiv \cos \theta, \quad (2.3)$$

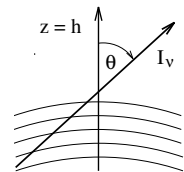
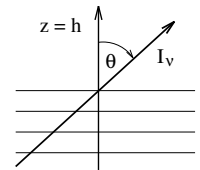
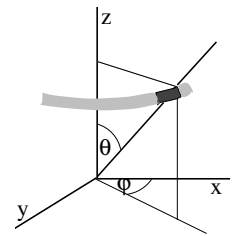
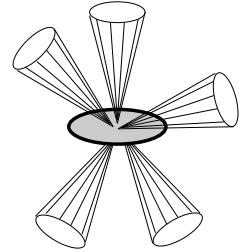
and so:

$$J_\nu(z) = \frac{1}{4\pi} \int_0^\pi I_\nu(z, \theta) 2\pi \sin \theta d\theta = \frac{1}{2} \int_{-1}^{+1} I_\nu(z, \mu) d\mu. \quad (2.4)$$

Question 2.17 A “Lambert surface” radiates intensity I_0 into all directions on one side of it. Is this a case of axial symmetry? What is J in a point of this surface? And what is J at a point a distance D from the surface if the latter is infinitely extended?

Question 2.18 How does the mean intensity of the solar radiation near Earth compare to the intensity? (The radius of the Sun is $R_\odot = 0.00465$ AU; approximate its surface by a Lambert one.)

Question 2.19 How do the intensity I_\odot and the mean intensity J_\odot of the sunlight near Saturn compare with those at Earth?



2.2.3 Flux

The *monochromatic flux* \mathcal{F}_ν is defined by:

$$\mathcal{F}_\nu(\vec{r}, \vec{n}, t) \equiv \int I_\nu(\vec{l} \cdot \vec{n}) d\Omega = \int I_\nu \cos \theta d\Omega = \int_0^{2\pi} \int_0^\pi I_\nu \cos \theta \sin \theta d\theta d\varphi. \quad (2.5)$$

Dimension \mathcal{F}_ν : [erg s⁻¹ cm⁻² Hz⁻¹] or [W m⁻² Hz⁻¹].

The flux \mathcal{F}_ν is the flow of energy per second through a surface of one cm² located at \vec{r} with normal \vec{n} . It is the *net* flow of energy through this surface because the perspective factor $\cos \theta$ counts the reversed contributions negatively, i.e., those along directions $\pi/2 < \theta \leq \pi$ with components counter to \vec{n} . If \vec{n} is upwards, we may write \mathcal{F}_ν as the net sum of upward and downward parts:

$$\begin{aligned} \mathcal{F}_\nu &= \int_0^{2\pi} \int_0^{\pi/2} I_\nu \cos \theta \sin \theta d\theta d\varphi + \int_0^{2\pi} \int_{\pi/2}^\pi I_\nu \cos \theta \sin \theta d\theta d\varphi \\ &= \int_0^{2\pi} \int_0^{\pi/2} I_\nu \cos \theta \sin \theta d\theta d\varphi - \int_0^{2\pi} \int_\pi^{\pi/2} I_\nu \cos \theta \sin \theta d\theta d\varphi \\ &= \int_0^{2\pi} \int_0^{\pi/2} I_\nu \cos \theta \sin \theta d\theta d\varphi - \int_0^{2\pi} \int_0^{\pi/2} I_\nu \cos(\pi - \theta) \sin(\pi - \theta) d(\pi - \theta) d\varphi \\ &\equiv \mathcal{F}_\nu^+ - \mathcal{F}_\nu^-, \end{aligned} \quad (2.6)$$

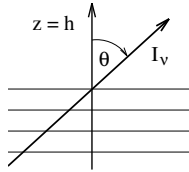
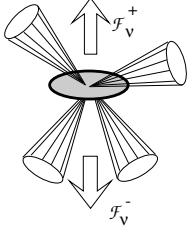
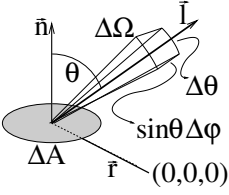
with the upward flux \mathcal{F}_ν^+ and the downward flux \mathcal{F}_ν^- both positive. For an isotropic radiation field $\mathcal{F}_\nu^+ = \mathcal{F}_\nu^- = \pi I_\nu$ and $\mathcal{F}_\nu = 0$. A Lambert radiator has $\mathcal{F}_\nu = \mathcal{F}_\nu^+ = \pi I_\nu$ and $\mathcal{F}_\nu^- = 0$ at its surface. For axial symmetry only the z -component of the flux is non-zero because the radiation field is then isotropic within (x, y) planes. In that case:

$$\begin{aligned} \mathcal{F}_\nu(z) &= 2\pi \int_0^\pi I_\nu \cos \theta \sin \theta d\theta \\ &= 2\pi \int_{-1}^{+1} \mu I_\nu d\mu \\ &= 2\pi \int_0^1 \mu I_\nu d\mu - 2\pi \int_0^{-1} \mu I_\nu d\mu, \end{aligned}$$

thus

$$\begin{aligned} \mathcal{F}_\nu^+(z) &= 2\pi \int_0^1 \mu I_\nu d\mu \\ \mathcal{F}_\nu^-(z) &= 2\pi \int_0^{-1} \mu I_\nu d\mu. \end{aligned} \quad (2.7)$$

Flux is a loose term. One should define it as a vector (e.g., Mihalas 1978 p. 9), but for simple geometries the direction of the vector is usually obvious—for example, outward in or from a star. Since we define flux per cm², “flux density” would be a better term; physicists employ it indeed, and use “flux” for $F_\nu = \int \mathcal{F}_\nu dA$. Flux is often used in place of irradiance for the energy that is detected from an object at the telescope—radio astronomers use “milli-flux units”, atmospheric physicists “actinic flux”. Flux is also often used instead of luminosity as measure of the energy which escapes from an object; “surface flux” then specifies what is defined as flux here, per cm². Often, the location and the orientation of the unit area are not explicitly specified. When axial symmetry applies, flux usually implies $\mathcal{F}_\nu(z)$ inside the object or $\mathcal{F}_\nu^+(z = 0)$ at its surface. Frequently, πF is written in place of \mathcal{F} (so that a Lambert radiator has $F = F^+ = I_0$), with F called “astrophysical flux”. However, sometimes \mathcal{F} is written as F without π . (Rybicki and Lightman 1979 do so; this is the only notation difference between their book and this one.)



- Question 2.20* How is the flux of the solar radiation near Earth related to the local intensity, mean intensity and irradiance?
- Question 2.21* How does the solar flux near Earth compare to that near Saturn?
- Question 2.22* A Lambert disk with radius R emits intensity $I_\nu(\theta, \varphi) = I_0$. Express J_ν and \mathcal{F}_ν in I_0 for a point P at a distance D from the disk on its axis. What are the results for $D \ll R$ and $D \gg R$?
- Question 2.23* Express the surface flux of a spherical star in the mean intensity \bar{I}_ν that is received from the stellar surface by a distant observer.
- Question 2.24* The segment of solar spectrum with the Na I D lines in Figure ?? is copied from the atlas of Kurucz *et al.* (1984). This is an atlas of the solar irradiance spectrum. Why is it called a “flux” atlas? How may one measure the irradiance spectrum from the Sun? Why should one want to?
- Question 2.25* There is a tight correlation between the excursions of the apparent solar limb due to the turbulence in the earth’s atmosphere and the fluctuations in the solar irradiance. Why?
- Question 2.26* Are stellar magnitudes a measure of intensity, mean intensity, flux, or luminosity? And absolute magnitudes and bolometric corrections?

2.2.4 Radiation density and radiation pressure

The *radiative energy density* u_ν is:

$$u_\nu = \frac{1}{c} \int I_\nu d\Omega. \quad (2.8)$$

Dimension u_ν : [erg cm⁻³ Hz⁻¹] or [J m⁻³ Hz⁻¹].

Isotropic radiation has $u_\nu = (4\pi/c)I_\nu$, filling a unit sphere in $1/c$ seconds.

The *radiation pressure* p_ν is:

$$p_\nu = \frac{1}{c} \int I_\nu \cos^2 \theta d\Omega. \quad (2.9)$$

Dimension p_ν : [dyne cm⁻² Hz⁻¹] or [N m⁻² Hz⁻¹].

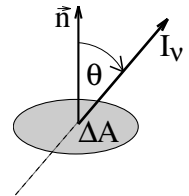
Radiation pressure is analogous to gas pressure, being the pressure of the photon gas. It is a scalar for isotropic radiation fields; a force is exerted only along a photon pressure gradient. Note that the term radiation pressure is often also used for the mechanical force on an object when it absorbs photons from a directional beam.

- Question 2.27* Derive equation (2.8) by first considering the energy content of the volume that is passed through by a single beam with intensity I_ν during a time dt , then integrating the result over a small volume ΔV which is pervaded by beams in different directions.

Question 2.28 Derive equation (2.9).

Question 2.29 Show that:

$$u_\nu = \frac{4\pi}{c} J_\nu \quad \text{and} \quad u = \frac{4\pi}{c} \int_0^\infty J_\nu d\nu.$$



Question 2.30 Demonstrate that isotropic radiation has $p_\nu = u_\nu/3$.

Question 2.31 Consider isotropic radiation within a reflecting enclosure. Show that the radiation pressure on the walls is given by:

$$p_\nu = \frac{2}{c} \int I_\nu \cos^2 \theta \, d\Omega.$$

Why is this result the same as eq. (2.9)?

2.2.5 Stokes parameters

When the radiation in a beam is fully or partially polarized, three more quantities are required to describe it completely in addition to its intensity. The wave representation of electromagnetic radiation provides the appropriate description in this case. Two parameters are needed to describe the time-dependent orientation of the electric wave vector \vec{E} in the vibration plane perpendicular to the direction of propagation; the orientation of the magnetic vector \vec{B} then follows from these because $|\vec{E}| = |\vec{B}|$ and $\vec{E} \perp \vec{B}$. The third parameter specifies the degree of polarization. In practice, this information is split in different fashion between the three *Stokes parameters* which furnish a description in observable quantities.

Decompose the harmonic vibration of the electric field vector \vec{E}_{rad} of a monochromatic light wave which propagates along the z -axis into its x and y components (Figure 2.4):

$$\begin{aligned} E_x &= A_x \cos(\omega t - \phi_x) \\ E_y &= A_y \cos(\omega t - \phi_y), \end{aligned} \quad (2.10)$$

where A_x and A_y are the amplitude maxima and ϕ_x and ϕ_y the phase offsets; $\omega = 2\pi\nu$ is the circular frequency. For a fully polarized wave, the four Stokes parameters are defined by:

$$\begin{aligned} I_\nu &\equiv A_x^2 + A_y^2 \\ Q_\nu &\equiv A_x^2 - A_y^2 \\ U_\nu &\equiv 2A_x A_y \cos(\phi_x - \phi_y) \\ V_\nu &\equiv 2A_x A_y \sin(\phi_x - \phi_y), \end{aligned} \quad (2.11)$$

with $I_\nu^2 = Q_\nu^2 + U_\nu^2 + V_\nu^2$. “Fully polarized” means that the vector \vec{E} is well-behaved, its tip harmonically travelling along a line, ellipse or circle in the (x, y) plane. In these cases the wave is said to be linearly polarized, elliptically polarized, or circularly polarized. Depending on whether the vector tip travels clockwise or counterclockwise, the elliptical and circular polarizations are called left-handed or right-handed. Usually right-handed implies clockwise as seen by the observer towards whom the beam travels, looking back along the line of sight, but sometimes the reverse definition is used. (Polarization theory is fraught with sign convention problems—see Rees 1987).

Radiation fields that one actually detects and measures tend to consist of many superimposed polarization states. An unpolarized contribution may also be present, and the polarization will generally vary with time. If the temporal changes are slow, the Stokes parameters for actual radiation are:

$$I_\nu = I_\nu^{\text{unpol}} + \langle A_x^2 + A_y^2 \rangle$$

$$\begin{aligned}
Q_\nu &= \langle A_x^2 - A_y^2 \rangle \\
U_\nu &= \langle 2A_x A_y \cos(\phi_x - \phi_y) \rangle \\
V_\nu &= \langle 2A_x A_y \sin(\phi_x - \phi_y) \rangle,
\end{aligned} \tag{2.12}$$

where Stokes I is the sum of the unpolarized and polarized contributions and with the time-independent expressions on the right hand sides in eqs. (2.11) replaced by temporal averages.

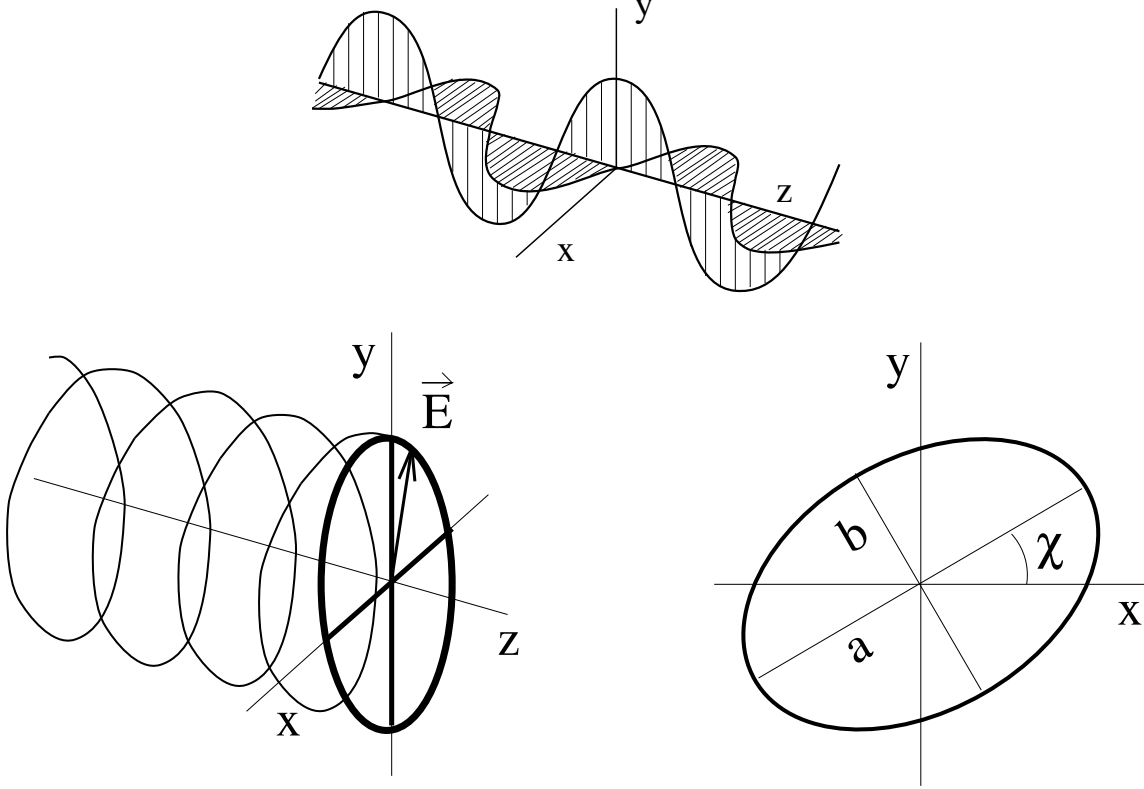


Figure 2.4: *Elliptical polarization. Top: decomposition of the electric wave vector \vec{E} into two sinusoidal components E_x and E_y . The two amplitudes A_x and A_y are unequal; there is a 90° phase lag $\phi_x - \phi_y$ between them. In that case, the tip of \vec{E} describes an ellipse in the (x, y) plane of which the axes are aligned with x and y (bottom left). For arbitrary amplitudes and phase lag, the tip of \vec{E} travels clockwise or counterclockwise along an (x, y) ellipse of which the axes are offset over an angle χ (bottom right).*

Figure 2.4 shows \vec{E} -tip orbits in the (x, y) plane. The angle χ measures the rotation of the ellipse axes from the x and y axes. The ratio of the major semi-axis a and the minor semi-axis b defines an angle β with $\tan \beta = b/a$. With these quantities the Stokes parameters for fully polarized radiation become:

$$\begin{aligned}
I_\nu &= A_x^2 + A_y^2 \equiv A^2 \\
Q_\nu &= A^2 \cos 2\beta \cos 2\chi \\
U_\nu &= A^2 \cos 2\beta \sin 2\chi \\
V_\nu &= A^2 \sin 2\beta.
\end{aligned} \tag{2.13}$$

These relations help to interpret the Stokes parameters in observational terms. In

fact, they were originally defined as such, namely as:

$$\begin{aligned}
 I_\nu &\equiv \text{total intensity} \\
 Q_\nu &\equiv I_0^{\text{linear}} - I_{90}^{\text{linear}} \\
 U_\nu &\equiv I_{+45}^{\text{linear}} - I_{-45}^{\text{linear}} \\
 V_\nu &\equiv I_{\text{right}}^{\text{circular}} - I_{\text{left}}^{\text{circular}}.
 \end{aligned} \tag{2.14}$$

Thus, Stokes Q and U describe intensity differences between measurements with crossed linear polarizers, while Stokes V specifies the difference between the amounts of right-handed and left-handed circularly polarized radiation in a beam.

These four parameters are often combined into the *Stokes vector* for use in matrix transformations (“Mueller calculus”) which quantitatively describe the effects of optical devices such as lenses, beam splitters, polarizers, retarders etc. on a beam of light. For more on polarization and polarized radiative transfer, see e.g., pp. 24–35 of Chandrasekhar (1950), Robson (1974), § 2.4 of Rybicki and Lightman (1979), Chapt. 4 of Kraus (1986), Rees (1987). Kliger *et al.* (1990), Chapt. 12 of Shu (1992a).

Question 2.32 Derive eqs. (2.13) from eqs. (2.11).

Question 2.33 How do eqs. (2.14) relate to eqs. (2.11) and (2.13)?

Chapter 3

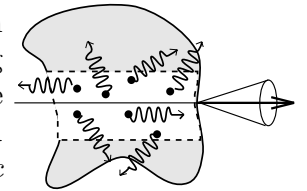
Transport equation

3.1 Introduction: emission and extinction

The intensity along a beam is constant unless local emission or extinction processes add photons to it or remove photons from it. If such processes occur (which requires the presence of matter), the local intensity increase and the local intensity decrease are defined with empirical proportionality constants, similarly to the definition of intensity. In this chapter these coefficients are defined and combined into the transport equation of radiative transfer. This equation is studied without detailing the actual processes.

3.2 Emission coefficient

Experience and physical insight teach that the local addition of photons to a beam of radiation is proportional, in the $d = \Delta \rightarrow 0$ limit, to the number of emitting particles, and to the time interval dt , the bandwidth interval $d\nu$ and the solid angle $d\Omega$ over which the beam is measured. The proportionality coefficient can be defined per particle or for all particles in a gram or cm^3 . In this book the *monochromatic emission coefficient* j_ν is defined per cm^3 , as the constant in:



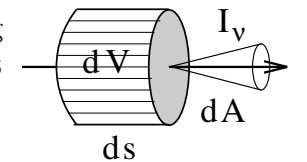
$$dE_\nu \equiv j_\nu dV dt d\nu d\Omega \quad (3.1)$$

with dE_ν the energy that is added in the form of photons to a beam with solid angle $d\Omega$, over the bandwidth $d\nu$, during a time dt , within the volume dV .

Dimension j_ν : $[\text{erg cm}^{-3} \text{ s}^{-1} \text{ Hz}^{-1} \text{ ster}^{-1}]$.

The coefficient j_ν depends on location, direction, time and frequency, just as the intensity I_ν .

A beam with cross-section dA traverses a volume $dV = dA ds$ while propagating over a path ds . Combination of definitions (3.1) and (2.1) shows that the amount of intensity added by local photon emission to a beam with intensity I_ν is:



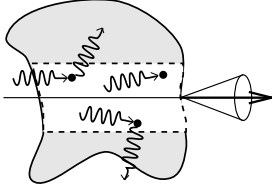
$$dI_\nu(s) = j_\nu(s) ds. \quad (3.2)$$

Question 3.1 A thin, homogeneous slab of thickness Δs is irradiated from one side with a beam of intensity $I_\nu(s)$. What is the emergent intensity $I_\nu(s + \Delta s)$ on the other side if the emission coefficient in the slab is j_ν and if there is no extinction? Is the result also valid for a thick slab, with large Δs ?

Question 3.2 Why is the emission coefficient defined in terms of intensity and not in terms of flux?

Question 3.3 How should one split the emission coefficient between two types of particles that contribute photon emission at the same frequency?

3.3 Extinction coefficient



Experience and physical insight also teach that the number of photons that is removed from a beam by extinction processes is proportional to both the supply of photons and to the number of extinguishing particles, again in the $d = \Delta \rightarrow 0$ limit. The proportionality constant is called the *extinction coefficient*. It may be defined per particle, per gram, or per cm^3 ; all three are specified here for completeness.

First the definition per particle. The monochromatic extinction coefficient (effective cross-section) σ_ν per particle, with dimension $[\text{cm}^2]$, is:

$$dI_\nu \equiv -\sigma_\nu n I_\nu ds, \quad (3.3)$$

with n the density of the absorbing particles ($[\text{cm}^{-3}]$).

The extinction per unit path length is:

$$dI_\nu \equiv -\alpha_\nu I_\nu ds \quad (3.4)$$

with α_ν the monochromatic linear extinction coefficient with dimension $[\text{cm}^{-1}]$. This measure is identical to measurement per unit volume:

$$dI_\nu = -\alpha_\nu I_\nu ds$$

with α_ν the monochromatic volume extinction coefficient (cross-section per unit volume) with dimension $[\text{cm}^2 \text{cm}^{-3}] = [\text{cm}^{-1}]$.

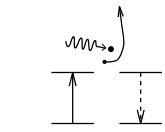
Finally, the extinction per unit mass is:

$$dI_\nu \equiv -\kappa_\nu \rho I_\nu ds \quad (3.5)$$

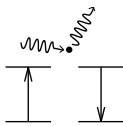
with κ_ν the “opacity”, the monochromatic mass extinction coefficient (cross-section per unit mass) with dimension $[\text{cm}^2 \text{g}^{-1}]$ and ρ the mass density ($[\text{g cm}^{-3}]$). The last definition is the one used most frequently in astronomy, but in this book I follow the notation of Rybicki and Lightman (1979) and use extinction per cm (definition 3.4).

The term “extinction” requires comment. Often “absorption” is used for what is called extinction here. When using “extinction”, no distinction is made between the removal of photons from a beam through photon destruction and the removal of photons from a beam through scattering and photon conversion. In the last processes, photons exist also after the extinction occurred. They are not destroyed, but they have a different direction and/or a different frequency than before, and they therefore count no longer for the beam under consideration. Extinction is here used to imply the sum of all processes by which photons are removed from the beam, including redirection and wavelength shift; absorption implies destruction of photons. Other authors use absorption for the total, and then use “true absorption” for photon destruction.

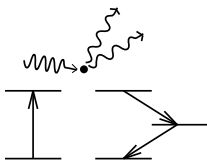
Question 3.4 Show that $\alpha_\nu = \sigma_\nu n = \kappa_\nu \rho$. Why is κ_ν preferred in astronomy and σ_ν in physics?



destruction



scattering



conversion

- Question 3.5* A thin homogeneous slab of thickness Δs is illuminated on one side by a beam with intensity $I_\nu(s)$. What is the emergent intensity $I_\nu(s+\Delta s)$ on the other side if the extinction coefficient is α_ν and if there is no local emission within the slab? Is the result valid for a thick homogeneous slab, with large Δs ? Why does one define j_ν and α_ν in the limit $d = \Delta \rightarrow 0$?
- Question 3.6* Show that $\alpha_\nu ds < 1$. When is $\alpha_\nu ds = 0$? Does $\alpha_\nu ds < 0$ imply local emission that should be added to $j_\nu ds$?
- Question 3.7* Does the index ν in α_ν have the same meaning as in I_ν and j_ν ? What is the conversion factor between α_ν and α_λ ? And between κ_ν and κ_λ ? Is it useful to introduce a total extinction coefficient $\alpha \equiv \int \alpha_\nu d\nu$?
- Question 3.8* In contrast to the emission coefficient j_ν in (3.1), the extinction coefficient α_ν is defined in (3.4) without reference to direction. Why? Is that correct in all circumstances?
- Question 3.9* Define coefficients for the emission and extinction by solid surfaces in similar fashion to the volume coefficients of equations (3.1) and (3.4). What are their dimensions?
- Question 3.10* If different types of particles or processes contribute to the extinction from a beam at the same frequency, how should partial extinction coefficients then be defined for each, and how should these be combined into a total extinction coefficient—for α_ν , σ_ν and κ_ν , respectively?
- Question 3.11* Kliger *et al.* (1990) write the following on page 162 of their book:

For absorbance measurements on solutions, the decadic molar extinction coefficient ϵ is the bulk property that is sought. The decadic molar extinction coefficient is related to the absorbance A by:

$$A = \epsilon l c = \log(I'/I'').$$

Here I' is the intensity of the beam at some point within the solution, and I'' is the intensity a distance l (in centimeters) later. The concentration of solute in moles/liter is given by c . An alternative quantity, the absorption coefficient α , defined by

$$\alpha l = \ln(I'/I''),$$

is sometimes reported instead and is useful where the concentration of the absorber is unknown.

How do these definitions correspond to our definitions (3.3)—(3.5)?

- Question 3.12* Spectral lines are always due to specific bound-bound transitions in compound particles (atoms, ions, molecules, nuclei). These provide extra emission and extinction processes at the line frequency $\nu = \nu_0$, with corresponding bound-bound extinction coefficient j_ν^{line} and extinction coefficient α_ν^{line} . Can you have one without the other? Are such bound-bound contributions always an increase, adding to the background continuum emission and extinction from other processes at the line frequency?
- Question 3.13* When the medium contains a magnetic field, the bound-bound extinction coefficient is split for many transitions into separate components that extinguish circularly or linearly polarized light, respectively, depending on the angle between the beam and the magnetic field lines. How should such selective Stokes extinction coefficients be defined?

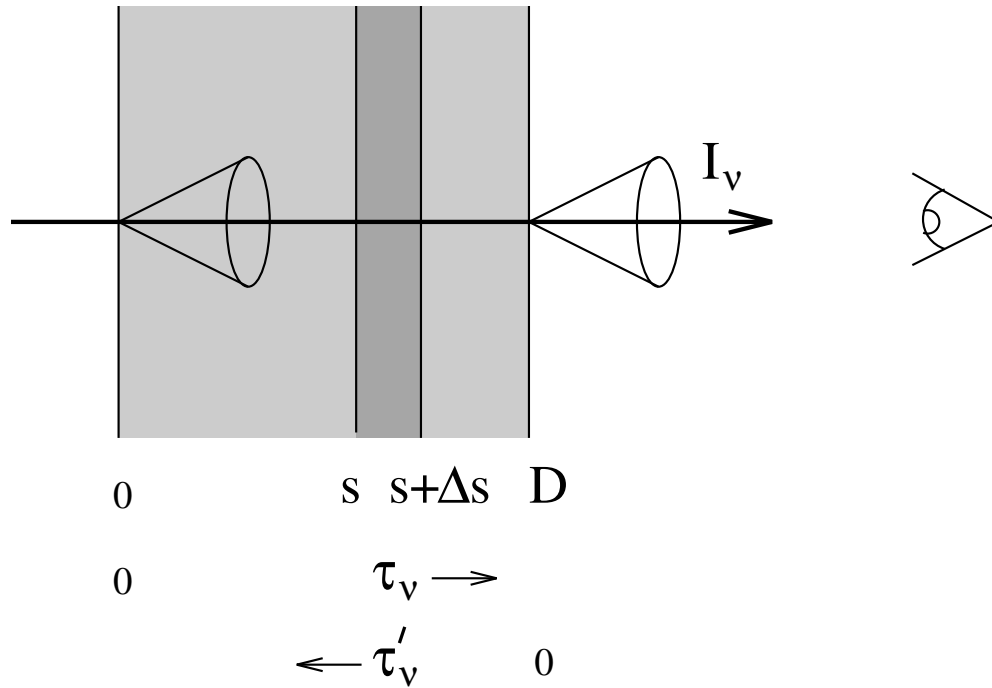
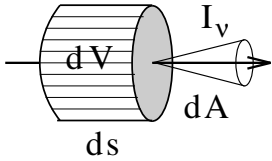


Figure 3.1: *Beam passing through a slab. The s coordinate measures geometrical path length along the propagation direction, from the entry at $s = 0$ to the exit at $s = D$. The optical path length τ_ν is also measured along the beam; the optical thickness of the whole slab is $\tau_\nu(D)$. The optical depth τ'_ν is measured along the line of sight, against the propagation direction.*

3.4 Transport equation



Consider a small cylinder with length ds and sides dA , oriented along a beam of radiation with intensity I_ν . Since I_ν is constant along the interval $(s, s+ds)$ except for local emission and extinction, the total intensity change combining (3.1) and (3.4) is

$$dI_\nu(s) = I_\nu(s+ds) - I_\nu(s) = j_\nu(s) ds - \alpha_\nu(s)I_\nu(s) ds,$$

or:

$$\frac{dI_\nu}{ds} = j_\nu - \alpha_\nu I_\nu. \quad (3.6)$$

This is the *transport equation*. It applies generally, except when the extinguishing particles are not small with respect to their separation, or when they are not randomly distributed over the medium.

Question 3.14 The transport equation rests on empirical definitions. What sort of experiment would demonstrate its validity? Is it a conservation law?

Question 3.15 A slab of thickness D is irradiated from one side with intensity $I_\nu(0)$. What is the emergent intensity $I_\nu(D)$ on the other side:

- in the case of pure emission ($\alpha_\nu = 0$)?
- in the case of pure extinction ($j_\nu = 0$)?

What are the results for a homogeneous slab?

3.5 Optical path length, optical thickness, optical depth

A beam passes at right angles through a slab of thickness D from $s = 0$ to $s = D$ (Figure 3.1). Per layer of thickness ds the corresponding increment of the *monochromatic optical path* $d\tau_\nu$ is defined by:

$$d\tau_\nu(s) \equiv \alpha_\nu(s) ds. \quad (3.7)$$

The total optical path through the slab is called its *monochromatic optical thickness* and is given by:

$$\tau_\nu(D) = \int_0^D \alpha_\nu(s) ds. \quad (3.8)$$

It represents an “optical” measure of thickness, in terms of photon penetration rather than geometrically. For pure extinction ($j_\nu = 0$), the transport equation reduces to

$$\frac{dI_\nu}{d\tau_\nu} = -I_\nu,$$

and to the solution

$$I_\nu(D) = I_\nu(0) e^{-\tau_\nu(D)}. \quad (3.9)$$

This result shows that $\tau_\nu(D)$ in $I_\nu(D)/I_\nu(0) = e^{-\tau_\nu(D)}$ is an exponential decay parameter which measures how much photon energy remains after penetration over $\Delta s = D$. The boundary between small extinction and large extinction lies at the $1/e$ decay value, i.e., at optical thickness $\tau_\nu(D) = 1$. A slab is called *optically thick* for $\tau_\nu(D) > 1$, *optically thin* for $\tau_\nu(D) < 1$.

How far do photons penetrate into the slab? At $s < D$, within the slab, the remaining energy fraction is

$$I_\nu(s) = I_\nu(0) e^{-\tau_\nu(s)},$$

with $\tau_\nu(s)$ the optical path from 0 to s , or the optical thickness of the corresponding part of the slab. The probability that an incident photon penetrates over an optical path $\tau_\nu(s)$ before an extinction process removes it from the beam is given by $e^{-\tau_\nu(s)}$, so that the *mean optical path* $\langle \tau_\nu(s) \rangle$ of the photons equals:

$$\langle \tau_\nu(s) \rangle \equiv \frac{\int_0^\infty \tau_\nu(s) e^{-\tau_\nu(s)} d\tau_\nu(s)}{\int_0^\infty e^{-\tau_\nu(s)} d\tau_\nu(s)} = 1. \quad (3.10)$$

The *mean geometrical path* l_ν of photons in a homogeneous medium is:

$$l_\nu = \frac{\langle \tau_\nu(s) \rangle}{\alpha_\nu} = \frac{1}{\alpha_\nu}. \quad (3.11)$$

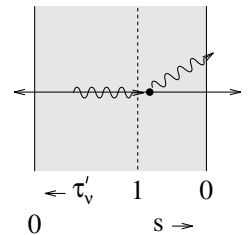
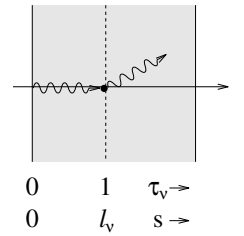
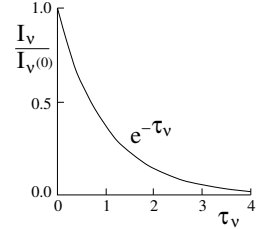
In an inhomogeneous medium this value represents the local photon free path.

In addition to optical thickness $\tau_\nu(D)$ and optical path $\tau_\nu(s)$, I will frequently use the *monochromatic optical depth* $\tau'_\nu(s)$. This is the optical path length along the line of sight, against the beam direction:

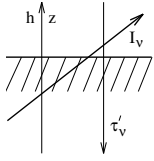
$$d\tau'_\nu(s) \equiv -\alpha_\nu(s) ds \quad (3.12)$$

where s is measured in the propagation direction, as in the definitions above.

In the case of axial symmetry, the *radial optical depth* is defined as the optical depth along the z or h axis, measured from $z = \infty$ well outside the object (or from



the eye of the beholder) down into the object along a line of sight that is normal to its surface. Thus, at a location $z = z_0$ inside the object:



$$\tau'_\nu(z_0) \equiv - \int_\infty^{z_0} \alpha_\nu dz. \quad (3.13)$$

In summary, optical path length and optical depth differ in direction and in zero point. Optical path length measures the penetration of photons into a medium; optical depth is used to measure the escape of photons from a medium (or, adhering to the ancient Greek belief that one's eyes illuminate the scene, the penetration of one's sight). The first measure is useful to describe radiative transfer within astrophysical objects; the second measure is useful to describe the radiation which we observe from them.



Question 3.16 What are the dimensions of $d\tau_\nu$, $\tau_\nu(D)$, and $\tau'_\nu(z_0)$? May one add optical thicknesses? And optical depths?

Question 3.17 How should $d\tau_\nu$ be defined when σ_ν or κ_ν is used instead of α_ν ?

Question 3.18 What is the meaning of the index ν in τ_ν ? How does one convert τ_ν into τ_λ ? What is the meaning of the integral $\int_0^\infty \tau_\nu d\nu$?

Question 3.19 Equation (3.10) relates $\langle \tau_\nu \rangle$ to the distribution function $e^{-\tau_\nu}$. Show that the expectation value of a quantity x which is characterized by a statistical distribution $f(x)$ is given by $\langle x \rangle = \int_0^\infty x f(x) dx / \int_0^\infty f(x) dx$.

Question 3.20 Derive (3.11) directly from the probability that a photon penetrates over a geometrical path length s .

Question 3.21 Are equations (3.10) and (3.11) also valid in the presence of emission? And in the presence of photon scattering?

Question 3.22 What is the the optical thickness of a homogeneous slab of thickness D with mean geometrical photon path l_ν ?

Question 3.23 How should one define optical thickness for a slanted beam, with angle of incidence θ below 90° ? What is the radial optical depth along a line of sight with $\mu < 1$? What is the definition of radial optical depth in terms of geometrical depth?

Question 3.24 Show that the escape probability of a photon at $z = z_0$ in the direction μ is $\exp(-\tau'_\nu(z_0)/\mu)$. Where does the bulk of the escaping photons come from? Is the mean photon escape depth given by $\langle \tau'_\nu \rangle = 1/\mu$?

Question 3.25 The earth's atmosphere and the solar corona are both transparent for visible radiation. What are the optical thickness and the optical depth of the corona in the visible?

The earth's ionosphere and the corona are both opaque for radio waves with $\nu = 10$ Mhz. Where should the optical depth integration begin in that case?

3.6 Source function

The emission coefficient j_ν and the extinction coefficient α_ν are quite different quantities. This is clear from their dimensions: j_ν has the dimension of intensity per cm path length, whereas α_ν is per cm only. Nevertheless, the ratio of these coefficients yields a very important quantity called the *source function*:

$$S_\nu \equiv j_\nu/\alpha_\nu, \quad (3.14)$$

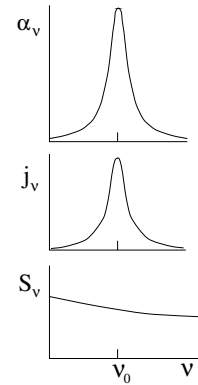
which has dimension $[\text{erg cm}^{-2} \text{ s}^{-1} \text{ Hz}^{-1} \text{ ster}^{-1}]$.

Since S_ν has the same dimension as I_ν , these two quantities may be added and subtracted. Their difference appears in the transport equation (3.6) when it is rewritten with definitions (3.7) and (3.14) into:

$$\frac{dI_\nu}{d\tau_\nu} = S_\nu - I_\nu. \quad (3.15)$$

This is the transport equation in the standard differential form. It provides an elegant description of the change in intensity per unit optical path along the beam. S_ν represents a source term in this equation, hence its name “source function”: it specifies the addition of new photons along the beam. When $S_\nu = 0$, the intensity simply decreases with the exponential decay of eq. (3.9).

We now have three quantities, j_ν , α_ν and S_ν , to describe the increase and decrease of I_ν along a beam. The combination α_ν and S_ν is usually employed, rather than the combination α_ν and j_ν . One reason to do so is the symmetry of equation (3.15), with α_ν contained in $d\tau_\nu$. A second reason is that α_ν and S_ν tend to be much more independent of each other than α_ν and j_ν . A bound-bound transition, for example, may produce large increase of both j_ν and α_ν at the corresponding line frequency, whereas these peaks nearly or completely cancel in the ratio $S_\nu = j_\nu/\alpha_\nu$ so that S_ν tends to be a much smoother function of frequency than j_ν . Finally, j_ν depends more directly on the local radiation field than α_ν does. In scattering processes, for example, j_ν increases with the number of photons that are scattered into the beam, and therefore with the quantity of photons that is locally available for scattering (i.e., the angle-averaged intensity J_ν). In contrast, α_ν measures the *fraction* of the incident photons that are extinguished, and does not directly depend on the number of available photons itself. It does so only indirectly, through the influence of the radiation on the state of the matter. We return to these properties in Chapter ??.



Question 3.26 How should the source function be defined with σ_ν or κ_ν as extinction coefficient?

Question 3.27 Rewrite (3.15) for a beam with exit angle μ using optical depth τ'_ν instead of optical path τ_ν .

Question 3.28 If different processes contribute emission and/or extinction at the frequency ν , how should the total source function S_ν^{total} be defined in terms of separate source functions per process?

Question 3.29 Spectral lines are always due to bound-bound transitions, with rapid variation of j_ν^{line} and α_ν^{line} across the line width. What is the corresponding source function S_ν^{line} ? What is the total source function S_ν^{total} if there is also continuous emission j_ν^{cont} and extinction α_ν^{cont} present at the line frequency? When is $S_\nu^{\text{total}} \approx S_\nu^{\text{line}}$, and when is $S_\nu^{\text{total}} \approx S_\nu^{\text{cont}}$? Show that the frequency variation of S_ν^{total} across the line width is small if $S_\nu^{\text{line}} \approx S_\nu^{\text{cont}}$.

Question 3.30 Does the value $S_\nu = 1$ have special meaning? And $S_\nu/I_\nu = 1$? Can $S_\nu > I_\nu$? And $S_\nu < 0$?

Question 3.31 In §?? Kirchhoff’s law $I_\nu = B_\nu(T)$ is presented, with $B_\nu(T)$ the Planck function. It holds when there is sufficient coupling between radiation and matter, if the latter obeys the Maxwell velocity distribution. Which quantity is then most likely to follow the Planck function also:

- the emission coefficient,
- the extinction coefficient,
- the source function?

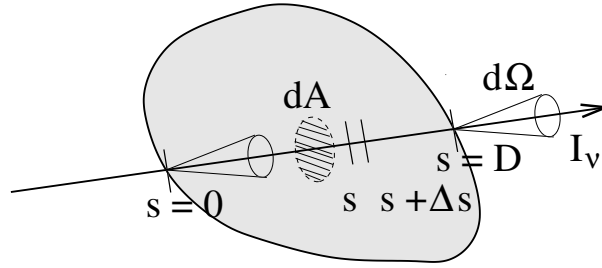


Figure 3.2: Geometry for the passage of a beam through a gaseous object. The s coordinate measures the geometrical path along the propagation direction, from the entry at $s = 0$ to the exit at $s = D$. The optical thickness of the object along the beam is $\tau_\nu(D)$.

Question 3.32 Demonstrate that $S_\nu = J_\nu$ if no photon creation, photon destruction or photon conversion occurs, i.e., if both α_ν and j_ν are due to monochromatic scattering alone.

Question 3.33 The extinction of radiation at visible wavelengths in the earth's atmosphere, at clear sky, consists primarily of elastic Rayleigh scattering (§??). What is the corresponding source function?

3.7 Formal solution of the transport equation

3.7.1 Integral form of the transport equation

Consider a gaseous medium through which a beam passes as in Figure 3.2. The beam has intensity $I_\nu(0)$ at the entry point at $s = 0$. What is the emergent intensity $I_\nu(D)$ at $s = D$?

First, the incident intensity $I_\nu(0)$ is attenuated within the medium. The optical path along the beam from $s = 0$ to an intermediate location $s = s'$ is given by

$$\tau_\nu(s') = \int_0^{s'} \alpha_\nu(s) ds;$$

the amount of incident radiation that remains at s' is:

$$I_\nu(s') = I_\nu(0) e^{-\tau_\nu(s')}.$$

Second, there is emission within the medium along the beam. At $s = s'$ it is given by

$$dI_\nu(s') = j_\nu(s') ds = S_\nu(s') d\tau_\nu(s')$$

across the path increase ds . This contribution is attenuated along the remainder of the path, between $s = s'$ and $s = D$:

$$[dI_\nu(D)]_{s=s'} = S_\nu(s') d\tau_\nu(s') e^{-[\tau_\nu(D) - \tau_\nu(s')]}.$$

The net result is obtained by summing the remainder of $I_\nu(0)$ and all attenuated contributions within the medium from $s = 0$ to $s = D$:

$$I_\nu(D) = I_\nu(0) e^{-\tau_\nu(D)} + \int_0^{\tau_\nu(D)} S_\nu(s) e^{-[\tau_\nu(D) - \tau_\nu(s)]} d\tau_\nu(s). \quad (3.16)$$

This is the integral form of the transport equation. It is often called its *formal solution*.

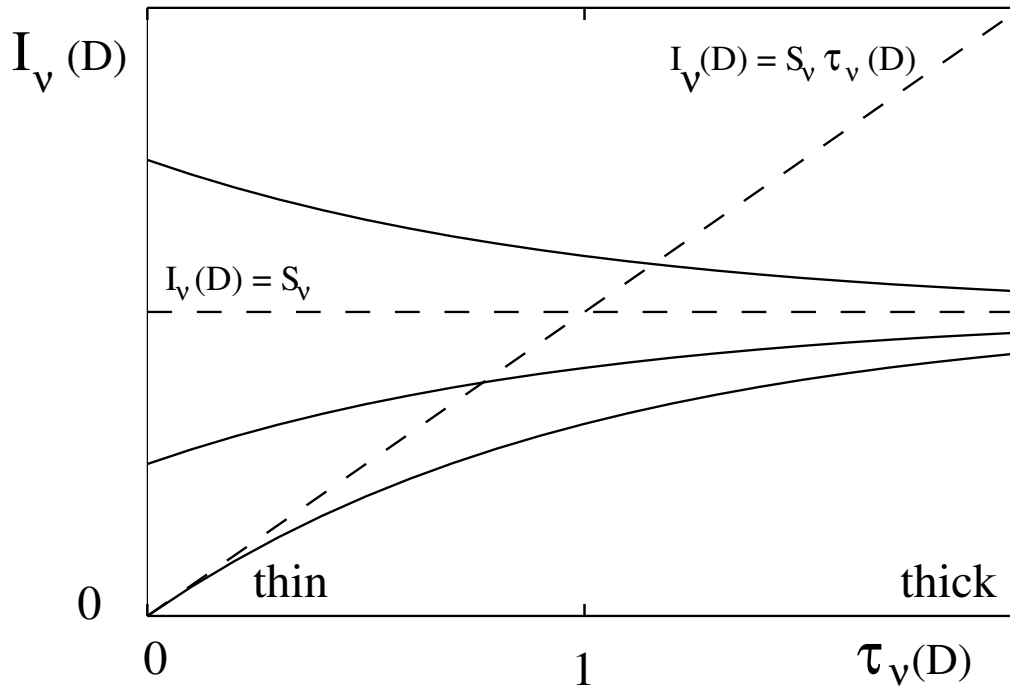


Figure 3.3: *Emergent intensity $I_\nu(D)$ from a homogeneous medium against its optical thickness $\tau_\nu(D)$. Optically thin, non-backlit objects produce $I_\nu(D) = S_\nu \tau_\nu(D) = j_\nu D$ (lower curve, at left). If a background intensity $I_\nu(0)$ illuminates the slab in the beam direction, there is enhancement of the intensity for $I_\nu(0) < S_\nu$ (middle curve), reduction for $I_\nu(0) > S_\nu$ (upper curve). For thick slabs with $\tau_\nu(D) > 1$, the emergent intensity $I_\nu(D) \approx S_\nu$ independent of $I_\nu(0)$.*

Question 3.34 Derive (3.16) directly from the differential form (3.15) by multiplying the latter with $\exp(\tau_\nu)$ followed by integration.

Question 3.35 Is (3.16) a general result? Does it hold for both thick and thin media? For inhomogeneous media? For fluids or solids rather than gases? Which parameters in (3.16) contain material properties of the medium?

Question 3.36 The formal solution (3.16) is rarely a true solution. In the presence of scattering, j_ν and S_ν depend on the local radiation field, i.e., on I_ν in all directions including the one for which I_ν is sought. Thus, to find $I_\nu(D)$ one needs to know $I_\nu(s, \theta, \varphi)$. What tactic would you try to solve this problem?

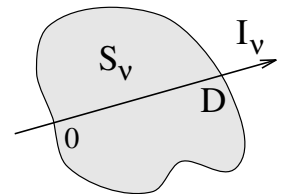
3.7.2 Radiation from a homogeneous medium

Let us now consider the unrealistic but instructive case of a homogeneous medium, in which neither j_ν nor α_ν varies through the medium. Then S_ν does not vary either, so that (3.16) yields:

$$I_\nu(D) = I_\nu(0) e^{-\tau_\nu(D)} + S_\nu [1 - e^{-\tau_\nu(D)}], \quad (3.17)$$

with D the geometrical thickness of the medium measured along the beam (Figure 3.2). The first term again measures the attenuation of the incident radiation $I_\nu(0)$ across the medium; the second term gives the total contribution from within the medium.

If the medium is *optically thick*, with $\tau_\nu(D) \gg 1$ and $\exp(-\tau_\nu(D)) \approx 0$, the result



is:

$$I_\nu(D) \approx S_\nu.$$

The incident radiation $I(0)$ does not penetrate to the other side; one receives an intensity equal to the source function within the medium.

In the *optically very thin* case, with $\tau_\nu(D) \ll 1$, the emergent intensity simply equals the incident one:

$$I_\nu(D) \approx I_\nu(0).$$

For the less extreme *optically thin* case, with $\tau_\nu(D) < 1$, use of $\exp(-\tau_\nu) \approx 1 - \tau_\nu$ yields:

$$\begin{aligned} I_\nu(D) &\approx I_\nu(0) - I_\nu(0)\tau_\nu(D) + S_\nu\tau_\nu(D) \\ &= I_\nu(0) + [S_\nu - I_\nu(0)] \tau_\nu(D). \end{aligned} \quad (3.18)$$

These results are shown in Figure 3.3. $I_\nu(D)$ equals $I_\nu(0)$ for $\tau_\nu(D) = 0$, and approaches S_ν for large $\tau_\nu(D)$. The approach is from larger to smaller intensity when $S_\nu < I_\nu(0)$, and reversedly when $S_\nu > I_\nu(0)$. Thus, $I_\nu(D) \leq I_\nu(0)$ when $S_\nu < I_\nu(0)$, and $I_\nu(D) \geq I_\nu(0)$ when $S_\nu > I_\nu(0)$.

Question 3.37 What is the emergent intensity for a homogeneous infinite half-space? How does it depend on the viewing angle θ ? What is the intensity within a homogeneous medium of infinite extent? Why are these intensities independent of the amount of extinction in the medium, or of its nature? Is that also the case for solid surfaces?

Question 3.38 Rewrite (3.17) for a slanted beam which crosses a plane-parallel slab with thickness D at an angle $\mu = \cos\theta$. Rewrite (3.17) also, for the same beam, using radial optical depth τ'_ν instead of optical thickness τ_ν .

Question 3.39 A radio astronomer states that the observed radio intensity from an interstellar cloud of diameter D is given by $I_\nu = \alpha_\nu S_\nu D$. What are her assumptions?

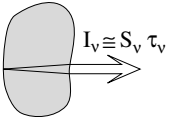
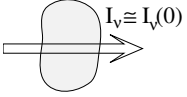
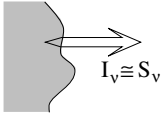
Question 3.40 What is the intensity at the surface of a non-backlit, homogeneous, optically thin, spherical cloud with radius R , extinction coefficient α_ν and source function S_ν ? Is the cloud a Lambert radiator? What is the surface flux of the cloud, and what is the irradiance from the cloud at earth?

Question 3.41 A homogeneous medium contains particles that cause continuous emission j_ν^{cont} and extinction α_ν^{cont} at the frequency ν_0 , and also particles that cause bound-bound emission j_ν^{line} and extinction α_ν^{line} that is centered at ν_0 . The two corresponding source functions are the same: $S_\nu^{\text{cont}} = S_\nu^{\text{line}}$. Express the emergent intensity at the line frequency, for a beam which crosses the medium as in Figure 3.2, in the above quantities for the following four cases:

- $\tau_\nu(D) \gg 1$,
- $\tau_\nu(D) < 1$ and $I_\nu(0) = 0$,
- $\tau_\nu(D) < 1$ and $I_\nu(0) < S_\nu^{\text{total}}$,
- $\tau_\nu(D) < 1$ and $I_\nu(0) > S_\nu^{\text{total}}$.

What is in each case the character of the resulting spectral line (emission or absorption)?

Question 3.42 If extra bound-bound emission occurs at the frequency of a spectral line, does that produce emission lines in the emergent spectrum? And do bound-bound extinction processes cause absorption lines? Do bound-free emission and extinction processes cause emission and absorption edges in the spectrum?



Question 3.43 Is a spectral line from a non-backlit optically thin homogeneous medium *always* an emission line? What if the slab is optically thick at the line wavelength but optically thin in the continuum? And vice versa?

Question 3.44 A beam with incident intensity $I_\nu(0)$ crosses an optically thin, homogeneous slab of thickness D . There is monochromatic scattering within the slab which increases with time. Do the optical thickness of the slab, the source function in the slab, and the emergent intensity $I_\nu(D)$ increase or decrease?

3.7.3 Radiation from a thick medium

The assumption of homogeneity is unrealistic; a better approximation is to adopt axial symmetry by assuming that the object consists of plane-parallel layers, i.e., that variations exist only in the z direction (= height h). In addition, for thick objects the observable emergent intensity has more interest than the intensity in the invisible layers at large optical depth; we therefore employ the radial optical depth $\tau'_\nu(h)$ defined by (3.13). It integrates extinction vertically into the object, along a radial line of sight, rather than along the beam from the far side onwards as is the case for the optical path length τ_ν .

Combination of (3.13), (3.16) and (2.3) gives for inward-directed radiation I_ν^- with $\mu < 0$ at an arbitrary height $h = h_0$:

$$I_\nu^-(h_0, \mu) = - \int_0^{\tau'_\nu(h_0)} S_\nu(\tau'_\nu) e^{-[\tau'_\nu - \tau'_\nu(h_0)]/\mu} d\tau'_\nu/\mu$$

and for the outward-directed radiation I_ν^+ with $\mu > 0$:

$$I_\nu^+(h_0, \mu) = + \int_{\tau'_\nu(h_0)}^\infty S_\nu(\tau'_\nu) e^{-[\tau'_\nu - \tau'_\nu(h_0)]/\mu} d\tau'_\nu/\mu,$$

where the following boundary conditions have been used:

$$I_\nu^-(\tau'_\nu=0, \mu) = 0$$

for I_ν^- (no incident radiation from above), and

$$S_\nu(\tau'_\nu) e^{-\tau'_\nu/\mu} \rightarrow 0 \text{ for } \tau'_\nu \rightarrow \infty$$

for I_ν^+ (the source function should not increase exponentially with optical depth).

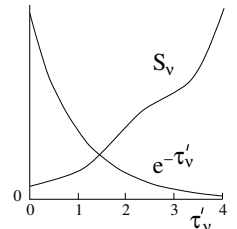
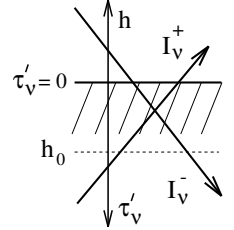
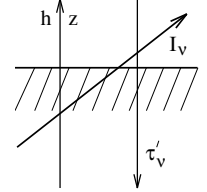
The emergent intensity is given by the value of I_ν^+ at a location far enough out from the object that it has $\tau'_\nu(h) = 0$:

$$I_\nu^+(\tau'_\nu=0, \mu) = \int_0^\infty S_\nu(\tau'_\nu) e^{-\tau'_\nu/\mu} d\tau'_\nu/\mu. \quad (3.19)$$

For $\mu = 1$, looking down vertically, we observe:

$$I_\nu^+(\tau'_\nu=0, \mu=1) = \int_0^\infty S_\nu(\tau'_\nu) e^{-\tau'_\nu} d\tau'_\nu. \quad (3.20)$$

This result shows that the emergent intensity is set by the source function, with its inward variation weighted with the attenuation factor $\exp(-\tau'_\nu)$. This factor rapidly diminishes with increasing optical depth and limits the integrand to the surface layers of the object.



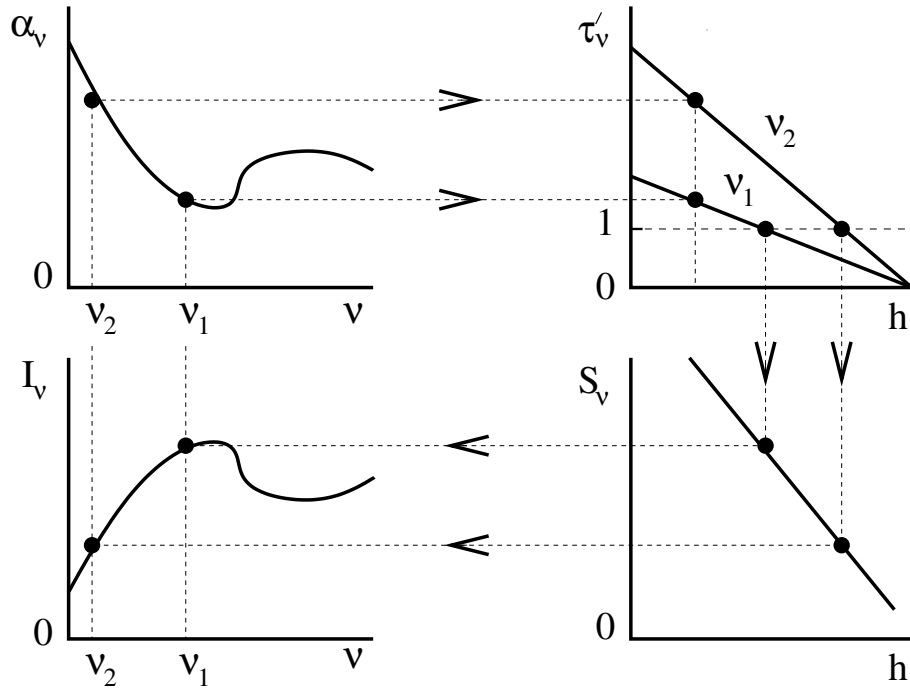


Figure 3.4: *Illustration of the Eddington-Barbier relation. Assumptions: height-independent extinction, frequency-independent source function, linear variation of the source function with height. The extinction coefficient α_ν (upper left) sets the optical depth scaling $\tau'_\nu(h)$ per frequency ν (upper right). The location where the optical depth reaches unity ($h(\tau'_\nu = 1)$; upper right) sets the height at which the source function $S_\nu(h)$ (lower right) is representative for the emergent intensity $I_\nu(0, \mu = 1)$ (lower left). Thus, the α_ν curve is mapped through the righthand curves into variation of the emergent intensity I_ν with ν .*

At which height does the radiation escape? Substitution of the expansion

$$S_\nu(\tau'_\nu) = \sum_{n=0}^{\infty} a_n \tau'^n_\nu = a_0 + a_1 \tau'_\nu + a_2 \tau'^2_\nu + \dots + a_n \tau'^n_\nu$$

in (3.19) and use of $\int_0^\infty x^n \exp(-x) dx = n!$ yields

$$I_\nu^+(\tau'_\nu=0, \mu) = a_0 + a_1 \mu + 2a_2 \mu^2 + \dots + n! a_n \mu^n.$$

Truncation of both expansions after the first two terms yields the important *Eddington-Barbier approximation*:

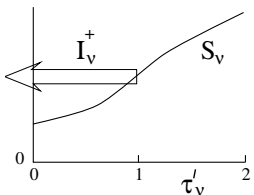
$$I_\nu^+(\tau'_\nu=0, \mu) \approx S_\nu(\tau'_\nu = \mu). \quad (3.21)$$

In particular, for $\mu = 1$:

$$I_\nu^+(\tau'_\nu=0, \mu=1) \approx S_\nu(\tau'_\nu = 1). \quad (3.22)$$

This relation is exact when S_ν varies linearly with τ'_ν .

The Eddington-Barbier approximation equates the emergent intensity for $\mu = 1$ to the source function at optical depth unity ($\tau'_\nu = 1$). This location lies at one mean optical photon path from the surface (§ 3.5); the Eddington-Barbier approximation



therefore says that the radiation which escapes from the medium represents the source function at one mean photon path below the surface.

The Eddington-Barbier approximation does *not* imply that the observed photons all escaped from optical depth $\tau'_\nu = 1$, although that is often said (“the photons come from optical depth unity”). The integrand $S_\nu \exp(-\tau'_\nu)$ extends over a wide range in τ'_ν , from the surface at $\tau'_\nu = 0$ to, say, $\tau'_\nu \approx 10$ where the factor $\exp(-\tau'_\nu)$ cuts it off. Photons escape from this entire slab; they are collectively *characterized* by the value of the source function at $\tau'_\nu = 1$.

For oblique viewing, with $\mu < 1$, the mean free photon path should be measured along the propagation direction. For such a slanted beam, the shallow layer with $\tau'_\nu = \mu$ is already at optical path length $\tau_\nu = 1$ from the surface. It constitutes the Eddington-Barbier depth in (3.21).

Figure 3.4 illustrates the Eddington-Barbier approximation for a somewhat unrealistic medium in which the source function $S(h)$ varies linearly with height (or depth) but not with frequency, whereas the extinction α_ν varies with frequency but not with height. The frequency dependence of the extinction coefficient (upper left panel) results in frequency dependence of the scaling between geometrical height h and optical depth τ'_ν (upper right panel). Since the extinction does not vary with h , the scaling relations are straight lines with different slopes. The values of h where they reach $\tau'_\nu = 1$ are marked; these are the characteristic Eddington-Barbier heights and differ with frequency. Since the $S(h)$ and $\tau_\nu(h)$ relations are linear, the Eddington-Barbier relation applies exactly. The emergent intensity I_ν in the lower left panel therefore equals $S_\nu(h[\tau'_\nu = 1])$ in the lower right panel. The frequency pattern seen in the emergent intensity is similar to the frequency pattern of the extinction coefficient, but it is mapped through the curves in the righthand panels. In this case, the mapping consists of sign reversal and linear amplitude rescaling.

We have now reached an important point. The radiation which we receive from a non-illuminated, optically thin object is approximately given by

$$I_\nu \approx S_\nu \tau_\nu = \alpha_\nu S_\nu D,$$

whereas the radiation from an optically thick object is approximately given by

$$I_\nu \approx S_\nu(\tau'_\nu = \mu).$$

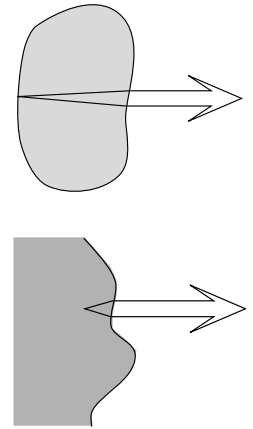
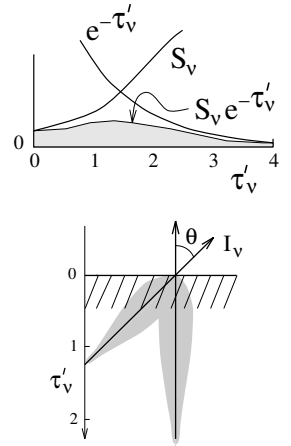
In both cases we need to specify both the extinction coefficient α_ν and the source function S_ν to compute the emergent intensity I_ν (in the optically thick case, α_ν is needed to determine the location where $\tau'_\nu = \mu$). We must therefore study these quantities, both for continua and for spectral lines. This is done in the following three chapters; we return to the transport equation and its solution in Chapter ??.

Question 3.45 Optically thin objects are often assumed to be homogeneous, while the conditions in optically thick objects are often assumed to vary radially, with axial symmetry. Why this difference?

Question 3.46 Does the Eddington-Barbier approximation hold for a homogeneous slab? May it also be written as $I_\nu^+(0, \mu) \approx S_\nu(z = -l_\nu \mu)$ with l_ν the mean geometrical photon free path? Use equation (3.19) to derive the mean contribution depth to the emergent intensity. Does this depth equal the mean photon escape depth? When is it unity? Do “the photons come from optical depth unity” in that case?

Question 3.47 Show that the flux from an optically thick object is given by:

$$\mathcal{F}_\nu^+(\tau'_\nu=0) = \pi S_\nu(\tau'_\nu=2/3)$$



when S_ν varies linearly with τ'_ν .

- Question 3.48* At which optical depth should one define the “surface” of the Sun?
- Question 3.49* The intensity in the visible part of the solar spectrum decreases from the center of the apparent solar disk to the limb. What does that imply for the variation of the source function with height in the solar atmosphere?
- Question 3.50* Assume that the continuous extinction coefficient $\alpha_{\nu_1}^{\text{cont}}$ at $\nu = \nu_1$ exceeds $\alpha_{\nu_2}^{\text{cont}}$ at $\nu = \nu_2$ by a factor of 10, but that the corresponding source function S_ν^{cont} is the same at both frequencies. What is the ratio of the emergent intensities at the two frequencies for:
- an optically thin, homogeneous, non-backlit, spherical cloud,
 - a homogeneous infinite half-space,
 - a spherical star with $S_\nu(\tau'_{\nu_1}) = S_\nu(\tau'_{\nu_1}=0) + \tau'_{\nu_1}$?
- And what is the ratio of the emergent fluxes at the two frequencies for these three cases?
- Question 3.51* Different continuous processes and different bound-bound processes may operate at the same frequency. What is the effect of such overlap on the total extinction, the total emission, the total optical thickness, and the total source function? If a line has $\eta = 2$, with $\eta_\nu \equiv \alpha_\nu^{\text{line}}/\alpha_\nu^{\text{cont}}$, does that imply doubling of the local emission at the line frequency? And of the emergent intensity?
- Question 3.52* Draw a four-panel diagram as in Figure 3.4 for the formation of a spectral line with $\eta_\nu = 3$ at line center, assuming height-independent extinction $\alpha_\nu^{\text{total}}$ and source function equality $S_\nu^{\text{line}} = S_\nu^{\text{cont}}$. When do you get absorption lines and when do you get emission lines? What changes are needed to describe the formation of a bound-free ionization edge in the spectrum?
- Question 3.53* Draw a four-panel diagram as in Figure 3.4 for the formation of a bound-free ionization edge in the spectrum, again assuming height-independent extinction and source function equality.
- Question 3.54* The Na I D lines in the solar spectrum are in absorption (Figure 1.2). What does that imply for their source functions S_ν^{total} ? Assume that these are equal. The extinction coefficient α_ν^{line} differs by a factor two between the two lines. Do their line strengths in the solar spectrum also differ by a factor two? Discuss which modifications of the four-panel diagram in Question 3.52 are needed to describe their actual formation.
- Question 3.55* The Ca II K line of Ca II is much stronger (i.e., broader and deeper) in the solar spectrum than the Na I D lines, as shown by comparing Figures 8.7 and 3.4. If the line source function S_ν^{line} is the same for all three lines, what makes the difference?
- Question 3.56* The Ca II K line in the solar spectrum exhibits two minuscule bumps on each side of line center (Figure 8.7). What source function behavior is required to explain these?
- Question 3.57* Show that emission lines may occur in the irradiance spectrum from a spherical star with an extended atmosphere, even if the source function $S_\nu^{\text{total}} = S_\nu^{\text{line}} = S_\nu^{\text{cont}} \equiv S_\nu$ does not vary with height.
- Question 3.58* A spectrometer onboard a spacecraft registers emission lines in the ultraviolet spectrum from an unknown source. What are the options for interpretation? Should they also be considered for a radio source with emission lines?

Chapter 4

Radiation and matter in equilibrium

4.1 Introduction: thermodynamical equilibrium

In this chapter we continue for the time being the macroscopic description with a discussion of ensemble averages. They serve to specify the quantity of particles and photons of a given type that are present within a medium. Averages over ensembles are most straightforward in *equilibrium situations*. These come in various types; in this chapter we confine ourselves to the assumption of a homogeneous medium in *thermodynamical equilibrium* (TE).

In TE *all* processes and states are in equilibrium with each other. Each process is in microscopic equilibrium with the reverse process: there is *detailed balance*. All macroscopic equipartition laws hold, and indeed with *the same* temperature for each one. For the *radiation* the equipartition laws are those of Kirchhoff, Planck, Wien and Stefan-Boltzmann; for the *matter* they are the laws of Maxwell, Boltzmann and Saha.

TE is the most stringent form of equilibrium, and does not often occur in nature. Further on the TE laws described here will also be used for situations with less stringent stipulations of equilibrium (such as for LTE = Local TE, in which the temperature may vary slowly through the medium), and in order to describe departures from the laws.

Radiation can occur in equilibrium with matter, thanks to the fact that photons have no mass. In contrast with fermions, no Pauli exclusion principle holds for photons, so that unlimited creation and destruction of photons is possible, and with it the establishment of an equilibrium.

4.2 Radiation in thermodynamical equilibrium

4.2.1 Kirchhoff laws

TE holds in a homogeneous, isothermal, isotropic medium, for example in a medium enclosed within isothermal walls for a sufficient length of time. Then according to equation (3.6), the following holds for *each* bundle, at *each* frequency and at *each* point in time:

$$\frac{dI_\nu}{ds} = j_\nu - \alpha_\nu I_\nu = 0 \quad \rightarrow \quad j_\nu = \alpha_\nu I_\nu$$

This is Kirchhoff's law for TE. Another law found by Kirchhoff is that the intensity in a medium in TE is isotropic, and at each frequency depends exclusively upon the

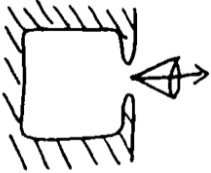
temperature:

$$I_\nu \equiv B_\nu(T),$$

regardless of the nature of the medium. In this equation B_ν is the Planck function. Taking these two laws together, we see that in TE we have:

$$j_\nu^{\text{TE}} = \alpha_\nu^{\text{TE}} B_\nu(T), \quad (4.1)$$

and thus that the source function $S_\nu \equiv j_\nu/\alpha_\nu$ in TE is equal everywhere to the Planck function B_ν .



A good source of TE radiation is a closed cylinder that is placed in an oven, so that the medium inside it is isothermal. Once equilibrium is established, we poke a small hole in it. If the hole is small enough, the radiation that escapes from it is a representative sample of the radiation within in the cylinder. From such a hole, then, emerges the same equilibrium radiation, which is completely specified by the temperature.



The second law is best made plausible by a thought experiment. Suppose that the intensity does depend upon the nature of the medium, and so that in two isothermal TE cylinders of the same temperature different intensities are found: $I_\nu^1 \neq I_\nu^2$, with I_ν^1 the intensity in the one cylinder and I_ν^2 the intensity in the other. Make an opening between the cylinders and slip in there a monochromatic filter that transmits only the frequency band $(\nu, \nu + d\nu)$. Photons with frequency ν will then migrate out of the cylinder with the greater intensity into the other, in contradiction with the second law of thermodynamics. Thus the assumption must be false, and we must have that $I_\nu^1 = I_\nu^2$.

A third law of Kirchhoff is that equation (3.6) also holds for the *walls* of the cylinder, with $\kappa_\nu^{\text{surface}}$ the coefficient of *true absorption* through a *surface*, not defined per unit path length but rather as dimensionless:

$$dI_\nu^{\text{abs}} \equiv -\kappa_\nu^{\text{surface}} I_\nu^{\text{incident}},$$

and likewise for a coefficient for the emission $\epsilon_\nu^{\text{surface}}$ of the wall (i.e., without the contributions of reflection or scattering off the wall):

$$dI_\nu^{\text{em}} \equiv \epsilon_\nu^{\text{surface}}.$$

Equilibrium then demands:

$$\epsilon_\nu^{\text{surface}} = \kappa_\nu^{\text{surface}} I_\nu^{\text{incident}} = \kappa_\nu^{\text{surface}} B_\nu.$$

Check that we have: $0 \leq \kappa_\nu^{\text{surface}} \leq 1$. The larger the absorption coefficient, the larger the associated radiation: the absorption determines the emission. A surface with $\kappa_\nu^{\text{surface}} = 1$ that absorbs all radiation falling on it is “black”. A “black body” therefore radiates in all directions an intensity $I_\nu = \epsilon_\nu^{\text{surface}} = B_\nu$; it radiates in a “Planckian” fashion.

A hole in a TE-cylinder can thus also be considered as a good approximation to a *black surface*: all photons that enter the cylinder through the hole do not leave by it if the hole is small enough — the hole is black because such an absorption coefficient is $\kappa_\nu^{\text{surface}} \approx 1$. The photons that do come out (by other means) are Planckian.

An expanded discussion of this topic can be found in Chandrasekhar (1939), Chapter V (page 199 in the Dover edition).

Question 4.1 Does the radiation that you observe from two TE-cylinders of the same temperature differ if the one cylinder is made of mirrored material and the other of black material?

Question 4.2 Is a TE-cylinder with a sufficiently small hole an optically thick or an optically thin source? Does the Eddington-Barbier relation hold for such a hole?

Question 4.3 Give a description of the radiation of a TE-wall that incorporates an *extinction coefficient*, i.e., including reflection and scattering off the wall.

Question 4.4 How would you define the source function of a surface? How large is it for a TE surface? Does it make a difference whether that surface is “black”?

4.2.2 Planck law

For the intensity and the source function in a medium in TE we have $I_\nu = S_\nu = B_\nu$, with B_ν given by the *Planck formula*.

In frequency units this is:

$$B_\nu(T) = \frac{2h\nu^3}{c^2} \frac{1}{e^{h\nu/kT} - 1} \quad (4.2)$$

Dimensions of B_ν : [erg cm⁻² s⁻¹ Hz⁻¹ ster⁻¹],
and in wavelength units:

$$B_\lambda(T) = \frac{2hc^2}{\lambda^5} \frac{1}{e^{hc/\lambda kT} - 1} \quad (4.3)$$

Dimensions of B_λ : [erg cm⁻² s⁻¹ cm⁻¹ ster⁻¹].

Representative Planck curves are illustrated in Figure 4.1.

Sometimes B_ν is defined a factor 4π larger: integrated over all directions rather than per steradian.

The Planck curves in Figure 4.1 never intersect one another: $B_\nu(T)$ rises monotonically with the temperature at all frequencies.

Question 4.5 Why do the factors ν^3 and λ^{-5} respectively appear in the two equations?

Question 4.6 Check that $B_\nu \downarrow 0$ for $T \downarrow 0$, and that $B_\nu \uparrow \infty$ for $T \uparrow \infty$.

4.2.3 Related radiation laws

4.2.3.1 Wien approximation

For sufficiently large ν/T , $\exp(h\nu/kT) \gg 1$ and the Planck formula simplifies to the *Wien approximation*:

$$h\nu/kT \gg 1 \quad \rightarrow \quad B_\nu \approx \frac{2h\nu^3}{c^2} e^{-h\nu/kT}. \quad (4.4)$$

These are the steep portions on the right-hand side of Figure 4.1.

4.2.3.2 Rayleigh-Jeans approximation

For sufficiently small ν/T , $\exp(h\nu/kT) - 1 \approx h\nu/kT$ and the Planck formula simplifies to the *Rayleigh-Jeans approximation*:

$$h\nu/kT \ll 1 \quad \rightarrow \quad B_\nu \approx \frac{2\nu^2 kT}{c^2}. \quad (4.5)$$

These are the linear portions on the left-hand side of Figure 4.1.

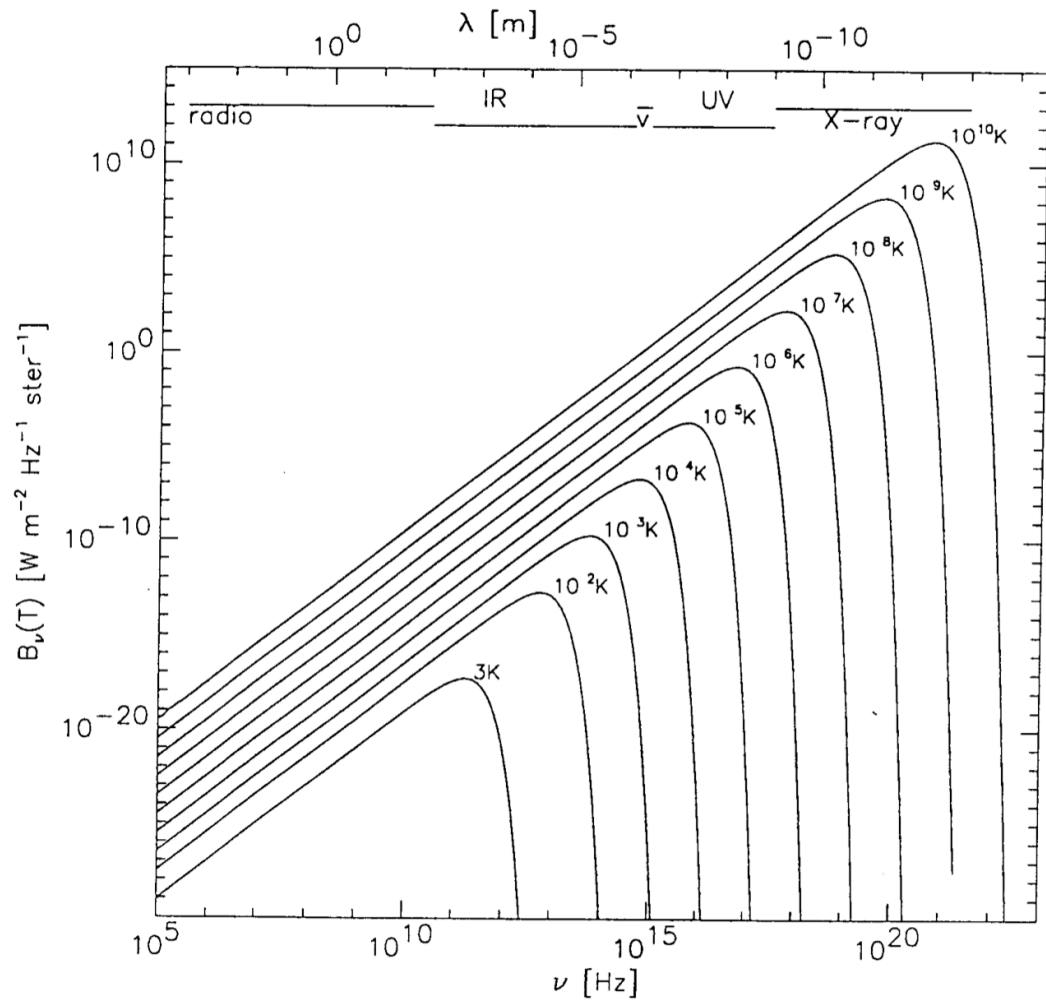


Figure 4.1: *The Planck function for various temperatures.*

Question 4.7 Give the Wien and Rayleigh-Jeans approximations for B_λ .

Question 4.8 In the book “Astrophysics or the Sun” of Zirin (1988) we find on pages 59–60:

... and the Planck function is

$$B_\nu d\nu = \frac{2h\nu^2}{c^2} \frac{1}{e^{h\nu/kT} - 1} d\nu$$

in the frequency scale, while in the wavelength scale

$$B_\lambda d\lambda = \frac{2\pi hc^2}{\lambda^5} \frac{1}{e^{hc/k\lambda T} - 1} d\lambda.$$

We must be careful of the differential factor $d\nu = -(c/\lambda^2)d\lambda$ which must be used as we transfer from the frequency scale Hz^{-1} to the wavelength scale cm^{-1} . The Planck function has two important asymptotic forms. At long wavelengths ($h\nu \ll kT$) the denominator in the equation for $B_\lambda d\lambda$ becomes $h\nu$ and we have:

$$B_\nu = \frac{2kT}{\lambda^2}$$

which is the Rayleigh-Jeans law. It tells us that when energy is not a factor, the radiation is proportional to the possible density of photons. For ($h\nu \gg kT$), the exponential in the denominator dominates, and

$$B_\nu = \frac{2h\nu^3}{kT} e^{-h\nu/kT},$$

which is the Boltzmann law from the fact that the distribution of higher-energy photons depends on the Boltzmann formula.

Comments?

4.2.3.3 Wien displacement law

The location of the maximum of the Planck curve follows the *Wien displacement law*, which is derived by taking $dB_\nu/d\nu = 0$ and $dB_\lambda/d\lambda = 0$ respectively.

The peak of B_ν falls at:

$$h\nu_{\max} = 2.82 kT \quad \rightarrow \quad \frac{\nu_{\max}}{T} = 5.88 \times 10^{10} \text{ Hz K}^{-1}. \quad (4.6)$$

The peak of B_λ falls at:

$$\lambda_{\max} T = 0.290 \text{ cm K}. \quad (4.7)$$

Question 4.9 Check that the maxima of the curves B_λ and of B_ν do not fall at the same place in the spectrum.

4.2.3.4 Stefan-Boltzmann law

Integration over the whole spectrum provides the *Stefan-Boltzmann law*:

$$B \equiv \int_0^\infty B_\nu d\nu = \frac{\sigma}{\pi} T^4 \quad (4.8)$$

with:

$$\sigma = \frac{2\pi^5 k^4}{15h^3 c^2} = 5.67 \times 10^{-5} \text{ erg cm}^{-2} \text{ K}^{-4} \text{ s}^{-1}.$$

The useful expression $B = \sigma T^4$ does not hold for intensity but for the outward flux $\mathcal{F}^+ = \pi I$ of an isotropically radiating black surface.

4.2.4 Radiation temperatures

Since the variation of the Planck function with frequency is determined exclusively by the temperature, the intensity observed from an object can often be best described by means of a temperature.

4.2.4.1 Brightness temperature

The *brightness temperature* T_b is the temperature for which the Planck function reproduces the observed intensity at a particular frequency:

$$B_\nu(T_b) = I_\nu^{\text{obs}}. \quad (4.9)$$

This measure is especially useful in the radio region. In that region the Rayleigh-Jeans approximation holds:

$$T_b = \frac{c^2}{2\nu^2 k} I_\nu^{\text{obs}}. \quad (4.10)$$

Question 4.10 How would the definition of brightness temperature appear if the intensity were observed per unit wavelength?

Question 4.11 Does the brightness temperature of a radio source depend on distance?

Question 4.12 Can you measure the brightness temperature of a point (i.e., unresolved) source such as a star? And of an extended source such as a nebula if it is not in TE?

Question 4.13 When is T_b a linear measure of the temperature of an optically thick radio source? And when for an optically thin radio source?

Question 4.14 Suppose that a homogeneous radio source radiates thermally, i.e., $I_\nu = B_\nu$. What is the frequency dependence of the radiation received? And what is the corresponding brightness temperature? Does the optical thickness of the source matter?

4.2.4.2 Antenna temperature

Radio astronomers often characterize the radiation received from a source by the *antenna temperature* T_A :

$$T_A \equiv \eta_A T_b, \quad (4.11)$$

with η_A the efficiency factor of the antenna.

T_A is the value of T_b as the antenna sees the source, i.e., the temperature of a “surrogate source of noise”: a source of black radiation that is coupled to the detector in place of the antenna. A stipulation is that the object fill the whole antenna array, for otherwise it would not be measuring intensity.

Question 4.15 How large is the antenna temperature of a radio source of size Ω_{source} (angular measure) if this size is smaller than the inherent angular resolution Ω_{antenna} of the telescope?

4.2.4.3 Color temperature

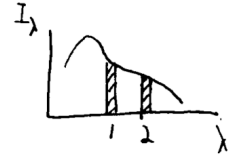
The *color temperature* T_c is the temperature for which the Planck function reproduces the slope of the observed spectrum at the observational frequency:

$$\left. \frac{dI_\nu^{\text{obs}}}{d\nu} \right|_{\nu=\nu_0} = \left. \frac{dB_\nu(T_c)}{d\nu} \right|_{\nu=\nu_0}. \quad (4.12)$$

For example in two-color photometry:

$$\frac{I_1}{I_2} \equiv \frac{B_{\lambda_1}(T_c)}{B_{\lambda_2}(T_c)}$$

the ratio of two observed intensities determines a temperature. A benefit of this definition is that it is a relative measurement: the absolute value of I_ν need not be known. Notation: $(B-V) \equiv 2.5 \log(I_V/I_B)$.



Question 4.16 Two-color photometry is frequently applied to stars. How is that related to the fact that stars are unresolved sources?

Question 4.17 What conditions must prevail in order for two-color photometry of a star to provide its temperature? Of what part of the star is that then the temperature?

Question 4.18 Check that T_c , just like T_b and T_A , is a function of frequency. From three-color photometry, two color temperatures can be found. Give three reasons why the color temperatures from the three-color photometry of a star can differ from one another.

4.2.4.4 Effective temperature

The *effective temperature* T_{eff} of a source of radiation is the temperature of a black body which radiates the same total flux:

$$\sigma T_{\text{eff}}^4 = \mathcal{F}_{\text{source}}^+, \quad (4.13)$$

thus it is the temperature for which an isotropically radiating black surface radiates the same total outward flux per cm^2 $\mathcal{F}^+ = \pi B = \pi \int_0^\infty B_\nu d\nu$ as does one cm^2 of the object.

Question 4.19 Express T_{eff} in terms of the emergent intensity of a spherically symmetric source.

4.3 Matter in thermodynamical equilibrium

4.3.1 Maxwell distribution

Where there is equipartition of kinetic energy, as is the case in TE, then the *Maxwellian velocity distribution* applies. For a type of particle with mass m we have: For each *component of velocity*:

$$\frac{n(v_x)}{N} dv_x = \left(\frac{m}{2\pi kT} \right)^{1/2} e^{-(1/2)mv_x^2/kT} dv_x, \quad (4.14)$$

and for the *speed*:

$$\frac{n(v)}{N} dv = \left(\frac{m}{2\pi kT} \right)^{3/2} 4\pi v^2 e^{-(1/2)mv^2/kT} dv, \quad (4.15)$$

with N the total number of particles of this type per unit volume and m the mass per particle.

The first distribution function is a Gaussian distribution. The second exhibits a “tail” as a result of the v^2 term, see Figure 4.2.

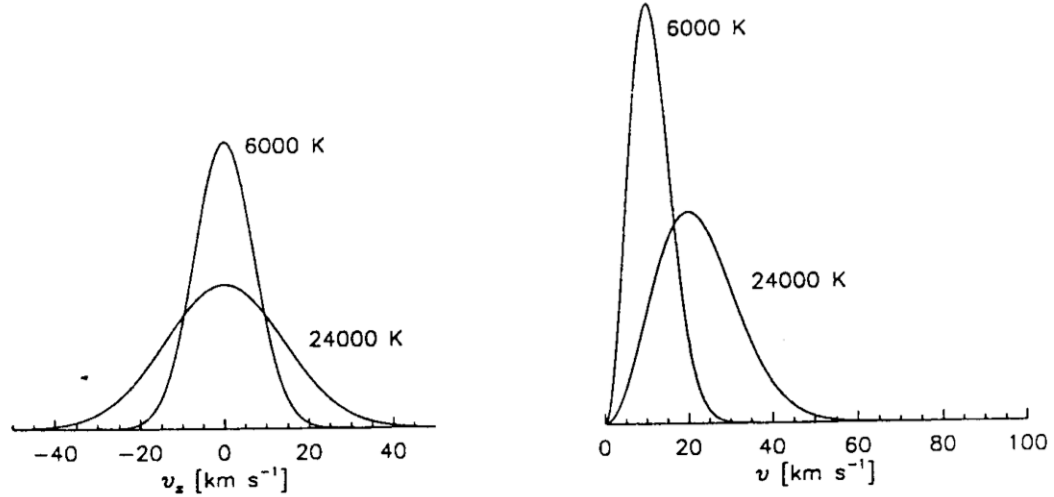


Figure 4.2: *The Maxwellian velocity distribution for hydrogen atoms, for a velocity component and for the speed.*

Question 4.20 Derive the second distribution from the first.

Question 4.21 Demonstrate that both distributions are normalized.

Question 4.22 Check by differentiating equation (4.15) with respect to v that the most probable velocity is given by:

$$v = \sqrt{2kT/m}.$$

How large is the most probable velocity component? The average particle energy? The average Doppler velocity along the line of sight?

4.3.2 Boltzmann distribution

In TE, the distribution of the particle populations of a specific type of atom (or ion or molecule) over the possible discrete excitation states (bound energy levels) is given by the *Boltzmann law*:

$$\left[\frac{n_{r,s}}{n_{r,t}} \right]^{\text{TE}} = \frac{g_{r,s}}{g_{r,t}} e^{-(\chi_{r,s} - \chi_{r,t})/kT}. \quad (4.16)$$

In which:

$n_{r,s}$ = number of atoms per cm^3 in level s of ionization state r ;

$g_{r,s}$ = statistical weight of level s of ionization state r ;

$\chi_{r,s}$ = excitation energy of level s of ionization state r , measured from the ground

state $(r, 0)$. Thus $\chi_{r,s} \equiv E_{r,s} - E_{r,0}$, and $\chi_{r,s} - \chi_{r,t} = h\nu$ for a radiative transition between states (r, s) and (r, t) , with the level s “higher” (has more internal energy) than level t .

Another form is:

$$\left[\frac{n_{r,s}}{N_r} \right]^{\text{TE}} = \frac{g_{r,s}}{U_r} e^{-\chi_{r,s}/kT} \quad (4.17)$$

with $N_r = \sum_s n_{r,s}$ the sum of the populations of all levels of ionization state r per cm^3 , and the *partition function* or *sum over all levels* U_r of ionization state r given by:

$$U_r \equiv \sum_s g_{r,s} e^{-\chi_{r,s}/kT}. \quad (4.18)$$

The Maxwell and Boltzmann distributions are both of the form

$$N^{\text{TE}} = \frac{1}{\sum} e^{-E/kT}$$

with \sum the integrated distribution, continuous and discrete respectively.

According to Boltzmann levels become *degenerate* because magnetic splitting only occurs in the presence of an external magnetic field; the consequent overlapping of levels is described by the statistical weights $g_{r,s}$.

The excitation energy $\chi_{r,s}$ is the “difference in potential energy” between the ground level $(r, 0)$ and the overlying level (r, s) . It is useful to measure energy differences between levels not in erg but in eV or in cm^{-1} . An energy of 1 eV amounts to 1.6021×10^{-12} erg (Allen 1976); wave numbers are defined as $\sigma = c_{\text{vac}}\nu$ (equation 1.1). In both cases a zero point must also be adopted; it is useful to measure excitation energy upwards from the ground level, within each ionization state, such as in the above and in Appendix ??; the ionization energy is likewise measured from the ground level of the ionization state in question. Once in a while, excitation energies are given in the reverse sense, increasing downwards from the ionization limit; that is in accord with the fact that energy is released in deexcitation, not in excitation.

A large collection of term diagrams and Grotrian diagrams can be found in the books of Bashkin and Stoner (1975). (Strictly speaking, *term diagrams* show only the energy and the identification of the levels, and *Grotrian diagrams* also contain the bb transitions. Figure 1.4 is a Grotrian diagram.)

Question 4.23 How much energy in eV does the potential difference between two levels amount to if the associated spectral line has a wavelength of 500 nm?

Question 4.24 Frequently the Boltzmann ratio between two levels is written as:

$$\log(n_2/n_1)^{\text{TE}} = \log(g_2/g_1) - \chi_{12} \theta,$$

with χ_{12} in eV. What is θ ?

4.3.3 Saha distribution

In TE, the distribution of particles over the ionization states of an element is given by the *Saha law*. There are also two versions of this law. For a ground level:

$$\left[\frac{n_{r+1,0}}{n_{r,0}} \right]^{\text{TE}} N_e = \frac{2g_{r+1,0}}{g_{r,0}} \left(\frac{2\pi m_e kT}{h^2} \right)^{3/2} e^{-\chi_r/kT} \quad (4.19)$$

with N_e the electron density and m_e the electron mass, $n_{r+1,0}$ and $n_{r,0}$ the populations of the ground states of two adjacent ionization levels, $g_{r+1,0}$ and $g_{r,0}$ their

statistical weights, and χ_r the ionization energy of level r , i.e., the minimal energy necessary to remove an electron from an atom in state $(r, 0)$. The factor 2 for the statistical weight $g_{r+1,0}$ is the statistical weight of the freed electron; each has $g_e = 2$ on account of the two possible orientations of its spin.

For the entire ionization state:

$$\left[\frac{N_{r+1}}{N_r} \right]^{\text{TE}} N_e = \frac{2U_{r+1}}{U_r} \left(\frac{2\pi m_e kT}{h^2} \right)^{3/2} e^{-\chi_r/kT}. \quad (4.20)$$

Or, with the electron pressure $P_e = N_e kT$:

$$\left[\frac{N_{r+1}}{N_r} \right]^{\text{TE}} P_e = \frac{2U_{r+1}}{U_r} \left(\frac{2\pi m_e}{h^2} \right)^{3/2} (kT)^{5/2} e^{-\chi_r/kT}.$$

See page 260 of Rybicki and Lightman for a derivation.

The Saha formula is a particular form (with $U_e = g_e = 2$ and $m_A = m_e \ll m_B = m_{\text{element}}$) of the *general* formula for the constant of equilibrium in the equilibrium reaction $A + B \rightleftharpoons AB$:

$$K_{AB} \equiv \frac{n_A n_B}{n_{AB}} = \left(\frac{2\pi kT}{h^2} \frac{m_A m_B}{m_A + m_B} \right)^{3/2} \frac{U_A U_B}{U_{AB}} e^{-E_{AB}/kT}$$

which also holds for example for the dissociation equilibrium of molecules.

4.3.4 Saha-Boltzmann partitioning

Together, the Boltzmann and Saha laws provide the ratio of populations within a single element; these are named in a single breath the Saha-Boltzmann distribution. To find the particle density in a specific state (number per cm^3) for an *arbitrary* gas mixture in TE we need besides these two laws:

- element conservation: $\sum_r N_r = N_{\text{element}}$;
- matter conservation: $\sum_{\text{element}} \sum_r Z_r N_r = N_e$.

These equations can be solved by numerical iteration. More often than not, only two ionization levels of an element are of interest at the same time. The trace elements with small χ_r must also be included, because these can contribute significantly to the electron density N_e (see the table with ionization energy and abundances in Appendix ??).

To become familiar with the Saha and Boltzmann laws, we give here a numerical example, borrowed from lecture notes of A. Schadee.

Take a hypothetical (but iron-like) element E with:

- ionization energy $\chi_0 = 7$ eV, $\chi_1 = 16$ eV, $\chi_2 = 31$ eV, $\chi_3 = 51$ eV;
- excitation energy: always with 1 eV increments, $\chi_{r,s} = s$ eV;
- statistical weights: $g_{r,s} = 1$ for all levels (r, s) ;
- three characteristic stellar atmospheres: $P_e = 10^3$ dyne/ cm^2 (for all three) and $T_1 = 5\,000$ K, $T_2 = 10\,000$ K and $T_3 = 20\,000$ K.

A straightforward calculation then gives the tables below, with $N = \sum N_r$ the total particle density of this element and with the notation (i) for the order of magnitude $\approx 10^{-i}$.

	U_r	5 000 K	10 000 K	20 000 K
Partition functions	U_0	1.11	1.46	2.25
	$U_1 = U_2 = U_3$	1.11	1.46	2.27

The partition functions appear to be scarcely sensitive to temperature. U_0 is a sum over only 7 levels; the higher levels with $r = 1$ etc. just barely become noticeable above $T = 10\,000$ K (1% difference in the last column). The lowest levels are the most important, as a result of the rapid decline of the Boltzmann factor $e^{-\chi/kT}$.

N_r^{TE}/N		5 000 K	10 000 K	20 000 K
Saha	$r = 0$	0.91	(-4)	(-10)
	1	0.09	0.95	(-4)
	2	(-11)	0.05	0.63
	3	(-36)	(-11)	0.37
	4	(-81)	(-30)	(-5)

In each column there are always only two ionization levels of interest. For $T = 5\,000$ K this element is primarily neutral (E I), for $T = 10\,000$ K it is singly ionized (E II), and only at higher temperatures do the second and third ionization states (E III and E IV) also appear.

$[n_{r,s}/N_r]^{\text{TE}}$		5 000 K	10 000 K	20 000 K
Boltzmann	$s = 0$	0.90	0.69	0.44
	1	0.09	0.22	0.25
	2	0.01	0.07	0.14
	3	(-3)	0.02	0.08
	4	(-4)	0.01	0.04
	5	(-5)	(-3)	0.02
	6	(-6)	(-3)	0.01
	10	(-10)	(-5)	(-3)
	15	(-15)	(-8)	(-4)

A steep decline is seen with $\chi_{r,s}$, but it is less steep at higher temperature.

Populations

The populations of the levels are given by the product of the two tables above:

$$\frac{n_{r,s}^{\text{TE}}}{N} = \left[\frac{n_{r,s}}{N_r} \right]^{\text{TE}} \frac{N_r^{\text{TE}}}{N}.$$

Level $s = 1$ contains a higher maximum population for $r = 1$ (at 10 000 K) than for $r = 0$ (at 5 000 K) because the Boltzmann factor increases with temperature. In general the population of an excited ($s > 0$) level first increases with increasing temperature, until the Saha factor N_r^{TE}/N depletes the population again. The excited levels are less populated than the neutral level. An excited level reaches its maximum population at a higher temperature than the ground level.

- Question 4.25* For $T = 5\,000$ K and $T = 10\,000$ K the sum of the populations is 1, but not for $T = 20\,000$ K. Why?
- Question 4.26* Account for the fact that in the spectrum of the Sun the CaII K line is much stronger than the $H\alpha$ line, while the abundance ratio of calcium and hydrogen in the Sun is $N_{\text{Ca}}/N_{\text{H}} = 1.7 \times 10^{-6}$.
- Question 4.27* A mythical hot star consists of 90% hydrogen and 10% titanium. In the photosphere hydrogen is 50% ionized. Estimate approximately the distribution of titanium over the different ionization states and estimate at the same time the electron density N_e as a fraction of the total particle density N .

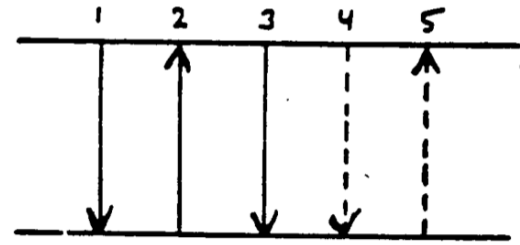
Chapter 5

Discrete processes

5.1 Introduction: bound-bound transitions

We turn now from the macroscopic description to the microscopic specification of the emission and extinction processes by particles. Between two energy levels there are five different processes possible:

1. spontaneous radiative deexcitation;
2. radiative excitation;
3. induced radiative deexcitation;
4. collisional deexcitation;
5. collisional excitation.



These occur both in bb transitions as well as in bf and ff transitions, and especially so in a system in which exchange is possible between internal energy and radiation, and in which consequently *energy levels* can be defined, whether discrete or continuous in energy.

In this chapter we examine these five processes for the bb transitions between *discrete levels*. The various types of discrete energy levels are:

- levels in the electron configurations of atoms and ions;
- levels in the electron configurations of molecules;
- the rotational levels of atoms in molecules about each other;
- the vibrational levels of atoms in molecules with respect to each other;
- the vibrational levels of atoms in a crystal;
- levels in the hadron configurations of atomic nuclei.

The nature of the configurations and the selection rules (which follow from the Pauli exclusion principle for fermions) are not treated here. See for example chapters 9 and 11 of Rybicki and Lightman.

5.2 Five transition processes

5.2.1 Spontaneous deexcitation

A particle in an upper level u can decay spontaneously to a lower energy level l , with spontaneous emission of a photon. The probability that this will occur is defined as the *Einstein coefficient* A_{ul} :

$$A_{ul} \equiv \text{transition probability for spontaneous deexcitation per second per particle in state } u. \quad (5.1)$$

This transition probability is an atomic (or molecular etc.) parameter which does not depend on external conditions such as pressure, temperature, or the radiation field. It differs from transition to transition. Its size differs between *permitted transitions*, with typical values $A_{ul} \approx 10^4 - 10^8 \text{ s}^{-1}$, and *forbidden transitions* with $A_{ul} \approx 1 - 10^2 \text{ s}^{-1}$. The differences are connected with the selection rules that determine the particle configuration. The values can in principle be calculated from quantum mechanics, but in practice must be experimentally determined for non-hydrogen-like transitions.

The number of deexcitations per second per cm^3 is given by:

$$R_{ul} = n_u A_{ul},$$

with n_u the density of the particles in state u (the *population*). R_{ul} is the *rate* of spontaneous deexcitation.

The depletion of the population as a result of spontaneous deexcitation is:

$$dn_u = -n_u A_{ul} dt$$

and so the population is diminished according to:

$$n_u(t) = n_u(0) e^{-A_{ul}t}.$$

If deexcitations to additional lower levels are possible, then the transition probabilities are summed:

$$\Gamma_u \equiv \sum_l A_{ul};$$

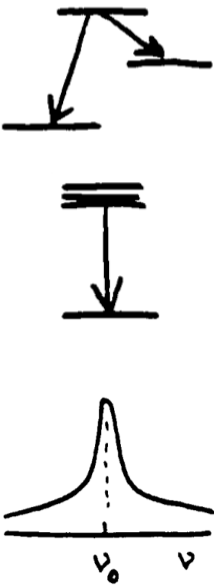
the average lifetime of a particle in state u is then Γ_u^{-1} seconds. The Heisenberg uncertainty principle provides that:

$$\Delta E = \hbar/\Delta t \approx \hbar\Gamma_u$$

so that the spread in the energy of a level that is associated with the finite lifetime is given by $\Delta\omega \approx \Gamma_u$. This is the *natural line width* or *radiative damping*, with Γ_u the *damping constant*. The associated distribution function $\psi(\nu - \nu_0)$ about the line frequency ν_0 is given by the *Lorentz profile*:

$$\psi(\nu - \nu_0) = \frac{\Gamma_u/4\pi^2}{(\nu - \nu_0)^2 + (\Gamma_u/4\pi)^2}. \quad (5.2)$$

This is the profile function for spontaneous emission. It is normalized according to $\int_0^\infty \psi(\nu - \nu_0) d\nu = 1$. Compared to the exponential decline of a Gaussian profile, the wings of the Lorentzian fall off much more slowly, only quadratically according to $\psi \sim 1/(\nu - \nu_0)^2$.



This Lorentz profile describes the constraint on the lifetime of the upper state imposed by spontaneous deexcitation. In practice there is also *collisional damping* as a result of disturbances by neighboring particles which also contribute to the damping constant Γ_u . And there is also macroscopic broadening of the emission profile because the particles are perturbed by each other and therefore emit photons with observable Doppler shifts. A Maxwell distribution leads to a Gaussian function; the resulting profile function is then the convolution of a Gaussian and a Lorentzian and is called a *Voigt function*.

Question 5.1 Demonstrate that the average lifetime in level u is given by Γ_u^{-1} seconds.

Question 5.2 Demonstrate that $\psi(\nu - \nu_0)$ is normalized. What are the dimensions of $\psi(\nu - \nu_0)$?

Question 5.3 How large is the full width at half maximum of $\psi(\nu - \nu_0)$? And of $\psi(\lambda - \lambda_0)$?

5.2.2 Radiative excitation

A photon $h\nu$ of the radiation field can be used for the excitation $l \rightarrow u$. The probability of such a process is determined by the product of a transition probability, which depends solely on the nature of the transition, and the probability of the existence of a suitable photon. Because such a photon may come from any direction, we describe the second probability with the angle-averaged intensity J_ν . As a result of the fuzziness of the levels, there is also some spread in the energy required. For this purpose we employ an *extinction profile function* $\varphi(\nu - \nu_0)$, normalized according to $\int_0^\infty \varphi(\nu - \nu_0) d\nu = 1$ and with dimension $[\text{Hz}^{-1}]$. The angle-averaged radiation field that can cause the excitation is weighted by that as follows:

$$\bar{J}_{\nu_0}^\varphi \equiv \frac{\int_0^\infty J_\nu \varphi(\nu - \nu_0) d\nu}{\int_0^\infty \varphi(\nu - \nu_0) d\nu} = \int_0^\infty J_\nu \varphi(\nu - \nu_0) d\nu, \quad (5.3)$$

and thus $\bar{J}_{\nu_0}^\varphi$ is the frequency-averaged, angle-averaged intensity. The dimensions of $\bar{J}_{\nu_0}^\varphi$ are $[\text{erg s}^{-1} \text{cm}^{-2} \text{Hz}^{-1} \text{ster}^{-1}]$, just as for J_ν and I_ν . (The index ν_0 implies that the calculation refers to the profile function of the bb extinction coefficient with central frequency ν_0 ; this index thus specifies the spectral line involved.)

The first probability we define by means of the *Einstein coefficient for extinction* B_{lu} so that:

$$B_{lu} \bar{J}_{\nu_0}^\varphi \equiv \text{number of radiative excitations per second per particle in state } l. \quad (5.4)$$

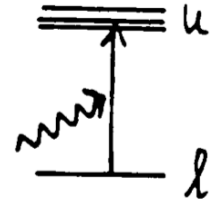
The *excitation rate* is given by $R_{lu} = n_l B_{lu} \bar{J}_{\nu_0}^\varphi$ excitations per second per cm^3 .

This definition shows that, if radiation falls on a particle from all directions with average intensity $\bar{J}_{\nu_0}^\varphi$, the probability of radiative excitation is given by the product $B_{lu} \bar{J}_{\nu_0}^\varphi$. Just like A_{ul} , B_{lu} is thus defined for the full 4π steradians. The definitions can also be given for a given bundle with vertex angle $d\Omega$ and frequency-averaged intensity \bar{I}_{ν_0} ; then $B_{lu} \bar{I}_{\nu_0} (d\Omega/4\pi)$ is the number of excitations per particle with photons in this bundle. In that case B_{lu} has the same numerical value.

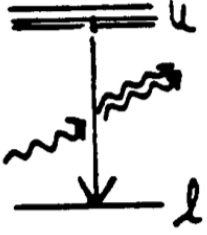
Sometimes A and B are defined to be smaller by a factor 4π , with the number of excitations per second per particle given by $B_{lu} \int \bar{I}_{\nu_0} d\Omega$, for example in Chandrasekhar (1939), page 191. Also the Einstein coefficients are often defined on the basis of energy density rather than intensity. These then differ by a factor of $c/4\pi$.

Question 5.4 Why do we have $\bar{J}_{\nu_0}^\varphi$ per Hz when this quantity is integrated over the frequency?

Question 5.5 What are the dimensions of B_{lu} ?



5.2.3 Induced deexcitation



In order to derive the Planck formula, Einstein introduced a third radiative process and a third coefficient:

$$B_{ul}\bar{J}_{\nu_0}^x \equiv \text{number of induced deexcitations per second per particle in state } u \quad (5.5)$$

This definition is analogous to the one for B_{lu} , but with

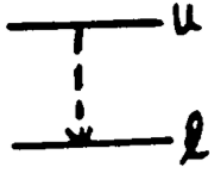
$$\bar{J}_{\nu_0}^x \equiv \int_0^\infty J_\nu \chi(\nu - \nu_0) d\nu$$

in which $\chi(\nu - \nu_0)$ is the normalized profile function for induced = stimulated emission.

Stimulated emission produces radiation moving in the same direction as the radiation which triggered the process. A definition per incident bundle is thus also possible here: then $B_{ul}\bar{I}_{\nu_0}(d\Omega/4\pi)$ is the number of deexcitations induced by a bundle with vertex angle $d\Omega$ that are contributed to the same bundle.

5.2.4 Collisional excitation and collisional deexcitation

For bb *collisional processes* transition probabilities are similarly defined as:



$$C_{ul} \equiv \text{number of collisional deexcitations per second per particle in state } u \quad (5.6)$$

and

$$C_{lu} \equiv \text{number of collisional excitations per second per particle in state } l. \quad (5.7)$$

The *collision rates* are: $n_u C_{ul}$ and $n_l C_{lu}$ per second per cm^3 .

These coefficients depend on the density and the particle velocities, and on the nature of the interaction.

For example, for transitions of state i to state j via collisions with electrons we have:

$$n_i C_{ij} = n_i N_e \int_{v_0}^\infty \sigma_{ij}(v) f(v) v dv$$

with v_0 the threshold energy, the minimum kinetic energy required $(1/2)mv_0^2 = h\nu_0$, N_e the electron density per cm^3 , σ the collisional cross section and $f(v)$ the velocity distribution (generally the Maxwellian distribution).

We are usually talking about Coulomb interactions here. For an ionized gas in which the Maxwellian distribution holds, the fraction of particles above the threshold energy is the same for each type of particle, but the particle velocities and therefore the collisional frequencies are not the same. From $\frac{1}{2}m \langle v^2 \rangle = \frac{3}{2}kT$ it follows that:

$$\frac{\text{number of electron collisions}}{\text{number of ion collisions}} \sim \frac{N_e \langle v_e \rangle}{N_{\text{ion}} \langle v_{\text{ion}} \rangle} = \frac{N_e}{N_{\text{ion}}} \left(\frac{m_H A}{m_e} \right)^{1/2}$$

with A the atomic weight on the C=12 scale and N_{ion} the ion density per cm^3 . For hydrogen this ratio is already $\sqrt{m_p/m_e} = 43$; with the more complete ionization of heavier atoms, the electrons win out even more convincingly because then $N_e > N_{\text{ion}}$.

In a partially *neutral* gas it can happen that hydrogen is mostly neutral and that free electrons are supplied only by elements with lower ionization energies, including Fe,

Mg and the alkali elements (see Appendix ??). Then collisions with neutral hydrogen atoms often dominate, on account of the large abundance of hydrogen and the large polarizability of the hydrogen atom (a consequence of its asymmetrical mass distribution).

The collisional cross sections σ are usually not well known for electron collisions, and for collisions with neutral atoms they are almost entirely unknown.

5.3 Einstein relations

Next we express the Einstein coefficients A_{ul} , B_{lu} and B_{ul} defined above in terms of each other, under the assumption of thermodynamical equilibrium. In TE *detailed* balance holds for each process, thus there are as many transitions downwards as upwards. This holds for each individual process as well: (as many *radiating* downwards as *radiating* upwards), and it holds also at each frequency, it being implicit that the profile functions ψ , φ , and χ are equal. Therefore in TE we have:

$$\begin{aligned} n_l B_{lu} \bar{J}_{\nu_0}^{\varphi} &= n_u A_{ul} + n_u B_{ul} \bar{J}_{\nu_0}^{\chi} \\ \bar{J}_{\nu_0} &\equiv \bar{J}_{\nu_0}^{\chi} = \bar{J}_{\nu_0}^{\varphi} \\ &= \frac{n_u A_{ul}}{n_l B_{lu} - n_u B_{ul}} \\ &= \frac{A_{ul}/B_{ul}}{\frac{n_l}{n_u} \frac{B_{lu}}{B_{ul}} - 1} \\ &= \frac{A_{ul}/B_{ul}}{\frac{g_l}{g_u} \frac{B_{lu}}{B_{ul}} e^{h\nu/kT} - 1}, \end{aligned}$$

in which we make use of the Boltzmann law, which holds in TE.

Furthermore, it is true in TE that $J_{\nu} = B_{\nu}$. Because B_{ν} changes only slowly with frequency over the small width of the extinction profile $\varphi(\nu - \nu_0)$ it is usually also true that $\bar{J}_{\nu_0} = B_{\nu}$, and so:

$$B_{\nu} = \frac{A_{ul}/B_{ul}}{\frac{g_l}{g_u} \frac{B_{lu}}{B_{ul}} e^{h\nu/kT} - 1}.$$

This formula holds for arbitrary temperature, just as the Planck formula does. Equating these, we find:

$$\frac{B_{lu}}{B_{ul}} = \frac{g_u}{g_l} \quad \text{and} \quad \frac{A_{ul}}{B_{ul}} = \frac{2h\nu^3}{c^2}. \quad (5.8)$$

These are the *Einstein relations*. There are two equations with three unknowns, and so you only have to know but a single one to determine the others.

Next we have a typically Einsteinian piece of reasoning. These relationships connect A_{ul} , B_{ul} and B_{lu} without regard to the temperature. Just above we noted that these coefficients are defined as atomic parameters that do not depend on external conditions. So if these relationships hold anywhere, they must hold everywhere. Thus the Einstein relations hold *generally*, even in media where the assumption of TE does not hold, or where $\bar{J}_{\nu_0} \neq B_{\nu}$ or where $\varphi \neq \chi$. These are “detailed balance” relationships which ensure that in the proper circumstances equilibrium certainly *can* occur. This forms a generalization of Kirchhoff’s law ($j_{\nu} = \alpha_{\nu} B_{\nu}$ in TE).

For the collisional rates there follows similarly for TE:

$$n_l C_{lu} = n_u C_{ul}$$

thus

$$\frac{C_{ul}}{C_{lu}} = \frac{g_l}{g_u} e^{E_{lu}/kT}, \quad (5.9)$$

with the application of the Boltzmann law. This relationship also holds generally, even outside TE. The knowledge of a single collisional transition probability is thus enough.

Question 5.6 Do the dimensions tally on the left- and right-hand sides of equation (5.8)?

5.4 Emission coefficient and extinction coefficient

Spontaneous deexcitation provides photons headed in all directions. We define the output of radiated energy per Hz and per steradian:

A_{ul} = number of spontaneous deexcitations per second per particle in state u ,

$n_u A_{ul} = R_{ul}$ = number of deexcitations per second per cm^3 ,

$h\nu_0 n_u A_{ul}$ = energy radiated per second per cm^3 ,

$h\nu_0 n_u A_{ul} \psi(\nu - \nu_0)$ = energy radiated per second per cm^3 per Hz,

$h\nu_0 n_u A_{ul} \psi(\nu - \nu_0)/4\pi$ = energy radiated per second per cm^3 per Hz per steradian.

Thus we have for the associated emission coefficient:

$$j_\nu^{\text{spont}} = h\nu_0 n_u A_{ul} \psi(\nu - \nu_0)/4\pi. \quad (5.10)$$

Now the radiative excitation. The total energy in a volume dV that is extinguished by radiative excitation during dt is:

$$\begin{aligned} dE^{\text{tot}} &= -h\nu_0 n_l B_{lu} \bar{J}_{\nu_0}^\varphi dV dt \\ &= -h\nu_0 n_l B_{lu} dV dt \int J_\nu \varphi(\nu - \nu_0) d\nu \\ &= -\frac{h\nu_0}{4\pi} n_l B_{lu} dV dt \iint I_\nu \varphi(\nu - \nu_0) d\Omega d\nu, \end{aligned}$$

thus the energy dE^{bundle} that is extinguished during a time dt in a given bundle with intensity I_ν , opening angle $d\Omega$ and bandwidth $d\nu$ in dV is:

$$dE^{\text{bundle}} = -\frac{h\nu_0}{4\pi} n_l B_{lu} I_\nu \varphi(\nu - \nu_0) dV dt d\Omega d\nu,$$

and from $dV = dA ds$ and the definitions of intensity and extinction coefficient it follows that:

$$\alpha_\nu^{\text{excitation}} = \frac{h\nu_0}{4\pi} n_l B_{lu} \varphi(\nu - \nu_0).$$

Now the stimulated emission. It seems obvious that we should introduce an extra emission coefficient and then sum this up with the coefficient for spontaneous emission. However, stimulated emission is much more similar to radiative excitation than to spontaneous deexcitation; just as before this is proportional to \bar{J}_{ν_0} . In practice, these processes always occur together. Consequently the stimulated emission is not usually included with the emission coefficient but is treated as “negative extinction”, i.e., as a correction to the extinction.

Thus we have the *line extinction coefficient* α_ν^l :

$$\alpha_\nu^l = \frac{h\nu_0}{4\pi} [n_l B_{lu} \varphi(\nu - \nu_0) - n_u B_{ul} \chi(\nu - \nu_0)] \quad (5.11)$$

and the *line emission coefficient* j_ν^l remains:

$$j_\nu^l = \frac{h\nu_0}{4\pi} n_u A_{ul} \psi(\nu - \nu_0).$$

The excitation coefficient $\alpha_\nu^{\text{excitation}}$ is a more fundamental quantity than the deexcitation coefficient j_ν^{spont} because the latter depends more strongly on the local radiation field. This occurs because j_ν contains the recent history of the excited particle in the term n_u . An atom or molecule can for example be excited to level u prior to the spontaneous deexcitation by radiative excitation in the same spectral line (*photon scattering*), by radiative excitation in another spectral line or by radiative deexcitation from a higher level (*photon conversion*), or by a collisional excitation or collisional deexcitation (*photon creation*). Each of these mechanisms counts, and thus the emission coefficient depends directly on the medium and on the radiation field. The excitation is a form of internal energy which, in the presence of substantial scattering and conversion of photons, can be determined primarily by *nonlocal* conditions; via photons transported from afar by the radiation field.

The situation is different for the excitation coefficient $\alpha_\nu^{\text{excitation}}$, since the exciting radiation field itself does not enter into the determination of the coefficient, nor is it sensitive to recently deposited internal energy. This coefficient is thus governed by the medium. While it is true that the state of the medium, and thus the population of the lower level, can be strongly dependent on whatever radiation field may be present, nevertheless the coupling is much less direct than for a recently excited level.

The introduction of a correction term for the stimulated emission in the line extinction coefficient blurs this distinction. The line extinction coefficient α_ν^l is then:

$$\alpha_\nu^l = \frac{h\nu_0}{4\pi} n_l B_{lu} \varphi(\nu - \nu_0) \left[1 - \frac{n_u B_{ul} \chi(\nu - \nu_0)}{n_l B_{lu} \varphi(\nu - \nu_0)} \right]$$

thus the correction factor is:

$$1 - \frac{n_u B_{ul} \chi(\nu - \nu_0)}{n_l B_{lu} \varphi(\nu - \nu_0)} = 1 - \frac{n_u g_l \chi(\nu - \nu_0)}{n_l g_u \varphi(\nu - \nu_0)}.$$

The correction is large (a large reduction) if the excited level has a relatively large population. In that case the extinction coefficient is also directly governed by the radiation field.

Einstein introduced the stimulated emission process only because without it he could only derive the Wien approximation and not the Planck function. The Wien approximation can readily be deduced because in this case $h\nu \gg kT$, so that according to the Boltzmann distribution the population n_u of the excited level is small and the contribution of stimulated emission is negligible.

With α_ν^l , B_{lu} , B_{ul} and A_{ul} , we have now *four* parameters that describe how readily a bb transition will occur: the bb transition probability. You have only to know but one (from calculation or measurement). For the most part however we employ none of these four but rather a *fifth* parameter: the *oscillator strength* f . The term stems from the classical description of a spectral line as a harmonic oscillator, in which the extinction coefficient per particle $\sigma(\nu)$ is given by (Chapter 6):

$$\sigma(\nu) = \frac{\pi e^2}{m_e c} \frac{\Gamma/4\pi^2}{(\nu - \nu_0)^2 + (\Gamma/4\pi)^2} = \frac{\pi e^2}{m_e c} \varphi(\nu - \nu_0)$$

with

$$\sigma \equiv \int_0^\infty \sigma(\nu) d\nu = \frac{\pi e^2}{m_e c} = 0.02654 \text{ cm}^2 \text{ Hz}.$$

The oscillator strength f_{lu} is introduced as a correction factor to this classical value, neglecting the correction for stimulated emission:

$$\sigma^l = \int_0^\infty \frac{\alpha_\nu^l}{n_l} d\nu = \frac{h\nu_0}{4\pi} B_{lu} \equiv \frac{\pi e^2}{m_e c} f_{lu}.$$

For resonance lines such as Ly α the classical oscillator is a good approximation so that $f_{lu} \approx 1$, and so the oscillator strength has a reasonable numerical size. Other permitted transitions have $10^{-4} \leq f_{lu} \leq 10^{-1}$; forbidden transitions have $f_{lu} \leq 10^{-6}$.

We derive the correction for stimulated emission in TE with the use of the Einstein relations, Boltzmann's law, and the equality $\varphi = \chi$ which is valid for TE, as:

$$1 - \frac{n_u B_{ul} \chi(\nu - \nu_0)}{n_l B_{lu} \varphi(\nu - \nu_0)} = 1 - e^{-h\nu_0/kT}.$$

This factor is often given as “the” correction for stimulated emission, but strictly speaking it holds only in TE. With this the line extinction coefficient is ultimately represented as:

$$\alpha_\nu^l = \frac{\pi e^2}{m_e c} n_l f_{lu} \varphi(\nu - \nu_0) \left[1 - e^{-h\nu_0/kT} \right].$$

And finally we have yet a sixth quantity: the product $g_l f_{lu}$ that is usually referred to as the “gf-value”. This is the quantity that you will encounter most frequently in the literature as the “transition probability”.

Question 5.7 What are the dimensions of α_ν^l , j_ν^l , f_{lu} and $g_l f_{lu}$?

Question 5.8 Express the photoexcitation rate R_{lu} in terms of $\alpha_\nu^{\text{excitation}}$ and I_ν .

Question 5.9 Express the line extinction coefficient α_λ^l in terms of f_{lu} and the profile function $\lambda(\nu - \lambda_0)$.

Question 5.10 The HI 21-cm line has $A_{ul} = 2.9 \times 10^{-15} \text{ s}^{-1}$. What is the oscillator strength of this line? How many hydrogen atoms are needed to provide an optical thickness of unity in this line?

5.5 Source function

Lastly, the *line source function* S_ν^l is given by:

$$S_\nu^l \equiv j_\nu^l / \alpha_\nu^l = \frac{n_u A_{ul} \psi(\nu - \nu_0)}{n_l B_{lu} \varphi(\nu - \nu_0) - n_u B_{ul} \chi(\nu - \nu_0)}.$$

Because the Einstein relations also hold outside of TE, we have a very general result for the line source function, and in fact for the source function of an arbitrary radiative transition:

$$\begin{aligned} S_\nu &= \frac{\frac{A_{ul} \psi}{B_{ul} \varphi}}{\frac{n_l B_{lu}}{n_u B_{ul}} - \frac{\chi}{\varphi}} \\ &= \frac{2h\nu^3}{c^2} \frac{\psi/\varphi}{\frac{g_u n_l}{g_l n_u} - \frac{\chi}{\varphi}}. \end{aligned} \quad (5.12)$$

The assumption of *complete redistribution* is frequently made. This states that in the case of elastic bb scattering, atoms have no “memory”: that the photon resulting from deexcitation is not correlated with the photon that was responsible for the excitation. In this case the three frequency distributions are equal because for each process the statistical distribution is represented anew: $\phi(\nu - \nu_0) = \psi(\nu - \nu_0) = \chi(\nu - \nu_0)$. In that case the general line source function simplifies to:

$$S_\nu^l = \frac{n_u A_{ul}}{n_l B_{lu} - n_u B_{ul}} = \frac{2h\nu^3}{c^2} \frac{1}{\frac{g_u n_l}{g_l n_u} - 1}. \quad (5.13)$$

Question 5.11 Using equation (5.13), demonstrate that $S_\nu = B_\nu$ for TE.

Question 5.12 What is the relationship between spontaneous deexcitation and stimulated emission in TE? Which deexcitation process dominates in the Wien limit, and which in the Rayleigh-Jeans limit?

Chapter 6

Continuous processes

6.1 Introduction: four types of interaction

In this chapter we treat the processes which give rise to *continuous* extinction and emission. For highly-energetic conditions the relativistic forms are of interest; because a complete treatment of these requires a knowledge of Maxwell's equations and relativity theory, what follows here is only a simplified summary of Chapters 3 through 8 of Rybicki and Lightman. See also Chapter 6 of Harwitt (1988).

There are four global types of continuous radiative processes of interest:

- extinction and emission as a result of the acceleration of a charged particle in an electric field (the electric field of an EM-wave itself);
- extinction and emission as a result of the acceleration of a charged particle in a magnetic field;
- effects resulting from collective electric fields;
- extinction and emission as a result of nuclear reactions.

6.2 Radiation from an accelerating charge

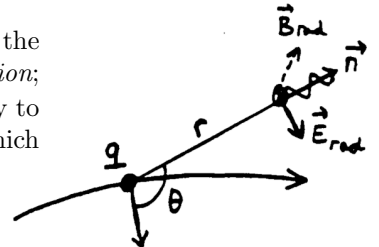
From Maxwell's equations it follows that a particle with an electric charge that experiences an acceleration emits EM radiation. If the acceleration is generated by incident electromagnetic radiation, a charged particle can also absorb or scatter. Consider *nonrelativistic* velocities $v \ll c$ in vacuum. It follows from Maxwell's equations that the EM field generated at a distance r from a charge q that experiences an acceleration $\vec{v} = d\vec{v}/dt$ is given by

$$\vec{E}_{\text{rad}}(r, t) = \left[\frac{q}{rc^2} \vec{n} \times (\vec{n} \times \vec{v}) \right] \quad (6.1)$$

$$\vec{B}_{\text{rad}}(r, t) = \left[\vec{n} \times \vec{E}_{\text{rad}} \right], \quad (6.2)$$

with c the speed of light and \vec{n} a unit vector in the direction of propagation of the light \vec{E}_{rad} lies in the plane of \vec{v} and \vec{n} ; \vec{B}_{rad} is perpendicular to this.

The square brackets on the right-hand sides refer to the fact that at distance r the acceleration of the charge q is felt only after r/c seconds. This delay is called *retardation*; the brackets indicate that the values on the right-hand sides of \vec{E}_{rad} and \vec{B}_{rad} apply to the “retarded times”: the time lag t amounts to r/c seconds from the moment at which \vec{v} , r and \vec{n} are determined. See §§ 2.5 and 3.1–3.2 of Rybicki and Lightman.



For the amplitudes we have:

$$|\vec{E}_{\text{rad}}| = |\vec{B}_{\text{rad}}| = \frac{q\dot{v}}{rc^2} \sin \theta$$

with θ the angle between \vec{v} and \vec{n} . The flow of energy in the direction \vec{n} in $\text{erg cm}^{-2} \text{ s}^{-1}$ (possibly measured monochromatically per Hz) is given by the *Poynting vector*

$$\vec{S} = \frac{c}{4\pi} \vec{E}_{\text{rad}} \times \vec{B}_{\text{rad}}$$

with amplitude:

$$S = \frac{c}{4\pi} E_{\text{rad}}^2 = \frac{c}{4\pi} \frac{q^2 \dot{v}^2}{r^2 c^4} \sin^2 \theta. \quad (6.3)$$

Through a surface dA during dt the flow of energy is:

$$dE = |\vec{S}| dt dA = \frac{q^2 \dot{v}^2}{4\pi c^3} \sin^2 \theta \frac{dt dA}{r^2}.$$

With $d\Omega = dA/r^2$, we have the angle-dependent power that the particle radiates in the direction \vec{n} (r/c seconds earlier):

$$\frac{dP}{d\Omega} \equiv \frac{dE}{dt d\Omega} = \frac{q^2 \dot{v}^2}{4\pi c^3} \sin^2 \theta. \quad (6.4)$$

The factor $\sin^2 \theta$ provides a *dipole pattern*: there is no radiation emitted parallel to \vec{v} , and a maximum perpendicular to \vec{v} .



Figure 6.1: Dipole radiation from an accelerated charge.

Integration of $dP/d\Omega$ over all directions provides the *Larmor formula* for the total amount of radiative power:

$$P = \frac{q^2 \dot{v}^2}{4\pi c^3} \int \sin^2 \theta d\Omega = \frac{2q^2 \dot{v}^2}{3c^3} \quad (6.5)$$

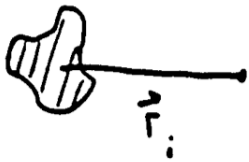
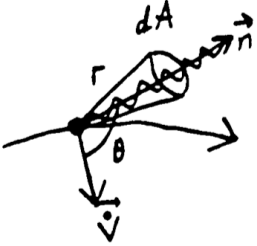
with the use of $\int \sin^2 \theta d\Omega = 2\pi \int_0^\pi \sin^3 \theta d\theta = 2\pi \int_{-1}^{+1} (1 - \mu^2) d\mu = 8\pi/3$ with $\mu = \cos \theta$.

These equations often hold (in the *dipole approximation*) for systems of primarily non-relativistic particles:

$$\begin{aligned} \frac{dP}{d\Omega} &= \frac{\ddot{d}^2}{4\pi c^3} \sin^2 \theta \\ P &= \frac{2\ddot{d}^2}{3c^3}, \end{aligned}$$

with the *dipole moment* $\vec{d} \equiv \sum_i q_i \vec{r}_i$ and θ the angle between \vec{d} and the direction of propagation of the radiation \vec{n} .

These equations give a *classical* description in which an EM-field is present all around an accelerated charge; in reality, however, the radiation field is quantized.



In the quantum mechanical formulation, not presented here, the Larmor equation is a *statistical distribution* for the emission of quanta of radiation, i.e., photons. There follow below additional classical descriptions which also always translate into photon processes. For the most part we are concerned with the emission or absorption of one single photon; the quantum mechanical probability of a second simultaneous photon is then negligibly small.

6.3 Electrons and electric fields

6.3.1 Free-free transitions

We first discuss the radiative processes that take place during the Coulomb acceleration of a free charged particle that moves in the electric field of another particle: *Bremsstrahlung* = *braking radiation* in German. Only those collisions between dissimilar particles are interesting here, because in collisions of similar particles (proton–proton, electron–electron etc.) $\vec{d} = \sum q_i \vec{r}_i \sim \sum m_i \vec{r}_i$. The center of mass of this system is a conserved quantity, and so $P = 0$ according to the last equation in the previous paragraph on dipole radiation. (Higher-order radiation such as quadrupole radiation we leave to outside sources – it is beyond the scope of this treatment.) Thus we are usually dealing with electron–ion collisions, i.e., with ff processes.

We take a classical (non-quantum-mechanical) approach. Place the ion at the origin so that $\vec{d} = -e\vec{r}$ with $-e$ the electron charge and consider it stationary on account of its much larger mass. The Larmor law then gives

$$P = \frac{2e^2}{3c^3} \dot{v}^2$$

where \dot{v} is the Coulomb acceleration between electron and ion. This is the instantaneously radiated power; the total ff emission per electron–ion collision we approximate by

$$E(b, v) = \int P dt \approx \frac{2e^2}{3c^3} (\Delta v)^2 \approx \frac{2e^2}{3c^3} (\Delta v_{\perp})^2,$$

assuming that the deflection of the electron is negligibly small so that only the component of the Coulomb acceleration perpendicular to the direction of incidence matters; this amounts to $\dot{v}_{\perp} = \dot{v} \cos(\pi/2 - \theta) = \dot{v} b/r$ with θ the angle between direction of incidence and the Coulomb acceleration, and with the distance of closest approach given by the *impact parameter* b . With the Coulomb force $m\dot{v} = Ze^2/r^2$ for an ion charge of size Ze it follows from the Pythagorean theorem that:

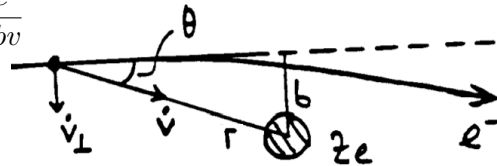
$$\Delta v_{\perp} = \int \dot{v}_{\perp} dt = \frac{Ze^2}{m_e} \int_{-\infty}^{\infty} \frac{b}{r^3} dt = \frac{Ze^2}{m_e} \int_{-\infty}^{\infty} \frac{b}{(b^2 + v^2 t^2)^{3/2}} dt = \frac{2Ze^2}{m_e b v}$$

so that

$$E(b, v) \approx \frac{8Z^2 e^6}{3c^3 m_e^2 b^2 v^2}$$

per electron–ion collision with parameters Z , b and v .

Conservation of energy requires that this radiated energy be provided at the expense of the kinetic energy. Assuming the ion to be immobile, we find $m_e v_1^2/2 = m_e v_2^2/2 + h\nu$ in ff emission and $m_e v_1^2/2 + h\nu = m_e v_2^2/2$ in ff absorption, with v_1



the velocity of the electron before the collision and v_2 the velocity afterwards. The *acceleration* perpendicular to the path therefore produces a *deceleration* along the direction of travel, from whence the name “braking radiation”. This last deceleration is neglected in the above derivation. In ff absorption this goes the other way round: the energy of an incoming photon is augmented by the Coulomb acceleration and results in an increase of kinetic energy.

To arrive at the total macroscopic energy transfer, $E(b, v)$ must be integrated over $2\pi b db$ about the ion and multiplied by the ion density N_{ion} , the flux $N_e v$ of electrons with velocity v and the velocity distribution $f(v) dv$. The integration boundaries b_{min} and b_{max} require closer analysis, which we skip here. The final result for the emission coefficient is:

$$j_\nu^{\text{ff}} = 5.4 \times 10^{-39} Z^2 N_e N_{\text{ion}} T^{-1/2} e^{-h\nu/kT} \bar{g}_{\text{ff}}$$

with N_e the electron density, $N_{\text{ion}} = \sum_{\text{element}} \sum_s n_{r,s}$ the ion density (of all ions with charge Z , for example H^+ and He^+ together) and \bar{g}_{ff} the velocity-averaged *Gaunt factor*. This gives the quantum mechanical correction to the classically deduced remainder of the formula; it is dimensionless, of order unity, and is determined by the values of b_{min} and b_{max} . (The wave and quantum mechanical corrections arise because the fact must be accounted for that the electrons describe stable Bohr orbits in an atom, rather than spiralling inward as they radiate in the manner predicted by this classical description. Consequently the above approach fails for small impact parameter b because quantum effects are neglected; the Gaunt factor measures the size of this error.)

The factor $T^{-1/2}$ appears in j_ν^{ff} because the generated emission is inversely proportional to the velocity v (v^{-2} per collision times v from the electron flux) and for the average velocity we have $\langle v \rangle \sim T^{1/2}$. The factor $\exp(-h\nu/kT)$ is a result of the lower boundary in the integration over the Maxwell distribution: there must be sufficient kinetic energy on hand to generate a photon of this frequency.

In the case of TE the ff source function is given by the Planck function $B_\nu(T)$. That is also true outside of TE provided that the particle motions are Maxwellian, because ff processes *always* exchange kinetic energy and radiative energy. In each ff emission process a photon is released from the “thermal pool”; there is no intrinsic record such as occurs for the bb processes by which the escaping photon can be equal (except in direction) to the photon just arrived. In such elastic scattering there is no exchange of radiation energy and kinetic energy; in inelastic scattering, which is the case for the ff processes, the memory of the collision is erased, with a new sample drawn from the Maxwell distribution. Thus the extinction coefficient, even outside of TE, is given by

$$\alpha_\nu^{\text{ff}} = j_\nu^{\text{ff}}/B_\nu(T) = 3.7 \times 10^8 Z^2 N_e N_{\text{ion}} T^{-1/2} \nu^{-3} (1 - e^{-h\nu/kT}) \bar{g}_{\text{ff}}.$$

In this expression T is the kinetic temperature, i.e., the temperature of the Maxwellian distribution; this is usually called the *electron temperature* T_e . “Outside of TE” means here that the Saha and Boltzmann equations do not hold for all states *a priori*, and that $I_\nu = B_\nu$ does not hold *a priori* for all directions and frequencies. The conclusion that $S_\nu^{\text{ff}} = B_\nu^{\text{ff}}$ implies that under conditions where at least the Maxwellian distribution holds, the *partial* source function for the free-free processes is *always* equal to the Planck function at that spot, even if that is not the case for other processes. If such other processes contribute to the particle populations these can deviate from the Saha and Boltzmann distributions.

The factor $1 - \exp(-h\nu/kT)$ follows from the -1 in the Planck law and describes the contribution of induced emission. This was not included in the emission coeffi-

cient above and therefore results in a reduction of the extinction coefficient. If the Wien approximation holds ($h\nu \gg kT$) this correction is negligible:

$$\alpha_{\nu}^{\text{ff}} \approx 3.7 \times 10^8 Z^2 N_e N_{\text{ion}} T^{-1/2} \nu^{-3} \bar{g}_{\text{ff}},$$

with frequency dependence $\alpha_{\nu}^{\text{ff}} \sim \nu^{-3}$. From a physical standpoint, the correction for large $h\nu/kT$ is negligible because the difference between the lower and the higher energy states is then much larger than can be bridged by thermal energy, thus the population of the higher state is negligible and the free-free analog of induced deexcitation hardly matters.

In the Rayleigh-Jeans region ($h\nu \ll kT$) it follows that:

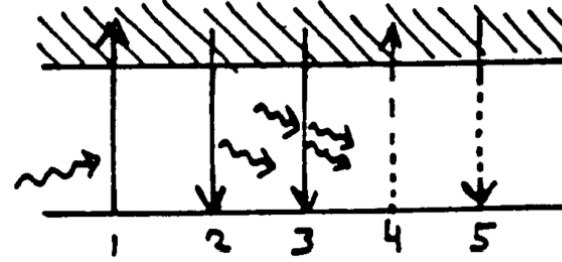
$$\alpha_{\nu}^{\text{ff}} \approx 0.018 Z^2 N_e N_{\text{ion}} \nu^{-2} T^{-3/2} \bar{g}_{\text{ff}},$$

thus there is a frequency dependence $\alpha_{\nu}^{\text{ff}} \sim \nu^{-2}$.

6.3.2 Bound-free transitions

There are once again five possible bf processes:

1. *photoionization*.
A photon of the right frequency is required;
2. *spontaneous photorecombination*.
A passing capturable electron is required;
3. *induced photorecombination*.
Both an available electron and a photon of the right frequency are required;
4. *collisional ionization*.
A passing colliding particle with sufficient energy is required;
5. *collisional recombination*.
A passing colliding particle and a capturable electron are required.



The last process is a 3-particle collision and is therefore usually rare. The processes 1 and 4 require an energy (from the photon or the collision) $E > E_{\infty} - E_n$. The extinction coefficient for each lower level i thus has a limiting value in ν ; the extinction and emission set in suddenly at the *series limit* $\nu = \nu_0$ of the line series with that lower level (Fig. 6.2).

For *hydrogen-like* spectra (H I, He II, Li III, etc.) the extinction coefficient per particle for radiative ionization (without correction for induced recombination) from a level with principal quantum number n for $\nu \geq \nu_0$ is given approximately as:

$$\sigma_{\text{bf}}^{\text{H}} = \frac{64}{3\sqrt{3}} \frac{\pi^4 m e^{10}}{c h^6} \frac{Z^4}{n^5} g_{\text{bf}} \nu^{-3} = 2.815 \times 10^{29} g_{\text{bf}} Z^4 n^{-5} \nu^{-3}$$

in cm^2 ; this formula is due to Kramers, except for the additional quantum mechanical correction factor g_{bf} which was added by Gaunt. The extinction falls off according to $\sigma \sim \nu^{-3}$ for $\nu > \nu_0$. For more elaborate spectra with more valence electrons (for example Fe I in which a half-filled shell provides a number of valence electrons and valence holes) the falloff is disturbed by a variety of peaks in $\sigma_{\text{bf}}(\nu)$ and must be determined experimentally.

These five processes are completely analogous to the discrete bb processes. *Detailed balance* relationships due to Milne hold, which agree with the Einstein relations

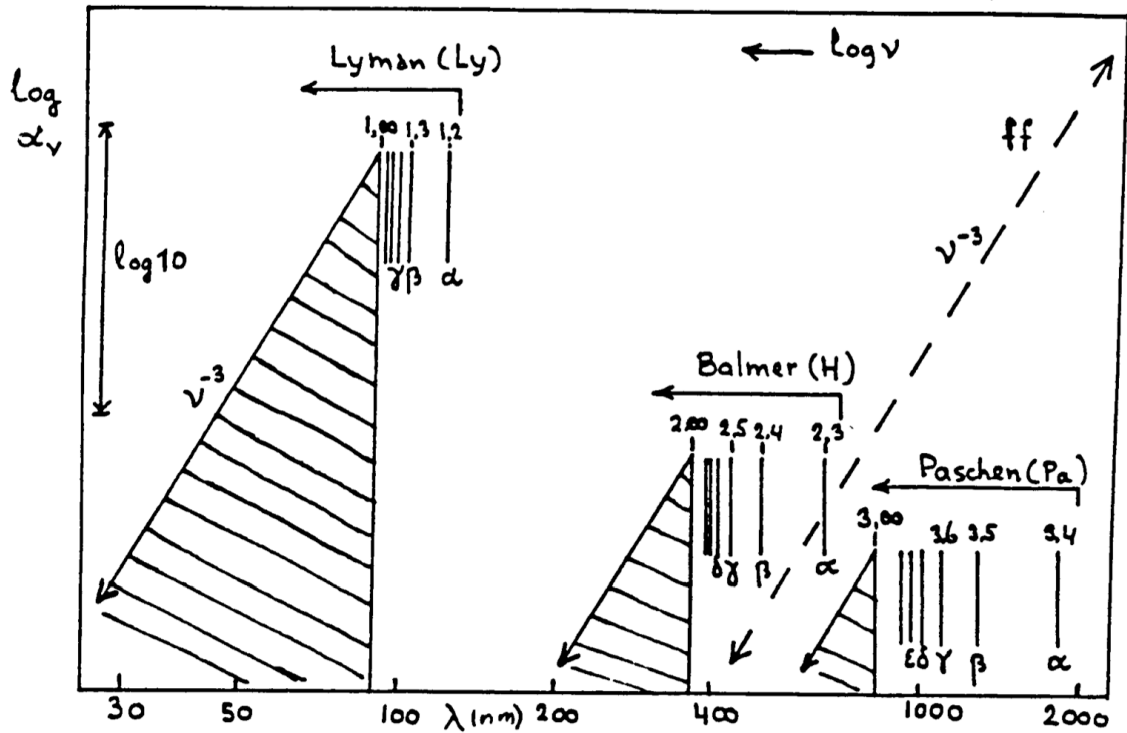


Figure 6.2: The extinction coefficient of neutral hydrogen (shaded). The HI bf extinction coefficient is indicated for the Lyman, Balmer and Paschen series limit continua. The dashed line gives the HI ff extinction coefficient. Several lines in the bb line series are indicated, with their name and the principal quantum numbers n of their lower and upper levels. Each line series becomes compressed towards the series limit. The ionization continuum near this limit goes as $\sim \nu^{-3}$, just like the HI ff coefficient. Sketch by C. Zwaan, for $T \approx 25\,000\text{ K}$.

for bb transitions (see Rybicki and Lightman page 284). In place of the profile functions ψ etc. we now need to integrate over the *series limit continuum* (ionization edge): the bf continuum above the series limit $\nu = \nu_0$. The photoionization rate per second per cm^3 from a bound level i to the continuum k is for example given by:

$$R_{ik} = 4\pi n_i \int_{\nu_0}^{\infty} \frac{\sigma_{ik}(\nu)}{h\nu} J_{\nu} d\nu$$

with ν_0 the frequency of the series limit (compare with question 5.8).

Just like the bb processes and in contrast to the ff processes the bf processes have an intrinsic “memory”: namely the internal part of the energy difference, given by $E_k - E_i$. The kinetic portion of the above is continually thermalized, just as for the ff processes; however, the fixed internal part provides a possibility for elastic scattering analogous to the elastic scattering in bb pairs of processes. Ionization from low-lying levels, with a large fraction of internal energy, more closely resembles bb transitions while ionization from levels close to the continuum more closely resembles ff transitions. The source function of bf transitions therefore is not simply given by $S_{\nu}^{\text{bf}} = B_{\nu}$; it can depend upon the radiation field J_{ν} at the ionization edge.

Question 6.1 The caption to Figure 6.2 implies that α_{ν}^{bf} depends on the temperature. How? Do the relative values of α_{ν}^{bf} at the different series wavelengths also depend upon the temperature? The density?

Question 6.2 Does the general expression for S_ν in equation (5.12) also hold for bf transitions? How then does the possible dependence of J_ν appear? What is the bf analog for the profile functions ψ , χ and φ ?

6.3.3 H^- transitions

A special source of bf and ff extinction is provided by the H^- ion. A neutral H atom, by virtue of its large polarizability, can capture a second electron. Only one bound state is known, with binding energy $E_\infty - E_1 = 0.75$ eV and $\lambda_{\text{limit}} = 1650$ nm. There are consequently no lines, and there is but one bf continuum which does not exhibit a sharp ionization edge but rather a broad peak at much higher frequency, with $\lambda_{\text{max}} = 850$ nm (Figure 6.3).

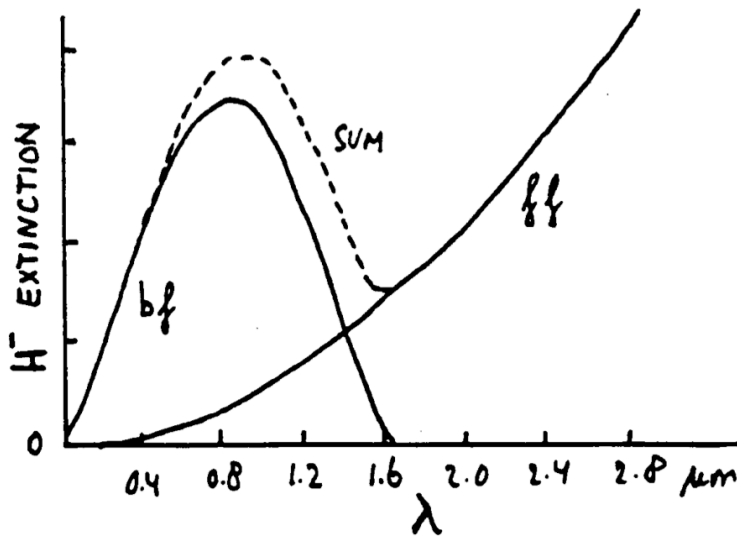


Figure 6.3: Extinction coefficient of the H^- ion. The bf extinction displays a maximum at 800 nm. The ff extinction varies as λ^2 . The sum goes through a minimum at 1.6 μm .

Note carefully the following terminology:

H_{ff} = proton + free electron;

H_{ff}^- = neutral H atom + free electron;

H_{bf} = ionization of an H atom to a proton, or recombination of a proton with an electron to form an H atom;

H_{bf}^- = ionization of H^- ion to an H-atom, or the recombination of an H-atom with electron to form an H^- ion.

These H^- bf and ff processes form the dominant source of visual and infrared extinction in the photospheres of cool stars. Hydrogen is neutral in these stars; the extra electrons come from elements such as Na, Mg, Si and Fe which have a relatively large abundance ($N/N_{\text{H}} \approx 10^{-6}$; see Appendix ??) and an ionization energy lower than that of hydrogen. The identification of this extinction source by Pannekoek and Wildt was an important breakthrough; prior to this the nature of the continuous extinction in cool stars was a large problem. (In Eddington's book "*The Internal Constitution of the Stars*" in 1926 the unknown continuous extinction, together with the similarly unknown source of internal energy of stars, constituted the *sole* remaining problems of the physics of stars; these two have since been solved but nevertheless there is still work to be done.)

Question 6.3 The ff extinction coefficient in Figure 6.3 has $\alpha_{\lambda}^{\text{ff}} \sim \lambda^2$ while in Figure 6.2 $\alpha_{\nu}^{\text{ff}} \sim \nu^{-3}$. Where does this difference come from?

Question 6.4 For these H^- extinction processes $S_{\nu} = B_{\nu}$ is a good assumption not only for the ff but also for the bf transitions. Why?

Question 6.5 The bf peak in Figure 6.3 looks anything but hydrogen-like although it relates directly to hydrogen. Why is that?

6.4 Electrons and photons

6.4.1 Elastic scattering

A charge can also be accelerated by a passing electromagnetic wave: then *scattering* occurs because the emitted radiation resulting from this acceleration can have a different direction from the incident radiation. We treat this scattering first for nonrelativistic conditions where the dipole approximation holds and for which the scattering is elastic, with constant frequency and energy and change only in direction.

A particle with charge q resonates with the incident EM-wave. The outward force that the charged particle experiences is:

$$\vec{F} = q(\vec{E} + \frac{1}{c}\vec{v} \times \vec{B}),$$

but the Lorentz force $(q/c)\vec{v} \times \vec{B}$ is negligible because $v \ll c$ and $E = B$, thus:

$$\vec{F} = qE_0\vec{e} \sin \omega t \quad (6.6)$$

with E_0 the amplitude of the wave with which the particle resonates, \vec{e} a unit vector with direction \vec{E} perpendicular to the incident beam and ω the circular frequency, defined as $\omega = 2\pi\nu$ with ν the frequency of the incident radiation.

We describe the resulting deflection x in the direction of \vec{E} as that of a damped, driven harmonic oscillator:

$$m\ddot{x} + m\Gamma\dot{x} + m\omega_0^2x = qE_0 e^{i\omega t}$$

with m the mass of the particle and ω_0 the resonant frequency of the oscillator. The damping term $m\Gamma\dot{x}$ describes the energy loss that occurs through the emission of the radiation. We use complex notation here because this simplifies the solution; below we retain only the real part \Re . Substitution of $x = x_0 \exp(i\omega t)$ provides

$$x = \Re \left[\frac{q(E_0/m) e^{i\omega t}}{\omega_0^2 - \omega^2 + i\Gamma\omega} \right]$$

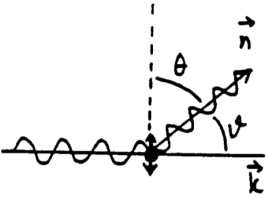
and with $|\ddot{x}|^2 = \ddot{x} \cdot \ddot{x}^*$ and $\ddot{x} = -x_0\omega^2 e^{i\omega t}$ it follows that:

$$|\ddot{x}|^2 = \frac{q^2 E_0^2}{m^2} \frac{\omega^4}{(\omega^2 - \omega_0^2)^2 + \Gamma^2 \omega^2}.$$

Substitution in the Larmor formula (equation 6.5) gives the power radiated:

$$P = \frac{2q^2 |\ddot{x}|^2}{3c^3} = \frac{q^4 E_0^2}{3m^2 c^3} \frac{\omega^4}{(\omega^2 - \omega_0^2)^2 + \Gamma^2 \omega^2}.$$

What is the extinction coefficient? In equation (3.3) the extinction coefficient per particle is defined with $dI_{\nu} = -I_{\nu}\sigma_{\nu}n ds$; for a single particle $n ds = 1 \text{ cm}^{-2}$. The



decrease $-dP$ of the incident energy P_0 is equal to the total energy P radiated (scattered) in all directions, thus

$$\sigma = \frac{-dI}{I} = \frac{-dP}{P_0} = \frac{P}{P_0}$$

where the incident energy P_0 (in erg cm⁻² s⁻¹) is given by the time average of the Poynting flux:

$$P_0 = \langle S \rangle = \frac{c}{4\pi} E_0^2 \langle \sin^2 \omega t \rangle = \frac{c}{8\pi} E_0^2$$

with the use of $\langle \sin^2 \omega t \rangle = 1/2$ ($= \langle \cos^2 \omega t \rangle = \langle [\Re \exp(i\omega t)]^2 \rangle$). Thus the extinction coefficient is:

$$\sigma(\omega) = 8\pi \frac{q^4}{3m^2 c^4} \frac{\omega^4}{(\omega^2 - \omega_0^2)^2 + \Gamma^2 \omega^2}.$$

We simplify this by introducing the *classical electron radius* r_0 , defined as

$$r_0 \equiv \frac{q^2}{mc^2}; \quad (6.7)$$

this is the size of the charged particle if its rest energy mc^2 is equal to the Coulomb energy q^2/r_0 , i.e., if the magnetic field \vec{B} and relativistic and quantum effects are negligible. Therefore:

$$\sigma(\omega) = \frac{8\pi}{3} r_0^2 \frac{\omega^4}{(\omega^2 - \omega_0^2)^2 + \Gamma^2 \omega^2}. \quad (6.8)$$

This extinction coefficient is (a factor of) $(m_p/m_e)^2 \approx 10^6$ times smaller for protons than for electrons and is smaller still for heavier ions; thus electron scattering will usually be the most important. With the classical electron radius

$$r_e = \frac{e^2}{m_e c^2} = 2.82 \times 10^{-13} \text{ cm}$$

and the *Thomson cross section* defined as

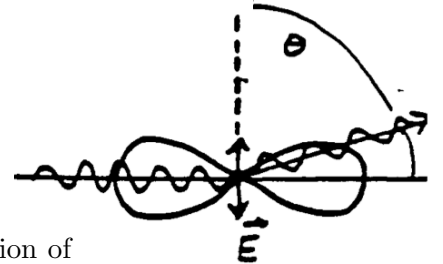
$$\sigma_T \equiv \frac{8\pi}{3} r_e^2 = 6.65 \times 10^{-25} \text{ cm}^2 \quad (6.9)$$

we obtain the extinction coefficient for elastic scattering by harmonically bound electrons:

$$\sigma_e(\omega) = \sigma_T \frac{\omega^4}{(\omega^2 - \omega_0^2)^2 + \Gamma^2 \omega^2}. \quad (6.10)$$

The scattering is not isotropic; the scattered radiation follows the dipole pattern of equation (6.4). The *differential cross section* for scattering into $d\Omega$ is then

$$\begin{aligned} \left[\frac{d\sigma(\theta, \omega)}{d\Omega} \right]_{\text{pol}} &= \frac{q^4}{m^2 c^4} \sin^2 \theta \frac{\omega^4}{(\omega^2 - \omega_0^2)^2 + \Gamma^2 \omega^2} \\ &= r_0^2 \sin^2 \theta \frac{\omega^4}{(\omega^2 - \omega_0^2)^2 + \Gamma^2 \omega^2}. \end{aligned}$$



The angle θ is the angle between the electric field direction \vec{E} and the direction of radiation \vec{n} . The scattering is the largest in the forward and reverse directions, measured along the incident radiation, because the acceleration is directed perpendicular

to the original direction of propagation and the dipole pattern of equation (6.4) and Figure 6.1 runs perpendicular to the acceleration. The index *pol* indicates that we are dealing here with a linearly polarized wave, in agreement with the fixed direction of \vec{E} that was assumed in equation (6.6). An *unpolarized* wave may be described as the superposition of two polarized waves perpendicular to one another:

$$\begin{aligned} \left[\frac{d\sigma}{d\Omega} \right]_{\text{unpol}} &= \frac{1}{2} \left[\frac{d\sigma(\theta)}{d\Omega} + \frac{d\sigma(\pi/2)}{d\Omega} \right] \\ &= \frac{r_0^2}{2} (\sin^2 \theta + 1) \frac{\omega^4}{(\omega^2 - \omega_0^2)^2 + \Gamma^2 \omega^2} \\ &= \frac{r_0^2}{2} (1 + \cos^2 \vartheta) \frac{\omega^4}{(\omega^2 - \omega_0^2)^2 + \Gamma^2 \omega^2}. \end{aligned} \quad (6.11)$$

Here \vec{E}_1 is chosen in the (\vec{k}, \vec{n}) surface with \vec{k} the direction of propagation of the incident radiation and \vec{n} the direction of propagation of the scattered radiation, \vec{E}_2 is chosen perpendicular to the (\vec{k}, \vec{n}) surface, and ϑ is the angle (\vec{k}, \vec{n}) with $\vartheta = \pi/2 - \theta$.

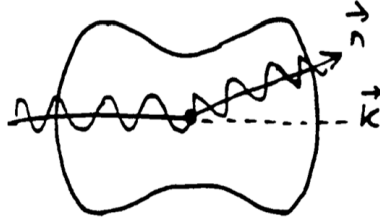


Figure 6.4: *The dipole phase function for elastic scattering of nonpolarized radiation.*

The distribution of the scattered radiation over the angle ϑ between incident and scattered radiation in equation (6.12) is thus $[d\sigma/d\Omega]_{\text{unpol}} \sim 1 + \cos^2 \vartheta$; this is the *dipole phase function*, see Figure 6.4. This does not differ markedly from isotropy: half as much as is scattered forward or backward is scattered in a perpendicular direction. Finally, the total extinction coefficient for the scattering of nonpolarized radiation through electrons amounts to:

$$\begin{aligned} [\sigma_e(\omega)]_{\text{unpol}} &= \int \left[\frac{d\sigma_e}{d\Omega} \right]_{\text{unpol}} d\Omega \\ &= \frac{r_0^2}{2} \frac{\omega^4}{(\omega^2 - \omega_0^2)^2 + \Gamma^2 \omega^2} \int_0^{2\pi} \int_0^\pi (1 + \cos^2 \vartheta) \sin \vartheta d\vartheta d\phi \\ &= \sigma_T \frac{\omega^4}{(\omega^2 - \omega_0^2)^2 + \Gamma^2 \omega^2}, \end{aligned}$$

equal to the cross section for polarized radiation given in equation (6.10). They are the same because an electron at rest has no preferred direction.

6.4.1.1 Rayleigh scattering

The extinction coefficient σ_e in equation (6.10) depends on the difference between the radiation frequency ω and the resonant frequency ω_0 . The last is given by the eigenfrequency of the harmonically bound electron, i.e., a bound electron in an atom or molecule which may resonate harmonically. The chance of such an oscillation is given for actual transitions by the *oscillator strength* f_{lu} which can be viewed as a

quantum mechanical correction factor to the classical harmonic oscillator. This is of order unity for resonance lines, i.e., for permitted bb transitions of the valence electron from the ground level of an atom or ion; for hydrogen for example, this is the Lyman series. For other transitions f_{lu} is much smaller. Then the extinction coefficient for elastic scattering by atoms or molecules per particle in the ground state l and per resonance transition lu is given by:

$$\sigma_e(\omega) = f_{lu} \sigma_T \frac{\omega^4}{(\omega^2 - \omega_0^2)^2 + \Gamma^2 \omega^2}, \quad (6.12)$$

with $\omega_0 = 2\pi\nu_{lu}$ the circular frequency of the bb transition.

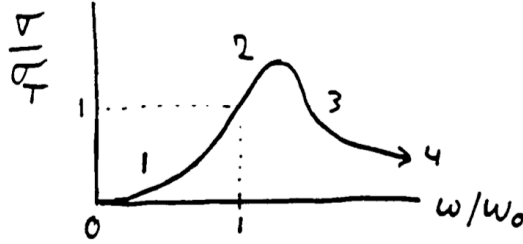


Figure 6.5: *Extinction as a result of electron scattering, in units of the Thomson cross section $\sigma_T = (8\pi/3)r_e^2$. 1 = Rayleigh scattering, 2 = resonance scattering, 3 = Thomson scattering, 4 = Compton scattering.*

Figure 6.5 shows the variation of σ_e/σ_T with ω/ω_0 . There are four different domains. The first domain is that of the *Rayleigh scattering* with $\omega \ll \omega_0$. For this we have:

$$\sigma_e^R(\omega) \approx f_{lu} \sigma_T \left(\frac{\omega}{\omega_0}\right)^4. \quad (6.13)$$

The incident wave vibrates so slowly with respect to the resonant frequency ω_0 that the valence electron resonates without inertia: for $\omega \ll \omega_0$ the fluctuations of the external electric field are experienced as quasistatic. Damping is negligible and higher frequencies are scattered much more strongly than lower ones.

6.4.1.2 Resonant scattering

The second domain in Figure 6.5 has $\omega \approx \omega_0$ so that:

$$\sigma_e(\omega) \approx f_{lu} \sigma_T \frac{\omega_0^2}{4(\omega - \omega_0)^2 + \Gamma^2}$$

A more precise specification of the radiative damping term Γ yields (Rybicki and Lightman §§ 3.5–3.6):

$$\Gamma = \frac{2e^2\omega_0^2}{3m_e c^3}$$

so that

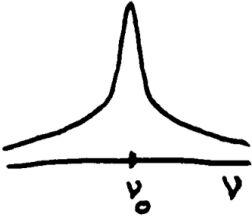
$$\sigma_T \omega_0^2 = \frac{4\pi e^2}{m_e c} \Gamma,$$

and

$$\sigma_e^l(\omega) = \frac{2\pi^2 e^2}{m_e c} f_{lu} \frac{\Gamma/2\pi}{(\omega - \omega_0)^2 + (\Gamma/2)^2}.$$

This is the extinction coefficient per particle for a spectral line with frequency $\omega = \omega_0$, as mentioned in § 5.4.

Without the correction factor f_{lu} this is the resonant oscillation of an undriven, bound oscillator, because such a free vibration can be excited by a pulse of incident radiation of the right frequency. It can also be derived directly from $\ddot{x} + \Gamma\dot{x} + \omega_0^2x = 0$. This is the classical description of a spectral line as a resonant oscillation and is therefore the reason that the most probable bb transitions are called “resonance transitions”, and the associated spectral lines “resonance lines”. The function



$$\psi(\omega - \omega_0) = \frac{\Gamma/2\pi}{(\omega - \omega_0)^2 + (\Gamma/2)^2}$$

is that given in equation (5.2) as the *Lorentz profile* that describes the broadening of the spontaneous emission profile through radiative damping.

6.4.1.3 Thomson scattering

The third domain in Figure 6.5 has $\omega \gg \omega_0$ so that $\sigma_e(\omega) \approx f_{lu} \sigma_T$. For bound electrons this approximation holds if the energy of the incident radiation is so large that the binding energy is negligible, i.e., if the electron behaves as a *free* particle. Then the classical harmonic oscillator is an exact description, thus $f_{lu} = 1$.

This does make one suppose that the Thomson cross section σ_T is the extinction coefficient for elastic scattering by free electrons, called *Thomson scattering*. That is correct; this can be derived directly from the equation of motion $m_e\ddot{x} = eE_0 \sin \omega t$ of a free electron that oscillates with the incident wave without damping and consequently follows here from equation (6.10) by setting to zero the resonant frequency ω_0 and the damping parameter Γ . Thus we have for Thomson scattering by free electrons:

$$\sigma_e^T(\omega) = \sigma_T = \frac{8\pi}{3} r_e^2 = 6.65 \times 10^{-25} \text{ cm}^2, \quad (6.14)$$

independent of the frequency of the incident radiation. The differential extinction coefficient for Thomson scattering of nonpolarized radiation is (equation 6.12):

$$\left[\frac{d\sigma_e^T}{d\Omega} \right]_{\text{unpol}} = \frac{r_e^2}{2} (1 + \cos^2 \vartheta) \quad (6.15)$$

with ϑ the angle between incident and scattered radiation.

Question 6.6 Explain the blue color of the sky. Does the light of the daytime sky contain spectral lines?

Question 6.7 Check that the extinction coefficient for Thomson scattering by free electrons is much larger than for Rayleigh scattering by bound electrons throughout the entire frequency regime where Rayleigh scattering occurs. In what circumstances will Rayleigh scattering nevertheless be important?

Question 6.8 What is the extinction coefficient α_T for Thomson scattering and what is its frequency dependence?

Question 6.9 What is the source function for Thomson scattering?

6.4.2 Inelastic scattering

6.4.2.1 Compton scattering

Just as with Thomson scattering, we are also concerned here with collisions between photons and free charges (electrons), but now, in the fourth domain of Figure 6.5, with photons of high energy for which the approximation no longer holds that the

Coulomb energy is the total energy of the particle, because now the energy $h\nu$ of the photon must also be included. The scattering is then *inelastic*: the EM-wave loses energy to the electron. The size of the energy loss follows by combining, for an initially stationary electron, energy conservation

$$h\nu_1 + m_e c^2 = h\nu_2 + m c^2$$

and momentum conservation

$$\frac{h\nu_1}{c} = \frac{h\nu_2}{c} \cos \vartheta + m v \cos \varphi \quad \text{and} \quad 0 = \frac{h\nu_2}{c} \sin \vartheta - m v \sin \varphi,$$

with $m_e c^2$ the rest mass energy and the mass m given by:

$$m = \frac{m_e}{\sqrt{1 - v^2/c^2}} = m_e \gamma$$

with $\gamma \equiv 1/\sqrt{1 - v^2/c^2}$. The elimination of φ and $m v$ provides:

$$h\nu_2 = \frac{h\nu_1}{1 + (h\nu_1/m_e c^2)(1 - \cos \vartheta)}$$

and consequently

$$\lambda_2 - \lambda_1 = \lambda_c (1 - \cos \vartheta) \quad (6.16)$$

with $\lambda_2 > \lambda_1$ and λ_c the *Compton wavelength*, defined as

$$\lambda_c \equiv \frac{h}{m_e c} = 2.4 \times 10^{-3} \text{ nm}, \quad (6.17)$$

The loss of energy of the photon is negligible for $h\nu \ll m_e c^2 = 0.5 \text{ MeV}$ or $\lambda \gg \lambda_c$; this is the *Thomson condition* for elastic scattering. The relative decrease $\Delta\nu/\nu = -\Delta\lambda/\lambda = -(\lambda_c/\lambda)(1 - \cos \vartheta)$ is large for γ -radiation and negligible in the optical spectral region.

The collisional cross section is given by the Klein-Nishina formula, which is not derived here. It varies with the photon energy. In the extremely relativistic domain where

$$x \equiv \frac{h\nu}{m_e c^2} \gg 1$$

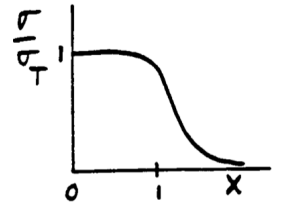
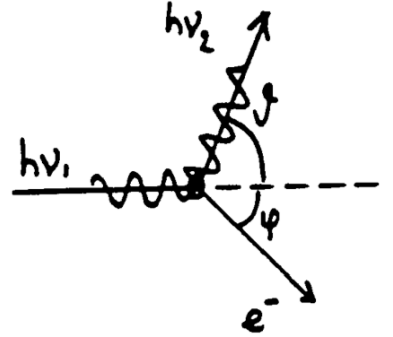
we have that

$$\sigma = \frac{3}{8} \sigma_T \frac{\ln 2x + 1/2}{x}.$$

6.4.2.2 Inverse Compton scattering

Instead of an energy transfer from energetic photons to charges “at rest” we now have the opposite: an energy transfer from energetic particles (usually relativistic electrons) to photons. We now need to make the relativistic distinction between the LRS = *laboratory reference system* = “observers reference frame” on the one hand and the PRS = *particle reference system* = “comoving system” = “rest frame” on the other hand.

First the Doppler effect. During one radiation cycle a source moves a distance $v\Delta t$ from point 1 to point 2 at an angle θ with respect to the line of sight. The path length difference projected onto the line of sight is $d = v\Delta t \cos \theta$.



Then the difference between the arrival times of the radiation emitted at point 1 and at point 2 at the position of the observer is:

$$\Delta t_{\text{obs}} = \Delta t - \frac{d}{c} = \Delta t [1 - (v/c) \cos \theta].$$

This time difference corresponds to one cycle of the radiation, thus the observed frequency $\nu_{\text{obs}} = 1/\Delta t_{\text{obs}}$ is given by

$$\nu_{\text{obs}} = \frac{\nu}{1 - (v/c) \cos \theta}.$$

This is the classical Doppler effect. The same formula holds for the relativistic Doppler effect, but then with an extra factor $\gamma \equiv 1/\sqrt{1 - v^2/c^2}$ as a result of time dilation:

$$\nu' = \nu \gamma (1 - \frac{v}{c} \cos \theta) \quad \text{and} \quad \nu = \nu' \gamma (1 + \frac{v}{c} \cos \theta'),$$

in which quantities that are measured in the PRS are designated with primes. The angle θ measured in the LRS between the wave vector and the source velocity \vec{v} is transformed into θ' in the PRS according to:

$$\sin \theta = \frac{\sin \theta'}{\gamma(1 + (v/c) \cos \theta')} \quad \text{and} \quad \sin \theta' = \frac{\sin \theta}{\gamma(1 + (v/c) \cos \theta)}.$$

Consider a radiating object that is moving towards us with relativistic velocity ($\gamma \gg 1$). Radiation that is emitted perpendicular to the line of sight *in* the rest frame of the object (PRS) ($\theta' = 90^\circ$) has $\sin \theta \approx \theta \approx 1/\gamma \ll 1$, and thus radiation that is emitted isotropically in the PRS is strongly peaked in the forward direction when observed in the LRS. This is the *relativistic beaming effect* (Figure 6.6).

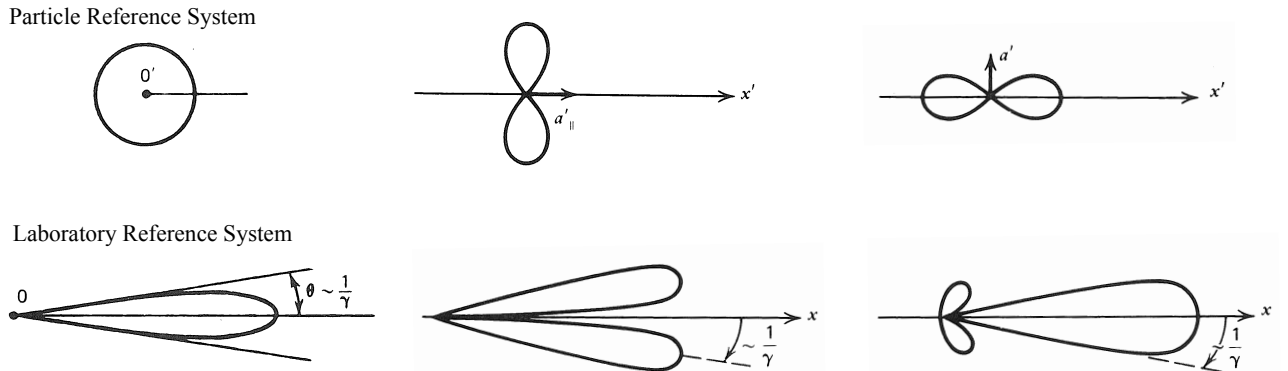


Figure 6.6: *The relativistic beaming effect. Isotropically emitted radiation is observed to be strongly peaked in the forward direction. Above: emission pattern in the PRS; at left, an isotropic distribution, in the middle, a dipole distribution with the dipole pointing towards the right, at right, a dipole distribution with the dipole pointing upwards. Below: the associated emission pattern in the LRS, for relativistic motion to the right. The beam width is only $\sim 2/\gamma$. The observer is to the right. (see Rybicki & Lightman Figure 4.3 and 4.11)*

Consider now a relativistic electron that scatters radiation. In an isotropic radiation field (isotropic in the LRS, thus in θ) that electron “sees” a radiation field

coming towards it that is strongly peaked in its direction, with a correspondingly higher frequency:

$$\nu'_1 = \nu_1 \gamma \left(1 - \frac{v}{c} \cos \theta\right)$$

where the index 1 indicates the situation before the scattering. For $\theta = 90^\circ$ the frequency increase is $\nu'_1/\nu_1 = \gamma$. The Thomson condition for elastic scattering in the PRS is $h\nu'_1 = h\nu_1 \gamma \ll m_e c^2 = 0.5 \text{ MeV}$; if this condition is satisfied then the scattering in the PRS is elastic and we have $\nu'_2 = \nu'_1$. In the LRS we then have for the scattered radiation:

$$\nu_2 = \nu'_2 \gamma \left(1 + \frac{v}{c} \cos \theta'\right) = \nu_1 \gamma^2 \left(1 + \frac{v}{c} \cos \theta'\right) \left(1 - \frac{v}{c} \cos \theta\right).$$

The scattering angle will follow the dipole phase function, and thus be roughly isotropically distributed; therefore we have:

$$\nu_2 \approx \frac{4}{3} \gamma^2 \nu_1. \quad (6.18)$$

For large γ there is thus a considerable energy increase (“hardening”) of the photons, which goes roughly as γ^2 . Thus X-ray photons can be created from a more moderate radiation field. The Thomson limit needs to be observed in the PRS. We must certainly have that $h\nu_1 \gamma \ll 0.5 \text{ MeV}$ we must have that $h\nu'_1 < 0.5 \text{ MeV}$, for example $h\nu'_1 = 100 \text{ keV}$. With $\gamma = 10$ you then can obtain 1 MeV LRS photons from 10 keV LRS photons. However the Thomson limit is easily violated; for $\gamma = 100$ (probably the case in AGN’s) this requires that $h\nu_1 < 5 \text{ keV}$.

Relativistic electrons in an intense radiation field will undergo inverse Compton scattering many times over. The radiation is hardened and the particles are slowed down; there is thus exchange of energy between the particles and the radiation field.

6.5 Electrons and magnetic fields

6.5.1 Cyclotron radiation

We now treat the acceleration of a charged particle (electron) in a magnetic field by the Lorentz force. First of all consider nonrelativistic velocities, $\gamma = 1$. An electron spirals around the magnetic field lines; we divide this motion into a single motion along the field and a circular motion perpendicular to it. Resolving the electron velocity \vec{v} into components $v_{\parallel} \parallel \vec{B}$ and $v_{\perp} \perp \vec{B}$ and setting the Lorentz force equal to the centripetal force yields:

$$\frac{m_e v_{\perp}^2}{R_B} = \frac{e v_{\perp} B}{c},$$

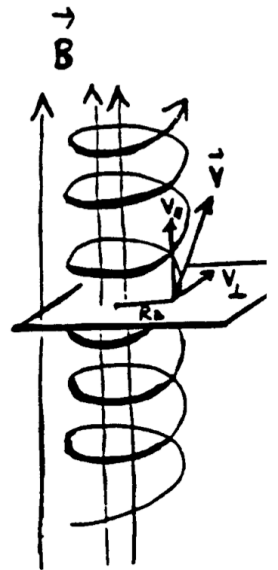
thus

$$R_B = \frac{m_e v_{\perp} c}{e B} \quad (\text{cgs}) = \frac{m_e v_{\perp}}{e B} \quad (\text{mksA}). \quad (6.19)$$

R_B is the *Larmor radius* or *gyro radius*. The acceleration is directed along R_B . The frequency of the associated radiation is given by the number of cycles per second:

$$\nu_B = \frac{v_{\perp}}{2\pi R_B} = \frac{e B}{2\pi m_e c} \quad (\text{cgs}) = \frac{e B}{2\pi m_e} \quad (\text{mksA}). \quad (6.20)$$

This is the *Larmor frequency* or *cyclotron frequency*.



The radiated power follows from the Larmor formula (equation 6.5):

$$P = \frac{2}{3} \frac{e^2}{c^3} \dot{v}_\perp^2.$$

The magnitude of the acceleration along R_B is given by the magnitude of the Lorentz force: $\dot{v}_\perp = (eB/m_e c)v_\perp$, and thus

$$P = \frac{2}{3} \frac{e^2}{c^3} \left(\frac{eB}{m_e c} \right)^2 v_\perp^2 = \frac{2}{3} \left(\frac{e^2}{m_e c^2} \right)^2 \frac{B^2}{c} v_\perp^2 = \frac{2}{3} \frac{r_e^2}{c} B^2 v_\perp^2$$

with $r_e = e^2/(m_e c^2)$ the classical electron radius. For an isotropic velocity distribution of the electrons we have:

$$\langle v_\perp^2 \rangle = \frac{v^2}{4\pi} \int \sin^2 \alpha \, d\Omega = \frac{2}{3} v^2$$

with α the *pitch angle* (\vec{B}, \vec{v}) using $\int \sin^2 \alpha \, d\Omega = 8\pi/3$. Thus:

$$\langle P \rangle = \frac{4}{9} r_e^2 \frac{v^2}{c} B^2 = \frac{4}{3} \sigma_T \frac{v^2}{c} \frac{B^2}{8\pi}$$

with the Thomson cross section $\sigma_T = (8\pi/3) r_e^2$.

In a homogeneous magnetic field there is monochromatic emission at the frequency ν_B : a single spectral line. Such *cyclotron lines* are observed in the X-ray spectra of pulsars.

6.5.2 Synchrotron radiation

Without proof we state that for relativistic velocities similar formulae hold as for cyclotron radiation, with an extra correction factor $\gamma = (1 - v^2/c^2)^{-1/2}$. The *gyro frequency* associated with the circular motion of an electron is then in cgs units:

$$\nu_g = \frac{\nu_B}{\gamma} = \frac{eB}{2\pi\gamma m_e c} \quad (6.21)$$

and the radiated power becomes:

$$P = \frac{4}{3} \sigma_T \frac{v^2}{c} \gamma^2 \frac{B^2}{8\pi},$$

for a homogeneous field and an isotropic velocity distribution. With respect to cyclotron radiation the frequency decreases and the power increases. Furthermore relativistic beaming also occurs here: the emission is strongly peaked in the forward direction along \vec{v} , with a half angle $1/\gamma$. As it sweeps around, this cone of radiation rapidly passes across the observer's view, and thus is visible for only a fleeting moment. The duration is only γ^{-3} times the period of revolution: one γ^{-1} from the vertex angle of the cone, and then γ^{-2} from the time dilation to and from the PRS via the LRS. These recurring bursts have a characteristic frequency:

$$\nu_c = \frac{3}{2} \gamma^2 \nu_B \sin \alpha = \frac{3}{2} \gamma^3 \nu_g \sin \alpha \quad (6.22)$$

in which α is again the pitch angle (\vec{B}, \vec{v}) . This is the *synchrotron frequency*. For $\gamma \gg 1$ we have $\nu_c \gg \nu_B$.



In Fourier terms: cyclotron radiation is a decent, continuous pure sine wave of EM radiation in which the spectrum, i.e., the Fourier transform, is a sharp spectral line. On the other hand, synchrotron radiation consists of sharp pulses. They follow one another with the cyclotron frequency but their pulse width is γ^3 times smaller. The spectrum, i.e., its Fourier transform, is a broad system of higher harmonics of the cyclotron frequency that extends up to the Nyquist-frequency $2\nu_c$. In other words: because of the short duration of the flash, the higher harmonics of the Larmor motion up to $2\nu_c$ are present. Because the radiation is so strongly peaked forwards, there are many of these higher harmonics of ν_B : the observed amplitude is no longer a sinusoid. Synchrotron radiation therefore has a broad spectrum consisting of higher harmonics of ν_B that extends to approximately ν_c . In the presence of smearing, for example by the distribution of particle velocities at a given spot (thus in γ , thus in the duration of the flash), or in spread in direction and strength of the magnetic field within a source, this gives rise to a continuum.

If the relativistic particles have an energy distribution that follows a power law:

$$N(E) dE \sim E^{-p} dE \quad \text{of} \quad N(\gamma) d\gamma \sim \gamma^{-p} d\gamma$$

then for the total emitted power we have:

$$P_{\text{tot}}(\nu) \sim \int P(\nu)\gamma^{-p} d\gamma \sim \nu^{-(p-1)/2},$$

thus the *spectral index* s in $P \sim \nu^{-s}$ is $s = (p - 1)/2$ for synchrotron radiation.

There is a direct analogy with the ff processes for charged particles accelerated in a Coulomb field. Thus synchrotron absorption can also take place: excitation of an electron into a “higher” Larmor orbit. There is likewise induced synchrotron emission: synchrotron deexcitation with the ambient radiation field. Finally: synchrotron radiation is polarized because the magnetic field defines a preferred direction.

6.6 Collective processes

In these lecture notes it is everywhere assumed that the index of refraction $n = 1$. Here we give a short summary of phenomena for which the index of refraction is of interest; a more extensive treatment is given in courses on plasma astrophysics.

6.6.1 Dust and droplets

Valence electrons in atoms and molecules, resonating with the incident radiation, give rise to Rayleigh scattering. For larger particles there is a transition, from Rayleigh scattering off dielectric globules to diffraction phenomena by particles locked into a medium with effective cross section $\sigma = \pi r^2$. Thus the phase function changes with respect to the dipole phase function for Rayleigh scattering towards increasingly stronger beaming in the forward direction. See Table 6.1. In all these processes we encounter partial polarization.

6.6.2 Cherenkov radiation

This is the radiation of a charged particle that moves with a velocity $v > c/n$ in a medium with index of refraction $n > 1$. Then c/n is the phase velocity of EM radiation in the medium, and the particle goes faster. Just as with the “sonic boom” of a supersonic jet, a shock wave occurs, with associated loss of energy. This is an efficient mechanism for slowing down the cosmic particle flux in the Earth’s atmosphere.

name	diameter	λ -dependence	phase function
Rayleigh	$d \ll \lambda$	$\sim \lambda^{-4}$	
Mie	$d \approx \lambda$	\Downarrow	
diffraction	$d \gg \lambda$	$\sim \lambda^0$	

Table 6.1: *Elastic scattering by larger particles.*

6.6.3 Plasma cutoff

The ions and the electrons in a plasma can be separated from one another by the Coulomb force of a passing EM wave because the electrons are much more mobile than the ions. For sufficiently low frequencies this separation provides a counterforce which works against the further propagation of the wave. This certainly happens for frequencies smaller than:

$$\nu_p = 9 \times 10^3 \sqrt{N_e} \text{ Hz} \quad (6.23)$$

with ν_p the *plasma frequency* below which EM waves *cannot* propagate. For $\nu > \nu_p$ the index of refraction is:

$$n_p = \sqrt{1 - \nu_p^2/\nu^2}.$$

6.6.4 Faraday rotation

The propagation of an EM wave in a plasma can be disturbed by a magnetic field. Speaking heuristically: a linearly polarized wave (\vec{E} in some preferred direction) can be thought of as a superposition of a left- and a right-circularly polarized wave. When propagation occurs parallel to the magnetic field, one circular polarization direction fits but the other does not. The result: the polarization is altered.

6.6.5 Razin cutoff

In a plasma with $n_p < 1$ no Cherenkov radiation can occur. The vertex angle of the cone of the relativistic beaming effect changes according to:

$$\theta_{\text{beam}} \approx \frac{1}{\gamma} = \sqrt{1 - v^2/c^2} \quad \rightarrow \quad \theta_{\text{beam}} \approx \sqrt{1 - n_p^2 v^2/c^2}.$$

For $n_p < 1$ the beaming effect is thus suppressed. Since it is this beaming which provides synchrotron radiation via pulsation, there is a *cutoff frequency* determined by n_p , thus ν_p , below which no synchrotron radiation can occur:

$$\nu_{\text{Razin}} = \gamma \nu_p$$

6.7 Nuclear reactions

Finally for the sake of completeness we present radiative processes resulting from nuclear reactions.

6.7.1 Fusion and fission reactions

For example $4p \rightarrow \alpha + 2\nu + 2\gamma$ occurs as a result of the various proton-proton cycles in hydrogen-burning stars. The whole star is optically thin to the two neutrinos. The two γ photons are the source of starlight.

6.7.2 Pair annihilation and pair creation

$$e^+ + e^- \rightarrow \gamma + \gamma$$

A highly energetic positron collides for example with a stationary electron and produces one γ -photon with large $h\nu$ and one γ -photon with $h\nu = m_e c^2$. This 0.511 MeV line is observed in solar flare spectra. Another example is the annihilation contribution to the 3 K background radiation.

Furthermore:

$e^+ + e^- \rightarrow \gamma$	only for bound electrons, otherwise momentum cannot be conserved;
$\gamma + \gamma \rightarrow e^+ + e^-$	with the condition that $h\nu_1 \times h\nu_2 > (m_e c^2)^2$;
$\gamma \rightarrow e^+ + e^-$	in a collision with an atom;
$\gamma \rightarrow \mu^+ + \mu^-$	in a collision with an atom;
$\pi^0 \rightarrow \gamma + \gamma$	etc.

Chapter 7

Radiative transfer

7.1 Introduction: different types of equilibrium

Chapter 3 discussed radiative transport in homogeneous slabs and the emergent intensity for slabs with a given source function S_ν . In this chapter we treat the radiation from inhomogeneous slabs and the source function itself. We do this for various types of equilibrium situations.

7.1.1 Thermodynamical Equilibrium (TE)

In *thermodynamical equilibrium* (TE) $S_\nu = B_\nu$ holds for each subprocess and also for the total source function; specification of the subprocesses is therefore not necessary. In TE it also is true that the profile functions are equal ($\chi = \varphi = \psi$) and for all radiative quantities the identity holds: $I_\nu = J_\nu = S_\nu = B_\nu(T)$. The populations are given by the Saha–Boltzmann distribution and the kinetic energy distribution follows the Maxwell law, with the same temperature in all distribution laws. There is “detailed balancing” between each process and its opposite, at each frequency and for each bundle. There is no net transport of energy: $\mathcal{F}_\nu = 0$, and there are no spectral lines. This is easy to calculate but not very helpful regarding evaluation of energy fluxes or diagnostic interpretation of spectral lines.

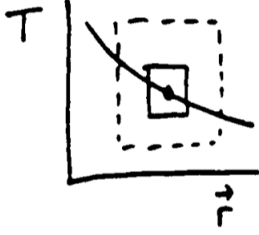
7.1.2 Local Thermodynamical Equilibrium (LTE)

In *local thermodynamical equilibrium* (LTE) it is assumed that the *matter* is in equilibrium with the *ambient* kinetic temperature. The radiation may, however, deviate from this temperature and the temperature may vary (slowly) through the medium. The Maxwell, Boltzmann and Saha laws hold, with T the ambient temperature that is determined by the thermal particle motions (*electron temperature*). It is also assumed that complete redistribution holds so that $\chi = \varphi = \psi$. With this assumption the populations follow the Saha-Boltzmann TE-distribution and the extinction coefficients are determined. For the source function it follows from the general expression (equation 5.12) that:

$$\begin{aligned} S_\nu &= \frac{2h\nu^3}{c^2} \frac{\psi/\varphi}{\frac{g_u n_l}{g_l n_u} - \chi/\varphi} \\ &= \frac{2h\nu^3}{c^2} \frac{1}{\left(\frac{g_u n_l}{g_l n_u}\right)^{\text{TE}} - 1} \end{aligned}$$

$$= \frac{2h\nu^3}{c^2} \frac{1}{e^{h\nu/kT} - 1} = B_\nu(T).$$

The essence of LTE is that the energy distribution of matter is *more locally* determined and maintained by collisions than that of radiation, so that the radiation but not the matter can depart somewhat from the local conditions:



$$S_\nu^l(\vec{r}) = B_\nu [T(\vec{r})] \quad I_\nu(\vec{r}) \neq B_\nu [T(\vec{r})] \quad J_\nu(\vec{r}) \neq B_\nu [T(\vec{r})] \quad \mathcal{F}_\nu(\vec{r}) \neq 0. \quad (7.1)$$

According to the assumption of LTE the matter resides in a sufficiently small TE-cylinder that the different thermal conditions elsewhere are not reflected in the populations. However, the ambient local radiation has indeed some knowledge of more distant regimes. The free path length for particles is thus assumed to be somewhat smaller than for photons, but the photons don't carry enough information about circumstances elsewhere to drive the populations from their local equilibrium values.

LTE is thus a very pleasant assumption that reconciles the convenience of TE with the need for at least some variation through the medium. It is a common assumption that sometimes is valid, notably for stellar photospheres. Both the extinction coefficient and the source function are determined in a simple way in LTE. Evaluation of the extinction coefficient α_ν demands only a knowledge of the extinction coefficient per particle σ_ν (or the equivalent transition probability A_{ul} , oscillator strength f_{ul} , gf -value), the chemical composition of the gas mixture and the critical quantities of pressure and temperature. From the Saha and Boltzmann laws $n_{r,s}^{\text{TE}}$ is derived for all populations and $\alpha_\nu = n_{r,s} \sigma_\nu$ is determined for all transitions of interest; their source function follows directly from the temperature by means of the Planck function. Thus you can analyze a single spectral line without being concerned with other transitions and wavelength regions. This applies to some extent to continuous processes as well as to spectral lines; a continuous transition can also be thought of as a jump between two levels.

Question 7.1 Which role does the relationship between collisional excitation, collisional deexcitation, collisional ionization, collisional recombination etc. on the one hand and radiative excitation, radiative deexcitation, radiative ionization, radiative recombination etc. on the other hand play in the applicability of LTE?

Question 7.2 Give examples of situations in which LTE truly holds and of situations in which LTE certainly does not hold.

7.1.3 Statistical Equilibrium (SE)

The assumption of *statistical equilibrium* (SE) implies a static situation: a time independence of the radiative fields and level populations. For the latter then the *statistical equilibrium equations* hold:

$$\frac{dn_i(\vec{r})}{dt} = \sum_{j \neq i}^N n_j(\vec{r}) P_{ji}(\vec{r}) - n_i(\vec{r}) \sum_{j \neq i}^N P_{ij}(\vec{r}) = 0 \quad (7.2)$$

with n_i the population of the level i in which we are interested, N the total number of levels that have influenced this population by means of one or another process, and P_{ij} the total transition probability per second for a transition from level i to level j :

$$P_{ij} = A_{ij} + B_{ij} \bar{J}_{\nu_0} + C_{ij},$$

with A_{ij} , B_{ij} and C_{ij} the Einstein coefficients for bb transitions from Chapter 5 or the analogous transition probabilities for other processes such as bf and ff transitions; \bar{J}_{ν_0} is the frequency-averaged, angle-averaged radiative field, for example, that for bf processes averaged over the series limit continuum. The first sum in equation (7.2) gives the increase of the population of level i from transitions from all other levels j to i ; the second sum gives the decrease of the population of i from transitions from i to all other levels j . These equations boil down to: per unit time there are as many transitions into a level as out of it, but no microscopic equilibrium per subprocess. The deficit in one process is made up by a surfeit of another.

These population equations for statistical equilibrium are coupled to the equations for radiative transport

$$\frac{dI_{\nu}(\vec{r})}{d\tau_{\nu}(\vec{r})} = S_{\nu}(\vec{r}) - I_{\nu}(\vec{r})$$

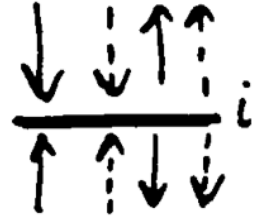
at all frequencies ν and along all bundles of interest for some population. The transition probabilities P_{ij} in the statistical equilibrium equations always depend on \bar{J}_{ν} and thus on I_{ν} in all directions, while the optical thickness τ_{ν} and the source function S_{ν} in the transport equations both again depend on the populations via α_{ν} . The connection between I_{ν} and S_{ν} is moreover usually not linear. The result is a system of nonlinear coupled equations, often quite large, that must be simultaneously (i.e., mutually consistently) solved for each place in the medium, for all frequencies and along all bundles that participate in the population processes.

If you may assume LTE you can bypass this detailed specification of P_{ij} and this involved solution of a large system of nonlinear equations. That's why the assumption of LTE is very often made without substantiation. Frequently that is incorrect; then there's nothing else to do but to assume SE only. If SE also does not hold then the time-dependent equations must be solved. If the Maxwellian distribution does not hold and axial symmetry cannot be assumed, then a supercomputer is soon required.

7.1.4 Non-Local Thermodynamical Equilibrium (NLTE)

The acronym NLTE or non-LTE means that the assumption of LTE is not valid. This does not indicate what is valid instead. Usually, however, it means that SE is assumed, that the Maxwell distribution holds and that complete redistribution (CRD) occurs. Then the populations can differ from the local Saha-Boltzmann values. That implies that the extinction coefficient can differ from its local LTE value and that the source function can differ from the local Planck function.

A more general step is to drop not only the Saha-Boltzmann population distribution but also the equality of the profile functions: $\psi \neq \varphi$. This is not complete but rather "partial" redistribution (NLTE-PRD). The line source function is then frequency-dependent: within a spectral line the source function varies with the frequency, depending on differences between the profile functions. Such differences may occur in strong lines with many scattering processes if the radiation fields vary across the line. That is quite possible because the free path length of a photon in the far wing of a strong line is much larger than in the core of the line so that the line wings have more knowledge of more distant radiative sources and radiative losses than the core. In that case the statistical equilibrium equations must be solved monochromatically, with a *redistribution function* that represents how much "crosstalk" there is with other parts of the line profile.



Question 7.3 Frequently *NLTE*-departure coefficients b_i are defined by:

$$b_l = n_l/n_l^{\text{LTE}} \quad b_u = n_u/n_u^{\text{LTE}}$$

that specify the departure of the true population with respect to the TE population following from the Saha and Boltzmann laws for the local temperature T . How do they appear in the line source function S_ν^l and in the line extinction coefficient α_ν^l ?

Demonstrate that in the Wien approximation the line source function scales linearly with b_u/b_l , and the line extinction coefficient with b_l .

Question 7.4 It is frequently thought that NLTE always means $S_\nu^l \neq B_\nu$ for the formation of a spectral line, but it is also possible that $S_\nu^l = B_\nu$ for a line that does not satisfy LTE. How is this?

7.2 Radiative transfer in LTE

If LTE holds the source function is simply determined by the ambient temperature, and the extinction coefficient by means of the Saha–Boltzmann laws. Radiative transport for a given source function has already been discussed in Chapter 3. All of the results there apply here with the simple substitution:

$$S_\nu(\vec{r}) = B_\nu [T(\vec{r})].$$

The transport equation (equation 3.15) therefore becomes

$$\frac{dI_\nu}{d\tau_\nu} = B_\nu(T) - I_\nu$$

for optical thickness,

$$\mu \frac{dI_\nu}{d\tau'_\nu} = I_\nu - B_\nu(T)$$

for radial optical depth and axial symmetry; in the Rayleigh-Jeans approximation we have for the brightness temperature

$$\frac{dT_b}{d\tau_\nu} = T - T_b.$$

The integral form (equation 3.16) becomes

$$I_\nu(\tau_\nu) = I_\nu(0) e^{-\tau_\nu} + \int_0^{\tau_\nu} B_\nu[T(t_\nu)] e^{-(\tau_\nu - t_\nu)} dt_\nu;$$

for a homogeneous slab this results in (equation 3.17)

$$I_\nu(D) = I_\nu(0) e^{-\tau_\nu(D)} + B_\nu(T) \left(1 - e^{-\tau_\nu(D)}\right)$$

and the Eddington-Barbier approximation for the intensity from an optically thick slab (equation 3.21) becomes

$$I_\nu^+(\tau'_\nu=0, \mu) \approx B_\nu [T(\tau'_\nu=\mu)].$$

7.2.1 Radiation from a thin LTE slab

For an optically thin homogeneous slab in LTE of thickness s the emergent intensity is

$$I_\nu(s) = I_\nu(0) + [B_\nu(T) - I_\nu(0)] \tau_\nu(s)$$

with the incident intensity in the direction of radiation equal to $I_\nu(0)$. In the Rayleigh-Jeans approximation this is:

$$T_b = T_b(0) + [T - T_b(0)] \tau_\nu(s); \quad (7.3)$$

this expression is often employed in radio astronomy. For an optically thick homogeneous LTE slab then we have just $T_b = T$, or $T_A = \eta_A T$ with T_A the antenna temperature.

7.2.2 Radiation within a thick LTE medium: the Rosseland approximation

In TE $S_\nu = B_\nu$ and $I_\nu = B_\nu$ holds. For the interior of optically very thick objects such as stars, this is a zero-order approximation: the free path length of the photons is small with respect to the scales on which the temperature and density change — a cubic centimeter of a stellar interior is a TE box to a good approximation. Yet this zero-order approximation is unsatisfactory because then there is no energy transport at all by radiation: the net flux $\mathcal{F}_\nu = 0$ if $I_\nu = B_\nu$ in all directions. In stellar interiors the net flux is indeed very small with respect to the angle-averaged intensity, but it is the net flux that interests us: it is what flows out that is important, both for us as observers in the form of a diagnostic as well as for the star itself in the form of a loss of energy, which determines its structure and lifetime. Thus the anisotropy of the radiation field, however small, must be explicitly included.

For axial symmetry and with the use of radial optical depth the transport equation is:

$$I_\nu(z, \mu) = S_\nu + \mu \frac{dI_\nu}{d\tau'_\nu}$$

Substitution of the zero-order approximation $I_\nu(z) \approx S_\nu(z) \approx B_\nu(z)$ provides

$$I_\nu(z, \mu) = B_\nu(z) + \mu \frac{dB_\nu(z)}{d\tau'_\nu},$$

in which the intensity differs from the Planck function only to first order. This approximation is valid provided that LTE holds and the correction $dB_\nu/d\tau'_\nu$ is small with respect to the isotropic part B_ν . The flux is then determined through the small anisotropic component $\mu dB_\nu/d\tau'_\nu$:

$$J_\nu(z) = \frac{1}{2} \int_{-1}^{+1} I_\nu d\mu = B_\nu(z)$$

and

$$\mathcal{F}_\nu(z) = 2\pi \int_{-1}^{+1} \mu I_\nu d\mu = \frac{4\pi}{3} \frac{dB_\nu(z)}{d\tau'_\nu}.$$

This monochromatic flux is however uninteresting in the unobservable stellar interior; of more interest is the total energy flow:

$$\mathcal{F}(z) = \int_0^\infty \mathcal{F}_\nu(z) d\nu$$

$$\begin{aligned}
&= -\frac{4\pi}{3} \int_0^\infty \frac{1}{\alpha_\nu} \frac{dB_\nu}{dz} d\nu \\
&= -\frac{4\pi}{3} \int_0^\infty \frac{1}{\alpha_\nu} \frac{dB_\nu}{dT} \frac{dT}{dz} d\nu.
\end{aligned}$$

where we used that the height dependence of B_ν is through the temperature variation: $B(T(z))$.

With the use of the Stefan-Boltzmann law we have

$$\int_0^\infty \frac{dB_\nu}{dT} d\nu = \frac{d}{dT} \int_0^\infty B_\nu d\nu = \frac{dB}{dT} = \frac{4\sigma}{\pi} T^3$$

and we define the *Rosseland mean extinction coefficient* α_R by

$$\int_0^\infty \frac{1}{\alpha_\nu} \frac{dB_\nu}{dT} d\nu \equiv 1/\alpha_R \int_0^\infty \frac{dB_\nu}{dT} d\nu$$

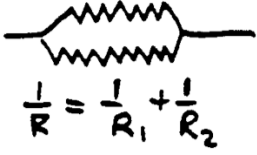
or

$$1/\alpha_R \equiv \left(\int_0^\infty \frac{1}{\alpha_\nu} \frac{dB_\nu}{dT} d\nu \right) / \left(\int_0^\infty \frac{dB_\nu}{dT} d\nu \right), \quad (7.4)$$

so that we arrive at:

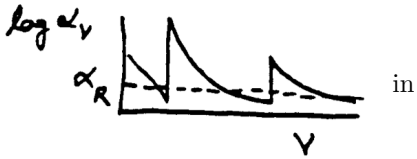
$$\mathcal{F}(z) = -\frac{16}{3} \frac{\sigma T^3}{\alpha_R} \frac{dT}{dz}. \quad (7.5)$$

This is the *Rosseland approximation* for the radiative flux. Its form is that of a diffusion equation with an effective conduction coefficient $16\sigma T^3/3\alpha_R$; this approximation is then also commonly called the *diffusion approximation*. Radiative energy transport deep inside a star is of the same nature as heat conduction. It shows that in LTE a net outward radiative flux is associated with an inwardly increasing temperature.



The Rosseland mean α_R of the extinction coefficient α_ν behaves analogously to an equivalent parallel resistance: the frequency bands with the smallest extinction contribute the most — the radiative flux “chooses” i.e., selectively leaks through the most transparent spectral windows. The weighting function

$$G_\nu(T) = \frac{dB_\nu/dT}{dB/dT} = \frac{\pi}{4\sigma T^3} \frac{dB_\nu}{dT}$$



$$1/\alpha_R \equiv \int_0^\infty (G_\nu/\alpha_\nu) d\nu$$

weights this choice of transparent windows by the temperature sensitivity of the Planck function. G_ν resembles the Planck function but peaks at $h\nu/kT \approx 3.8$ instead of 2.8, and thus at a somewhat shorter wavelength. Examples in Novotny, Fig. 3-12.

7.2.3 Radiation from a thick LTE medium

For an optically thick slab in LTE, we have in Eddington-Barbier approximation:

$$I_\nu^+(\tau'_\nu=0, \mu) \approx B_\nu [T(\tau'_\nu=\mu)].$$

Figure 7.1 shows an adaptation of the diagram in Figure 3.4 for LTE line formation in such a slab. The observed line profile (below left) is determined by:

- the variation of the extinction coefficient $\alpha_\nu^{\text{tot}} = \alpha_\nu^l + \alpha_\nu^c$ with the frequency (above left, illustrated for a specific location z). A bb transition can enhance the total extinction by many orders of magnitude compared to the value of the continuous extinction;

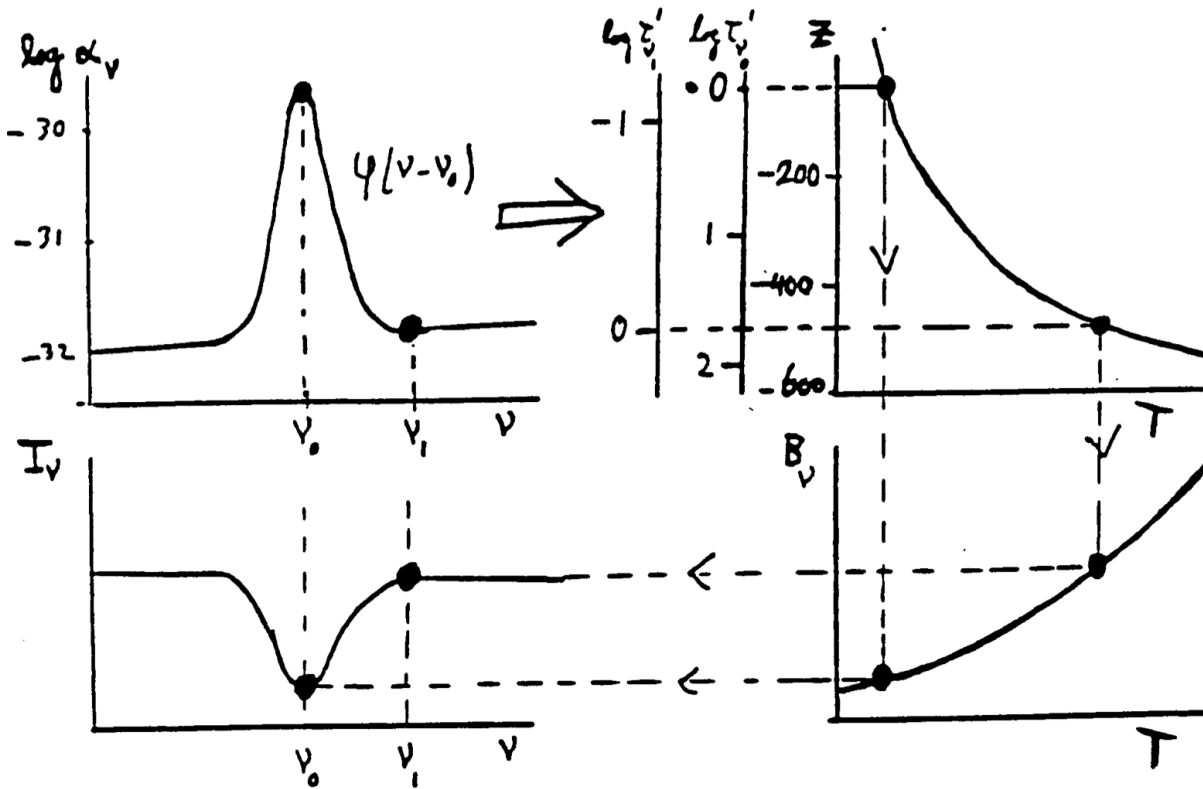


Figure 7.1: *Diagram for LTE line formation in optically thick media. The depth-dependent extinction coefficient (above left) determines the optical depth scale (above right). When convolved with the temperature dependence of the Planck function (below right), the variation of the temperature with the monochromatic optical depth determines the emergent intensity at each frequency (below left). The larger the extinction α_ν , the farther out the Eddington-Barbier representative height of formation $\tau'_\nu(z) = 1$. Where the temperature is falling towards the surface, absorption lines are the result.*

- the variation of the extinction coefficient with position (not illustrated). Here axial symmetry (plane parallel slabs) is assumed, so we are dealing here with the variation of $\alpha_\nu(z)$ with the height z . Because the density in an optically thick cloud of gas (which is probably gravitationally bound by its own mass) falls off roughly exponentially outward, α_ν usually falls off steeply with z ;
- the variation of the monochromatic optical depth $\tau'_\nu(z)$ with the geometrical height (or depth $-z$, above right, sketched for two frequencies along the y -axis). This variation follows from the two given above and is strongly frequency-dependent. With an exponential falloff of the density we have approximately that $\log \tau'_\nu \sim -z$, with departures dependent on $\alpha_\nu(z)$; the optical depth scales for different frequencies differ and are shifted with respect to one another; the geometrical surface $z = 0$ is here defined at $\log \tau'_{\nu_0} = 0$ or $\tau'_{\nu_0} = 1$ (often the geometrical surface is defined at $\tau'_{\text{cont}} = 1$);
- the variation of the temperature with z (above right); the temperature is decreasing with height; τ'_{ν_0} is at larger height ($z = 0$) and lower temperature than $\tau'_{\nu_1} = 1$ ($z \approx -500$);

- the variation of the Planck function with the temperature. The temperature sensitivity of the Planck function varies across the spectrum (Figure 7.2); and so this curve is also frequency-dependent (so strictly two different curves for B_{ν_0} and B_{ν_1} should be drawn, however, over small frequency domain the two curves would be indistinguishable). The slope dB/dT is always positive.

The line is in absorption if the temperature falls outward and is in emission if the temperature rises outward.

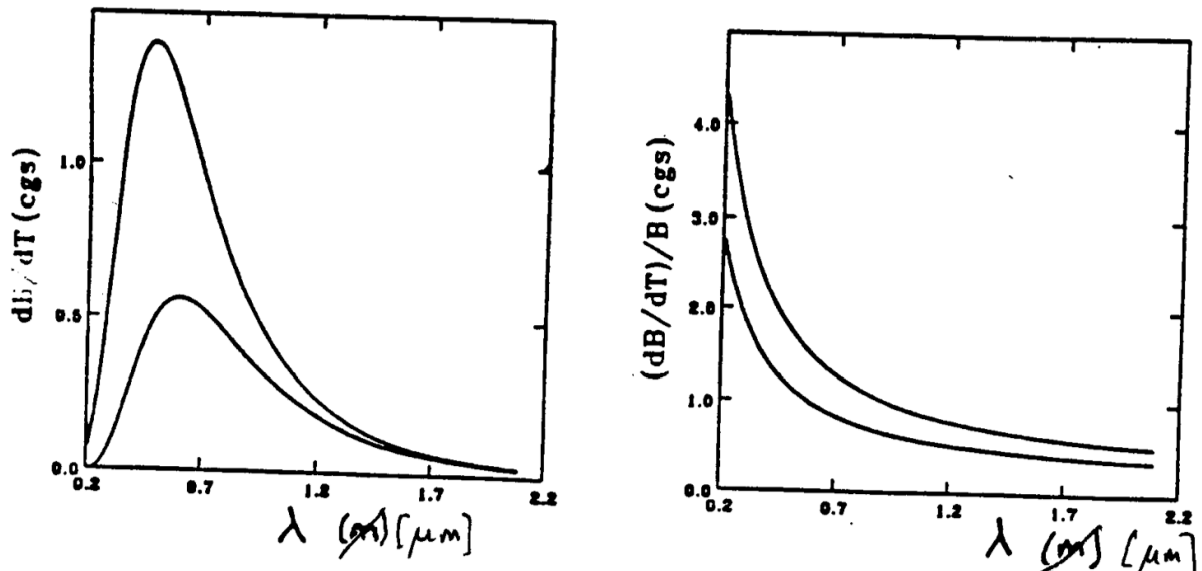


Figure 7.2: The temperature sensitivity of the Planck function B_λ , absolute (left) and relative (right), for $T = 4000$ K and $T = 5000$ K.

Question 7.5 How can you tell in Figure 7.1 that the Eddington-Barbier approximation is assumed? Is the assumption correct?

Question 7.6 Does the diagram in Figure 7.1 apply also for the formation of the continuum at radically different wavelengths?

Question 7.7 What kind of spectral lines do you have in LTE from an optically thin homogeneous slab? And from an optically thick homogeneous slab? And from

a homogeneous slab which is optically thin in the continuum and optically thick in the spectral line?

Question 7.8 From the observation that the solar Na I D lines are absorption lines and the assumption of LTE for these lines, what can we say about the temperature structure of the solar atmosphere?

Question 7.9 How does the intensity in the line center of the Na D lines change from the center to the limb of the Sun?

Question 7.10 Just outside the limb of the Sun during a total solar eclipse the *chromosphere* appears. This is a thin layer of tenuous gas. During a solar eclipse you look transversely through it; even then the whole chromosphere is optically thin along the line of sight in the visible region of the spectrum. Explain why the chromosphere shows the yellow Na D lines in emission. Does that say something about the temperature of the chromosphere, if LTE is a good assumption?

Question 7.11 In the spectrum of the center of the solar disk the $H\alpha$ line is an absorption line but the $Ly\alpha$ line is in emission. How is that explained with the assumption of LTE?

7.3 Radiative transfer with photon scattering

The essence of LTE is that the source function is determined *locally*, due to sufficient local coupling of particle energy and radiative energy. If however it is not the collisional processes but the scattering processes which dominate, this local determination is lost —the photons to be scattered come from somewhere else. Scattering contributes both to j_ν and to α_ν , thus both together to S_ν .

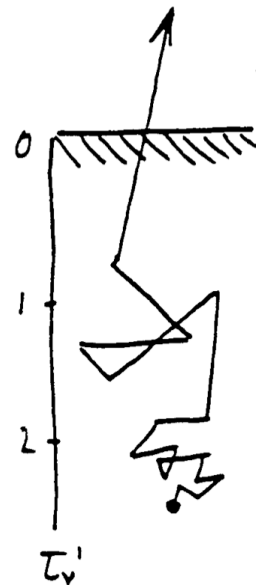
The free path length of a photon between two successive extinction processes, according to equation (3.11), is:

$$l_\nu = 1/\alpha_\nu$$

but if most extinction processes are elastic scattering processes, the *identity* of the quantum of radiative energy remains constant between successive scatterings: the photon changes in direction but not in energy in each scattering. The distance between creation and destruction or between creation and escape of a photon can thus be effectively much larger than l_ν .

For example in a stellar atmosphere. The outgoing photons emerge from the slab at an optical thickness roughly $\tau_\nu = 1$, measured along the line of sight, that is from a radial optical depth $\tau'_\nu = \mu$. But this depth of escape is merely the place where the photons experienced their last interaction, i.e., where they were scattered. Their *creation depth* can be much larger. From that point they diffused by a “random walk” in scattering steps towards the surface.

It doesn't matter here what type of photon scattering is involved. Below we will always be discussing bb scattering because the creation and destruction probabilities can then be conveniently expressed via the Einstein transition probabilities, but the treatment holds for each type of elastic scattering: Thomson, Rayleigh, etc. In bb resonant scattering the line photon is also scattered elastically, with conservation of energy. That can be the case precisely (*coherent scattering*) or there can be a redistribution over the width of the line profile (*frequency redistribution*). In spontaneous deexcitation the new direction then is arbitrary (*complete angular redistribution*) while in self-induced deexcitation the direction of the induced photon is fixed.



Question 7.12 Why do the scattering steps become larger towards the surface?

Question 7.13 According to the Eddington-Barbier approximation the escaped photons exhibit the source function of the depth $\tau'_\nu = \mu$. Does that also hold for scattering?

7.3.1 Pure scattering

Consider a homogeneous slab of gas in which in a bb transition there is only scattering. There is no photon conversion, no photon absorption and no thermal emission, thus there is no photon creation or photon destruction. Assume that the scattering is isotropic and elastic (= “coherent” = monochromatic: $\nu_2 = \nu_1$). In each extinction process the photons then change only in direction. Instead of the line extinction coefficient α_ν^l we use a scattering coefficient α_ν^s that gives the scattering cross section in cm^2 per cm^3 , defined as

$$dI_\nu = -\alpha_\nu^s I_\nu ds.$$

What is the emission coefficient j_ν^s ? Each “new” photon is a scattered “old” photon from the extant radiative field. Thus we must have that the total emission per cm^3 in all directions is equal to the total extinction per cm^3 from all bundles:

$$\int j_\nu^s d\Omega = \int \alpha_\nu^s I_\nu d\Omega.$$

The angle-averaged radiative field is $J_\nu = (1/4\pi) \int I_\nu d\Omega$, and so the emission coefficient is given by

$$j_\nu^s = \alpha_\nu^s J_\nu$$

and the line source function by

$$S_\nu^l = j_\nu^s / \alpha_\nu^s = J_\nu.$$

The radiative transport equation then becomes:

$$\frac{dI_\nu}{ds} = \alpha_\nu^s [J_\nu - I_\nu]$$

The average intensity J_ν must thus be known in order to determine I_ν , and so we must know I_ν in all directions in order to calculate J_ν for a specific bundle. Here the analytical treatment ends; for a precise evaluation an iterative numerical calculation is necessary.

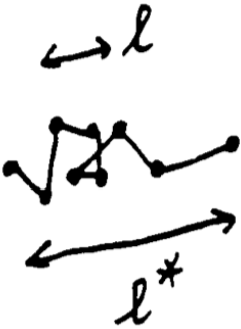
In these paragraphs about scattering we must therefore limit ourselves to approximations. We begin with an estimate of the radiative transport under pure scattering, with “random walk” arguments applied to individual photons. The free path length of a photon between two successive scatterings is given by (equation 3.11):

$$l_\nu = \frac{\langle \tau_\nu \rangle}{\alpha_\nu} = \frac{1}{\alpha_\nu^s}.$$

What is the total path length l^* traveled by a quantum after N scatterings? A description as a 1-dimensional diffusion process provides (Rybicki and Lightman §1.7):

$$l_\nu^* \approx \sqrt{N} l_\nu. \quad (7.6)$$

After how many scattering steps does a photon migrate through a slab with thickness D ? There are roughly as many steps required so that the ultimate path length l_ν^*



is equal to D , thus $N \approx (l_\nu^*)^2/l_\nu^2 \approx D^2/l_\nu^2$. With $l_\nu = 1/\alpha_\nu^s$ and $\tau_\nu = \alpha_\nu^s D$ follows $N \approx \tau_\nu^2$ provided that the slab is sufficiently thick ($\tau_\nu \gg 1$) that the diffusion description applies.

For a thin slab with $\tau_\nu \ll 1$ the photon usually escapes immediately — with a small chance of being retained, roughly equal to $\tau_\nu = \alpha_\nu^s D \ll 1$.

7.3.2 Absorption and scattering in a two-level atom

Consider now a medium that for convenience consists only of *two-level atoms*: particles with only one lower level l and one upper level u . In such a situation only discrete transitions are possible, namely the five processes of Figure 1.5 that were discussed in Chapter 5. We assume as well that the upper level u is sharp, Heisenberg's uncertainty principle notwithstanding, so that the transition is strictly monochromatic with frequency $\nu = \nu_0$. In all equations of Chapter 5 in which the frequency-averaged angle-averaged intensity \bar{J}_{ν_0} appears, we have the monochromatic angle-averaged intensity J_{ν_0} instead.

The five processes can be combined according to Figure 1.6 into the pairs of processes *photon creation*, *photon destruction* and *photon scattering*.

The fourth pair, collisional excitation followed by collisional deexcitation, involves no interaction with photons and is not of interest here, aside from the fact that it helps to maintain the Maxwellian distribution (also assumed here).

These assumptions provide a medium with strictly elastic scattering, without any photon conversion. There is no radiative excitation followed by excitation or deexcitation to another level or continuum, neither per photon nor per collision. Each line photon that is created by means of a creation pair of processes (collisional excitation followed by radiative deexcitation) keeps undergoing a random walk, continuously being monochromatically scattered, until such time as it is destroyed by a destruction pair of processes (radiative excitation followed through collisional deexcitation) — or leaves the medium altogether.

This is a convenient approximation for the illustration of radiative transport with scattering without having to be troubled by coupling to other spectral regions and to other parts of the medium via various other transitions into and out of the two levels. We arrive upon a good description of the *nonlocal nature* of radiative transport as a result of photon scattering, while passing over for the time being the *nonmonochromatic nature* that results from photon conversion.

Each radiative excitation of a two-level atom is followed either by radiative deexcitation (scattering), or by collisional deexcitation (destruction). The total extinction (all radiative excitations) is the sum of these pairs of processes; therefore we divide the bb extinction coefficient $\alpha_{\nu_0}^l$ in two parts: an absorption part $\alpha_{\nu_0}^a$ that describes photon extermination and a scattering part $\alpha_{\nu_0}^s$ that describes elastic scattering. The total transition probability for deexcitation per excited particle per second is (equations 5.1–5.6):

$$P_{ul}^{\text{tot}} = A_{ul} + B_{ul}J_{\nu_0} + C_{ul}.$$

The first two terms on the right-hand side together comprise the creation and scattering fractions, the third term is the fraction undergoing destruction = absorption. These are the fractions per excited particle, thus also per radiative excitation. The two partial extinction coefficients are:

$$\alpha_{\nu_0}^a = \frac{h\nu_0}{4\pi} n_l B_{lu} \frac{C_{ul}}{P_{ul}} \left[1 - e^{-h\nu_0/kT} \right] \quad (7.7)$$

$$\alpha_{\nu_0}^s = \frac{h\nu_0}{4\pi} n_l B_{lu} \frac{A_{ul}}{P_{ul}} \quad (7.8)$$

with

$$\alpha_{\nu_0}^l \equiv \alpha_{\nu_0}^a + \alpha_{\nu_0}^s.$$

A full derivation is given in Rutten 2003 Sect. 3.4.1 which involves separating all up-down sequences in the two-level atom between $\alpha_{\nu_0}^a$ and $\alpha_{\nu_0}^s$. The factor $[1 - e^{-h\nu_0/kT}]$ is the TE correction factor for induced emission which is taken as negative absorption according to convention.

What are the associated emission coefficients? With thermal destruction there is similarly thermal creation; the source function associated with the collisional processes is the Planck function. Thus it follows for the first part, i.e., the destruction process:

$$j_{\nu_0}^a = \alpha_{\nu_0}^a B_{\nu_0}.$$

The scattering is monochromatic and isotropic, and so the emission coefficient for the second part, i.e., as a result of scattering per cm^3 per second per Hz and per steradian radiated energy, is again equal to the average energy extinguished by scattering per cm^3 per second per Hz and per steradian:

$$j_{\nu_0}^s = \alpha_{\nu_0}^s J_{\nu_0}.$$

The corresponding bb source function $S_{\nu_0}^l$ is

$$S_{\nu_0}^l \equiv \frac{\sum j_{\nu_0}}{\sum \alpha_{\nu_0}} = \frac{\alpha_{\nu_0}^a B_{\nu_0} + \alpha_{\nu_0}^s J_{\nu_0}}{\alpha_{\nu_0}^a + \alpha_{\nu_0}^s},$$

and the transport equation becomes :

$$dI_{\nu_0} = -\alpha_{\nu_0}^a I_{\nu_0} ds - \alpha_{\nu_0}^s I_{\nu_0} ds + \alpha_{\nu_0}^a B_{\nu_0} ds + \alpha_{\nu_0}^s J_{\nu_0} ds,$$

where the first two terms on the right-hand side are the absorption part and the scattering part of the extinction, the third and fourth terms are the creation and the scattering parts of the emission, along the bundle. With

$$d\tau_{\nu_0} \equiv \alpha_{\nu_0} ds = (\alpha_{\nu_0}^a + \alpha_{\nu_0}^s) ds$$

and the corresponding source function we recover the standard form:

$$\frac{dI_{\nu_0}}{d\tau_{\nu_0}} = \frac{dI_{\nu_0}}{(\alpha_{\nu_0}^a + \alpha_{\nu_0}^s) ds} = S_{\nu_0}^l - I_{\nu_0}.$$

We now introduce the probability ε_{ν_0} that a photon is extinguished following an extinction process:

$$\varepsilon_{\nu_0} \equiv \frac{\alpha_{\nu_0}^a}{\alpha_{\nu_0}^a + \alpha_{\nu_0}^s} = \text{destruction probability per extinction.} \quad (7.9)$$

The probability that it is scattered in the next extinction process is then:

$$1 - \varepsilon_{\nu_0} = \frac{\alpha_{\nu_0}^s}{\alpha_{\nu_0}^a + \alpha_{\nu_0}^s} = \text{scattering probability per extinction.}$$

Expressed in terms of Einstein coefficients ε_{ν_0} is:

$$\varepsilon_{\nu_0} = \frac{C_{ul}}{A_{ul} + B_{ul}B_{\nu_0} + C_{ul}}. \quad (7.10)$$

This important parameter measures the fractional absorption per extinction, thus the amount of coupling to the local temperature. The two-level line source function then becomes:

$$S_{\nu_0}^l = (1 - \varepsilon_{\nu_0})J_{\nu_0} + \varepsilon_{\nu_0}B_{\nu_0}. \quad (7.11)$$

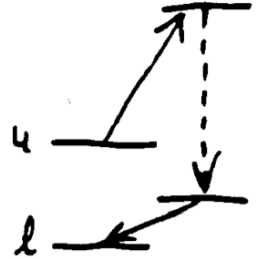
This is an important result. The source function is equal to the Planck function if $\varepsilon_{\nu_0} \approx 1$; on the contrary the source function is dominated by the angle-averaged radiative field J_{ν_0} if $\varepsilon_{\nu_0} \ll 1$. In intermediate cases the source function is an average of J_{ν_0} and B_{ν_0} weighted by ε_{ν_0} . When does $S_{\nu_0}^l = B_{\nu_0}$ hold? If $\varepsilon_{\nu_0} \approx 1$ or if $J_{\nu_0} \approx B_{\nu_0}$, or if both conditions are satisfied at the same time.

The term J_{ν_0} is the *reservoir term*: the quantity of available photons. The term $\varepsilon_{\nu_0}J_{\nu_0}$ is the *loss term* (“photon sink”); this specifies the energy of the photons that disappear from the reservoir per extinction. The term $\varepsilon_{\nu_0}B_{\nu_0}$ is the *source term* (“photon source”); this is the energy of the photons newly created per extinction. This source term can not be neglected because otherwise no photons would be created for scattering, unless a large radiative field were imposed. That means that also whenever ε_{ν_0} is very small, the photon source $\varepsilon_{\nu_0}B_{\nu_0}$ usually must be evaluated precisely: it builds up the radiative field J_{ν_0} by which the source function then is largely determined. This *inhomogeneous term* makes the numerical solution of the transport equation difficult for the case $\varepsilon_{\nu_0} \ll 1$.

For simplicity the above is presented for a two-level atom with monochromatic scattering, but the resulting source functions are illustrative for every extinction process. The source function is always a weighted average over the different subprocesses. The line source function of a bb transition in a multi-level atom can for example be written as:

$$S_{\nu_0}^l = (1 - \varepsilon_{\nu_0} - \eta_{\nu_0})\bar{J}_{\nu_0} + \varepsilon_{\nu_0}B_{\nu_0}(T_e) + \eta_{\nu_0}B_{\nu_0}(T^*),$$

where \bar{J}_{ν_0} is the angle-averaged intensity averaged over the extinction profile, T_e is the kinetic temperature (electron temperature), and T^* a typical or mean temperature for which the Planck function provides the source function of all processes by which an atom can eventually go from the upper level to the lower level other than by direct deexcitation. $B_{\nu_0}(T^*)$ is then the aggregate source function for all pathways from u to l ; the parameter η_{ν_0} measures the probability of such a pathway per $l \rightarrow u$ extinction.



Question 7.14 Derive from the statistical equilibrium equations that in the case of complete redistribution over the line profile and pure scattering (no collisions), the line source function in a two-level atom is given by $S_{\nu_0}^l = \bar{J}_{\nu_0}$. Demonstrate also that $S_{\nu_0}^l = B_{\nu_0}$ if the populations of the two levels are completely determined by collisions.

Question 7.15 Here ε_{ν_0} is defined as the destruction probability *per extinction process*. Other usage is that $\varepsilon'_{\nu_0} = \alpha_{\nu_0}^a / \alpha_{\nu_0}^s$, i.e., is the destruction probability *per scattering*. Express ε'_{ν_0} in ε_{ν_0} and in Einstein coefficients. What does equation (7.11) become with the use of ε'_{ν_0} ?

Question 7.16 Derive equation (7.11) *ab initio* from the equations of Chapter 5.

Question 7.17 Demonstrate that for a two-level atom with the profile functions ψ , φ and χ of Chapter 5 (and so with a broadened upper level) we have in the case of complete redistribution:

$$S_{\nu_0}^l = (1 - \varepsilon_{\nu_0})\bar{J}_{\nu_0} + \varepsilon_{\nu_0}B_{\nu_0}.$$

How must ε_{ν_0} be defined for this?

Show that in this case the line source function does not vary with frequency across the line profile, while the “coherent” line source function in equation (7.11) does. Is there a difference in the emergent intensity between these two cases?

7.3.3 Effective optical thickness

Consider once again a homogeneous medium with photons wandering at random. The free path length of a photon between two successive extinction processes is (equation 3.11):

$$l_\nu = \frac{\langle \tau_\nu \rangle}{\alpha_\nu} = \frac{1}{\alpha_\nu^a + \alpha_\nu^s}, \quad (7.12)$$

but it is more interesting to know over what distance a photon’s *identity* is preserved, i.e., what the path length is between its creation and destruction. The extinction probability per step is ε_ν , thus the average number of steps that a photon can make while being scattered is:

$$N = 1/\varepsilon_\nu$$

and from equation (7.6) it follows that:

$$l_\nu^* \approx l_\nu / \sqrt{\varepsilon_\nu} \quad (7.13)$$

with l_ν^* the characteristic distance between creation and destruction, i.e., the *identity conservation path length*, or the *diffusion length*, or the *thermalization length*, or the *effective free path length* of a photon.

For $\varepsilon_\nu = 1$ ($\alpha_\nu^s = 0$, no scattering) we have: $l_\nu^* = l_\nu$.

For $\varepsilon_\nu \ll 1_\nu$ ($\alpha_\nu^s \gg \alpha_\nu^a$, much scattering) we have: $l_\nu^* \gg l_\nu$.

For $\varepsilon_\nu = 0$ ($\alpha_\nu^a = 0$, scattering only) we have: $l_\nu^* = \infty$.

With equations (7.12) and (7.9) it follows that:

$$l_\nu^* \approx 1 / \sqrt{\alpha_\nu^a (\alpha_\nu^a + \alpha_\nu^s)} \quad (7.14)$$

and we define, as a sequel to equations (3.7) and (3.11), the:

- optical path length τ_ν as $d\tau_\nu = (\alpha_\nu^a + \alpha_\nu^s) ds$;
- absorption path length τ_ν^a as $d\tau_\nu^a = \alpha_\nu^a ds$;
- scattering path length τ_ν^s as $d\tau_\nu^s = \alpha_\nu^s ds$;
- and lastly the *effective optical path length* $d\tau_\nu^*$ as $d\tau_\nu^* = \sqrt{\alpha_\nu^a (\alpha_\nu^a + \alpha_\nu^s)} ds$.

For a homogeneous slab of thickness D the *effective optical thickness* τ_ν^* is:

$$\tau_\nu^* = D/l_\nu^* \approx \sqrt{\tau_\nu^a (\tau_\nu^a + \tau_\nu^s)}, \quad (7.15)$$

with $\tau_\nu^* < \tau_\nu$ because

$$\tau_\nu^* / \tau_\nu = \sqrt{\tau_\nu^a / (\tau_\nu^a + \tau_\nu^s)}.$$

The slab is *effectively thin* if $\tau_\nu^* < 1$ and *effectively thick* if $\tau_\nu^* > 1$.

7.3.4 Radiation from a thin scattering slab

We look now at radiation from homogeneous layers in which scattering occurs. First for a thin slab. Assume homogeneity in the sense that the temperature, density and extinction coefficient do not depend on position, but that the source function can vary because of scattering. The total monochromatic luminosity from an *effectively thin* object is then:

$$L_\nu \approx 4\pi\alpha_\nu^a B_\nu V \quad (7.16)$$

with V the volume of the object. The term $\alpha_\nu^a B_\nu$ describes all the photons created from thermal energy which contribute to a given bundle; multiplication by $4\pi V$ gives the total number of photons escaping from the object under the assumption that all photons ever created at some point leave the object, however often they may be scattered. The direction is thereby lost, which is why an expression is given here for the luminosity.

This assumption of homogeneity is not internally consistent: if the source function varies as a result of scattering, the relative populations do also, and therefore also the populations and the extinction coefficients. For a two-level atom, for example, overexcitation of the excited level goes hand in hand with an underpopulation of the ground level, thus an increase in the source function is accompanied by a decrease in the extinction coefficient. On account of the Boltzmann factor, however, the decrease for the lower level is usually a smaller fraction of the population than for the increase of the upper level; to first order the source function does change considerably but the extinction coefficient does not.

Question 7.18 What is the luminosity of a homogeneous, effectively thin sphere with absorption coefficient α_ν^a and scattering coefficient α_ν^s ?

Question 7.19 Can an object be effectively thin and optically thick at the same time? Does equation (7.16) hold in consequence?

7.3.5 Radiation within a thick scattering inhomogeneous medium: the Eddington approximation

We now look at a thick object in which the conditions do indeed vary. The Rosseland approximation of §7.2.2 demands that the intensity differ only to first order from the Planck function. A more broadly applicable approximation is to assume that I_ν once again departs only to first order from isotropy, but that it may be nonthermal as well. The addition of photons to a bundle takes place isotropically both for the thermal creation of new photons as well as for the scattering of already extant photons (provided that spontaneous deexcitation dominates over induced deexcitation); therefore this approximation can also hold if scattering is important ($\varepsilon_\nu \ll 1$) and has a broader domain of applicability than the Rosseland approximation. We assume axial symmetry once again and set:

$$I_\nu(z, \mu) \equiv a_\nu(z) + b_\nu(z) \mu,$$

then the first three “moments” of the intensity I_ν with respect to μ are:

$$J_\nu(z) \equiv \frac{1}{4\pi} \int I_\nu(z, \mu) d\Omega = \frac{1}{2} \int_{-1}^{+1} I_\nu d\mu = a \quad (7.17)$$

$$H_\nu(z) \equiv \frac{1}{4\pi} \int \cos \theta I_\nu(z, \mu) d\Omega = \frac{1}{2} \int_{-1}^{+1} \mu I_\nu d\mu = b/3 \quad (7.18)$$

$$K_\nu(z) \equiv \frac{1}{4\pi} \int \cos^2 \theta I_\nu(z, \mu) d\Omega = \frac{1}{2} \int_{-1}^{+1} \mu^2 I_\nu d\mu = a/3. \quad (7.19)$$

The dimensions of the *Eddington flux* H_ν and the *K integral* K_ν are [$\text{erg cm}^{-2} \text{s}^{-1} \text{Hz}^{-1} \text{ster}^{-1}$], just as for I_ν and J_ν . J_ν and K_ν are always positive; H_ν can also be negative.

From this there follows the important *Eddington approximation*

$$J_\nu = 3K_\nu. \quad (7.20)$$

From the transport equation (for radial optical depth τ'_ν and axial symmetry, cf. question 3.23) it follows by integrating over μ :

$$\begin{aligned} \mu \frac{dI_\nu}{d\tau'_\nu} &= I_\nu - S_\nu \\ \frac{1}{2} \int_{-1}^{+1} \mu \frac{dI_\nu}{d\tau'_\nu} d\mu &= \frac{1}{2} \int_{-1}^{+1} I_\nu d\mu - \frac{1}{2} \int_{-1}^{+1} S_\nu d\mu \\ \frac{dH_\nu}{d\tau'_\nu} &= J_\nu - S_\nu \end{aligned}$$

with S_ν assumed isotropic, this being usually the case. Multiplication by μ and a second integration over μ provides

$$\begin{aligned} \frac{1}{2} \int_{-1}^{+1} \mu^2 \frac{dI_\nu}{d\tau'_\nu} d\mu &= \frac{1}{2} \int_{-1}^{+1} \mu I_\nu d\mu - \frac{1}{2} \int_{-1}^{+1} \mu S_\nu d\mu \\ \frac{dK_\nu}{d\tau'_\nu} &= H_\nu = \frac{1}{3} \frac{dJ_\nu}{d\tau'_\nu} \end{aligned}$$

with use of the Eddington approximation.

This leads to:

$$\frac{1}{3} \frac{d^2 J_\nu}{d\tau'^2_\nu} = J_\nu - S_\nu. \quad (7.21)$$

For elastic scattering we have $S_\nu = (1 - \varepsilon_\nu)J_\nu + \varepsilon_\nu B_\nu$ and therefore

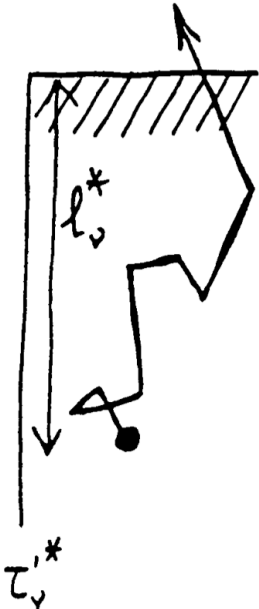
$$\frac{1}{3} \frac{d^2 J_\nu}{d\tau'^2_\nu} = \varepsilon_\nu (J_\nu - B_\nu). \quad (7.22)$$

This is the radiative transport equation in the Eddington approximation with elastic scattering. Provided that the boundary conditions are known, this provides from $T(z)$ and $\varepsilon_\nu(z)$ first $J_\nu(z)$, then $S_\nu(z)$, and finally $I_\nu(z)$ from the transport equation. This historically much-used approximation holds thus if the radiative field is not too anisotropic, i.e., within slabs that are at least effectively thick.

7.3.6 Radiation from a thick scattering medium

Now consider an effectively thick slab with $\tau_\nu^* \gg 1$, also with homogeneous conditions. Photons which originate more deeply than l_ν^* from the surface do not escape, but are extinguished after $N = 1/\varepsilon_\nu$ random-walk steps. Photons that are created less than l_ν^* from the surface can escape. Assuming that they always do, they then provide an upper limit for the emergent luminosity. The volume from which they escape is given by:

$$V = Al_\nu^*$$



with A a piece of the upper surface. Thus it follows with equation (7.16)

$$L_\nu \approx 4\pi\alpha_\nu^a A l_\nu^* B_\nu$$

and with equations (7.14) and (7.9)

$$L_\nu \approx 4\pi\sqrt{\varepsilon_\nu} B_\nu A,$$

and finally

$$\mathcal{F}_\nu^+ = L_\nu/A \approx 4\pi\sqrt{\varepsilon_\nu} B_\nu.$$

This is somewhat too large. Consider $\varepsilon_\nu = 1$, for which $S_\nu = B_\nu$; the surface flux of a black body is $\mathcal{F}_\nu^+ = \pi B_\nu$ instead of $4\pi B_\nu$. A better approximation follows from the Eddington approximation (see exercise 1.10 of Rybicki and Lightman) with the effective optical thickness defined by $\tau_\nu^* \equiv \sqrt{3}\varepsilon_\nu\tau_\nu = \sqrt{3}\tau_\nu^a(\tau_\nu^a + \tau_\nu^s)$ and the effective optical depth by $\tau_\nu'^* = \sqrt{3\varepsilon_\nu}\tau_\nu'$, thus a factor of $\sqrt{3}$ larger than in equation (7.15). For the outgoing flux this approximation yields

$$\mathcal{F}_\nu^+ \approx \frac{4\pi}{\sqrt{3}} \frac{\sqrt{\varepsilon_\nu}}{1 + \sqrt{\varepsilon_\nu}} B_\nu$$

and for the source function

$$S_\nu(\tau') = B_\nu \left[1 - (1 - \sqrt{\varepsilon_\nu}) e^{-\tau_\nu'^*} \right].$$

The source function at the surface is only

$$S_\nu(\tau_\nu' = 0) = \sqrt{\varepsilon_\nu} B_\nu \tag{7.23}$$

and with much scattering ($\varepsilon_\nu \ll 1$) the emergent intensity is only barely larger:

$$I_\nu(\tau_\nu' = 0) \approx S_\nu(\tau_\nu' = 1) \approx (1 + \sqrt{3})\sqrt{\varepsilon_\nu} B_\nu.$$

With very much scattering ($\varepsilon_\nu \ll 1$) thus much *less* radiation than B_ν emerges from the slab — in spite of the fact that the emergent photons actually originate from a deeper level than that from which you see them emerging. With scattering you receive photons from deeper layers than the depth $\tau_\nu' = 1$, but you receive fewer of them than you would from a black body. That happens because with much additional scattering the visible radiating volume becomes smaller and the representative depth $\tau_\nu' = 1$ lies much closer to the surface.

Consider Figure 7.3. The crosses are photon-creating atoms. Throw in quite a few scattering atoms (dots): $q \gg 1$ times as many, thus $\alpha^s = q\alpha^a$ and $\varepsilon_\nu = 1/(1 + q) \approx 1/q$. Then the size of the volume in which emergent photons are produced in the case of no scattering (no dots) is proportional to the free absorption path length l_ν^a , i.e., the creation of emergent photons takes place within the absorption thickness $\tau_\nu^a = 1$ from the surface. With scattering (extra dots) the production of emergent photons is proportional to $l_\nu^* = l/\sqrt{\varepsilon_\nu} = l\sqrt{q} = (l_\nu^a/q)\sqrt{q} = l_\nu^a/\sqrt{q}$, i.e., the production of emergent photons now takes place only within the effective optical thickness $\tau_\nu^* = 1$ from the surface. The place with extinction depth $\tau_\nu' = 1$ lies even closer to the surface.

There are then only $1/\sqrt{q} = \sqrt{\varepsilon_\nu}$ photon creations involved. The rest of the manufactured photons are trapped. That occurs because the effective lifetime of the photons is larger when there is a great deal of scattering, so that the probability of photon destruction increases. The probability of photon creation does not increase proportionally because *photon loss* occurs. Any escaping quantum, not just scattered ones, leaves behind a non-excited atom that is not directly compensated statistically. There are fewer

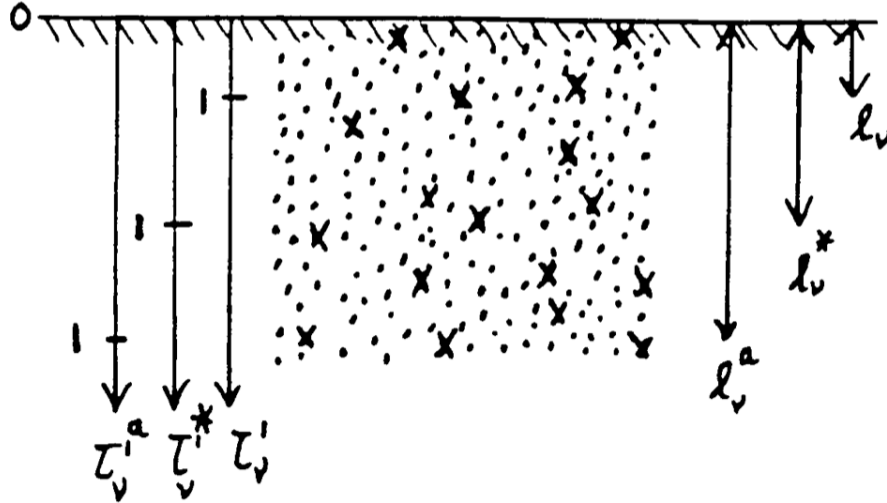


Figure 7.3: Schematic explanation of the small intensity from an effectively thick slab in the presence of much elastic scattering. The radial optical depth $\tau_\nu^i = 1$ at which the source function is representative of the emergent intensity lies only one average step length from the surface; that is much closer to the surface than the path length that a photon would traverse if there were no scattering ($\tau_\nu^a = 1$). The effective path length that a photon can randomly traverse after its creation falls between these values; this determines the effective depth of escape $\tau_\nu^* = 1$ at which the local Planck function is representative of the intensity of the emergent radiation.

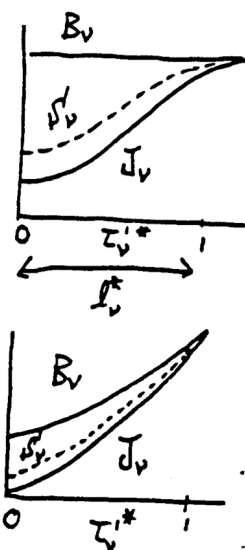
excited and more non-excited atoms than is the case in equilibrium, thus the emission coefficient j_ν is smaller, the extinction coefficient α_ν is larger, and the source function $S_\nu \equiv j_\nu/\alpha_\nu$ is smaller than in equilibrium.

The average radiative field J_ν decreases outwards from approximately the depth $l_\nu^* = 1/\sqrt{\varepsilon_\nu}$ where this radiative loss begins; from there on photons can reach the outer edge by random walks and be lost¹ before they happen to be extinguished. The source function is given by $S_\nu = (1 - \varepsilon_\nu)J_\nu + \varepsilon_\nu B_\nu$ and thus always falls between J_ν and B_ν . At the surface we have $S_\nu = \sqrt{\varepsilon_\nu}B_\nu$ and J_ν is even less than this. In sufficiently deep slabs $J_\nu \rightarrow B_\nu$ because no photons escape from there. The existence of an outer edge, which marks the sudden cessation of the homogeneity of the medium, is not yet felt by the radiative field and the source function. Thus we have there $S_\nu = (1 - \varepsilon_\nu)J_\nu + \varepsilon_\nu B_\nu \approx B_\nu$, whatever the value of ε_ν . The latter determines however where this “thermalization” appears.

The decrease of S_ν/B_ν near the surface of an optically thick medium as a result of radiative losses is actually a decrease in the *potential energy* of the radiative field that is available to excite or ionize etc. If there is some coupling between the radiative field and the kinetic energy distribution ($\varepsilon_\nu \neq 0$), then the radiative losses also lead to a decrease in temperature near the surface. An entirely homogeneous thick slab of gas can thus actually not exist. The existence of a surface as a transition to empty space into which photons disappear irrevocably results in a loss of the local energy density available for the excitation of atoms and the motions of atoms.

Question 7.20 What do you expect for the behavior of the photon destruction probability ε_ν with increasing depth, starting at the surface of a star?

¹from the medium, but available for observation.



Question 7.21 What is the region of applicability of respectively the Rosseland approximation and the Eddington approximation in terms of optical depth?

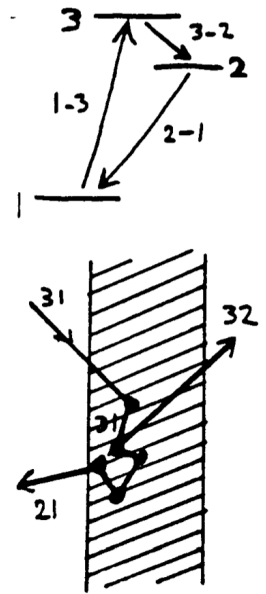
7.4 Radiative transfer with photon conversion

In the preceding paragraphs, the nonlocality of the source function in the presence of much elastic scattering was stressed: in that case the source function is determined at a different place from that from which the emergent radiation is observed. With inelastic scattering it can also happen that the source function is influenced *by another frequency* than the observed frequency. In the extreme case of photon conversion the observed radiation may have scarcely anything to do with the observed object.

We look at this again from a schematic standpoint. Postulate once again a slab which is homogeneous in its thermodynamical state variables and extinction coefficients but in which the source function can vary locally as a result of scattering and conversion. Suppose also that the medium consists of three-level atoms, with strong permitted bb transitions between the levels, all three with the same transition probability A_{ul} . Photon conversion is then possible via conversion of 3–1 photons into 3–2 plus 2–1 photons, and vice versa. Assume that the populations are distributed in a Boltzmann-like fashion. Then the population of level 1 is much larger than the populations of levels 2 and 3; thus it is entirely possible that the slab is optically thick in the lines 2–1 and 3–1 (equally thick in both – why?) but optically thin in the line 3–2. Let us assume that that is indeed the case.

Suppose then that the slab has a low temperature and a low density, and is irradiated from the left by a hot source with much stronger radiation at λ_{31} than at longer wavelengths. What happens in the slab to the incoming photons at the wavelengths λ_{21} , λ_{31} and λ_{32} ? For the latter, the slab is optically thin: a 3–2 photon will pass through unhindered for the most part; a few might give rise to 2–3 photon excitation. The 2–1 and 3–1 photons however will be confined. The 2–1 photons will provide for photon excitation into level 2. In view of the low density, 2–1 collisional deexcitation is less probable than radiative deexcitation, thus resonant scattering is especially prevalent: 2–1 photons will either random-walk through the medium until they leave the slab entirely, will be extinguished by a rare 2–1 collision, or will lose their identity via a rare 2–3 excitation (by a 3–2 photon or collision). Finally, the numerous incident 3–1 photons undergo photon excitation to level 3. Collisional deexcitation from level 3 to level 1 or 2 is relatively infrequent, and so spontaneous deexcitation dominates, with an equal probability (“branching ratio”) for 3–1 and 3–2. The first case is again resonant scattering and the new 3–1 photon will not go much farther than an original one. In the second case, the 3–2 photon on the contrary will usually escape the scene — because at that wavelength the slab is optically thin. There then remains an atom in level 2. That will usually add a 2–1 photon to the 2–1 radiative field already present.

The result: each incident 3–1 photon provides, possibly after a few 3–1 resonant scatterings, an escaping 3–2 photon; their number is much larger than the number of 3–2 photons from the source itself. The number of 3–2 photons escaping from the slab is thus a good measure of the number of 3–1 photons falling on the slab. That is a situation which indeed lies very far from LTE: the observed 3–2 intensity is determined by the intensity of a totally different object at an entirely different wavelength. Assume for example that you are looking at λ_{32} through the slab towards the hot source. The slab is optically thin and cold and, in the absence of



conversion, would cause an absorption line to be observed in the continuum of the hot source, analogous to the telluric lines in the solar spectrum; but now the slab provides a very strong emission line that has nothing whatsoever to do with the temperature of the slab but is very dependent on the temperature of the source.

It is improbable that the populations will follow Boltzmann distribution if collisions are hardly involved. The statistical-equilibrium equations for the three levels are then:

$$\begin{aligned} n_1(B_{12}\bar{J}_{21} + B_{13}\bar{J}_{31}) &= n_2(A_{21} + B_{21}\bar{J}_{21}) + n_3(A_{31} + B_{31}\bar{J}_{31}) \\ n_2(A_{21} + B_{21}\bar{J}_{21}) &= n_1B_{12}\bar{J}_{21} + n_3A_{32} \\ n_3(A_{31} + B_{31}\bar{J}_{31} + A_{32}) &= n_1B_{13}\bar{J}_{31}. \end{aligned}$$

These must be solved together with the radiative transport equations for the three lines (at a number of frequencies in each line) in order to find the populations and radiative fields.

In more realistic term diagrams photon conversion can take place in various ways, for example by means of bf transitions or making use of a coincidence in wavelength with a strong spectral line of another element such as $\text{Ly}\alpha$ (“optical pumping”). It is also possible that the 2–1 transition is not permitted or has a very small transition probability. Then level 2 accumulates a large overpopulation whose growth is ultimately capped, whether by collisional deexcitation to level 1 which then results in heating of the local medium, or by radiative deexcitation in such a “forbidden” line that then will be notably strong.

Question 7.22 Within the slab \bar{J}_{21} can be larger than in the incident radiative field – why?

Question 7.23 Show what happens in the example above if the slab is not optically thin but is effectively thin in line 3–2.

Question 7.24 Suppose that the slab consists of two-level-plus-continuum atoms, with bf transitions for 3–1 and 3–2. Does this differ from the example?

Chapter 8

Applications

8.1 Introduction: between thick and thin

This extra chapter gives a few applications of radiative processes and radiative transport to various astrophysical circumstances. These examples illustrate where this course material can be applied and at the same time provide insightful practical material.

There are many more applications in astronomy; this chapter contains only a first selection. In the future more will certainly be included; suggestions are welcome.

All the applications treated here have in common that they pertain to the domain between optically thick and optically thin. That is not surprising because $\tau_\nu \approx 1$ properly typifies the circumstances in which radiative transport is on the one hand important and on the other hand complex. For optically very thick conditions radiative transport is simple because the free path length of the photons in the medium is usually small with respect to typical scale lengths of changes in temperature and pressure; in these circumstances the Rosseland approximation usually holds. Optically very thin circumstances usually only involve the evaluation of the local extinction coefficient and source function, without complications brought on by radiative transport.

8.2 Spectra from stellar photospheres

8.2.1 Continua from the Sun

8.2.1.1 Extinction coefficient

The *photosphere* of a star is the layer from which the visible light emerges. In the photosphere of the Sun ($T_{\text{eff}} = 5770$ K, $N_e \approx 10^{14}$ cm⁻³) H is neutral but Na, Fe, Mg, Si are singly ionized (Saha). These “metals” are abundant and supply many electrons; therefore H⁻ provides the largest contribution to the continuous extinction in the visual (H_{bf}⁻) and infrared (H_{ff}⁻). At radio frequencies H_{ff} contributes the most. In the ultraviolet the extinction coefficient is determined by an assortment of mutually overlapping series limit continua (Al I, Mg I, Si I, C I, Fe I); in the far UV by the H and He I Lyman continua, and in the X-ray region by series limit continua of species with a high degree of ionization, e.g., Fe XXIV bf. See Figure 8.1.

Figure 8.1 holds for one specific electron pressure P_e (why?) but has about the same shape for values which do not deviate too much from P_e (see Novotny for examples). How does the *size* of the extinction vary with P_e ?

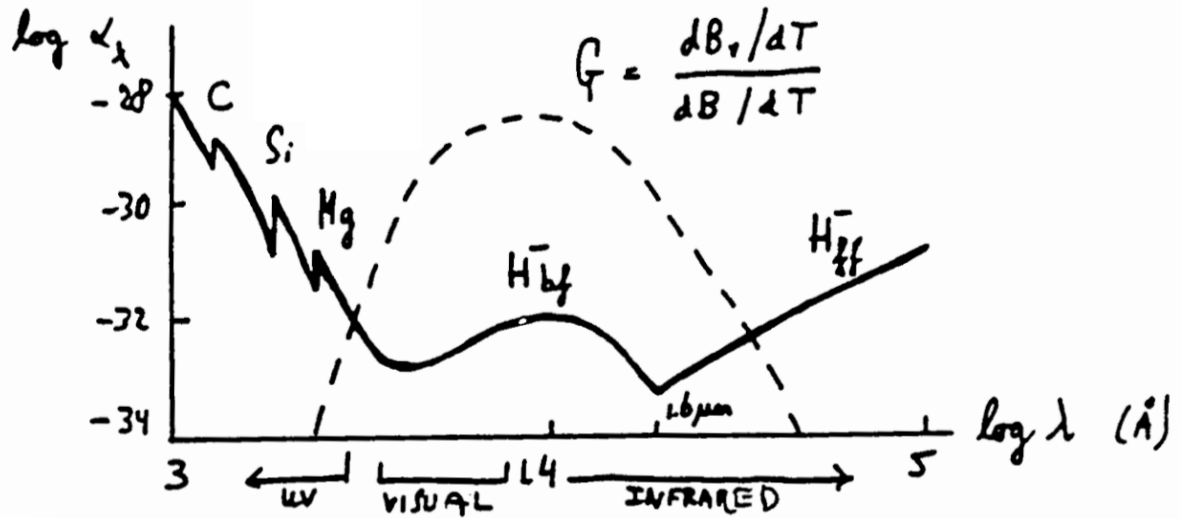


Figure 8.1: Sketch of the continuous extinction coefficient in the photosphere of the Sun.

The Sun is smallest in the visual region: you look most deeply into the Sun at $\lambda = 1.6 \mu\text{m}$ in the near infrared.

The Rosseland weighting function $G_\nu(T)$ is also included. The major portion of the solar flux runs between $\log \lambda = 3.5$ and $\log \lambda = 4.5$, why? (Note: the maximum of $B_\nu(T = 5770 \text{ K})$ falls at $\log \lambda = 3.9$ or $\lambda = 800 \text{ nm}$ but $B_\lambda(T = 5770 \text{ K})$ reaches its maximum at 600 nm .)

8.2.1.2 Height of formation

The continuous extinction coefficient changes by orders of magnitude across the spectrum, see Figure 8.1. Thus the location of $\tau'_\nu = 1$ varies strongly with wavelength. According to the Eddington-Barbier approximation, this location is the one that is representative of the emergent intensity. Moreover, the extinction of the line wavelengths of very highly probable bb transitions such as the Balmer and Lyman lines of H I, the H & K resonance lines of Ca II and the h & k resonance lines of Mg II is even larger by many order of magnitude than the continuous extinction.

Figure 8.2 shows the resulting heights of formation. The temperature and the height in the solar atmosphere are plotted against each other, with the height increasing to the left. The temperature is a type of horizontal average over the inhomogeneities the Sun shows in actuality. The zero point of the height scale is defined by taking $h = 0$ where $\tau'_\nu = 1$ for the continuum at $\lambda = 500 \text{ nm}$, thus approximately the location where the visual continuum the Sun arises. The second abscissa shows the density, in the conventional form of the mass column density $m \equiv$ the mass of an infinitely long column of 1 cm^2 cross section above the given height.

The density drops roughly exponentially outward (why?) so that the geometrical height scale ($h \equiv z$) is reasonably linear in $\log m$. The $\log \tau'_\nu$ scale varies roughly linearly with $\log m$ as well. Why? What is the frequency dependence of τ_ν ?

The temperature declines in the *photosphere* up to the location where the principal continua (with $\log \lambda = 3.5 - 4.5$ for λ in Å) become optically thin: $\tau'_\nu < 1$. The falloff of the temperature is in accord with energy transport by solar radiation where

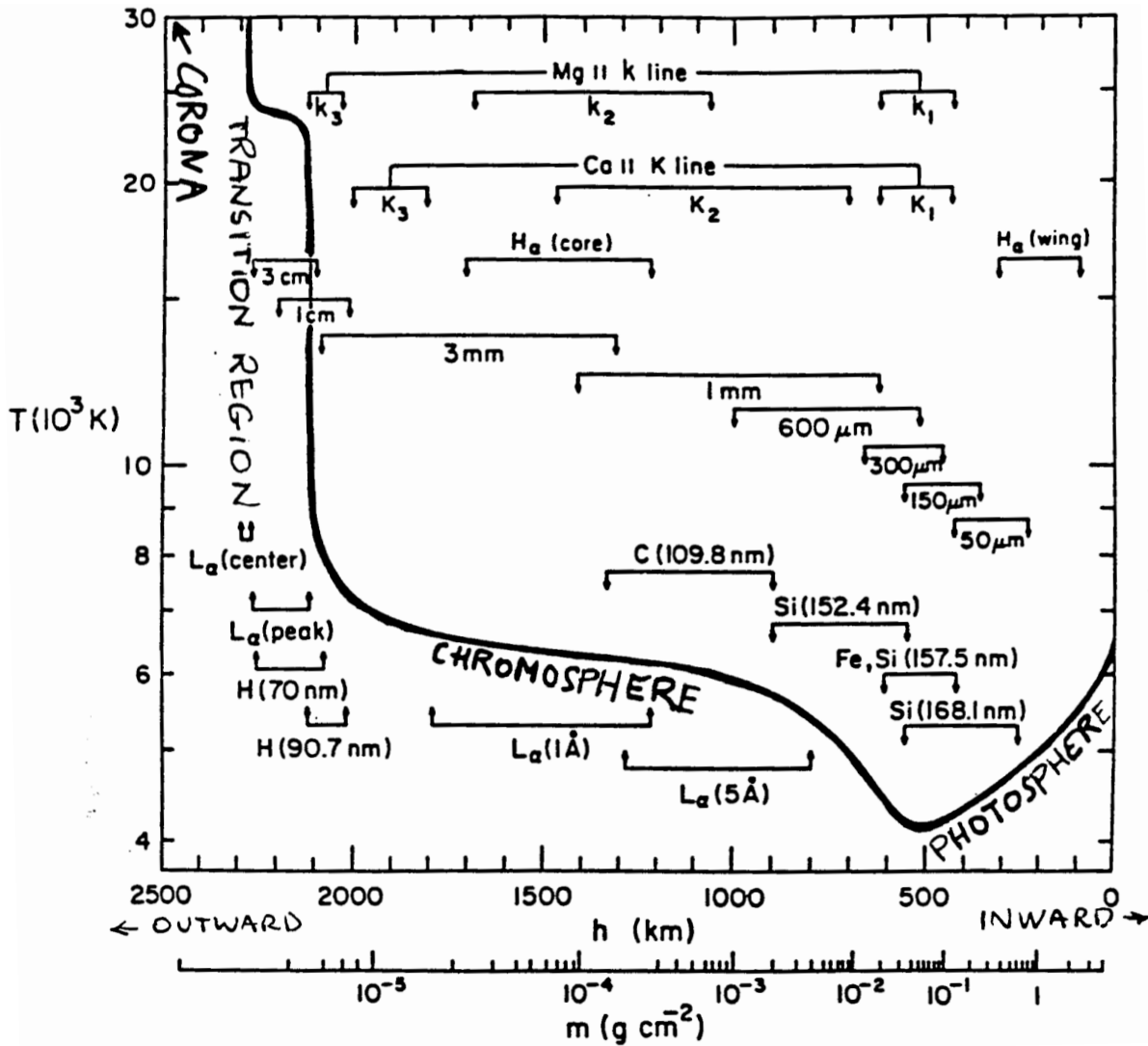


Figure 8.2: The height of formation of continua and strong spectral lines in the solar atmosphere. From Vernazza, Avrett and Loeser (1981).

this still dominates the medium (*radiative equilibrium*). The more superficial layers, however, are not coupled to \mathcal{F} because the visual solar radiation passes through them without being disturbed; they therefore may deviate from T_{eff} just as they do in the earth's atmosphere. In these higher layers the temperature once again rises, first moderately in the *chromosphere* and then very rapidly in the *transition region* to the very hot (2×10^6 K) *corona*.

The heights of formation of the various continua are determined by the extinction coefficient in Figure 8.1: the larger the extinction, the higher the formation; the same holds for spectral lines. For large extinction the photosphere is optically thick: the representative Eddington-Barbier location $\tau_\nu = 1$ then lies higher up. That is the case both in the far infrared and in the far ultraviolet; and for radio and X-ray radiation, the continuum arises in the chromosphere and the corona. The core of the Ly α line also has a very large extinction (why?) and becomes optically thin only just in the transition region to the corona.

Each piece $T(\log m)$ is a rough indicator of the behavior of $S_\nu(\log \tau'_\nu)$ for the

corresponding piece of spectrum with $\log \tau'_\nu \approx 0$. It is a good indicator where LTE is valid. That is certainly the case for the infrared continuum because H_{ff} is the principal extinction source there and the density in the photosphere is sufficiently large that the Maxwellian distribution applies there (Figure 8.3).

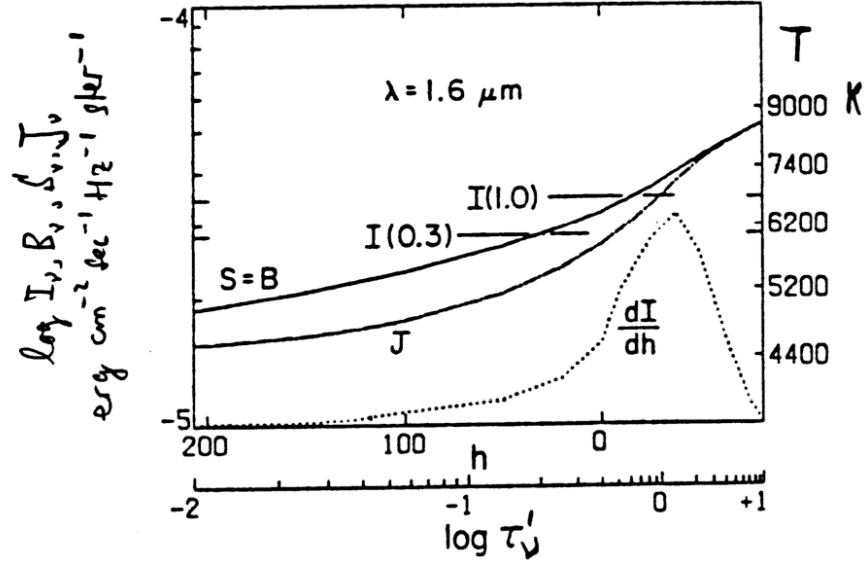


Figure 8.3: B_ν, J_ν and S_ν in the photosphere of the Sun for $\lambda = 1.6 \mu\text{m}$. From Vernazza, Avrett and Loeser (1981).

Figure 8.3 shows the formation of the solar radiation at $\lambda = 1.6 \mu\text{m}$. Compare the height scale and the $\log \tau'_\nu$ -scale with Figure 8.1 and Figure 8.2. Is the continuum at $\lambda = 500 \text{ nm}$ formed higher or lower than the $1.6 \mu\text{m}$ radiation? What determines the sides of the contribution function dI/dh with

$$dI/dh = \frac{d}{dh} \int_0^\infty S e^{-\tau'} d\tau' = -\frac{d}{dh} \int_{+\infty}^{-\infty} j e^{-\tau'} dh = j e^{-\tau'}?$$

Why isn't the top of this integrand at $\tau'_\nu = 1$? Do the emergent intensities $I_\nu(\mu=1.0)$ and $I_\nu(\mu=0.3)$ tally with the Eddington-Barbier relation? Above an isotropically radiating surface we have $J_\nu = \frac{1}{2}I_\nu$. Does that work here? If LTE holds somewhere it must do so at this wavelength, why? How does this figure indicate that LTE holds? And that $\varepsilon_\nu \approx 1$? Is it true that $S_\nu(\tau'_\nu=0) = \sqrt{\varepsilon_\nu}B_\nu$? And that $J_\nu \approx B_\nu$ for $\tau'_\nu = 1$? Where does $\tau'_{\nu^*} = 1$ occur?

8.2.1.3 Variation of emergent intensity and temperature stratification

The observed continuous spectrum $I_\nu(0, \mu)$ is a convolution of:

- the temperature behavior $T(h)$;
- the behavior of the source function, given by $S_\nu(h) = B_\nu[T_e(h)]$ where the assumption of LTE holds, and by $S_\nu(h) = (1 - \varepsilon_\nu(h))J_\nu(h) + \varepsilon_\nu(h)B_\nu[T_e(h)]$ where elastic scattering (such as Thomson scattering) is important;
- the behavior of the extinction $\alpha_\nu(m)$;
- the density stratification $m(h)$ (column mass).

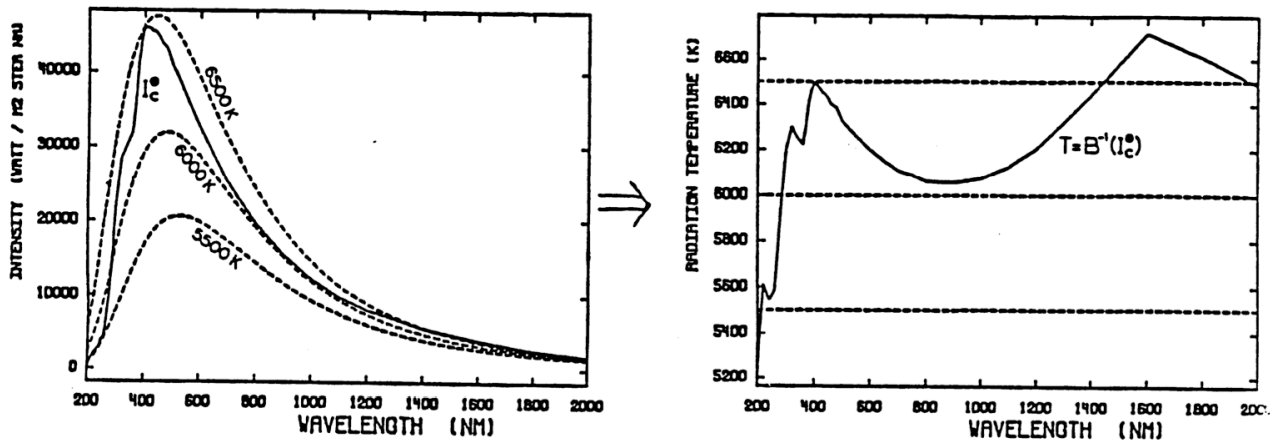


Figure 8.4: Left: the emergent intensity $I_\lambda(\tau'_\nu=0, \mu=1)$ for the middle of the solar disk compared to the three Planck functions $B_\lambda(T = 5500, 6000, 6500 \text{ K})$. Right: the same, in the form of brightness temperatures.

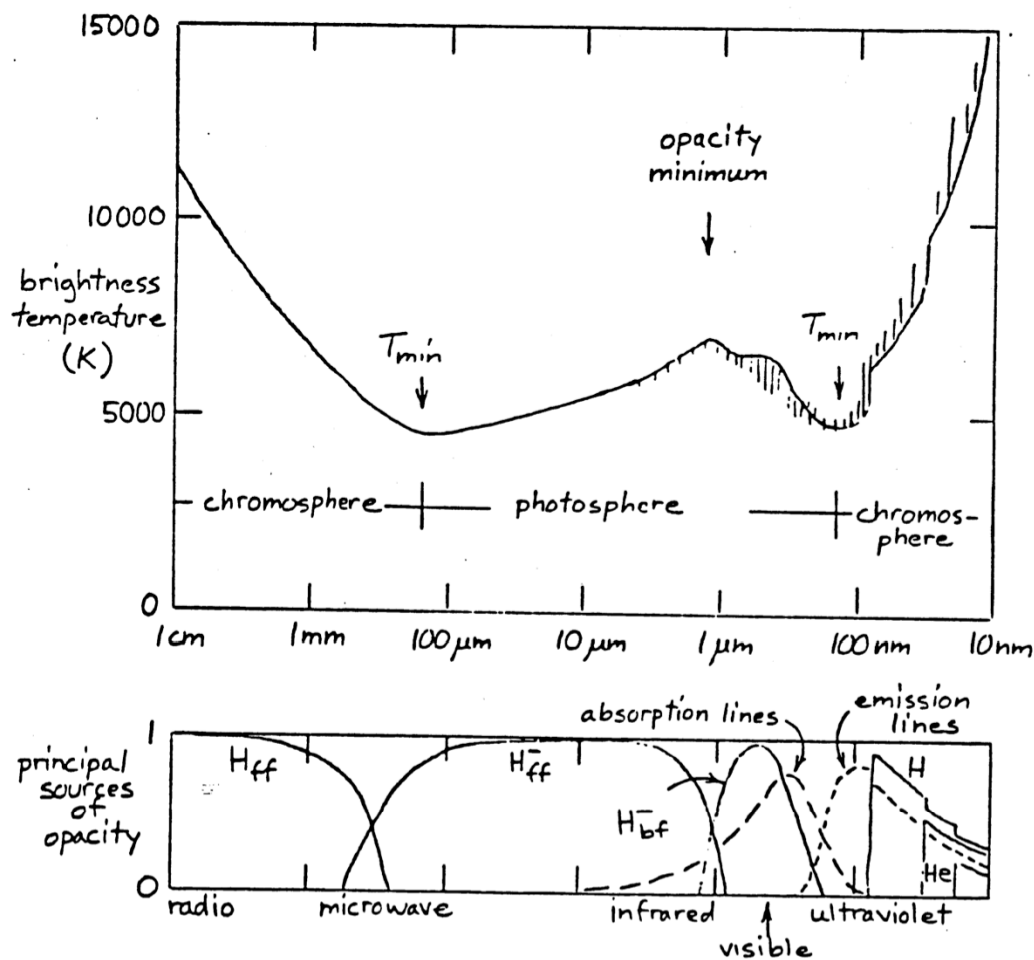


Figure 8.5: Brightness temperature of the Sun (above) and the relative contribution of the principal sources of continuous extinction, always at the height where $\tau'_\nu = 1$, as a function of frequency. Avrett (IAU Symposium 138, 1990).

You look through to a depth $\tau'_\nu \approx 1$ and see the source function at that spot. Better expressed: the value of the source function at the Eddington-Barbier depth $\tau'_\nu \approx 1$ is representative of the emergent intensity; this formulation is better because the integrand

$$\frac{dI}{dh} = \frac{d}{dh} \int_0^\infty S e^{-\tau'} d\tau' = -\frac{d}{dh} \int_{+\infty}^{-\infty} j e^{-\tau'} dh = j e^{-\tau'}$$

is reasonably broad, see Figure 8.3.

Figure 8.4 shows the intensity of the Sun compared to Planck functions, as energy and as brightness temperature T_b with $B_\nu(T_b) = I_\nu(0, 1)$. Why doesn't $I_\lambda(0, 1)$ follow a single Planck relation if LTE holds well for $\lambda > 400$ nm? Which quantities determine the run of the brightness temperature T_b^\odot at the right? Where did you previously see this shape?

Figure 8.5 shows the brightness temperature variation of the Sun for the whole spectrum, with the principal contributors to the continuous extinction indicated below. With a knowledge of this $\alpha_\nu(h)$, a *model atmosphere* $T(h)$ can be deduced from the observed intensities $I_\nu(0, 1)$. Vernazza *et al.* did that for all the spectral regions in Figure 8.2 to determine the temperature behavior shown there: this is an “empirical” model atmosphere determined from various continua and individual strong spectral lines, observed at the center of the Sun.

To this end Vernazza *et al.* had to carry out detailed NLTE radiative transport calculations for the ultraviolet bf transitions of H I, Mg I, Si I, Fe I and C I in the high photosphere because the ionization equilibria for these producers of extinction and contributors of electrons do not behave according to LTE. Their ultraviolet bf energy jumps are larger (3–5 eV) than the typical kinetic energy (1–2 eV) available in collisions in the cool layer between photosphere and chromosphere, so the radiative processes dominate in determining the ionization equilibrium: radiative ionization and spontaneous radiative recombination. (Why no induced recombination and collisional recombination?) In the ultraviolet the energy difference from a bound level to the ionization limit is so much larger than the kinetic part of the energy above, which falls off as ν^{-3} , that these ionization edges behave essentially as resonance lines, including resonant scattering.

8.2.1.4 Center-limb variation

Obliquely emergent radiation comes from more superficial layers according to equation (3.19):

$$I_\nu^+(0, \mu) = \int_0^\infty S_\nu(\tau'_\nu) e^{-\tau'_\nu/\mu} d\tau'_\nu/\mu.$$

The visual radiation comes from the photosphere; there LTE holds for the continuum (because H_{bf}^- provides the extinction, see Figure 8.1). The temperature decreases toward the outer layers of the photosphere (Figure 8.2, right side), thus $S_\nu(h) = B_\nu[T(h)]$ also decreases outward, and so the Sun shows *limb darkening*: the observed intensity diminishes from the center towards the limb of the solar disk. If LTE and the Eddington-Barbier relation (equation 3.21) apply, we have:

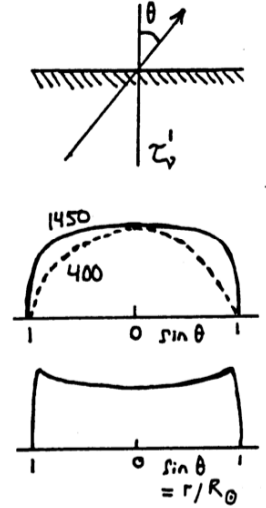
$$\frac{I_\nu(0, \mu)}{I_\nu(0, 1)} = \frac{a + b\mu}{a + b} = 1 - \beta + \beta\mu$$

with $\beta \equiv b/(a + b)$ the limb-darkening coefficient.

The limb darkening of the Sun was historically very important in:

- the conclusion that the photosphere is in radiative equilibrium, thus that the energy transport is provided primarily by radiation. Convection dominates up to just below the photosphere, due to the escape of radiation;
- the conclusion that H^- is the principal source of continuous extinction and emission;
- the empirical determination of the run of $T(h)$ before the infrared and ultraviolet intensities became available.

Radiation at $\lambda = 400$ nm and $\lambda = 1450$ nm emerge from approximately the same layer (Figure 8.2, Figure 8.4 right). Yet the limb darkening at $\lambda = 400$ nm is larger, why? In the far infrared the Eddington-Barbier relation is satisfied if the temperature increases linearly with τ'_ν . Why? Is that also true if the temperature declines inward linearly with τ'_ν ? For $\lambda > 1$ mm, limb brightening is observed instead of limb darkening. Why? Do you expect limb darkening or limb brightening in the Lyman continuum ($\lambda \leq 90.6$ nm)?



8.2.2 Spectral lines from the Sun

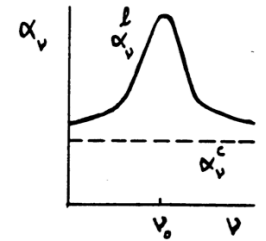
8.2.2.1 Extinction coefficient

A spectral line is always the result of a positive peak in the extinction coefficient. The size of the peak is given by

$$\alpha_\nu^l(\nu = \nu_0) = \frac{\pi e^2}{m_e c} b_l n_l^{\text{TE}} f_{lu} \varphi(\Delta\nu = 0) \left[1 - \frac{b_u}{b_l} e^{-h\nu_0/kT} \right]$$

with f_{lu} the bb oscillator strength and $\varphi(\Delta\nu = 0)$ the maximum of the extinction profile function. The amount of extinction varies to first order in proportion to the population of the lower level n_l . This is determined by the local density and temperature according to the Saha and Boltzmann LTE equations (n_l^{TE}), with a correction factor (b_l) for departures from LTE if nonlocal radiative fields play a role in the population equations. To the next level of approximation, the line extinction is also dependent on the population of the upper level, because of sensitivity to departures from LTE in the source function via the negative correction for induced emission ($1 - b_u/b_l e^{-h\nu/kT}$) if $S_\nu^l \neq B_\nu$.

The shape of the peak, given by $\phi(\nu - \nu_0)$, is the convolution of a Gaussian profile and a Lorentzian profile, determined by the local Doppler broadening, the radiative damping and the local collisional damping. These line-broadening mechanisms are treated extensively elsewhere: see Gray (1976) or Mihalas (1978).



8.2.2.2 Height of formation

Once again the extinction coefficient determines from which layer the radiation escapes. In this case it does not vary across a wide spectral domain such as for the continua above, but rather across a very small spectral domain, that of the line profile. Once again the source function at the monochromatic depth of escape is representative of the emergent intensity according to the Eddington-Barbier approximation

$$I_\nu^+(0, \mu) = \int_0^\infty S_\nu(\tau'_\nu) e^{-\tau'_\nu/\mu} d\tau'_\nu/\mu \approx S_\nu(h[\tau'_\nu = \mu]),$$

now with the total source function S_ν which is composed of the line source function S_ν^l and the continuum source function S_ν^c according to

$$S_\nu = \frac{\alpha_\nu^c S_\nu^c + \alpha_\nu^l S_\nu^l}{\alpha_\nu^c + \alpha_\nu^l}.$$

Where LTE holds, $T(h)$ also determines directly $S_\nu = B_\nu[T_e]$ and therefore the emergent intensity. Where LTE does not hold, the line source function is given by

$$S_\nu^l = (1 - \varepsilon_\nu) \bar{J}_\nu + \varepsilon_\nu B_\nu[T_e]$$

in the two-level approximation, or by

$$S_\nu^l = (1 - \varepsilon_\nu - \eta_\nu) \bar{J}_\nu + \varepsilon_\nu B_\nu[T_e] + \eta_\nu B_\nu[T^*]$$

if, besides resonant scattering, photon conversion also contributes, with η_ν the chance per extinction of multilevel processes and T^* a representative process temperature for such circuitous routes.

8.2.2.3 The Na I D lines

Figure 1.2 shows the two yellow Na I D lines in the solar spectrum. In question 1.24 it was stated that by the end of these lecture notes an answer could be given to the question of how far the textbooks' analogy goes between a radiating flame sprinkled with salt and the solar spectrum. The mistake of the textbooks is that cows and horses are compared: the flame is optically thin so that the interpretation demands no radiative transport, but the Sun is optically thick. Whether the Na I D lines in the solar spectrum are in emission or in absorption does not follow simply from equation (3.18), as it does for the flame, but from the Eddington-Barbier relation and the behavior of the source function.

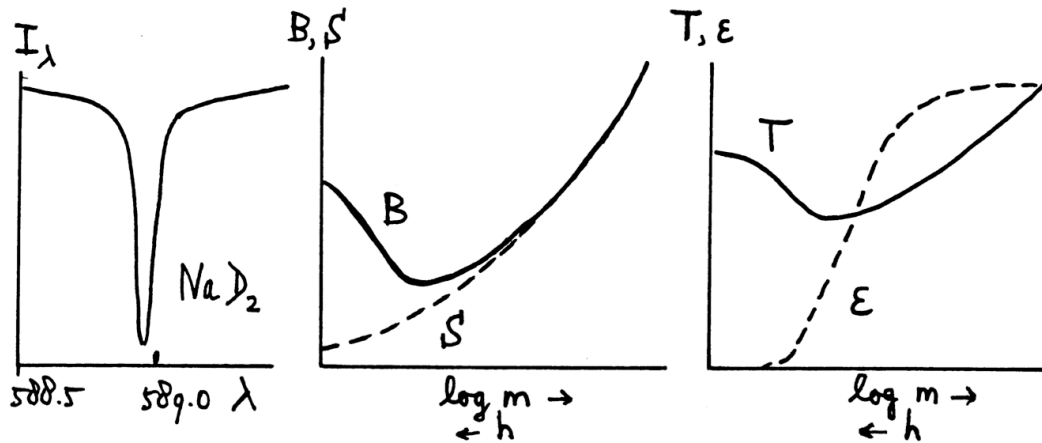


Figure 8.6: *Formation of the Na I D lines in the solar spectrum. The probability of destruction ε declines as $\varepsilon \approx 1$ in the deep photosphere to $\varepsilon \approx 10^{-4}$ above the temperature minimum. The source function follows the Planck function only in the deep layers; in higher layers the source function follows the angle-averaged intensity \bar{J}_{ν_0} , with $\bar{J}_{\nu_0} < B_\nu$ on account of photon losses. For the wings of the lines LTE holds, but the line cores are deeper than they would be in LTE; the Na I D lines are “scattering lines” in the core.*

Detailed numerical solution of the statistical-equilibrium equations for the excitation and ionization of sodium atoms in the solar atmosphere shows that the two-level approximation is a good one for these resonance lines. Therefore the result in Figure 8.6 is readily understood. As the density drops, the collisional probability C_{ul} falls sharply with the height h ; since A_{ul} is large for these resonance lines and does not depend on the height, the photon destruction probability $\varepsilon \approx C_{ul}/A_{ul}$ also falls sharply with h ; in deep layers $\varepsilon \approx 1$ holds. The line source function follows \bar{J}_{ν_0} in the higher layers and approaches the Planck function only in the deep photosphere where $\varepsilon \approx 1$.

The line wings are formed in deep layers; thus LTE holds for them. The line extinction α^l in the wings decreases monotonically with the distance in wavelength from the line center $\Delta\lambda = \lambda - \lambda_0$; the larger $\Delta\lambda$, the deeper the emergent intensity is determined. Moreover, for sufficiently large $\Delta\lambda$, $\alpha^l \ll \alpha^c$; then the continuum source function dominates the total source function and LTE formation is ensured.

The line cores have $\alpha^l \gg \alpha^c$. The cores are formed much higher; for them, the emergent intensity is determined in the regime where $S_\nu \approx \bar{J}_{\nu_0}$. This is much lower than the Planck function at that height. In consequence the source function (\approx line source function) is not influenced by the ambient temperature there. The existence of the temperature minimum does not affect the line source function or the emergent line profile; the line cores formed there are entirely determined by the strong resonant scattering of photons formed deeper, and so their intensities drop much lower than they would under LTE. The physical cause of this is the occurrence of large photon losses whose effect on the source function is noticeable until well below the $\tau \approx 1$ height of formation.

So there is after all an analogy with the flame experiment: in both cases resonant scattering plays an important role in the line extinction. The manner in which they affect the observed intensity is however completely different in the two cases — even if both cases result in dark Na I D lines.

8.2.2.4 The Ca II K line

Figure 8.8 sketches an extension of Figure 7.1 for the formation of the strong Ca II K line in the solar spectrum (Figure 8.7).

The extinction coefficient (top left panel) varies strongly with the wavelength because the bb processes offer an extra possibility for absorption and scattering. The size of the bb peak varies strongly with height, being dependent on the level populations which are sensitive to the density, the temperature and (in NLTE) the radiative field. The shape of the bb peak varies with height, being dependent on the density (collisional damping) and the temperature (collisional damping and Doppler broadening).

The extinction coefficient determines where the representative height of formation h , with $\log \tau'_\nu(h) = 0$, lies (top middle panel). Each frequency has its own optical depth scale $\tau'_\nu(h)$, roughly exponential in h near $\log \tau_\nu(h) = 0$. The intensity $I_\nu(0, 1)$ of the emergent radiation in the Eddington-Barbier approximation is given by the value of the monochromatic source function S_ν at the representative $\log \tau'_\nu = 0$ depth.

The monochromatic (total) source function S_ν (bottom middle panel) is the convolution of the continuum source function S^c and the line source function S^l (bottom right panel). (Because of this convolution the total source function is always frequency-dependent, even if the line source function S^l does not vary across the

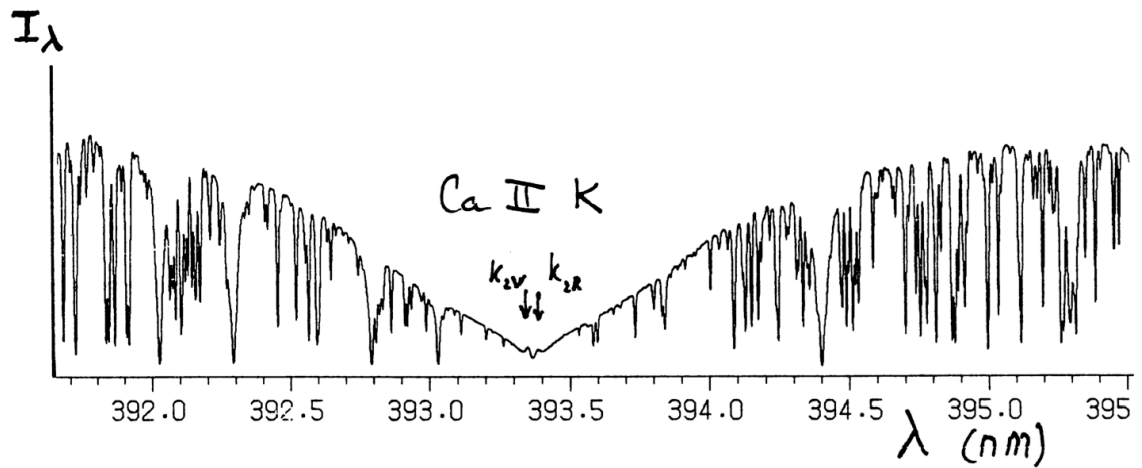


Figure 8.7: The Ca II K line in the solar spectrum. The broad deep absorption in this part of the solar spectrum was christened by Fraunhofer the “K” resonance line of the Ca^+ ion. This is the strongest line in the visually observable part of the solar spectrum. Superimposed on the broad line wings are many weaker spectral lines (“blends”); most arise from neutral “metals” such as Fe I. In its core the K line shows two minuscule peaks which are extensively studied in the Sun and stars: the K_{2V} and K_{2R} peaks (V for violet and R for red – signifying the peak on the violet or red side of line center, K_3).

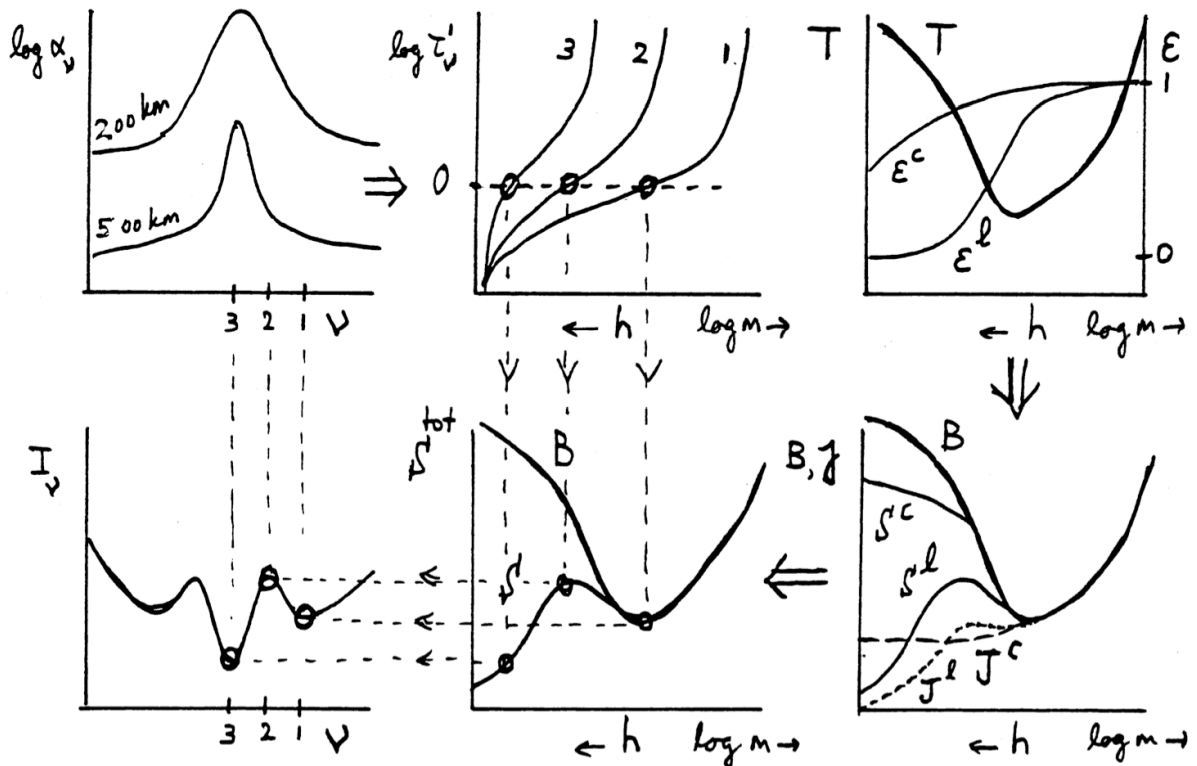


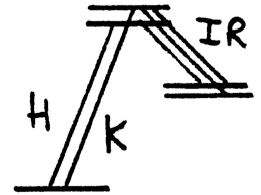
Figure 8.8: 6-panel diagram for the formation of the Ca II K resonance line (393.3 nm) in the solar spectrum and the K_3 , K_2 , and K_1 features.

line profile, as a result of complete redistribution over the line profile, as is assumed here.) Both source functions are determined by the temperature variation $T(h)$ and the amount of coupling to it, given by the destruction probabilities ε^c and ε^l which are small if scattering is dominant in the extinction. The line source function dominates in the Ca II K core because of the large line extinction in the layers where the radiation escapes; scattering is important there. In the deep photosphere where it participates in the formation of the far line wings, the continuum source function is to a good approximation equal to the Planck function, with $\varepsilon_\nu^c \approx 1$.

The Ca II K line is just strong enough that the line source function is sensitive to the temperature rise at the base of the chromosphere before photon scattering losses start dominating and induce decoupling from the Planck function. The result is a small increase in S^l that is evident as two small emission peaks in the observed line profile: the K_2 peaks (bottom left panel).

Once again the Eddington-Barbier approximation is assumed. How do you know that? What would be different if the Eddington-Barbier approximation did not hold? Scattering plays an important role in the shape of the observed line core (K_3). How do you know that? How is the strong scattering expressed in the behavior of the line source function? In the far wings, on the contrary, LTE is a good approximation. How can you tell that?

Only the lower part of the term diagram of Ca II is included in the sketch in the margin. The uppermost part is not important, why? Also the bf processes from Ca II to Ca III and Ca I are not important, why? The transitions marked IR refer to the Ca II infrared triplet lines (at $\lambda = 8498, 8542$ and 8662 \AA).



Photon conversion is possible from the Ca II H & K lines to the three “infrared” Ca II lines and vice versa because they share common upper levels. The two lower levels of the infrared lines are *metastable* because there are no permitted radiative transitions from them to the ground level. Such photon conversion is not really important for the H & K lines because they have larger transition probabilities: the *branching ratio* from the common upper levels favors the resonance lines. Conversion is quite important for the three infrared lines because their extinction is smaller (Boltzmann): where they become optically thin, their line source function faithfully follows the Planck function because coupling occurs via conversion to the still optically thick H & K lines.

The diagram illustrates the formation of the Ca II K line according to Jefferies and Thomas (1960). With this analysis these authors set forth the basics of the NLTE interpretation of spectral lines of the Sun and stars. This description was however by no means final. For one thing, there is also some partial frequency redistribution so that the line source function itself is frequency dependent: different parts of the line have their own source function, which each in their own fashion differs from the Planck function (Uitenbroek 1989). For another, the small emission peaks at the K_2 wavelengths actually originate exclusively in regions on the Sun with an enhanced concentration of magnetic field. The actual line formation is thus more complicated than is sketched here.

8.2.2.5 Emergent intensity and temperature stratification

How is the photospheric temperature variation expressed in the spectral lines? In LTE that is clear: $S_\nu = S_\nu^l = S_\nu^c = B_\nu[T(h)]$, and the line profile “illustrates the $T(\tau_\nu^l)$ variation”, convolved with the (strongly depth dependent) profile of the

extinction coefficient and the temperature sensitivity of the Planck function. The temperature declines outward, thus the lines are absorption lines.

But if scattering or photon conversion is important, it is possible that the observed line profile does not say much about the temperature variation. That is for example the case in the core of the Ca II K line: the fact that the K_3 line core is darker than the K_2 emission peak does not imply that the temperature drops again after an initial rise, but is the result of the NLTE photon losses in a scattering line.

For the Ca II K line LTE holds in the line wings (how can you tell that in Figure 8.8?). The observed intensity variation $I_\nu(0,1)$ for $\Delta\lambda = \lambda - \lambda_0 = 0.1\text{--}1$ nm can serve to determine the temperature variation in the photosphere. Which quantities must be known for this and how would you attack the problem?

Violet spectral lines have a much lower central intensity than the corresponding spectral lines in the red for equal $\alpha_\nu^l(h)$ and $\tau_\nu^c(h)$ scales. Explain that on the basis of the temperature sensitivity of the Planck function.

Spectral lines with $\lambda \leq 180$ nm and with $\lambda \geq 150$ μm are not absorption lines but emission lines. Explain that, bearing in mind that the continua at 180 nm and 150 μm are formed just in the region of the temperature minimum between photosphere and chromosphere (Figure 8.2), and that spectral lines are always formed higher than the adjacent background continuum.

8.2.2.6 Center-limb variation

Assume for convenience that the source functions fall off linearly outward: $S_\nu^l = a^l + b^l \tau_\nu^l$ and $S_\nu^c = a^c + b^c \tau_\nu^c$, so that the Eddington-Barbier approximation holds exactly (Figure 8.9).

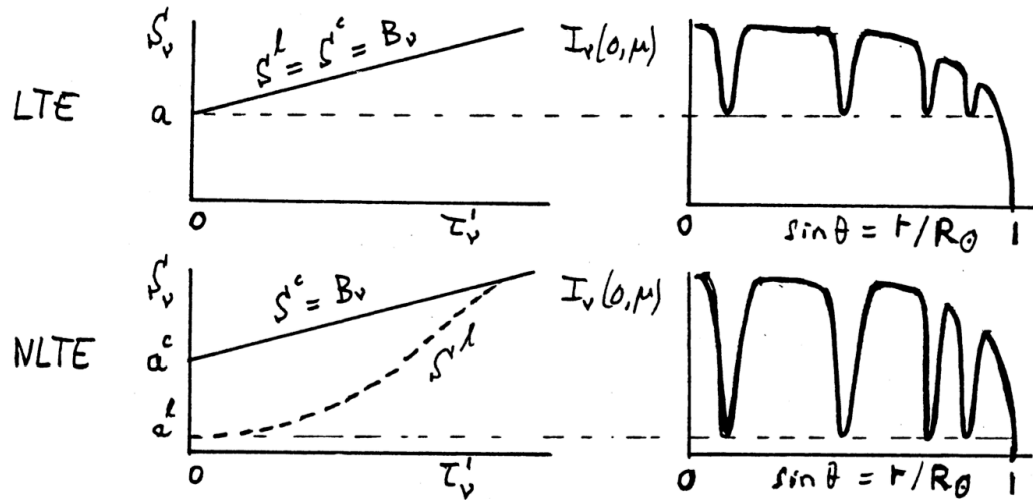


Figure 8.9: *The center-limb variation of photospheric spectral lines.*

In going from the center to the limb of the observed solar disk, the contrast of absorption lines diminishes because the total source function falls outwards. For LTE we have $S_\nu^l = S_\nu^c$ and the contrast of the strongest lines weakens up to $I_\nu = a$; near the solar limb the lines disappear completely. If $\varepsilon \ll 1$, however, then S_ν^l falls much more steeply than S_ν^c . The central intensities of the strongest lines are then much deeper than in LTE, and they do not disappear at the solar limb ($a^l \ll a^c$).

In the real Sun the temperature rises again into the chromosphere. Nearer the limb the radiation arises from higher layers; for many lines the height of formation

near the solar limb lies completely above the temperature minimum. The fact that these lines exhibit no emission cores near the solar limb *proves* that they have $\varepsilon \ll 1$, thus a NLTE source function.

8.2.2.7 Outside the limb

Beyond the solar limb *all* lines become emission lines, whatever their mechanism of formation. (Why? Recall that the “solar limb” is seen where the total continuous optical thickness of the Sun along the line of sight is approximately unity.) For lines of sight sufficiently far outside the solar limb the Sun also becomes optically thin in the strongest lines. Then the intensity of such a line is directly proportional to the population of the upper level (why?).

The strongest visual line in the eclipse spectrum is $H\alpha$: it appears as a reddish-purple arc at the limb of the Sun at the beginning and end of a total solar eclipse. Hence the name *chromosphere*.

8.2.3 Spectra of stellar photospheres

With the above insights, we can readily understand most photospheric lines in the solar spectrum (that is, the lines in the *visual* spectral region, why?). Therefore the spectrometry of stellar photospheres has become a “classical” discipline. For the most part, LTE is assumed and abundance determination is the goal.

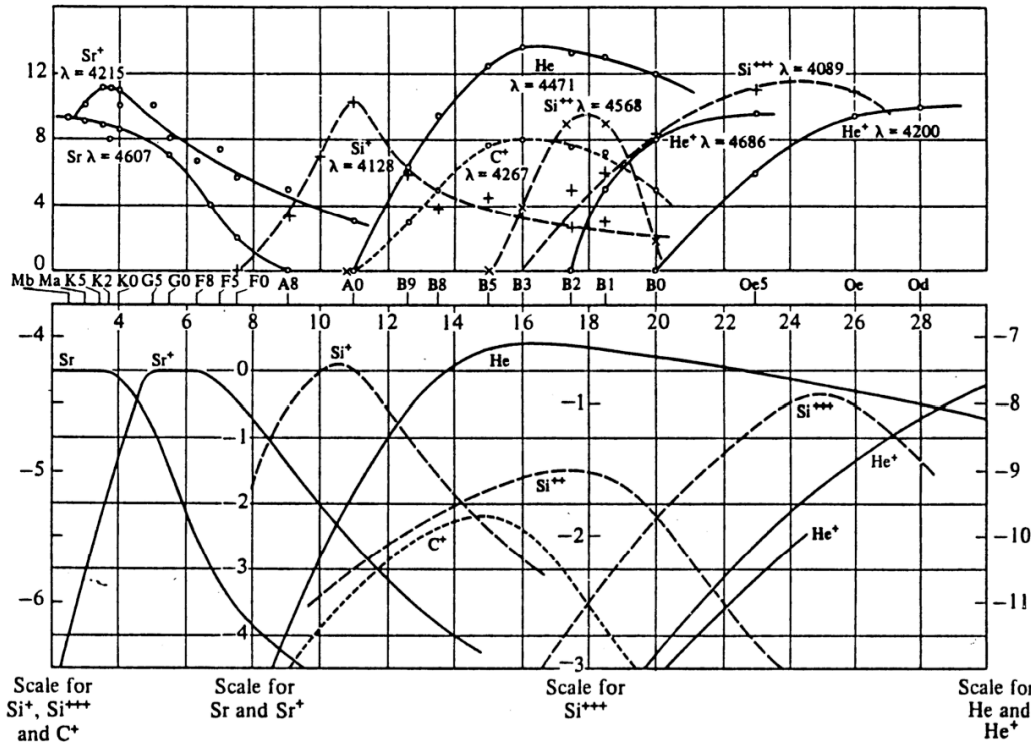


Figure 8.10: *Spectral classification.* The upper graph gives estimates (by eye, from photographic plates) of the strengths of representative spectral lines as a function of the empirically assigned spectral type. Below are given the population ratios as a function of temperature, calculated from Saha and Boltzmann for $P_e = 131 \text{ dyne cm}^{-2}$. After Payne.

The differences in stellar spectra across the HR-diagram, however, are hardly due to abundance differences, but rather to the effects of T_e and P_e on the populations via Boltzmann and Saha. That was not understood for a long time; the spectral classification arose long before the role of the temperature became clear and the Hertzsprung-Russell diagram could be translated from pure empiricism into astrophysics. That happened in the most famous doctoral thesis in astronomy, by Cecilia Payne (1925, Harvard): spectral classification was shown to be temperature classification (Figure 8.10).

The continuous extinction mechanisms vary across the HR-diagram. In cool stars such as the Sun hydrogen is predominantly a neutral atom, and H_{bf}^- dominates in the visual spectral domain and H_{ff}^- in the infrared. The free electrons involved in this come from the ionization of those metals that have both a reasonable abundance and a low ionization potential: Na, Mg, Al, Si, Ca and Fe. In the solar photosphere these elements are predominantly singly ionized. LTE is a good approximation for these processes because they are coupled with collisions. Furthermore, in G and K stars Rayleigh scattering off hydrogen also occurs. That is especially important in the visual because the resonance lines of hydrogen, i.e., the Lyman lines, lie in the far ultraviolet (how do you know that?) and especially for Population II stars with a low abundance of metals (why?). The spectral lines come primarily from neutral metals (visual) and singly ionized metals (near ultraviolet), with a few molecular bands.

In hotter stars hydrogen is however mostly ionized and thus H^- is not a factor any more; most of the free electrons then come from hydrogen. Thomson scattering provides a large contribution to the continuous extinction in O stars, with the consequence that LTE cannot be assumed for the corresponding continua. The scattered photons are then created as a rule in H_{ff} processes. Moreover, in O stars He II comes into play (the $n = 2$ ionization edge coincides with the Lyman continuum, why?) as does He I in B stars. The metals are all ionized and therefore show few lines in the visible spectral region (the neutral levels of metals such as Fe I have many lines in the visible; for higher ionization levels the electron energy differences are larger so that their lines fall in the ultraviolet). Many important resonance lines lie beyond the Lyman limit (91.2 nm) and can only be observed from space.

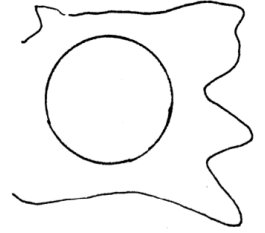
Situated between the hot and the cool stars are the A stars. In them H_2^+ ions provide extra extinction: a singly-ionized molecule with two protons and one electron.

In the coolest stars there is much Rayleigh scattering off molecules, especially off H_2 . H_2^- also contributes at long wavelengths via ff processes. The line spectrum of M stars is dominated by strong molecular bands, especially in the infrared where the majority of vibration and rotation transitions lie. If there is more carbon than oxygen in the star then all the oxygen is taken up into CO and there appear as well the lines of many carbon compounds (e.g., C_2 , CN, HCN, C_2N_2 , SiC_2); conversely, if oxygen dominates all carbon is locked up in CO and there appear the lines of many oxygen compounds (e.g., OH, H_2O , TiO, ZrO, VO).

8.3 Stellar envelopes

8.3.1 Stellar coronae

Coronae are very hot ($T_e \geq 10^6$ K), tenuous ($N_e \leq 10^7$ cm $^{-3}$), more or less spherical envelopes of stars. The majority of late-type stars have a corona. Here we discuss



radiative processes in the solar corona.

At $T_e = 10^6$ K the solar corona for $\lambda \leq 10$ cm is optically thin. That means that there are no complications due to radiative transport; specification of the rate equations provides the emergent intensities directly. The situation is however far from LTE, so that for this specification all possible population mechanisms must be evaluated to see if they are influential, and those that are must be evaluated explicitly. Table 8.1 provides an overview of the atomic processes; ions are especially involved in coronal processes because the combination of very high temperature and low density results in a high degree of ionization.

Process	Incoming	Outgoing	Rate
Absorption	photon + atom	excited atom	$u_\nu B_{mn} N_m$
Stimulated emission	phot. + excited atom	2 phots. + atom	$u_\nu B_{nm} N_n$
Spontaneous emission	excited atom	photon + atom	$N_{nm} A_{nm}$
Photo-ionization	photon + atom	ion + electron	$u_\nu N_m B_{m\kappa}$
2-Body recombination	electron + ion	photon + atom	$N_e N_i A_{\kappa m}$
Dielectronic Recomb.	electron + ion	phot. + excited atom	$N_e N_i \alpha_{diel}$
Dielectronic Absorption (Auto-ionization)	phot. + excited atom	ion + electron	$N_n u_\nu \kappa_{diel}$
Thomson scattering	photon + electron	phot. + electron	$\sigma_T N_e$
Free-free emission (Bremsstrahlung)	electron + ion	elec. + ion + phot.	$N_e N_i \kappa \kappa'$
Free-free absorption	phot.+electron+ion	ion + electron	$N_e N_i B_{\kappa' \kappa} u_\nu$
Collisional excitation	electron + atom	elec. + excited atom	$N_m N_e C_{mn}$
Collisional de-excitation	elec.+ excited atom	electron + atom	$N_n N_e C_{nm}$
Collisional Ionization	electron + atom	2 electrons + atom	$N_m N_e C_{m\kappa}$
3-Body Recombination	2 elecs. + atom	electron + atom	$N_e^2 N_i C_{\kappa m}$

Table 8.1: *Atomic processes. After Zirin.*

In coronal circumstances, both radiative excitation and ionization and the induced radiative processes are negligible with respect to the corresponding collisional processes because the electron temperature $T_e \approx 10^6$ K is much higher than the typical radiative temperature $T_{\text{eff}} \approx 6000$ K of the local radiation field, generated in the underlying photosphere. Therefore radiative excitation is negligible, and excitation is collisional:

$$P_{lu} \approx C_{lu}$$

radiative ionization is negligible, and ionization is collisional:

$$P_{lk} \approx C_{lk}$$

collisional and radiatively-induced deexcitation are negligible, and deexcitation is spontaneous radiative:

$$P_{ul} \approx A_{ul}$$

collisional and radiatively-induced recombination are negligible, and recombination is spontaneous radiative:

$$P_{kl} \approx A_{kl}^{\text{bf}} \quad (8.1)$$



with A_{kl}^{bf} the transition probability analogous to the Einstein coefficient A_{ul} for spontaneous radiative recombination. Thus the population equations become:

$$\frac{dn_i}{dt} \approx \sum_{j<i} (n_j C_{ij} - n_i A_{ij}) + \sum_{i<j} (n_j A_{ji} - n_i C_{ij}),$$

(with A_{ki}^{bf} also written as A_{ji}). The excitation of a two-level atom is given by statistical equilibrium:

$$n_1 C_{12} = n_1 N_e \int_{v_0}^{\infty} \sigma_{12} f(v) v dv \approx n_2 A_{21},$$

in which the population ratio $n_2/n_1 \approx C_{12}/A_{21}$ depends not only on the temperature (which enters into the velocity distribution $f(v)$), but also on the electron density, and remains far below the Boltzmann ratio $n_2/n_1 = C_{12}/C_{21}$ (itself barely temperature-dependent) which is achieved at much larger density. The two-level photon destruction probability $\varepsilon_\nu \approx C_{ul}/A_{ul}$ is very small; the two-level line source function becomes

$$S_\nu^l \approx J_\nu \approx (1/2) B_\nu(T_{\text{eff}}) \ll B_\nu(T_e)$$

in accord with

$$S_\nu^l \approx \frac{b_u}{b_l} B_\nu(T_e).$$

Even though the excitation is achieved through collisions, i.e., with a knowledge of the local temperature, the collisional frequency is too low to bring the population of the excited level up to the Boltzmann value. Each ion that is excited then promptly decays spontaneously, and the escape of the bb photon represents a large NLTE loss of energy; local detailed balance, which demands as many collisions upwards as collisions downwards, is not achieved by a long shot.

For the bf ionization-equilibrium, on the contrary, the electron density just drops out because an ion waits a long time for a passing electron for photorecombination. The probability for that is proportional to the electron density, just as for collisional ionization; the rate equations then result in Boltzmann-like ionization ratios which are independent of the temperature, which strongly simplifies their calculation and makes diagnostic applications easier. On the contrary, the Saha formula for the TE ionization ratio depends on N_e ; that arises because collisional recombination is proportional to N_e^2 . The second colliding electron in this three-particle process provides the Saha N_e but only counts if collisions are sufficiently dominant. In coronal circumstances the dependence of excitation and ionization on N_e is thus just reversed with respect to TE circumstances.

This description of the bb and bf processes is incomplete. In coronal circumstances, one should also consider *dielectronic processes*, for which two electrons undergo energetic transitions at the same time. Configurations in which two electrons are excited at the same time can have *autoionization*-energy levels, lying above the ionization limit of the configuration for a single valence electron. The excitation of such a level can lead to ionization by a radiation-free transition in which one electron is released (*autoionization*). That would occur if an already excited atom encountered a photon or electron suitable for a second excitation; however, the probability for this is small in coronal circumstances because for both encounters the rate is small with respect to the rate of spontaneous deexcitation (i.e., the probability of spontaneous deexcitation is higher than the probability of encountering a suitable photon or electron for the excited atom).

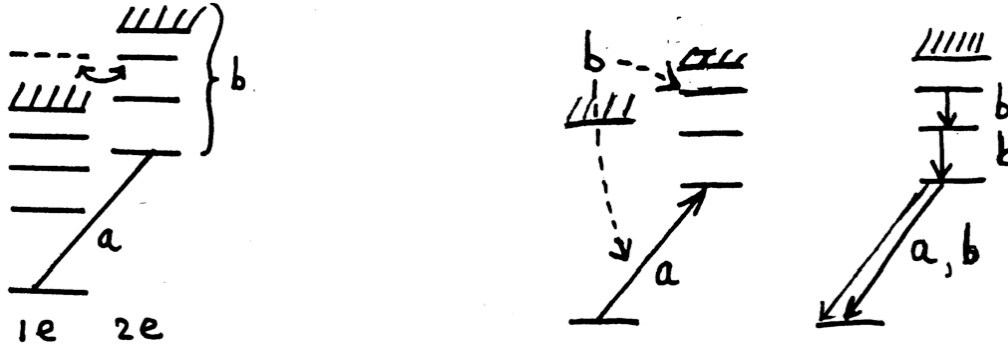


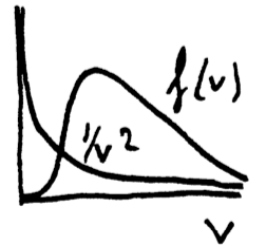
Figure 8.11: *Dielectronic recombination.* The left pair of diagrams sketches how the term diagram of an atom with two excited electrons (right diagram, marked $2e$) can have excited levels that are above the ionization limit of an atom with a single excited electron ($1e$). The right pair of diagrams sketches how first, an energetic free electron excites a bound electron in an ion as it itself is captured into another excited level (left diagram). Then, spontaneous deexcitation of both electrons, possibly in a cascade or series of transitions to progressively lower levels, provides line photons and leaves the ion in the ground state, one ionization level lower (right).

The reverse process, dielectronic recombination, is important, however. In this process a passing energetic electron excites a bound electron and at the same time is itself captured into an autoionization state. From here the atom can undergo a nonradiative ionization which leaves it in its original state of ionization; but the atom can also undergo doubly spontaneous radiative deexcitation of both electrons – there is plenty of time – leaving it in the next lower ionization stage. At high temperature this recombination process is more efficient than radiative recombination, ten times more so in the solar corona, because the collisional excitation of the bound electron helps to reduce the kinetic energy of the captured electron – much more energetic electrons can participate than those rather scarce ones near the ionization edges. (Slower electrons are captured more easily: the capture cross section σ_{fb} for photon recombination for hydrogen-like ions decreases quadratically with the electron energy: $\sigma_{fb} \sim 1/v^2$. Energy loss from extra bb excitation compensates this decrease.)

The ratio between the probability of photon recombination and the probability of dielectronic recombination depends solely on T_e and not on N_e , why? The conclusion above that the ionization equilibria depend only on the temperature thus doesn't hold. At high temperature dielectronic recombination wins because the peak of the Maxwellian distribution and the $1/v^2$ -dependence of the photon recombination are shifted further apart from one another with increasing temperature.

Figure 8.12 by Carole Jordan shows coronal ionization ratios in a Cecilia Payne-like diagram for successive ionization stages of iron. At any given temperature there are several stages of ionization present at the same time. The levels with filled shells are difficult to ionize and exhibit broad maxima ($7+$, $16+$). The ions one stage below ($6+$, $15+$) have many dielectronic recombination levels which provide a long high-energy tail.

Because of the low density the ionization equilibria are established slowly: after a temperature disturbance this takes several minutes. The attainment of statistical equilibrium between the populations takes even longer.



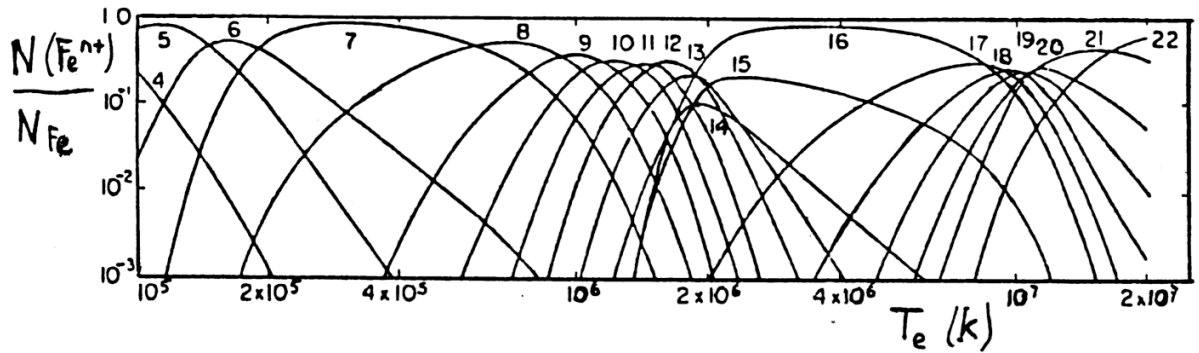


Figure 8.12: Ionization stages of iron in the solar corona. After Jordan.

The many dielectronic recombinations are evidenced by spectral lines: each recombination is always followed by two bb emissions, or even more if the deexcitation of the excited level to the ground state goes via intermediate levels. That provides a *cascade spectrum*, characteristic of circumstances in which recombination from excited levels is important. The spectral lines can thus be much stronger than predicted from the two-level approximation.

The spatial dependence of electron temperature T_e is smoothed by the large free path lengths of the particles over large distances. If a magnetic field is present, this smoothing only occurs parallel to the magnetic field, not perpendicular to it, because the electrons then spiral around the field lines (coronal loops). Then large temperature and density gradients are possible across the field lines. These indeed occur, because the dissipation of “mechanical” energy appears to take place via such magnetic structures. These lead to sharply defined structures with different temperature and density parameters and therefore with different emission coefficients; because the immediate surroundings are optically thin these structures are also readily observable. The best far-UV images of the Sun (from NASA’s Hi-C instrument, launched on a rocket in 2012) show coronal fine structure all the way to the instrumental resolution of 0.2 arc second or 150 km on the Sun.

8.3.1.1 The solar corona in X-rays

The coronal X-ray spectrum consists of overlapping series limit continua with superimposed emission lines (why in emission?), see Figure 8.13. There are several ionization stages evident at the same time (seven due to iron are seen here) which provide good temperature diagnostics. Coronal X-ray spectra are very rich in spectral lines.

Each photon represents the destruction of thermal energy and its disappearance from the local medium: i.e., each photon provides *radiative loss*. The line strengths are proportional to $n_u A_{ul}$ (why?), the loss per spectral line is proportional to $N_e N_H$ (why?), and because we have approximately that $N_e = N_H(1 + 2B)$, with B^1 the fraction N_{He}/N_H , it follows that the loss per transition is proportional to N_H^2 . The sum over all lines and continua then provides the total radiative loss; Figure 8.14 gives an example as a function of temperature. The indicated curve is unreliable for $T_e \leq 5 \times 10^4$ K because the corona is then no longer optically thin in the strongest lines such as Ly α . There the corona is still effectively thin so that all photons created

¹NB: This B is the fifth B in these lecture notes.

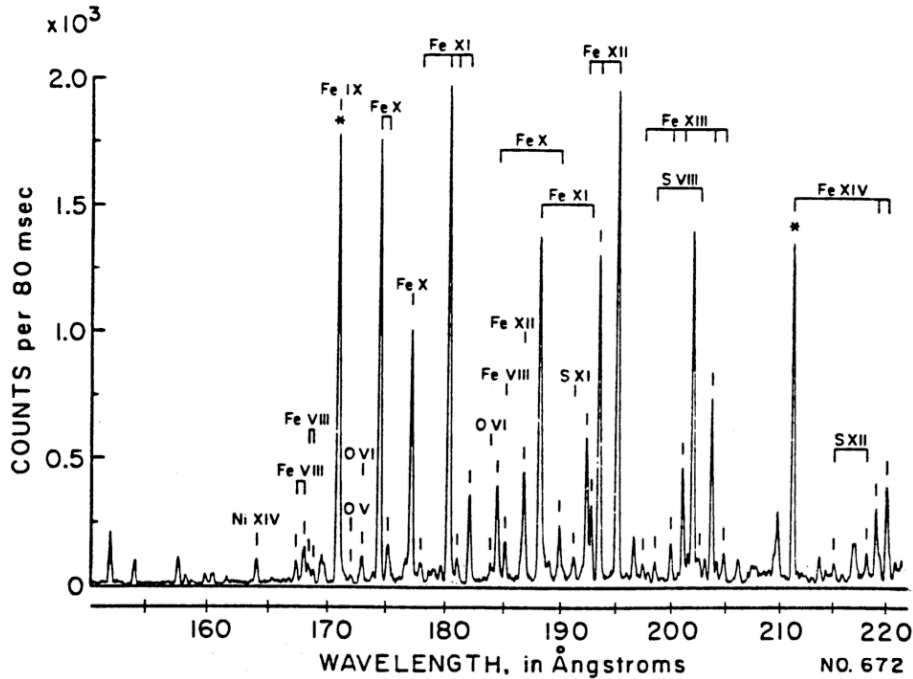


Figure 8.13: An X-ray spectrum of the Sun, taken from a rocket. Plasmas found in coronal circumstances (optically thin, hot, and tenuous) produce spectra with numerous emission lines from high ionization stages.

still count, but the term $B_{ij}J_\nu$ then is involved in the excitation processes so that the populations also depend on the radiation field.

8.3.1.2 The solar corona in the visible

There are various “coronae” = circles of light visible around the Sun, see Figure 8.15.

The F-corona arises from scattering of photospheric sunlight by interplanetary dust with cross section $d \approx 1 \mu\text{m} \approx \lambda$; this scattering is therefore “white” ($\sim \lambda^0$) and strongly peaked in the forward direction. The scattering is elastic, thus its spectrum is the photospheric line spectrum (*Fraunhofer spectrum*, from which the F is taken). Because these photons are strongly scattered forwards, viewed from Earth they principally appear near the Sun: the intensity increases towards the Sun. That holds also for the sky background at sunset, resulting from the scattering off dust and water droplets in the Earth’s atmosphere. For the brighter sky, however, Rayleigh scattering off molecules dominates, with the associated dipole phase function, and is scarcely increasing with proximity to the solar disk. (A good criterion for sky brightness is then to hold your thumb in front of the Sun and then to see how close to the Sun the sky remains blue.)

The *K corona* refers to the radiation of the corona itself, i.e., the emission from the tenuous shell of hot gas around the Sun. The largest contribution to the continuous extinction (and emission) is given by Thomson scattering. The electrons move with an average velocity

$$\bar{v} = \sqrt{\frac{2kT}{m_e}} \approx 10^9 \text{ cm s}^{-1},$$

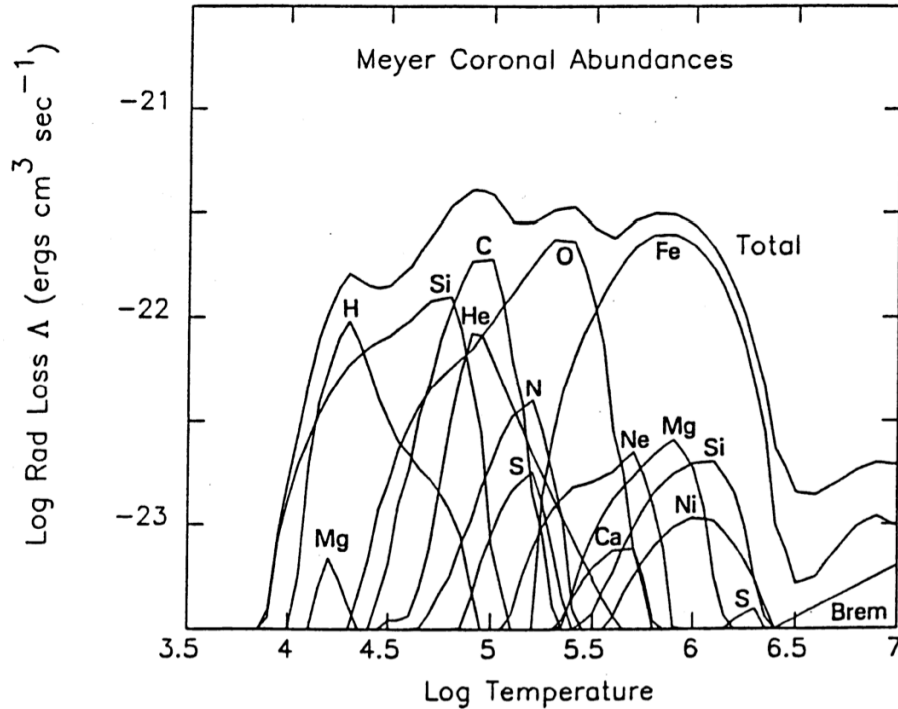


Figure 8.14: *Radiative losses curve.* On the vertical axis is plotted the loss of energy from photon emission divided by the product of electron density N_e and hydrogen density N_H ; temperature is plotted on the horizontal axis. The curve holds for an optically thin gas plasma with solar abundances (Cook et al. 1989).

thus the associated typical Doppler shift is

$$\Delta\lambda_D = \lambda \frac{\bar{v}}{c} \approx 10 \text{ nm}.$$

These shifts are quite large; although the scattering is elastic (monochromatic in the PRS, in the “frame of the particle”), the Fraunhofer line spectrum appears smeared out to an observer on Earth. Only the broadest lines are seen, notably in the case of the Ca II H and K lines where two broad, shallow absorption troughs remain; on this basis Grotrian first proposed that the corona contains fast-moving scattering electrons, and thus it must be very hot.

wavelength	identification	$\Delta\lambda_D$	\bar{v}	A_{ul}
530.3 nm	[Fe XIV]	0.051 nm	29 km/s	60 s^{-1}
569.4	[Ca XV]	0.087	46	95
637.4	[Fe X]	0.049	23	69

Table 8.2: *Coronal emission lines in the visible spectrum during a solar eclipse.*

The visible spectrum also exhibits individual well-known emission lines, see Table 8.2. Together these form the *E corona*. These *forbidden* transitions with $A_{ul} \approx 10^2 \text{ s}^{-1}$ (the notation [Fe XIV] means a forbidden transition in the spectrum of Fe^{13+} . All permitted transitions (with $A_{ul} \approx 10^4\text{--}10^8 \text{ s}^{-1}$) fall in the far ultraviolet and the X-ray region for such high stages of ionization). From the assumption that the observed line width is due to thermal Doppler shifts \bar{v} , we have

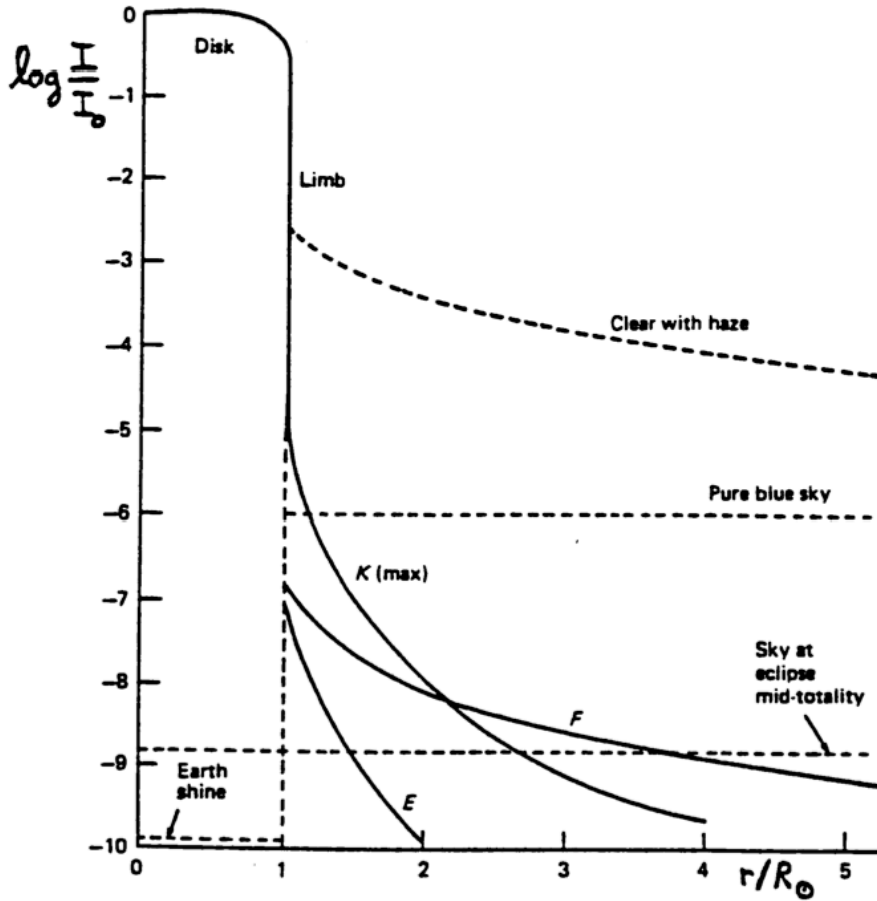


Figure 8.15: *The visual corona of the Sun. The radiation from the solar corona itself falls off with distance from the solar limb according to the curve K . This changes with the activity of the Sun. The F corona describes the contribution to the intensity observed about the Sun resulting from scattering by interplanetary dust. The “earth-shine” is light scattered from the moon back to Earth during a total solar eclipse. After Van de Hulst.*

for the temperature: $T \approx 2 - 5 \times 10^6$ K. The [Ca XV] line is the only one observable in highly active regions; there the corona is apparently hotter.

Why are these lines visible although they are forbidden? Once again it is thanks to the combination of very high temperature and low density: radiative deexcitation dominates over collisional deexcitation even for these long lifetimes in the upper level.

These coronal lines long remained a puzzle. They are very strong in coronal spectra taken during total solar eclipses; in a “coronal sky” (blue all the way up to your thumb) they can also be measured with a *coronagraph*: a telescope with an internal disk which eclipses the Sun. They were ascribed to a new element *Coronium* although no place for this element was available in the periodic table. Finally Grotrian and Edl nd provided the explanation based on the above identifications.

8.3.1.3 The solar corona in radio waves

Figure 8.16 shows the variation from the photosphere to the Earth's orbit for three characteristic frequencies:

1. $\nu_B =$ gyro frequency $= 2.8 \times 10^6 B$, with the magnetic field strength B in Gauss. Cyclotron radiation occurs for $\nu = (1 - 5) \times \nu_B$; synchrotron radiation for $\nu = (10 - 1000) \times \nu_B$. Of interest for $9 < \log \nu < 12$, and only in active regions (why?).
2. $\nu_p =$ plasma frequency $= 9 \times 10^3 \sqrt{N_e}$. There is no wave propagation for $\nu < \nu_p$. Strong *plasma radiation* can be generated by exciting disturbances with frequency $\nu = \nu_p$ and at the higher harmonics $\nu = 2\nu_p$ etc. Such plasma radiation dominates in the solar wind near the Earth for frequencies $\nu < 1$ GHz. Its measurement is carried out with space vehicles because the ionosphere is not transparent to such long waves ($\nu_p \approx 10^7$ Hz).
3. $\nu(\tau_{\text{ff}}=1) =$ frequency at which the continuous Bremsstrahlung extinction reaches an optical thickness $\tau_{\text{ff}} = 1$ over one scale height. Thus the corona is optically thin for the ff processes to the right of the dashed curve and is optically thick to the left; the curve shows where thermal Bremsstrahlung photons of this frequency typically originate.

The thermal Bremsstrahlung provides the temperature. The observed antenna temperature is:

$$T_A \equiv \eta_A T_b = T(0) e^{-\tau} + T_{\text{cor}} (1 - e^{-\tau})$$

so that the coronal temperature T_{cor} is measured provided that $\tau_{\text{ff}} > 1$. That however isn't the case for regions where $\nu(\tau_{\text{ff}} = 1) < \nu_p$ because waves of the frequencies which reach that depth are bent or deflected. (Figure 8.17). This doesn't happen for $10^8 < \nu < 10^9$ Hz because at those frequencies ν_p is reached deeper than at $\tau_{\text{ff}} = 1$. At $\nu \approx 150$ MHz for example the turnaround point is at $\tau_{\text{ff}} \approx 5$.

Even though the place where $\nu = \nu_p$ for $10^8 < \nu < 10^9$ Hz lies much deeper than $\tau_{\text{ff}} = 1$, plasma radiation is observable at those frequencies because:

- the brightness temperature in the most active regions can readily reach $T_b \approx 10^{15}$ K. With $\tau = 10$ and $e^{-\tau} = 2 \times 10^{-4}$ there still remains $T_b = 10^{10}$ K;
- the corona is strongly inhomogeneous, thus $\tau_{\text{ff}} = 1$ fluctuates strongly. Radiation from an optically thick coronal loop can escape in between the loops.

In the low-frequency domain (30 kHz — 1 GHz) we observe *flares* with a negative frequency drift, caused by a shock front (*Type II*) or a fast-moving packet of electrons (*Type III*) that are rapidly moving towards the outer part of the corona. The plasma radiation then follows ν_p , thus the local frequency shift $\sim \sqrt{N_e}$.

The high frequency domain (1 GHz — 30 GHz) is dominated by gyro radiation. Figure 8.18 shows characteristic spectra for homogeneous sources. The slopes are given and the arrows show how the curves shift as the various parameters increase.

Consider for example Bremsstrahlung spectrum (ff processes). For the Rayleigh-Jeans portion we have $S_\nu = B_\nu = 2k\nu^2 T/c^2$ (why does LTE hold?), thus

$$T_b = \frac{c^2}{2k\nu^2} I_\nu \begin{cases} = T_e & \text{for } \tau_\nu \gg 1 \\ = T_e \tau_\nu = (c^2/2k\nu^2) j_\nu L & \text{for } \tau_\nu \ll 1 \end{cases}$$

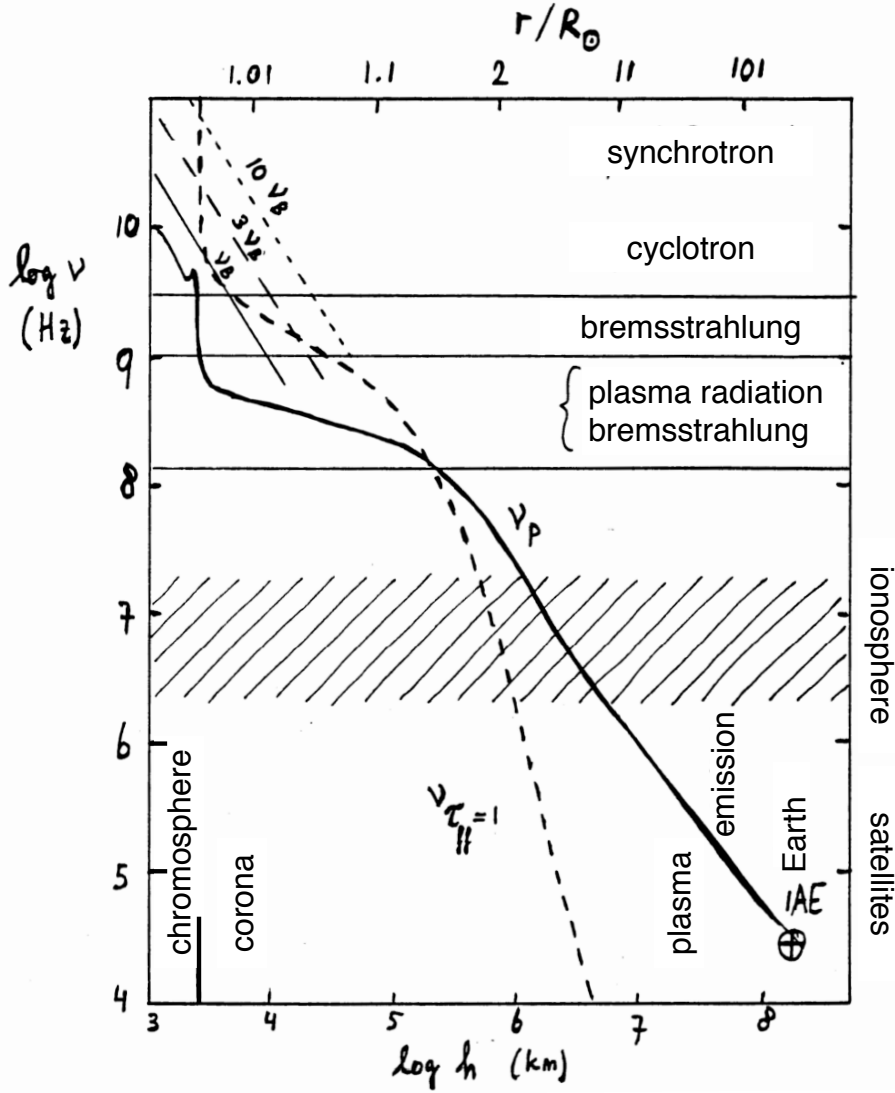


Figure 8.16: Typical spatial scales for three characteristic radio frequencies between Sun and Earth: the gyro frequency ν_B , the plasma frequency ν_p and the formation frequency ν_τ^{ff} . After a preprint by Gary and Hurford.

with L the source diameter. The emission coefficient $j_\nu \sim N_e^2$, why? The flux density (irradiance) is:

$$R_\nu = \Delta\Omega I_\nu \begin{cases} = \Delta\Omega B_\nu & \text{for } \tau_\nu \gg 1 \\ = \Delta\Omega j_\nu L = \Delta\Omega B_\nu k_\nu L & \text{for } \tau_\nu \ll 1. \end{cases}$$

Note the frequency dependence: for T_b this is $\sim \nu^0$ for $\tau \gg 1$ and $\sim \nu^{-2}$ for $\tau \ll 1$; for R_ν on the contrary $\sim \nu^2$ for $\tau_\nu \gg 1$ and $\sim [\nu^2 \nu^{-3}(1 - e^{-h\nu/kT})] = \nu^0$ for $\tau_\nu \ll 1$.

For synchrotron spectra the pitch angle θ , the magnetic field B , the number of particles N above the threshold energy and the spectral index δ of the particles energy distribution $n(E) = kE^{-\delta}$ join in. The peak of the curve always falls at the frequency with $\tau_\nu \approx 1$ (why?).

These curves can be compared against observations to decide among mechanisms and to determine parameters of the source. The upper figures then can be applied

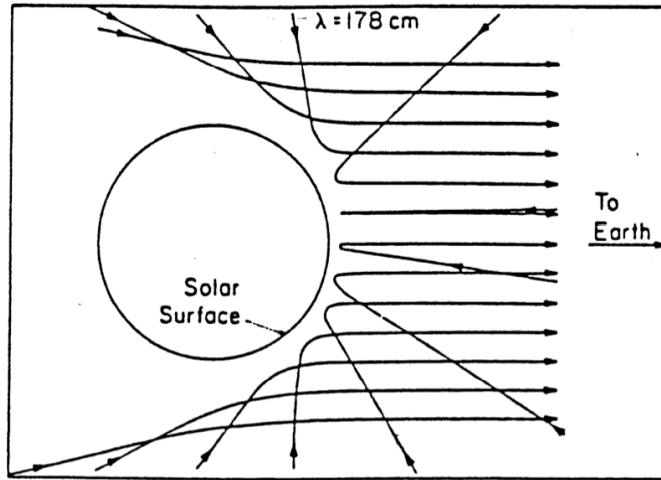


Figure 8.17: *Curvature and reflection of radio waves in the corona. Here spherical symmetry is assumed; in actuality the corona is strongly inhomogeneous.*

to resolved sources, while the lower ones can also be used if the true source diameter is unknown (why?).

8.3.2 Stellar winds

Many stars release not only photons and neutrinos into space as a sign of their existence, but also shed matter. The hydrodynamical solar wind (the evaporation of the hot corona) does not interest us here, but the radiatively driven winds of hot stars do. They are discussed at some length in radiative transport theory (see Chapters 14 and 15 of Mihalas 1978). At the heart of this lies the fact that the line extinction coefficient is systematically shifted in wavelength in the presence of systematic velocity structure within an object.

The formation of *P Cygni profiles* is geometrically determined. The unshifted emission line emerges from the parts of the extended atmosphere on each side of the star (A in Figure 8.19) that expand at right angles to the line of sight and give no Doppler shift. (Why is this contribution in the form of emission?) In the direction of the star, the layers with the largest expansion velocity give the largest blue shift in their absorption contribution (why absorption?). Such P Cygni profiles are a good indication of the occurrence of a stellar wind and mass loss. The P Cygni profiles are observed in the visible spectrum but are the most evident in the ultraviolet spectra of hot stars because the resonance lines of the most important ionization levels fall in the ultraviolet. With the first ultraviolet spectrometer (Morton in 1967, with a rocket for which the retrieval misfired and so it had to be dredged up from the sea floor) it was unexpectedly discovered that O and B supergiants have Si IV lines (140.28 nm and 154.95 nm) which show outwardly streaming velocities up to 2000 km s^{-1} . That is much larger than the escape velocity:

$$v_{\text{esc}} = 620 \left(\frac{M}{M_{\odot}} \right)^{\frac{1}{2}} \left(\frac{R}{R_{\odot}} \right)^{-\frac{1}{2}} \text{ km s}^{-1}.$$

The visual lines arise in the photosphere or in layers above the surface and only reach a terminal velocity $v_D \approx 300 \text{ km s}^{-1}$, but the ultraviolet resonance lines have

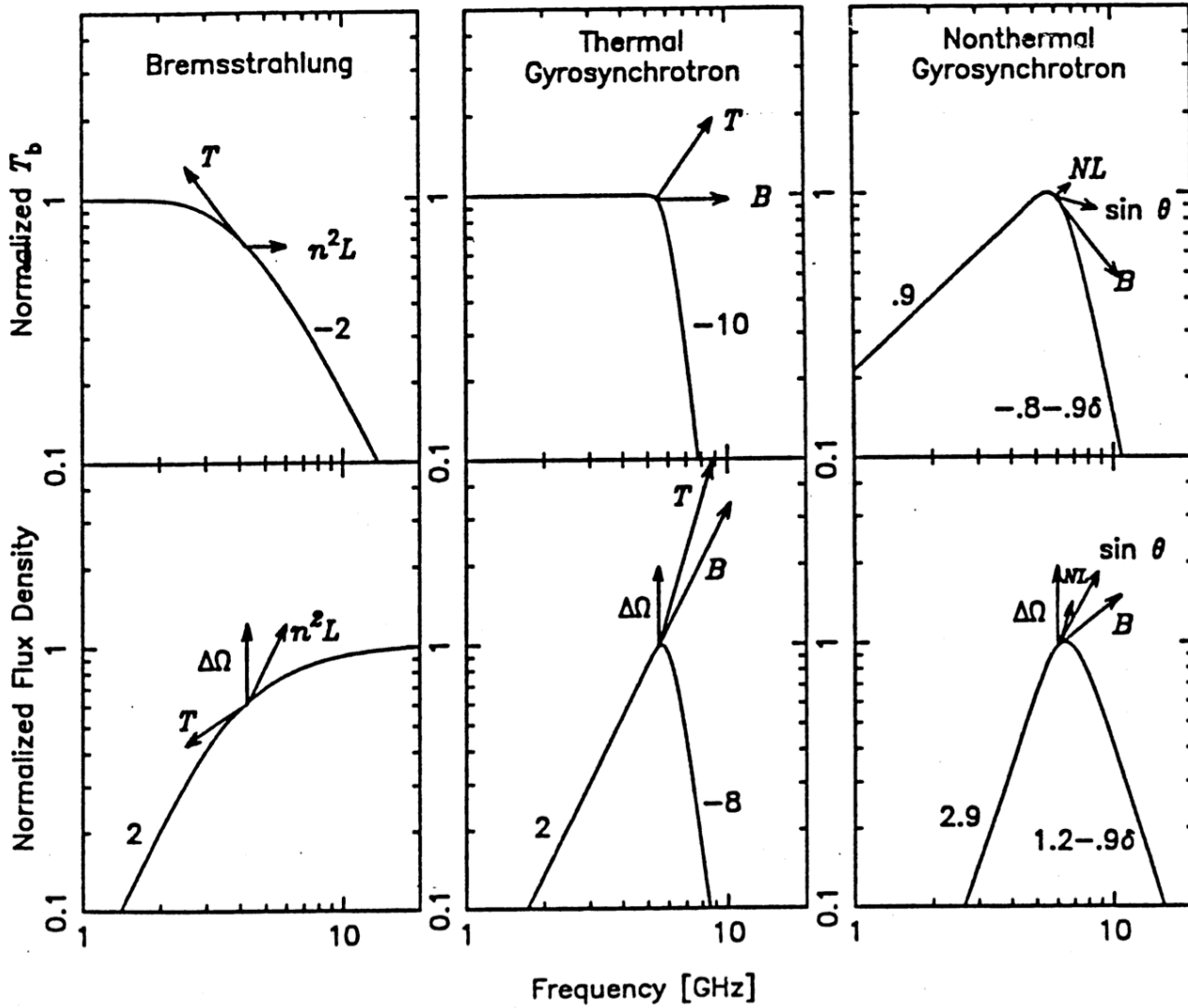


Figure 8.18: *Characteristic radio spectra for Bremsstrahlung, thermal synchrotron radiation and nonthermal synchrotron radiation, given as irradiance (below) and as brightness temperature (above). The numbers indicate the slope; in these log-log plots the slope is the power of the frequency dependence. The arrows indicate in which direction the curves shift (their shapes are roughly conserved) with a variation of a factor two in the parameters n (electron density), T (temperature), B (magnetic field strength), L (layer depth), N (number of fast-moving particles above the threshold energy), θ (pitch angle of the spiral movement) and δ (spectral index for the energy distribution of the particles $n(E) = kE^{-\delta}$). After a preprint by Gary and Hurford.*

much more extinction so that the outermost layer involved (shell D in Figure 8.19) lies much farther out: they show $v_D \approx 1500 - 3000 \text{ km s}^{-1}$.

How does this fast-moving stellar wind originate? The idea of Lucy and Solomon (1970) was that the momentum transfer from these ultraviolet lines powers the wind. Consider a thin shell at radius C . Photon excitation by means of outwardly directed stellar radiation followed by isotropic reemission provides an acceleration outwards with a sum in which the momentum transfer of the photon excitation contributes

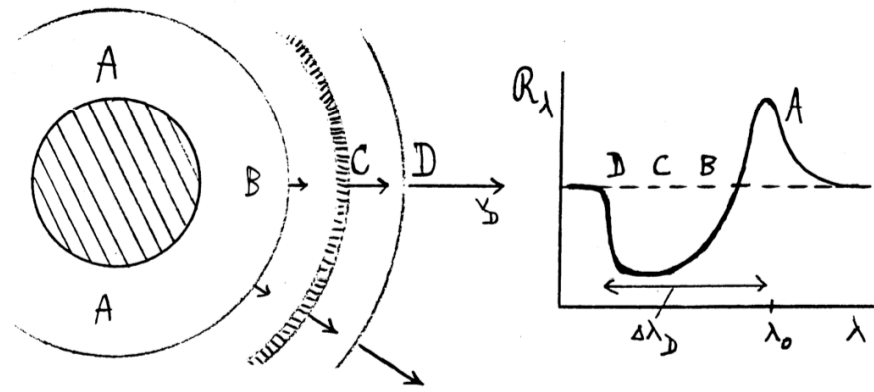


Figure 8.19: *P Cygni profiles*. An expanding extended atmosphere around a hot star provides spectral lines with an emission peak at the rest wavelength and an absorption trough towards shorter wavelengths.

but that of the photon deexcitation does not, on account of its isotropy:

flow of energy [$\text{sec}^{-1} \text{cm}^{-2}$]	\mathcal{F}_ν
with momentum	\mathcal{F}_ν/c
momentum transfer [cm^{-2}]	$\alpha_\nu \mathcal{F}_\nu/c$
contribution to the acceleration	$\alpha_\nu \mathcal{F}_\nu/\rho c$
total acceleration	$g_r = (1/\rho c) \int_0^\infty \alpha_\nu \mathcal{F}_\nu d\nu$

We evaluate this acceleration first for the continuum. The continuous extinction in O stars is dominated by Thomson scattering. This is frequency independent, thus

$$g_r^{\text{es}} = \frac{1}{\rho c} N_e \sigma^{\text{es}} \mathcal{F} = \frac{N_e \sigma^{\text{es}} L}{\rho c 4\pi r^2},$$

and the relationship to the inwardly directed gravitational acceleration $g = GM/r^2$ is

$$\Gamma^{\text{es}} \equiv \frac{g^{\text{es}}}{g} = \frac{N_e \sigma^{\text{es}} L}{4\pi \rho c GM}.$$

This ratio is the *Eddington limit*; if $\Gamma^{\text{es}} > 1$, the photosphere is blown off by the continuous radiation. Stable stars thus have $\Gamma^{\text{es}} < 1$.

Now for the radiation pressure of spectral lines. In deep layers the Rosseland approximation holds:

$$\mathcal{F}_\nu = \frac{4\pi}{3} \int_0^\infty \frac{1}{\alpha_\nu} \frac{dB}{dT} \frac{dT}{dz} d\nu,$$

thus

$$g_r = \frac{1}{\rho c} \int_0^\infty \alpha_\nu \mathcal{F}_\nu d\nu = \frac{4\pi}{3\rho c} \int_0^\infty \mathcal{F}_\nu \frac{dB}{dT} \frac{dT}{dz} d\nu$$

is independent of α_ν : the spectral lines are not effective in deep layers. They do increase the extinction but the radiative flux leaks out through just those spectral windows with small extinction.

But above the surface that is no longer so. There radiative flux doesn't know what lies above it and larger line extinction in an overlying shell counts as long as the shell is optically thin. The contribution per spectral line:

$$g_r^l = \frac{1}{\rho c} \alpha^l \Delta\nu_D \mathcal{F}_\nu \approx \frac{1}{\rho c} \alpha^l \Delta\nu_D B_\nu(T_{\text{eff}})$$

with $\Delta\nu_D = \nu\xi/c$ the Doppler width of the line, determined by the average thermal velocity ξ of the scattering particles in the shell. The peak of B_ν falls in the ultraviolet; for strong ultraviolet resonance lines such as C IV 154.8 nm with $\mathcal{F}_\nu = B_\nu(T_{\text{eff}})$ we have $g_r^l/g \approx 300$. This is then a large effect; moreover, there are hundreds of such strong lines available in the ultraviolet.

But now add radiative transport. An optically very thin layer captures few photons; in an optically thick layer the lines saturate and there is no more $B_\nu(T_{\text{eff}})$ radiation. Thus we introduce the optical thickness of the shell τ^l for the line frequency $\nu = \nu^l$. With radiation from below by the undisturbed continuum of the star there follows from

$$\tau^l \langle g_l \rangle = g_l(0) \int_0^{\tau^l} e^{-\tau'} d\tau'$$

that

$$\langle g_l \rangle = \frac{\alpha^l \Delta\nu_D}{\rho c} \mathcal{F}_\nu \frac{1 - e^{-\tau^l}}{\tau^l}.$$

How large is τ^l ? For a static atmosphere we have $\tau^l = \int_R^\infty \alpha^l dr$, but for an expanding atmosphere the extinction profile shifts in wavelength with the expansion velocity as it increases outwards. Then we have the important *Sobolev approximation*:

$$\tau^l \approx \alpha^l \frac{\xi}{dv/dr},$$

a type of effective optical thickness per line in an expanding shell. For sufficiently large dv/dr each shell absorbs a new piece of the continuum because the line extinction profile for this shell is shifted with respect to that of any other shell; this shell is not shielded by the inner shells. Each photon that traverses a path length of about τ^l (for example by scattering) escapes, in whatever direction; yet above and below the shell there are atoms which can absorb the line photons at this Doppler shift. For sufficiently large dv/dr this shell of interaction is also so thin that it can be assumed to be homogeneous. Thus:

$$\begin{aligned} \text{for strong lines } (\tau^l \gg 1) \quad \langle g_l \rangle &= \frac{\mathcal{F}_\nu}{\rho c} \frac{\Delta\nu_D}{\xi} \frac{dv}{dr} \\ \text{for weak lines } (\tau^l \ll 1) \quad \langle g_l \rangle &= \frac{\mathcal{F}_\nu}{\rho c} \Delta\nu_D \alpha^l \end{aligned}$$

For strong lines the line extinction coefficient α^l drops out: only their number matters. Their contribution is proportional to dv/dr because for larger dv/dr there is less self-screening.

8.3.3 Planetary nebulae

Planetary nebulae are the result of the loss of stellar material: shells of previously ejected material are heated and made to reradiate by the central star. They have nothing whatsoever to do with planets. The so-called H II regions are similar objects: emission nebulae of H^+ around hot stars. References: Bowers & Deeming Volume II, chapters 20, 24. Here follows a description of relevant radiative processes taken from the lecture notes of C. Zwaan.

8.3.3.1 Zanstra mechanism

Stellar radiation in the Lyman continuum ($\lambda < 91.2$ nm) ionizes the nebula – the nebula is thus heated. A recombining electron contributes to the *recombination spectrum* – not only Lyman photons but also Balmer, Paschen, etc. photons are released (thus: photon conversion, or photon degradation).

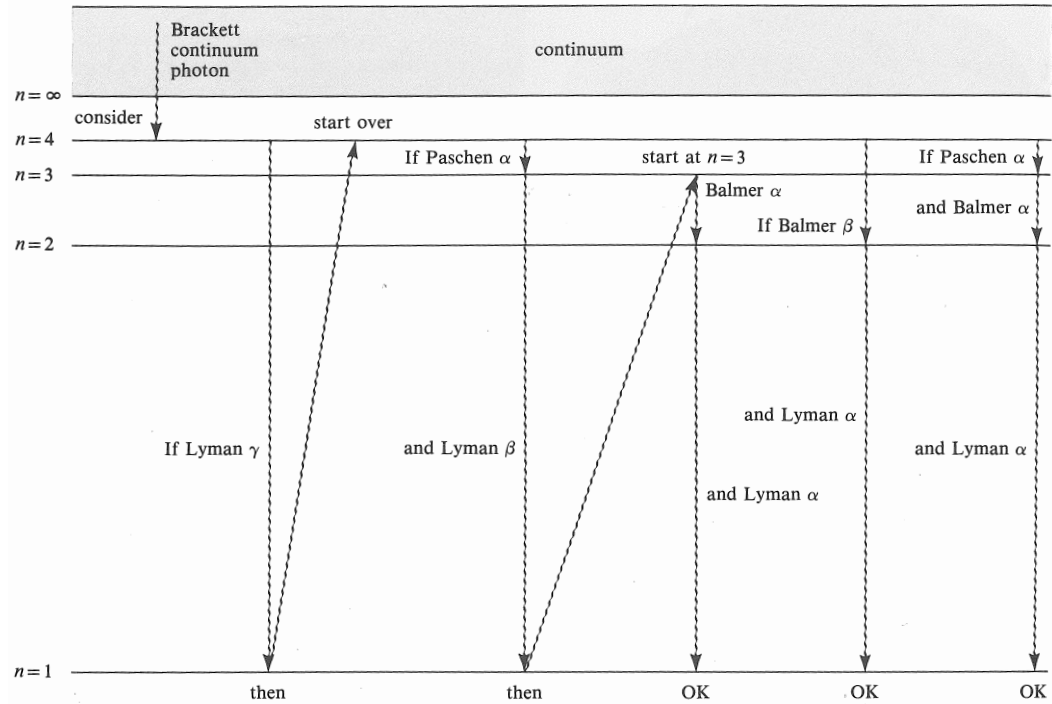


Figure 8.20: *The Zanstra mechanism for planetary nebulae. The recombination cascade which produces hydrogen emission lines in HII regions and planetary nebulae can take many possible paths. But in a nebula that is optically thick to the Lyman transitions, all such paths ultimately produce one Balmer photon plus one Ly α photon plus, perhaps, lower-energy continuum and line photons (the paths marked OK). Taken from Shu “The Physical Universe” 1982, Figure 11.9.*

Zanstra assumed that a (planetary) nebula is *optically thick* to all Lyman photons, but *optically thin* to Balmer, Paschen, and other photons. Zanstra established that the Ly β , Ly γ , ... and Lyman continuum photons originating in the star, after many extinctions and reemissions in the nebula, were eventually degraded into Ly α photons and Balmer, Paschen, etc. photons (Figure 8.20). He noted that *each* Lyman photon (from β up to the continuum) produced one Ly α and one Balmer photon. By means of many scattering processes, the Ly α photons leak out of the nebula path, the Balmer photons leave the nebula as soon as they are created. So by counting all Balmer photons *from the nebula*, one counts all Lyman photons (from Ly β on, for which the Lyman continuum is the most important) which originate *from the star*. Equating this with the photons in the optical *stellar* spectrum provides a *color index* which is a very sensitive measure of the stellar temperature. In this way one determines for the central stars of planetary nebulae the *Zanstra temperature*: $3 \times 10^4 \text{K} \leq T_{\text{eff}}^* \leq 3 \times 10^5 \text{K}$.

One can naturally draw up a detailed description, without making extreme as-

assumptions about the optical thickness of the nebula, and in which more is recovered from the Balmer spectrum of the nebula. The populations of the energy levels of hydrogen are completely determined by the radiative field of the star: as a result of the low electron densities, collisional processes are negligible compared to all non-forbidden line transitions.

The radiative field of the star has a very extreme character: the average intensity in the nebula as a result of the radiation is:

$$J_\nu = W_\nu \frac{2h\nu^3/c^2}{e^{h\nu/kT_r} - 1},$$

with T_r the (very high) radiative temperature of the star in the relevant line or series limit continuum and W_ν is the very small radiative dilution factor:

$$W_\nu = \frac{R^2}{4r^2} e^{-\tau_\nu(r)}.$$

The first factor is the geometric dilution factor, with R the radius of the star, and r the distance to the star. Assuming $r \gg R$, $R^2/4\pi r^2$ is very small: $\approx 10^{-15}$. The second factor is the extinction factor, in which τ_ν stands for the optical distance of the star to the particular element in the nebula – this contains the density of the (hydrogen) atoms along this distance. The radiative field is thus very “hot” though extremely thin.

Because the nebula is optically thin to all transitions except the Lyman spectrum, the radiative field of the nebula “itself” is negligible (except perhaps in Ly α). From this scenario it follows that the statistical equilibrium is completely determined by:

1. photon-ionization and photon excitation, exclusively from the ground level, as a result of Lyman radiation of the star;
2. photon-recombination and photon deexcitation (levels are thus populated only via processes from the ground level and from higher levels or the continuum).

The system of equations for statistical equilibrium is thus relatively simple – one can solve the problem using models for the stellar radiation and the density in the nebula, and calculate from these e.g. the relative strengths of the Balmer lines and the Balmer continuum (the Balmer decrement), and compare these with the observed Balmer decrement – from this there then follow unique model parameters.

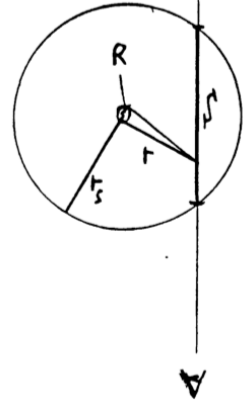
A result of the strongly diluted radiative field is that the local H atoms are practically exclusively in the ground level $n = 1$. If the nebula is optically very thick in Ly α , then the Ly α photons are efficiently trapped. Then the radiative field in Ly α builds up to an average intensity that exceeds the diluted radiation field of the star; however, the net flux remains small. An enhanced radiation field in Ly α then leads to an enhanced population of the level $n = 2$.

Since the hydrogen in the nebula is almost completely (singly) ionized, practically all emission in the Balmer, Paschen, etc. spectrum is produced by *recombination*. So the emission per volume element is thus proportional to $n_H \times N_e$. The surface brightness I_ν of the nebula is thus determined by the so-called *emission measure EM*:

$$EM = \int_S n_H \times N_e ds$$

in which S is the segment along the line of sight inside the nebula.

The nebula has a sharp edge, especially as a result of the extinction factor in the dilution factor W_ν . At a certain distance from the star the intensity of the



stellar radiation in the Lyman continuum decreases, consequently the fraction of neutral hydrogen in the nebula becomes larger, the extinction coefficient for Lyman radiation rises rapidly, and so on. The emission nebula extends to the so-called *Strömngren radius* r_s :

$$r_s = r_{s,1} N_H^{-(2/3)}.$$

In this n_H is the density of hydrogen particles. The Strömngren radius naturally depends strongly on the effective temperature of the central star – see the table.

Spectral type:	O5	O8	B0	B3	B9	A2
T_{eff}	55000	49000	42000	28000	15500	12300 K
$r_{s,1}(n_H = 1 \text{ cm}^{-3})$	130	80	50	15	2	0.6 pc

Table 8.3: *Effective temperatures and Strömngren radii for hot stars*

Since the particle density is somewhat nonuniform, the edge of the nebula will have an irregular shape – certainly for diffuse nebulae and H^+ regions.

The above scenario for the hydrogen spectrum in nebulae can also be applied to the He II spectrum of singly-ionized helium – the wavelengths are shifted: the resonance line corresponding to $\text{Ly}\alpha$ falls at 30.3 nm and the series limit corresponding to the Lyman continuum at 22.8 nm. Owing to the lower helium abundance, the nebula is somewhat less thick in He II lines and continua than in H. With a few modifications the preceding arguments also apply to He I: here there is also photoelectric heating and photon degradation.

8.3.3.2 Fluorescence

In planetary nebulae individual strong UV lines are encountered, especially in O III, which are noteworthy because other closely related lines from the same spectrum are completely absent.

Bowen (1935) demonstrated that these lines arise from fluorescence resulting from pumping in a strong line of the nebula (see Figure 8.21). The resonance line of He II λ 30.3780 nm is very strong: just as for $\text{Ly}\alpha$ a rather strong radiative field can build up in the line. This helium line overlaps the O III 30.3799 nm line, with the result that O^{++} is excited from the ground level to the very specific fine-structure level $3d^3P_2$. From there the O^{++} ion decays back to the ground state by spontaneous emissions, via a whole cascade of lines, most of which lie in the optical UV. The last transition O III λ 37.4436 nm overlaps two lines in the N III spectrum, which cause an excitation to the $3d^2D$ term of N^{++} , which once again results in a number of spontaneous emissions, also in the visible spectral region.

8.3.3.3 Forbidden lines

In the spectrum of emission nebulae spectral lines are seen which do not occur in the laboratory – among which are the two blue-green “nebulium” lines N_1 and N_2 , that are brighter than all the remaining lines combined in the visible spectrum of practically all nebulae. These lines were explained (by Bowen and others) as forbidden lines (i.e. not electronic dipole radiation) of O^{++} : [O III]. The metastable levels (1D and 1S in that case) are excited by collisions with electrons – that can happen at the typical electron temperatures in nebulae, $T_e \approx 1 - 2 \times 10^4$ K, because the energy jumps are only a few eV. Because of the low N_e the probability for a

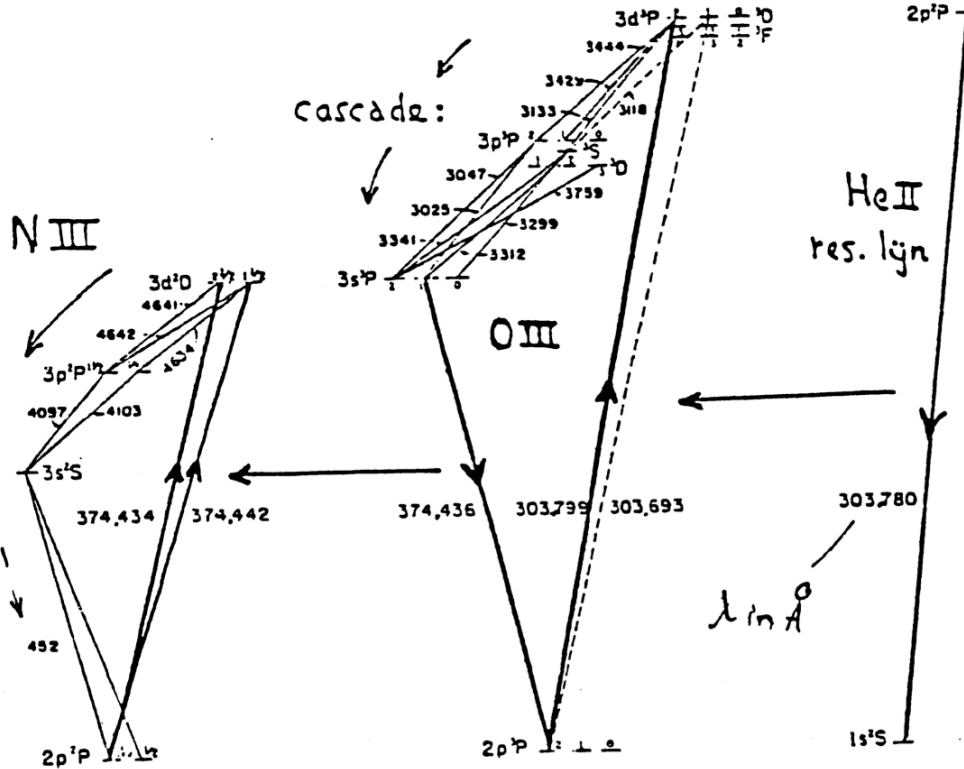


Figure 8.21: *The Bowen mechanism for fluorescence. Due to fortuitous wavelength coincidences, high levels can be excited by photons from the spectra of other elements. The wavelengths are given in Ångstrom.*

collisional deexcitation is still considerably smaller than the probability for photodeexcitation, by which forbidden lines appear. Note (carefully) that the presence of forbidden lines occurs optimally in a fairly hot gas of electrons, just dense enough to provide collisional excitation, but indeed not so dense that collisions dominate the deexcitation of the metastable levels.

8.3.3.4 Radio emission

Given that an emission nebula is practically completely (singly) ionized, free-free radiation is emitted – this is especially natural in the radio region (why?). This is an important diagnostic which provides the electron temperature of the nebula; in the radio region there is no continuous extinction. Do check if in the radio region a nebula is optically thick – (or an intermediate case) – or optically thin, but that can be discerned from the $I(\nu)$ spectrum itself. If it is optically thick we have $I(\nu) \sim \nu^2$; if it is optically thin we have $I(\nu) \sim \nu^0$.